

**ÉCOLE DOCTORALE DE PHYSIQUE ET CHIMIE PHYSIQUE**  
**Laboratoire d'Ingénierie des Polymères pour les Hautes Technologies-**  
**LIPHT- ECPM**

**THÈSE** présentée par :  
**Hale ÖZTÜRK DÜŞKÜNKORUR**

soutenue le : **7 Décembre 2012**

pour obtenir le grade de : **Docteur de l'université de Strasbourg**  
Discipline/ Spécialité : **CHIMIE DES MATÉRIAUX**

**BIOPOLYESTER SYNTHESIS BY ENZYMATIC  
CATALYSIS AND  
DEVELOPMENT OF NANOHYBRID SYSTEMS**

**THÈSE dirigée par :**

**M. AVEROUS Luc**  
**Mme GÜVENİLİR Yüksel**

Prof., Université de Strasbourg  
Prof., Istanbul Technical University

**RAPPORTEURS :**

**Mme DELAITE Christelle**  
**M. ELNEKAVE Moiz**

Prof., Université de Haute Alsace  
Prof. Assoc., Istanbul Technical University

---

**AUTRES MEMBRES DU JURY :**

**Mme DEVECİ Nuran**  
**Mme ÖNEN Ayşen**  
**M. POLLET Eric**

Prof., Istanbul Technical University  
Prof., Istanbul Technical University  
Dr., Université de Strasbourg

**ISTANBUL TECHNICAL UNIVERSITY ★ GRADUATE SCHOOL OF SCIENCE**  
**ENGINEERING AND TECHNOLOGY**  
**UNIVERSITY OF STRASBOURG ★ E.D. PHYSICS AND PHYSICAL CHEMISTRY**

**BIOPOLYESTER SYNTHESIS BY ENZYMATIC CATALYSIS  
AND DEVELOPMENT OF NANOHYBRID SYSTEMS**

**Ph.D. THESIS**

**Mediha Hale ÖZTÜRK DÜŞKÜNKORUR**

**Department of Chemical Engineering - Chemical Engineering  
Programme (ITU)  
Laboratory of Polymer Engineering for High Technologies - LIPHT  
(UdS)**

**DECEMBER 2012**



**ISTANBUL TECHNICAL UNIVERSITY ★ GRADUATE SCHOOL OF SCIENCE**  
**ENGINEERING AND TECHNOLOGY**  
**UNIVERSITY OF STRASBOURG ★ E.D. PHYSICS AND PHYSICAL CHEMISTRY**

**BIOPOLYESTER SYNTHESIS BY ENZYMATIC CATALYSIS  
AND DEVELOPMENT OF NANOHYBRID SYSTEMS**

**Ph.D. THESIS**

**Mediha Hale ÖZTÜRK DÜŞKÜNKORUR  
(506042005)**

**Department of Chemical Engineering - Chemical Engineering  
Programme (ITU)  
Laboratory of Polymer Engineering for High Technologies - LIPHT  
(UdS)**

**Thesis Advisor: Prof. Dr. Yüksel GÜVENİLİR  
Co-Advisor: Prof. Dr. Luc AVEROUS**

**DECEMBER 2012**



**İSTANBUL TEKNİK ÜNİVERSİTESİ ★ FEN BİLİMLERİ ENSTİTÜSÜ**  
**STRAZBURG ÜNİVERSİTESİ ★ FİZİK ve FİZİKSEL KİMYA Y.O**

**ENZİMATİK KATALİZ YOLUYLA BİYOPOLİESTER SENTEZİ  
VE NANOHİBRİT SİSTEMLERİN GELİŞTİRİLMESİ**

**DOKTORA TEZİ**

**Mediha Hale ÖZTÜRK DÜŞKÜNKORUR**  
**(506042005)**

**Kimya Mühendisliği Anabilim Dalı - Kimya Mühendisliği Programı**  
**(İTÜ)**  
**Yüksek Teknolojiler Polimer Mühendisliği Laboratuvarı - LIPHT (UdS)**

**Tez Danışmanı: Prof. Dr. Yüksel GÜVENİLİR**  
**Eş Danışman: Prof. Dr. Luc AVEROUS**

**ARALIK 2012**



**M.Hale ÖZTÜRK DÜŞKÜNKORUR, a Ph.D.** student of ITU **Graduate School of Science Engineering and Technology**, student ID 506042005 and student of Uds **E.D. of Physics and Physical Chemistry**, student ID 20918964 successfully defended the **thesis** entitled “**BIOPOLYESTER SYNTHESIS BY ENZYMATIC CATALYSIS AND DEVELOPMENT OF NANOHYBRID SYSTEMS**”, which she prepared after fulfilling the requirements specified in the associated legislations,

**Thesis Advisor :**      **Prof. Dr. Yüksel GÜVENİLİR** .....  
Istanbul Technical University

**Co-Advisor :**        **Prof. Dr. Luc AVEROUS** .....  
University of Strasbourg

**Jury Members :**     **Prof. Dr. Nuran DEVECİ** .....  
Istanbul Technical University

**Prof. Dr. Ayşen ÖNEN** .....  
Istanbul Technical University

**Prof. Dr. Christelle DELAITE** .....  
University of Haute Alsace

**Assoc. Prof. Dr. Moiz ELNEKAVE** .....  
Istanbul Technical University

**Dr. Eric POLLET** .....  
University of Strasbourg

**Date of Submission : 17 October 2012**

**Date of Defense : 7 December 2012**







**1926-2005**

*Çok sevdiğim dedem, değerli insan,  
edebiyat öğretmeni Reha Köseoğlu'nun anısına...  
Beni uzaklardan seyrettiğini biliyorum.  
Bu tezi, senin gibiengin bilgili, değer yargılarına ve doğrulara her zaman sahip  
çıkan bir öğretmene layık olmaya çalışan bir öğrenci, ve bana gösterdiğin  
emeklere teşekkürlerini sunan torunun olarak sana ithaf ediyorum.*

*To my dear grandfather,  
to the memory of Reha Köseoğlu, valuable and lovely literature teacher...  
I know that you are watching me from far away.  
I am dedicating this thesis to you, as a student trying to be worthy of such a  
teacher as you, with a vast knowledge and always defending his own values and  
the truth, and also as your granddaughter presenting her expression of gratitude.*



## FOREWORD

To start, I would like to record my gratitude to my supervisors for accepting the co-direction of this PhD project and for their guidance, support and suggestions from the beginning to the end of this research.

I would like to thank to my supervisor Prof. Dr. Yüksel GÜVENİLİR for permitting me to pursue my PhD abroad and supporting and encouraging me along this long journey with her technical and moral advices and her presence besides me within the ITU family.

I would like to thank to my supervisor Prof. Luc AVEROUS for giving me the opportunity to pursue my PhD within his “BioTeam” group and providing to introduce me into the world of biopolymers with his vast knowledge and deep experience in this domain.

I would like to express my sincere gratitude to Dr. Eric POLLET for his continuous assistance during my thesis, his tremendous help, the countless time he spent and his vast knowledge that have helped me to pursue the experimental work and understand this subject. His endless encouragement, understanding, patience and meticulous contributions worthy of appreciation were for me the most important supports and enabled me to complete this thesis.

I would like to acknowledge Dr. Vincent PHALIP for sharing his knowledge in enzymology, for guiding me in the experiments and welcoming me in his group. His kind and positive attitude during my stay and along the discussions always recomforted me.

I am thankful to Dr. Philippe DEBEIRE for teaching me his sound expertise in enzyme science and his sophisticated skills in the experimental work and also for important contributions that he made to the project. His kind and joyful personality brightened the days in the lab.

I would like to thank to the thesis supervising committee members within I.T.U, Prof. Dr. Nuran DEVECİ and Prof. Dr. Ayşen ÖNEN for their valuable comments.

I would like to thank to Prof. Christelle DELAITE and Assoc. Prof. Moiz ELNEKAVE for having accepted to be the rapporteurs of my thesis.

I would like to thank Prof. Pierre BUCHER, director of Ecole Doctorale de Physique et chimie physique for having kindly approved my inscription to the PhD programme within the University of Strasbourg.

I am grateful to Mrs. Annette WINTER for her kindness, her help and attention that she paid for my inscription and official procedures.

I am also indebted to Ecole Doctorale of University of Strasbourg for providing me some financial support for the international mobility to travel between France and Turkey during the project.

I would like to thank to the director of the LIPHT, Prof. Guy SCHLATTER for receiving me in the lab and the SEM images that he performed.

Thanks to Prof. Dr. Özgül TAŞPINAR from I.T.U for providing the silicate samples which were used in this study.

I am thankful to Mr. Michel SCHMIDT for several NMR analyses that he performed for this study and for his gentleness.

Many thanks to Christophe SUTTER, Sébastien GALLET and Christophe MELART for their technical assistance and limiteless help, and also their positive energy and smiley faces warming the lab atmosphere.

I am grateful to Chheng NGOV who helped me in every difficult condition with an appreciable patience and also for the SEC analyses that she performed for this project.

I would like to acknowledge Catherine KIENTZ for her courtesy, for whole official papers and procedures that she made gladly for me.

I am grateful to ESBS group: Anne, Jérôme, Olivier and Cédric, for their warm welcome and cordial help. The crosswords in french that they were teaching me at lunch time will always remain as sweet memories in my mind.

I am thankful to all the LIPHT group members with whom I shared this lab journey; Marie, Florence, Maria-Clara, Alice, Deepak, Ikram, Murielle, Jérôme, Stéphanie, Véronique, Camille, İbrahim for their friendship. Thanks to Antoine for his contribution to this project. Thanks to Veronica Martino for her technical assistance, guidance and friendly dialogue.

Thanks to my thesis that I met Inès, Seher and Patricia. Our acquaintance made me know different worlds which enriched my culture and embellished my days and their accompany and friendship always encouraged me morally.

I would like to express my appreciation to my friends Berrak, Zeynep, Özlem, Aygöl, Ceren and Alper who came to visit me in Strasbourg and made me feel inexpressibly happy.

I would like to extend my sincere gratitude to my dear grandmother Nevin and Köseoğlu family for their remote support and to Düşkünkörur family.

It is a pleasure to express my gratitude to my valuable parents Güldal and Okay. Their endless love, encouragement and presence in any condition beside me, were the sources of strength and motivation for me throughout these days and whole my life. Words would be insufficient to describe the feelings that I grow for them in my heart.

I am thankful to my dear husband Melih for sharing with me this period with a great understanding and patience. I am grateful for his accompany, love, support and his jokes to absorb my stress and to keep me happy.

December 2012

M.Hale ÖZTÜRK DÜŞKÜNKÖRUR  
(Chemical Engineer)

## TABLE OF CONTENTS

	<u>Page</u>
<b>FOREWORD</b> .....	<b>ix</b>
<b>TABLE OF CONTENTS</b> .....	<b>xi</b>
<b>ABBREVIATIONS</b> .....	<b>xv</b>
<b>LIST OF TABLES</b> .....	<b>xvii</b>
<b>LIST OF FIGURES</b> .....	<b>xix</b>
<b>SUMMARY</b> .....	<b>xxv</b>
<b>ÖZET</b> .....	<b>xxix</b>
<b>RÉSUMÉ</b> .....	<b>xxxiii</b>
<b>1. INTRODUCTION</b> .....	<b>1</b>
<b>2. LITERATURE REVIEW</b> .....	<b>5</b>
2.1 Short Introduction on Biodegradable Polymers .....	5
2.2 Biodegradable Polyesters .....	7
2.2.1 Petroleum-based polyester: polycaprolactone .....	7
2.2.2 Bio-based polyester: poly(lactic acid) .....	10
2.3 Ring Opening Polymerization (ROP) of Lactones and Lactides by “Chemical Catalysis” .....	14
2.3.1 ROP of lactones and lactides by organo-metallic compounds .....	14
2.3.1.1 Anionic ROP .....	14
2.3.1.2 Coordination-insertion ROP .....	15
2.3.1.3 Cationic ROP .....	19
2.3.1.4 Organo-metallic catalyst concerns .....	20
2.3.2 ROP of lactones and lactides by “metal-free” organic catalysts .....	20
2.4 Enzyme Catalysis .....	25
2.4.1 Introduction .....	25
2.4.2 Advantages of enzyme catalyzed polymerization over chemical polymerization for the synthesis of biopolyesters .....	26
2.4.3 Lipases for polyester and polycarbonate synthesis .....	27
2.4.4 Lipase catalyzed ROP of lactones and lactides into polyesters .....	32
2.4.4.1 Proposed mechanisms .....	32
2.4.4.2 Lipase catalyzed ROP of $\epsilon$ -CL .....	36
2.4.4.3 Lipase catalyzed ROP of lactides .....	40
2.4.5 PCL/PLA copolymerizations by lipase catalysis .....	44
2.4.6 Immobilization of lipases .....	48
2.4.6.1 CALB immobilization and Novozym <sup>®</sup> -435 commercial catalyst .....	49
2.4.6.2 Clays as enzyme supports .....	52
2.5 Organic/Inorganic Nanohybrids .....	54
2.5.1 Clays .....	56
2.5.1.1 Sepiolite .....	59
2.5.1.2 Montmorillonite .....	60
2.5.1.3 Organomodification of clays .....	61

2.5.2 Polymer/clay nanocomposites .....	63
2.5.3 Elaboration routes and morphologies of polymer/clay nanohybrids .....	64
2.5.4 Biopolyester/clay nanohybrids .....	65
2.5.4.1 PCL/clay nanobiocomposites .....	65
2.5.4.2 PLA/clay nanobiocomposites .....	70
2.6 Main Conclusions of The Bibliographic Review and Objectives of The Present Study .....	72
<b>3. MATERIALS AND METHODS.....</b>	<b>77</b>
3.1 Materials .....	77
3.2 Methods .....	78
3.2.1 Measurement of lipase activity .....	78
3.2.2 Determination of the protein content .....	78
3.2.3 Immobilization of lipase.....	80
3.2.4 Surface modification of clays .....	80
3.2.5 Polymerization reactions .....	81
3.2.6 Nanohybrid synthesis .....	82
3.3 Characterization Techniques .....	83
3.3.1 Nuclear magnetic resonance (NMR).....	83
3.3.2 Size exclusion chromatography (SEC) .....	83
3.3.3 Thermogravimetric analysis (TGA).....	84
3.3.4 Scanning electron microscopy (SEM).....	84
3.3.5 Differential scanning calorimetry (DSC) .....	84
3.3.6 X-Ray diffraction analysis (XRD) .....	84
3.3.7 Energy dispersive X-ray fluorescence spectroscopy (EDX).....	85
3.3.8 Transmission electron microscopy (TEM).....	85
<b>4. RESULTS AND DISCUSSIONS .....</b>	<b>87</b>
4.1 PCL Synthesis by ROP Catalyzed by NOV-435 and Free CALB .....	87
4.2 PCL Synthesis by ROP Catalyzed by NOV-435 and Free CALB in Presence of Clays.....	90
4.2.1 PCL synthesis in presence of sepiolite .....	90
4.2.2 PCL synthesis in presence of montmorillonite .....	91
4.2.3 PCL synthesis in presence of organomodified montmorillonite (Cloisite <sup>®</sup> 30B) .....	92
4.2.4 Scale-up of PCL synthesis in presence of clays.....	94
4.3 Lipase (CALB) Immobilization on Clays .....	95
4.3.1 Influence of the type of clay support: MMT, MMTMOD, SEP or SEPMOD .....	96
4.3.2 Influence of lyophilization and glutaraldehyde treatment.....	101
4.4 Synthesis of PCL Catalyzed by CALB Immobilized on Clays .....	109
4.5 Elaboration and Characterization of PCL/Clay .....	116
4.5.1 Nanohybrids synthesized by NOV-435.....	116
4.5.2 Nanohybrids synthesized by CALB immobilized on Cloisite <sup>®</sup> 30B .....	123
4.6 Nanohybrid Characterization for Evidencing Polymer Grafting on Clay .....	131
4.7 Test of Different Lipases for the ROP of $\epsilon$ -CL .....	145
4.8 Synthesis of PCL Catalyzed by Lipase Immobilized on Alternative Inorganic Supports .....	148
4.9 Synthesis of PLA by Enzymatic Catalytic Systems .....	153
4.9.1 Synthesis of PLA by NOV-435 and free CALB .....	153
4.9.2 PLA synthesis catalyzed by lipase (CALB) immobilized on montmorillonite .....	157

4.9.3 PLA synthesis catalyzed by an alternative lipase: Amano lipase PS.....	158
4.10 Copolymerizations of $\epsilon$ -CL and Lactide Isomers Catalyzed by NOV-435..	160
<b>5. CONCLUSIONS AND PERSPECTIVES .....</b>	<b>171</b>
<b>REFERENCES.....</b>	<b>177</b>
<b>CURRICULUM VITAE.....</b>	<b>195</b>





## ABBREVIATIONS

<b>ASTM</b>	: American Society for Testing and Materials
<b>BSA</b>	: Bovine serum albumin
<b>CALB</b>	: <i>Candida antarctica</i> Lipase B
<b>CCL</b>	: <i>Candida cylindracea</i> lipase
<b>CDCl<sub>3</sub></b>	: Deuterated chloroform
<b>ε-CL</b>	: Epsilon caprolactone
<b>DP<sub>n</sub></b>	: Degree of polymerization
<b>DSC</b>	: Differential Scanning Calorimetry
<b>EAM</b>	: Enzyme Activated Monomer Complex
<b>EDX</b>	: Energy Dispersive X-ray Fluorescence Spectroscopy
<b>FDA</b>	: American Food and Drug Administration
<b>GA</b>	: Glutaraldehyde
<b>LA</b>	: Lactic acid
<b>M<sub>n</sub></b>	: Number average molecular weight
<b>M<sub>w</sub></b>	: Weight average molecular weight
<b>MMT</b>	: Montmorillonite
<b>MMTL</b>	: CALB immobilized on montmorillonite
<b>MMT-MOD</b>	: Organomodified montmorillonite
<b>MMTMODL</b>	: CALB immobilized on organomodified montmorillonite
<b>MMT-Na<sup>+</sup></b>	: Unmodified sodium montmorillonite
<b>NMR</b>	: Nuclear Magnetic Resonance
<b>NOV-435</b>	: Novozym <sup>®</sup> -435
<b>OD</b>	: Optical density
<b>OMMT</b>	: Organomodified montmorillonite
<b>PC</b>	: <i>Pseudomonas cepacia</i> lipase
<b>PCL</b>	: Polycaprolactone
<b>PDI</b>	: Polydispersity index
<b>PPL</b>	: Porcine pancreatic lipase
<b>PS</b>	: Polystyrene
<b>pNPB</b>	: Para nitro phenyl butyrate
<b>pNP</b>	: Para nitro phenol
<b>SEC</b>	: Size Exclusion Chromatography
<b>SEM</b>	: Scanning Electron Microscopy
<b>SEP</b>	: Sepiolite
<b>SEPL</b>	: CALB immobilized on sepiolite
<b>SEP-MOD</b>	: Organomodified sepiolite
<b>SEPMODL</b>	: CALB immobilized on organomodified sepiolite
<b>T<sub>c</sub></b>	: Crystallization temperature
<b>T<sub>g</sub></b>	: Glass transition temperature
<b>T<sub>m</sub></b>	: Melting temperature
<b>TEM</b>	: Transmission Electron Microscopy
<b>TGA</b>	: Thermogravimetric Analysis

<b>PDLA</b>	: Poly(D-lactic acid)
<b>PDLLA</b>	: Poly(DL-lactic acid)
<b>PLA</b>	: Poly(lactic acid)
<b>PLLA</b>	: Poly(L-lactic acid)
<b><math>\delta</math>-VL</b>	: $\delta$ -valerolactone
<b>wt%</b>	: Weight percent
<b>XRD</b>	: X-Ray Diffraction Analysis

## LIST OF TABLES

	<u>Page</u>
<b>Table 2.1 :</b> Lipase catalyzed ROP of $\epsilon$ -CL at various temperatures and media with corresponding monomer conversion rates (C) and molecular weights ( $M_n$ ) of PCL chains .....	37
<b>Table 2.2 :</b> Lipase catalyzed ROP of lactide isomers at various temperatures and media with corresponding monomer conversion rates (C) and molecular weights ( $M_n$ ) of poly(lactide) .....	41
<b>Table 2.3 :</b> The nine groups of phyllosilicates (Bergaya et al., 2012) .....	57
<b>Table 2.4 :</b> Classification and examples of clay minerals (Alexandre and Dubois, 2000) .....	58
<b>Table 2.5 :</b> Commercial organomodified clays (Bordes et al., 2009) .....	63
<b>Table 4.1 :</b> Immobilization loading of lipase on different supports .....	96
<b>Table 4.2 :</b> Immobilization loading of lipase on different clay supports .....	97
<b>Table 4.3 :</b> Stability test on glutaraldehyde treated derivatives .....	108
<b>Table 4.4 :</b> Immobilization of lipase on modified clay supports.....	109
<b>Table 4.5 :</b> Immobilization of lipase on different clay supports to test the effect of GA.....	112
<b>Table 4.6 :</b> Larger scale $\epsilon$ -CL polymerization experiments catalyzed by NOV-435 in presence of different types of clay .....	117
<b>Table 4.7 :</b> Molecular weights and thermal properties of PCL and PCL/clay nanohybrids synthesized by NOV-435 and clay percentages present in the hybrid structures determined by SEC, DSC and TGA analyses .	117
<b>Table 4.8 :</b> Effect of immobilization media and drying techniques on final specific activity of the lipase derivatives (CALB immobilized onto Cloisite <sup>®</sup> 30B) .....	124
<b>Table 4.9 :</b> $\epsilon$ -CL conversion percentages and molar masses of PCLs observed in polymerizations catalyzed by A1 and B2 catalysts .....	125
<b>Table 4.10 :</b> Thermal properties of resulting PCL/Cloisite <sup>®</sup> 30B nanohybrids synthesized by CALB immobilized onto Cloisite <sup>®</sup> 30B and clay percentages present in the nanohybrids as determined by DSC and TGA .....	127
<b>Table 4.11 :</b> Percentages and ratios of analytes present in neat PCL, Cloisite <sup>®</sup> 30B (MMTMOD), clay-rich and PCL rich fractions of PCL/MMTMOD nanohybrid determined by EDX .....	141
<b>Table 4.12 :</b> Specific activities of lipases depending on different types of substrate.....	145
<b>Table 4.13 :</b> The use of different lipases for polymerization of $\epsilon$ -CL; specific activities on <i>p</i> NPB substrate, monomer conversion and reaction time at different temperatures .....	146

<b>Table 4.14 :</b> Molecular weights ( $M_n$ ) of PCLs synthesized at 70°C by different lipases for different reaction times. $M_n$ values determined by $^1\text{H}$ NMR .....	147
<b>Table 4.15 :</b> Immobilization of CALB onto various silicates .....	149
<b>Table 4.16 :</b> Use of silica type derivatives as catalyst for $\epsilon$ -CL polymerization reactions .....	150
<b>Table 4.17 :</b> Characteristics of PCLs synthesized by silica type derivatives .....	151
<b>Table 4.18 :</b> Lactide polymerization reactions carried out with 1 g of lactide, 3 ml of toluene and 150 mg of NOV-435 catalyst.....	155
<b>Table 4.19 :</b> Lactide polymerization reactions carried out with 1 g of lactide, 2 ml of toluene and 50 mg of free CALB catalyst.....	156
<b>Table 4.20 :</b> Lactide polymerization reactions carried out with 1g of D- lactide in 3 ml of toluene and 200 mg of CALB/clay derivatives as catalysts ...	158
<b>Table 4.21 :</b> Reaction conditions for ROP of $\epsilon$ -CL and D-, L-lactides catalyzed by Amano lipase PS .....	159
<b>Table 4.22 :</b> Monomer conversion evolution for the copolymerization of 1 ml of $\epsilon$ -CL and 1 g of D-lactide in 2 ml of toluene catalyzed by 100 mg NOV-435.....	162
<b>Table 4.23 :</b> Time evolution of D-lactide monomer conversion after its Subsequent addition in copolymerization medium composed of ~1 g PCL, 5 ml of toluene and 100 mg NOV-435 catalyst.....	163
<b>Table 4.24 :</b> Results of $\epsilon$ -CL/PCL- lactide copolymerizations catalyzed by NOV-435.....	165

## LIST OF FIGURES

	<u>Page</u>
<b>Figure 2.1</b> : Polymerization reaction of PCL from $\epsilon$ -CL .....	8
<b>Figure 2.2</b> : Synthesis of PLA by direct condensation polymerization or by ROP of lactide (Becker and Dove, 2011).....	10
<b>Figure 2.3</b> : The lifecycle of poly(lactide) (Becker and Dove, 2011).....	12
<b>Figure 2.4</b> : Initiation of ring opening polymerization of lactones by anionic initiators (Albertsson and Varma, 2003).....	14
<b>Figure 2.5</b> : Ring-opening polymerization mechanisms (Zinck, 2011) .....	16
<b>Figure 2.6</b> : Tin alkoxide complex initiated polymerization of lactones (Albertsson and Varma, 2003) .....	16
<b>Figure 2.7</b> : Proposed mechanism for the ROP of lactide by DMAP .....	21
<b>Figure 2.8</b> : Proposed monomer-activated mechanism for the ROP of lactide by IMes (Dove, 2009).....	22
<b>Figure 2.9</b> : The active site pocket of CALB partitioned into two sides: an acyl and an alcohol side (Uppenberg et al., 1995).....	29
<b>Figure 2.10</b> : 3D-structure of CALB (Uppenberg et al., 1994).....	29
<b>Figure 2.11</b> : Less mobile water molecules at the surface of CALB. Location of less mobile water molecules, with a B-factor lower than 40 Å <sup>2</sup> , at the surface of the last snapshot of CALB during the simulation (A) in water and (B) in cyclohexane; water molecules are displayed as red and white spheres (Trodler and Pleiss, 2008) .....	31
<b>Figure 2.12</b> : Lipase catalyzed ring-opening polymerization of lactones (Matsumura, 2006) .....	33
<b>Figure 2.13</b> : Postulated mechanism of lipase-catalyzed ring-opening polymerization of lactones (Albertsson and Srivastava, 2008).....	34
<b>Figure 2.14</b> : Illustration of suggested mechanism for the lipase catalyzed ROP of lactones showing the involvement of ionic intermediates at the enzyme active site (Puskas et al., 2011).....	34
<b>Figure 2.15</b> : A general illustrative mechanism of lipase-catalyzed ROP of lactones involving the acylation step and/or the deacylation step as rate-determining step, depending on the structure of R in monomer (Kobayashi, 2006) .....	35
<b>Figure 2.16</b> : Hypothesis concerning the enzymatic ROP of L-lactide (LLA) and D-lactide (DLA) by Novozym <sup>®</sup> -435, (i) initiation and (ii) chain propagation step (Hans et al., 2009).....	42
<b>Figure 2.17</b> : Lipase catalyzed copolymerization of $\epsilon$ -CL and lactide .....	46
<b>Figure 2.18</b> : $\epsilon$ -CL and lactide copolymerization initiated from benzyl alcohol using enzymatic (CALB) and/or carbene catalysis (Xiao et al., 2009).....	47

<b>Figure 2.19 :</b> The enzyme distribution throughout the center section of the NOV-435 bead (Mei et al., 2003b) .....	50
<b>Figure 2.20 :</b> Common particle reinforcements/geometries and their respective surface area-to-volume ratios (Thostenson et al., 2005) .....	55
<b>Figure 2.21 :</b> Structure of sepiolite (Duquesne et al., 2007) .....	59
<b>Figure 2.22 :</b> Structure of montmorillonite .....	60
<b>Figure 2.23 :</b> Organoclay preparation (Chen and Yoon, 2005) .....	62
<b>Figure 2.24 :</b> Scheme of the three main different types of polymer/layered silicate composite structures : (a) phase separated microcomposite; (b) intercalated nanocomposite and (c) exfoliated nanocomposite (Alexandre and Dubois, 2000) .....	64
<b>Figure 2.25 :</b> Illustration of PCL chain grafting on clay, for the case of organomodified montmorillonite .....	67
<b>Figure 2.26 :</b> Schematic representation of the performed studies .....	74
<b>Figure 3.1 :</b> BSA standard curve .....	79
<b>Figure 4.1 :</b> Typical $^1\text{H}$ NMR spectrum of PCL synthesized by lipase catalyzed ROP of $\epsilon$ -CL at 70 °C. The proton assignments and corresponding peaks integral areas are shown in the spectrum.....	87
<b>Figure 4.2 :</b> Zoomed view of $^1\text{H}$ NMR spectrum of a reaction mixture showing the methylene signals of monomer, polymer and chain-end .....	88
<b>Figure 4.3 :</b> Time-evolution curves of $\epsilon$ -CL conversion ( $\blacklozenge$ ) and molecular weight ( $M_n$ ) of obtained PCL ( $\bullet$ ), as determined by $^1\text{H}$ NMR analyses, for polymerizations carried out with (a) <i>NOV-435 (100 mg) catalyst</i> and (b) <i>“free” CALB (50 mg) catalyst</i> .....	89
<b>Figure 4.4 :</b> Time-evolution curves of $\epsilon$ -CL conversion ( $\blacklozenge$ ) and molecular weight ( $M_n$ ) of obtained PCL ( $\bullet$ ), as determined by $^1\text{H}$ NMR analyses, for <b>free CALB</b> (50mg) catalyzed polymerizations carried out (a) <i>in absence of clay</i> and (b) <i>in the presence of 10 mg of sepiolite</i> .....	90
<b>Figure 4.5 :</b> Time-evolution curves of $\epsilon$ -CL conversion ( $\blacklozenge$ ) and molecular weight ( $M_n$ ) of obtained PCL ( $\bullet$ ), as determined by $^1\text{H}$ NMR analyses, for <b>NOV-435</b> (100 mg) catalyzed polymerizations carried out in the presence of (a) <i>10 mg of sepiolite</i> and (b) <i>100 mg of sepiolite</i> .....	91
<b>Figure 4.6 :</b> Time-evolution curves of $\epsilon$ -CL conversion ( $\blacklozenge$ ) and molecular weight ( $M_n$ ) of obtained PCL ( $\bullet$ ), as determined by $^1\text{H}$ NMR analyses, for <b>NOV-435</b> (100 mg) catalyzed polymerizations carried out (a) in the presence of <i>10 mg of MMT-<math>\text{Na}^+</math></i> and (b) in the presence of <i>100 mg of MMT-<math>\text{Na}^+</math></i> .....	92
<b>Figure 4.7 :</b> Time-evolution curves of $\epsilon$ -CL conversion ( $\blacklozenge$ ) and molecular weight ( $M_n$ ) of obtained PCL ( $\bullet$ ), as determined by $^1\text{H}$ NMR analyses, for <b>NOV-435</b> (100 mg) catalyzed polymerizations carried out (a) in the presence of <i>10 mg of Cloisite<sup>®</sup> 30B</i> and (b) <i>100 mg of Cloisite<sup>®</sup> 30B</i> ..	93
<b>Figure 4.8 :</b> Time-evolution curves of $\epsilon$ -CL conversion ( $\blacklozenge$ ) and molecular weight ( $M_n$ ) of obtained PCL ( $\bullet$ ), as determined by $^1\text{H}$ NMR analyses. Reaction mixture constituents as (a) 2 ml toluene; 1 ml $\epsilon$ -CL; 20 mg NOV-435; <i>10 mg sepiolite</i> and (b) 10 ml toluene; 5 ml $\epsilon$ -CL; 100 mg NOV-435; <i>50 mg sepiolite</i> .....	94

<b>Figure 4.9 :</b> Time-evolution curves of $\epsilon$ -CL conversion ( $\blacklozenge$ ) and molecular weight ( $M_n$ ) of obtained PCL ( $\bullet$ ), as determined by $^1\text{H}$ NMR analyses. Reaction mixture constituents as (a) 2 ml toluene; 1 ml $\epsilon$ -CL; 20 mg NOV-435; 10 mg Cloisite <sup>®</sup> 30B and (b) 10 ml toluene; 5 ml $\epsilon$ -CL; 100 mg NOV-435; 50 mg Cloisite <sup>®</sup> 30B.....	95
<b>Figure 4.10 :</b> XRD patterns of natural montmorillonite (MMT- $\text{Na}^+$ ); modified montmorillonite (Cloisite <sup>®</sup> 30B); natural montmorillonite onto which CALB is immobilized (MMTL1); modified montmorillonite onto which CALB is immobilized (MMTMODL1).....	98
<b>Figure 4.11 :</b> XRD patterns of natural sepiolite (Sep- $\text{Na}^+$ ); modified sepiolite (Sep-Mod); natural sepiolite onto which CALB is immobilized (SEPL1); modified sepiolite onto which CALB is immobilized (SEPMODL1).....	99
<b>Figure 4.12 :</b> Reaction of glutaraldehyde with proteins under acidic or neutral conditions (Walt and Agayn, 1994) .....	101
<b>Figure 4.13 :</b> SEM pictures of natural sepiolite (SEP) at 2000x magnification (left) and 8000x magnification (right).....	103
<b>Figure 4.14 :</b> SEM pictures of natural sepiolite after the immobilization of CALB (SEPL) at 2000x magnification (left) and 8000x magnification (right).....	104
<b>Figure 4.15 :</b> SEM pictures of modified sepiolite (SEPMOD) at 2000x magnification (left) and 8000x magnification (right).....	104
<b>Figure 4.16 :</b> SEM pictures of modified sepiolite after immobilization of CALB (SEPMODL) at 2000x magnification (left) and 8000x magnification (right).....	105
<b>Figure 4.17 :</b> SEM pictures of modified sepiolite after immobilization of CALB and treated with GA (SEPMODL G) at 2000x magnification (left) and 8000x magnification (right).....	105
<b>Figure 4.18 :</b> SEM pictures of natural montmorillonite (MMT) at 2000x magnification (left) and 8000x magnification (right).....	106
<b>Figure 4.19 :</b> SEM pictures of natural montmorillonite after immobilization of CALB (MMTL) at 2000x magnification (left) and 8000x magnification (right).....	106
<b>Figure 4.20 :</b> SEM pictures of modified montmorillonite (MMTMOD) at 2000x magnification (left) and 8000x magnification (right).....	106
<b>Figure 4.21 :</b> SEM pictures of modified montmorillonite after immobilization of CALB (MMTMODL) at 2000x magnification (left) and 8000x magnification (right).....	107
<b>Figure 4.22 :</b> SEM pictures of modified montmorillonite after immobilization of CALB and treated with GA (MMTMODL G) at 2000x magnification (left) and 8000x magnification (right).....	107
<b>Figure 4.23 :</b> Time-evolution curves of $\epsilon$ -CL conversion ( $\square$ ) and molecular weight ( $M_n$ ) of obtained PCL ( $\bullet$ ), as determined by $^1\text{H}$ NMR analyses for polymerizations (10 ml toluene; 3 ml $\epsilon$ -CL) catalyzed by (a) 300 mg of MMTMODL1c G LYOPH (488 U) and (b) 300 mg of SEPMODL1c G LYOPH (215 U) .....	110



<b>Figure 4.24 :</b> Time-evolution curves of $\epsilon$ -CL conversion (♦) and molecular weight ( $M_n$ ) of obtained PCL (●), as determined by $^1\text{H}$ NMR analyses for polymerizations (10 ml toluene; 3 ml $\epsilon$ -CL) catalyzed by (a) 50 mg NOV-435, (b) 50 mg NOV-435 in presence of 300 mg Cloisite® 30B .....	111
<b>Figure 4.25 :</b> Time-evolution curves of $\epsilon$ -CL conversion (♦) and molecular weight ( $M_n$ ) of obtained PCL (●), as determined by $^1\text{H}$ NMR analyses, for polymerizations (10 ml toluene; 3 ml $\epsilon$ -CL) catalyzed by (a) 300 mg of SEPMODL1d (120 U) and (b) 300 mg of SEPMODL1d G (304 U) .....	113
<b>Figure 4.26 :</b> Time-evolution curves of $\epsilon$ -CL conversion (♦) and molecular weight ( $M_n$ ) of obtained PCL (●), as determined by $^1\text{H}$ NMR analyses, for polymerizations (10 ml toluene; 3 ml $\epsilon$ -CL) catalyzed by (a) 300 mg of MMTMODL1d (317 U) and (b) 300 mg of MMTMODL1d G (393 U) .....	114
<b>Figure 4.27 :</b> Schematic representation of polymerization reactions catalyzed by NOV-435 in the presence of nanoclays .....	116
<b>Figure 4.28 :</b> XRD patterns of neat PCL (NOV0 PCL), Cloisite® 30B and PCL/Cloisite® 30B nanohybrids (NOV2-3 PCLs) .....	119
<b>Figure 4.29 :</b> XRD patterns of neat PCL (NOV0 PCL), natural sepiolite (Sep- $\text{Na}^+$ ) and PCL/sepiolite nanohybrid (NOV4 PCL) .....	119
<b>Figure 4.30 :</b> XRD patterns of neat PCL (NOV0 PCL), non-modified montmorillonite (MMT- $\text{Na}^+$ ) and PCL/MMT- $\text{Na}^+$ nanohybrid (NOV5 PCL).....	120
<b>Figure 4.31 :</b> SEM pictures of PCL/clay nanohybrids (a) NOV2 PCL (3% Cloisite® 30B); (b) NOV5 PCL (3% MMT- $\text{Na}^+$ ); (c) NOV4 PCL (3.5% SEP- $\text{Na}^+$ ) with their zoomed view on the right hand side .....	121
<b>Figure 4.32 :</b> TEM pictures of PCL/clay nanohybrids (a) (scale is 500 nm), (b) and (c) (scale is 200 nm).....	122
<b>Figure 4.33 :</b> Schematic representation of polymerization reactions catalyzed by CALB immobilized on nanoclays .....	123
<b>Figure 4.34 :</b> Procedures for immobilization in aqueous and organic media with two different drying techniques.....	124
<b>Figure 4.35 :</b> TGA curves (weight loss and its temperature derivative) of the PCL/clay nanohybrids obtained from the polymerization catalyzed by A1, A2 and B2 derivatives .....	127
<b>Figure 4.36 :</b> TGA spectrum of A1 PCL synthesized by CALB immobilized onto Cloisite® 30B, and NOV3 PCL synthesized by NOV-435 in the presence of Cloisite® 30B .....	128
<b>Figure 4.37 :</b> XRD patterns of modified montmorillonite (Cloisite® 30B) and PCL/ Cloisite® 30B nanohybrids (NOV3, A1, A2, B2 PCLs) .....	129
<b>Figure 4.38 :</b> SEM pictures of PCL/Cloisite® 30B nanohybrids synthesized by A1 and B2 catalysts (a) A1 PCL (7.6 wt% Cloisite® 30B); (b) B2 PCL (9.2 wt% Cloisite® 30B) .....	130
<b>Figure 4.39 :</b> Schematic representation of the separation procedure for different types of nanohybrids .....	131
<b>Figure 4.40 :</b> Weight loss curves of neat SEP, SEP-rich fraction and PCL-rich fraction of PCL/clay nanohybrid obtained from NOV-435 catalyzed polymerization. TGA performed under air atmosphere .....	132

<b>Figure 4.41 :</b> Weight loss curves of neat SEP, SEP-rich fraction and PCL-rich fraction of PCL/clay nanohybrid obtained from NOV-435 catalyzed polymerization. TGA performed under air atmosphere ...	133
<b>Figure 4.42 :</b> Weight loss curves of neat MMTMOD, MMTMOD-rich fraction and PCL-rich fraction of PCL/clay nanohybrid obtained from NOV-435 catalyzed polymerization. TGA performed under air atmosphere .....	134
<b>Figure 4.43 :</b> Weight loss curves of neat SEP, SEP-rich fraction and PCL-rich fraction of PCL/clay nanohybrid obtained from the polymerization catalyzed by CALB immobilized on sepiolite (SEPL3). TGA performed under air atmosphere.....	136
<b>Figure 4.44 :</b> Weight loss curves of neat modified SEP (SEPMOD), SEPMOD-rich fraction and PCL-rich fraction of PCL/clay nanohybrid obtained from the polymerization catalyzed by CALB immobilized on modified sepiolite (SEPMODL1). TGA performed under air atmosphere.....	137
<b>Figure 4.45 :</b> Weight loss curves of neat modified SEP (SEPMOD), SEPMOD-rich fraction and PCL-rich fraction of PCL/clay nanohybrid obtained from the polymerization catalyzed by CALB immobilized on modified sepiolite (SEPMODL1G). TGA performed under air atmosphere.....	138
<b>Figure 4.46 :</b> Weight loss curves of neat modified MMT (MMTMOD), MMTMOD-rich fraction and PCL-rich fraction of PCL/clay nanohybrid obtained from the polymerization catalyzed by CALB immobilized on modified montmorillonite (MMTMODL1). TGA performed under air atmosphere .....	139
<b>Figure 4.47 :</b> Weight loss curves of neat modified MMT (MMTMOD), MMTMOD-rich fraction and PCL-rich fraction of PCL/clay nanohybrid obtained from the polymerization catalyzed by CALB immobilized on modified montmorillonite (MMTMODL1G). TGA performed under air atmosphere .....	140
<b>Figure 4.48 :</b> SEM pictures of organo-modified montmorillonite after immobilization of CALB and treated with GA (MMTMODL G) at 2000x magnification (left) and 8000x magnification (right).....	143
<b>Figure 4.49 :</b> SEM pictures of the clay-rich fraction of PCL/montmorillonite nanohybrid obtained from the polymerization catalyzed by MMTMODL G and showing the PCL chains grafting on clay surface at 2000x magnification (left) and 8000x magnification (right).....	143
<b>Figure 4.50 :</b> SEM pictures of modified sepiolite after immobilization of CALB and treated with GA (SEPMODL G) at 2000x magnification (left) and 8000x magnification (right).....	144
<b>Figure 4.51 :</b> SEM pictures of the clay-rich fraction of PCL/sepiolite nanohybrid obtained from the polymerization catalyzed by SEPMODL G PCL at 2000x magnification (left) and 8000x magnification (right).....	144
<b>Figure 4.52 :</b> Weight loss curves of neat Ca+Mg silicate and PCL produced by the catalysis of CALB/Ca+Mg silicate.....	151
<b>Figure 4.53 :</b> TEM micrograph of calcium-magnesium silicate from rice hull ash (scale is 200 nm).....	152

<b>Figure 4.54 :</b> SEM pictures of PCL synthesized by CALB immobilized on Ca+ Mg silicate at 100x magnification (left) and 400x magnification (right).....	152
<b>Figure 4.55 :</b> Typical $^1\text{H}$ NMR spectrum of PLA synthesized by lipase catalyzed ROP of at 70 °C. The proton assignments and corresponding peaks are shown in the spectrum .....	154
<b>Figure 4.56 :</b> Zoomed view of $^1\text{H}$ NMR spectra of samples withdrawn from the reaction mixture of D-lactide polymerization by NOV-435 showing the methylene signals of monomer, polymer and chain end recorded after (A) t=2 h and (B) t=48 h of reaction .....	154
<b>Figure 4.57 :</b> $^1\text{H}$ NMR spectrum of poly( $\epsilon$ -CL-co-D-lactide) copolymer synthesized by NOV-435, with proton assignments and corresponding peaks .....	161
<b>Figure 4.58 :</b> Zoomed view of $^1\text{H}$ NMR spectra of samples withdrawn from the reaction mixture (A) at t=2 h and (B) at t=48 h .....	162
<b>Figure 4.59 :</b> Representation of a two steps copolymerization where PCL is firstly synthesized from $\epsilon$ -CL by lipase catalysis followed by subsequent addition and polymerization of the lactide monomer .....	163
<b>Figure 4.60 :</b> Zoomed view of $^1\text{H}$ NMR spectra of samples (A) at t=0, where D-lactide monomer is added to the reaction mixture containing the preformed PCL chain, (B) at t=48 h, final purified copolymer .....	163
<b>Figure 4.61 :</b> Carbonyl signals in $^{13}\text{C}$ NMR spectra of copolymerization products of PCL+ D-lactide system; (A) at t=2 h and (B) at t=48 h .....	164
<b>Figure 4.62 :</b> TGA spectrum of hybrid random copolymer (CLDMMT), its polymer rich and clay rich fractions .....	168
<b>Figure 4.63 :</b> DSC thermograms of CLDMMT hybrid random copolymer and its purified polymer-rich fraction .....	169

## BIOPOLYESTER SYNTHESIS BY ENZYMATIC CATALYSIS AND DEVELOPMENT OF NANOHYBRID SYSTEMS

### SUMMARY

Biosynthetic pathway, like enzymatic ring opening polymerization (ROP) of lactones draws attention as a new trend of biodegradable polymer synthesis due to its nontoxicity, mild reaction requirement and recyclability of immobilized enzyme. The enzymatic polymerization can thus be regarded as an environment-friendly synthetic process for polymeric materials, providing a good example of green polymer chemistry and sustainable development. The conventional organo-metallic catalysts used for the ROP of lactones or lactides are based on derivatives of metals such as Zn, Al, Sn or Ge, which may be very toxic. The required complete removal of these metallic residues is an important issue when considering the biomedical applications of these biopolyesters. Enzymes are natural catalysts and therefore good candidates for the elaboration of such biopolyesters e.g., for biomedical applications.

Lipases, belonging to the family of hydrolases, are found in most organisms from microbial, plant and animal kingdom and can hydrolyze triglycerides (or esters) to glycerols and fatty acids at water-oil interface. Interestingly, in some cases, the lipase-catalyzed hydrolysis in water can be easily reversed in non-aqueous media into ester synthesis or transesterification. Due to this specific behavior, lipases can catalyze the ring-opening polymerization (ROP) of lactones (small to large rings), cyclic diesters (lactides) and cyclic carbonates to produce aliphatic polyesters or polycarbonates.

Various process parameters of enzyme catalyzed reactions such as: operational and thermal stability and easier separation from the reaction mixture, can be modified by enzyme immobilization. Immobilization of lipases is often performed by adsorption through hydrophobic interactions between the enzyme and the support.

Among the immobilized lipases, the most common and preferred system is the physically immobilized form of *Candida antarctica* lipase B (CALB) commercially available and known as Novozym<sup>®</sup> 435 (NOV-435). This efficient and versatile catalyst is based on a porous acrylic resin as the enzyme carrier. Alternative enzyme supports such as porous ceramic (silica) or other polymer-based supports for the development of immobilized lipase catalyst for efficient production of polymers are also investigated. In parallel, the use of phyllosilicates (clays) as possible inorganic porous supports to immobilize enzymes has also been described in the literature. Interestingly, the use of such nanoclays as lipase carriers could bring numerous advantages such as the high specific surface availability, the facility of water dispersion/recuperation, the high water uptake capacity, and the excellent mechanical resistance of these materials.

Besides, important researches are conducted nowadays on the elaboration of composites materials in combination with inorganic (nano)particles to further improve some of these polyester properties for specific applications. Till now,

mainly hydroxyapatite, wollastonite and bioactive glass have been studied as the inorganic phase, mainly for the development of materials for tissue engineering (e.g., implants, bone reconstruction). All studies show that these materials are very promising, the inorganic moiety bringing enhanced mechanical strength, bioactivity and tailored degradation rate, but need further studies and improvement. Among the possible developments, the use of inexpensive and largely available clays as inorganic reinforcements is attentively considered.

Among the clays, montmorillonite is by far the most studied for the elaboration of polyester/clay nano-biocomposite materials. Montmorillonite is a crystalline 2:1 layered silicate mineral, composed of platelets formed of alumina-silicate sheets separated by an inter-layer spacing full with inorganic cations ( $\text{Na}^+$ ,  $\text{Ca}^{2+}$ ,...). This feature gives a hydrophilic character to the clay which is not appropriate for its compatibility with polymers mostly organophilic. With a simple cation exchange, the polymer/montmorillonite affinity can be modified. Another clay representing a particular interest for the elaboration of organic/inorganic nanohybrid materials, is sepiolite. Sepiolite is a non swelling, lightweight, fibrous and porous clay with a large specific surface area and having particles of needle-like morphology. It is a hydrated magnesium silicate having rather a high surface area (around  $400 \text{ m}^2/\text{g}$ ) and lower contact area between needles when compared to the contact area between montmorillonite platelets.

This thesis aims at presenting the use and development of original catalytic systems based on lipases immobilized on clays which are efficient for the synthesis of biopolyesters and allowing the preparation of organic/inorganic nanohybrids based on clay nanoparticles (sepiolite and montmorillonite) grafted with such polyesters.

For this,  $\epsilon$ -caprolactone ( $\epsilon$ -CL) polymerization catalyzed by *Candida antarctica* lipase B (CALB) was carried out in the presence of montmorillonite and sepiolite to obtain organic/inorganic nanohybrids through polymer chain grafting and growth from the surface of the clay.

Besides being widely used and studied in nanocomposites based on biodegradable polymers (nano-biocomposites), these two nanoclays are also good candidates for enzyme immobilization procedures and thus their natural and organomodified forms were used as lipase supports. Free form, commercial resin-immobilized form (NOV-435) and clay-immobilized forms of CALB have been tested as catalytic systems and their efficiency has been compared. The polymerization kinetics and resulting materials were fully characterized with NMR, SEC, DSC, TGA, SEM and EDX analyses.

The first steps of the study consisted in testing and defining the most appropriate experimental techniques and operational conditions proper to the synthesis of polycaprolactone (PCL) by enzymatic ROP. Polymerization reactions were catalyzed by commercial enzymatic systems as CALB immobilized on acrylic resin (NOV-435) and its equivalent free lipase. Once this step was achieved, optimization of operational conditions for the synthesis of biopolyesters in organic solvent and in bulk was performed by analyzing the effect of temperature, concentration of the reactants and reaction time. This part was essentially based on the determination of the polymerization reactions' kinetics and characterization of the obtained polyesters in terms of molecular weights.

As a second task, an important work was carried out on the development of original catalytic systems obtained by immobilization of lipases on inorganic clay

nanoparticles, i.e natural and modified forms of sepiolite and montmorillonite. Different conditions for immobilization were tested and resulting lipase/clay systems were characterized, selected and optimized in function of their performances with respect to the polymerization efficiency. The main results obtained from this part of the study concern the differences in catalytic performance between montmorillonite and sepiolite-based systems as well as the influence of clay-organomodification. Indeed, it has been demonstrated that lipases immobilized on montmorillonite show better performances compared to the ones immobilized on sepiolite. In addition, the clay surface organo-modification performed with quaternary ammonium salts has proved to greatly enhance the lipase immobilization procedure efficiency and thus the catalytic activity of the corresponding systems. It has been suggested that such differences in the catalytic behavior of the systems could be explained by the differences in the strength of electrostatic interactions between the enzyme and the clay surface. Finally, the more efficient catalytic systems identified were then tested for the elaboration of organic/inorganic nanohybrids.

The chosen approach was thus to elaborate such nanohybrids using the "grafting from" strategy by promoting the polyesters chain anchoring and growth directly from the hydroxyl groups present at the surface of clay nanoparticles and thus in direct vicinity of the immobilized lipase. This original route was compared to the more direct one which was performed by conducting the "grafting from" polymerization using the NOV-435 catalyst in presence of corresponding clays in the reaction medium. The effective grafting of PCL chains from the clay surface was demonstrated using selective separation methods followed by thermogravimetric analyses.

In parallel, lipase-based catalytic systems were also tested for the polymerization of the lactide D-, L- and D/L- isomers, highlighting the selectivity of the enzyme toward the different types of isomers. Finally, copolymerization reactions between  $\epsilon$ -caprolactone and the lactide isomers were performed using the NOV-435 catalytic system with the aim to obtain PCL/PLA copolymers. Random copolyesters were successfully obtained when copolymerizing D-lactide with  $\epsilon$ -caprolactone.



## ENZİMATİK KATALİZ YOLUYLA BİYOPOLİESTER SENTEZİ VE NANOHİBRİT SİSTEMLERİN GELİŞTİRİLMESİ

### ÖZET

Laktonların enzimatik halka açılımı ile polimerizasyonu (ROP), toksik sonuçlar doğurmaması, ılımlı reaksiyon koşullarında gerçekleşmesi ve immobilize enzimlerin tekrar kullanılabilmesi açısından biyobozunur polimer sentezinde yeni bir eğilim olarak dikkat çekmektedir. Enzimatik polimerizasyon, polimer malzemelerinin üretimi için çevre dostu sentetik bir proses olarak görülmekte ve yeşil polimer kimyası ve sürdürülebilir gelişme için iyi bir örnek oluşturmaktadır. Laktonların ve laktidlerin ROP'u için kullanılan geleneksel organo-metalik katalizörler, Zn, Al, Sn veya Ge gibi çok toksik olabilecek metal türevleri bazındadır. Biyopoliesterlerin biyomedikal uygulamaları söz konusu olduğunda, bu metalik kalıntıların tümüyle giderilmesi gereksinimi, önemli bir sorun olarak ortaya çıkar. Enzimler doğal katalizörler olduklarından, biyopoliesterlerin biyomedikal uygulamalar için üretiminde tercih edilebilecek en iyi adaylar arasında yer alırlar.

Hidrolazlar sınıfına dahil olan lipazlar, mikrop, bitki ve hayvan dünyasından organizmaların birçoğunda bulunur ve su-yağ arayüzeyinde, trigliserit veya esterleri, gliserol ve yağ asidine hidrolizleyebilirler. İlginç olarak, lipazların sulu ortamdaki bu hidrolizleme yetenekleri, susuz çözücü ortamında, ester sentezi veya transesterifikasyon kabiliyetine dönüşebilir. Bu özel davranış sayesinde lipazlar, laktonların (küçük ve geniş halka yapıda), siklik diesterlerin (laktidler) ve siklik karbonatların halka açılım polimerizasyonunu, alifatik poliester veya polikarbonat üretimi için katalizleyebilirler.

Enzim katalizli reaksiyonlarda, işletimsel, termal kararlılık ve reaksiyon ortamından ürünün ayrıştırılabilmesi gibi birçok proses parametresi, enzimlerin immobilizasyonu ile iyileştirilebilir. Lipazların immobilizasyonu, genellikle enzim ile taşıyıcı arasındaki hidrofobik etkileşimler sonucu adsorpsiyonla gerçekleşmektedir. Bu bağlanmanın kovalant olmayan yapısı, enzimatik reaksiyonun susuz ortamda gerçekleştiği durumlarda herhangi bir sorun yaratmamaktadır, çünkü bu koşullarda lipazın yüzeyden desorplanması olası değildir.

İmmobilize lipazlar arasında en yaygın ve tercih edilen sistem, *Candida antarctica* lipaz B (CALB) enziminin fiziksel olarak immobilize edilmiş ve ticari olarak Novozym® 435 (NOV-435) adı altında bulunan şeklidir. Bu etkili ve çok yönlü katalizörde, enzim taşıyıcısı olarak gözenekli akrilik bir reçine kullanılmıştır. Bunun yanı sıra, polimerlerin etkin üretiminde kullanılabilecek immobilize lipaz katalizörlerinin geliştirilmesi için, gözenekli seramik (silika) veya diğer polimer bazlı alternatif taşıyıcıların kullanımı araştırılmaktadır.

Buna paralel olarak, enzimlerin immobilizasyonunda killerin, inorganik, gözenekli taşıyıcılar olarak kullanımı da uygulamalar arasında görülmektedir. Bu nanokillerin lipaz taşıyıcısı olarak kullanılması, yüksek spesifik yüzey alanı, kolay su dispersiyonu ve geri kazanılması, yüksek su tutma kapasitesi ve mükemmel mekanik



direnç gibi bu maddelerin yapılarından ileri gelen birçok avantajı beraberinde getirmektedir.

Biyopoliesterlerin enzimatik olarak sentezinin yanı sıra, inorganik nanopartiküllerle birleştirilerek, belirli biyomedikal uygulamalar için özelliklerinin iyileştirilmesi adına, nano-biyokompozit malzemelerin geliştirilmesi üzerine günümüzde önemli çalışmalar yürütülmektedir. Şu ana kadar, hidroksiapatit, wollastonit ve biyoaktif cam, doku mühendisliği için malzemelerin geliştirilmesinde; implantlar ve yeniden kemik yapılanması alanlarında inorganik faz olarak kullanılmış ve araştırılmıştır. Malzeme içindeki inorganik yarı; geliştirilmiş mekanik kuvvet, biyoaktivite ve istenilen bozunma hızı gibi avantajlar sağladığından, tüm çalışmalar bu malzemelerin çok umut verici olduğunu göstermiştir. Fakat bu alanda daha ileri derecede çalışmaların ve geliştirmelerin yapılması gerekmektedir. Olası geliştirmeler arasında, ucuz ve çokça mevcut olan killerin, inorganik güçlendiriciler olarak kullanımı önemli ölçüde dikkate çekmektedir.

Killer arasında montmorillonit, poliester/kil nano-biyokompozitlerinin hazırlanmasında şu ana kadar en çok kullanılan kil olmuştur. Montmorillonit, kristalin yapıda, 2:1 katmanlı silikat esaslı bir mineraldir. Katmanları oluşturan alümina-silikat tabakalarının arası, inorganik katyonlarla ( $\text{Na}^+$ ,  $\text{Ca}^{2+}$ , v.b) dolu olan bir boşlukla ayrılmıştır. Bu yapı kile, hidrofilik bir özellik kazandırmaktadır ki bu durum, çoğunluğu organofilik olan polimerlerle uyumluluğu açısından avantajlı değildir. Basit bir katyon değişim prosedürü ile, polimerlerle montmorillonit arasındaki afinite olumlu yönde değiştirilebilir. Organik/inorganik nanohibritlerin hazırlanması için ilgi çeken diğer bir kil ise sepiyolittir. Sepiyolit gözenekli yapıda, hafif ağırlıklı, geniş spesifik yüzey alanına sahip, suda şişmeyen bir kildir ve iğne yapılı tanecikler içerir. Hidratlı doğal bir magnezyum silikat olan sepiyolit, katmanlı filossilikatlarla (örneğin montmorillonit) karşılaştırıldığında, iğne yapılı tanecikleri arasında daha zayıf bir kontak alanına sahiptir. Bunun yanı sıra yüksek bir yüzey alanı ( $\sim 400 \text{ m}^2/\text{g}$ ) sergilemektedir.

Bu tezin amacı, biyopoliester sentezi için etkili olabilecek, sepiyolit ve montmorillonit nanokilleri üzerine immobilize edilmiş lipazlarla yeni ve özgün katalizörlerin geliştirilmesi ve aynı zamanda bu yeni katalik sistemler sayesinde poliesterlerin kil nanopartikülleri üzerine aşılması ile organik/inorganik nanohibrit malzemelerin üretilmesidir. Bu amaçla,  $\epsilon$ -kaprolakton'un ( $\epsilon$ -KL) CALB ile katalizlenen halka açılım polimerizasyonu, reaksiyon ortamına montmorillonit ve sepiyolit killerin konulmasıyla gerçekleştirilmiştir. Bu sayede, polimer zincirlerinin kil yüzeyine aşılaraq uzayıp büyümeleri ile organik/inorganik nanohibrit malzemelerin üretimi amaçlanmıştır.

Biyopolimer bazlı nanokompozitler için fazlaca kullanılan ve üzerinde bilimsel çalışmalar yapılan bu iki nanokil, ayrıca enzim immobilizasyonu için olası taşıyıcı adayları arasında yer almaktadır. Bu amaçla, doğal ve organomodifiye edilmiş formları lipaz taşıyıcı olarak kullanılmıştır. CALB'nin serbest, reçine üzerine immobilize edilmiş ticari formu (NOV-435) ve kil üzerine immobilize edilmiş formu katalitik sistemler olarak denenmiş ve polimerleştirme etkinlikleri karşılaştırılmıştır. Polimerizasyon kinetiği ve elde edilen ürünlerin karakterizasyonu, NMR, SEC, DSC, TGA, SEM, XRD ve EDX analizleri gerçekleştirilerek yapılmıştır.

Çalışmanın ilk aşaması, enzimatik ROP ile polikaprolakton (PKL) sentezi için en uygun deneysel tekniklerin ve reaksiyon koşulların belirlenmesine dayanmıştır. Polimerizasyon reaksiyonları, CALB'nin ticari serbest formu ve immobilize formu

NOV-435 tarafından katalizlenmiştir. Çalışmanın bu ilk aşaması tamamlandıktan sonra, reaksiyon koşullarının optimizasyonu için biyopoliester sentezi, organik çözücülerde ve yığılma gerçekleştirilmiş; sıcaklık, reaktanların konsantrasyonu ve reaksiyon süresi gibi parametrelerin etkisi incelenmiştir. Bu bölüm daha çok, polimerizasyon kinetiğinin incelenmesine ve elde edilen poliesterlerin molekül ağırlıklarının belirlenmesine dayanmaktadır.

İkinci bölümde, lipazın inorganik kil nanotaneceklerinin (sepiyolit ve montmorillonitin doğal ve modifiye formları) üzerine immobilizasyonu ile elde edilecek özgün katalitik sistemlerin geliştirilmesi için önemli bir çalışma gerçekleştirilmiştir. Immobilizasyon için farklı koşullar denenmiş ve elde edilen lipaz/kil katalitik sistemleri karakterize edilerek, amaçlanan polimerizasyon reaksiyonlarındaki etkinliklerine göre seçilerek optimize edilmiştir.

Çalışmanın bu kısmından elde edilen başlıca sonuçlar, montmorillonit ve sepiyolit bazlı sistemlerin katalitik etkinliklerindeki farklılıkları ve killerin organomodifikasyonun bu sistemler üzerindeki etkisini sergilemektedir. Şöyle ki, montmorillonitler üzerine immobilize edilen lipazlar, sepiyolit üzerine immobilize edilenlerden daha iyi etkinlik göstermektedir. Ayrıca, kuaterner yapılu amonyum tuzları ile kil yüzeylerine yapılan organomodifikasyon işleminin, lipaz immobilizasyonunun etkinliğini ve ilgili katalitik sistemin performansını büyük ölçüde arttırdığı gözlenmiştir. Sistemlerin katalitik davranışlarındaki farklılıkların, enzim ile kil yüzeyi arasındaki elektrostatik etkileşimlerin güçlerindeki farklılıklardan ileri gelebileceği düşünülmüştür. Son olarak, en etkin olduğu belirlenen katalitik sistemler, organik/inorganik nanohibritlerin sentezi için denenmiştir.

Seçilen yaklaşımda, “grafting from” stratejisi ile poliester zincirlerinin sentezleri sırasında, kil nanotaneceklerinin yüzeyinde bulunan hidroksil gruplarına doğrudan aşılmalara ve büyümeleri, ve aynı zamanda bu reaksiyonu katalizleyen kil üzerine immobilize edilmiş lipazın hemen çevresinde, nanohibritlerin oluşturulması amaçlanmıştır. Bu özgün yol, yine “grafting from” stratejisine dayanan, fakat bu kez NOV-435 lipazının katalizinde, killerin reaksiyon ortamına konulmasıyla daha direkt bir yolla gerçekleştirilen polimerizasyonlarla karşılaştırılmıştır. Bu yöntemler sonucunda PKL zincirlerinin kil yüzeyine etkin olarak aşılması, seçici ayırma yöntemleri ve bunu takip eden termogravimetrik analiz ile kanıtlanmıştır.

Buna paralel olarak, lipaz bazlı katalitik sistemler, D-, L- ve D/L- laktid izomerlerinin polimerizasyonunda denenmiş ve farklı izomer tipleri için farklı seçicilikler gösterdikleri tespit edilmiştir. Son olarak, PKL/PLA kopolimer eldesi için,  $\epsilon$ -KL ile laktid izomerleri arasında NOV-435 katalitik sistemi kullanılarak kopolimerizasyon reaksiyonları gerçekleştirilmiştir.  $\epsilon$ -KL ile D-laktidin kopolimerleşmesi ile rastgele kopolimerler başarıyla elde edilmiştir.



## **SYNTHÈSE ENZYMATIQUE DE BIOPOLYESTERS ET DÉVELOPPEMENT DES SYSTÈMES NANOHYBRIDES**

### **RÉSUMÉ**

Les réactions de biosynthèse, telle que la polymérisation par ouverture de cycle catalysée par les enzymes, sont considérées comme de nouvelles voies prometteuses pour la synthèse des polymères biodégradables de par leur non-toxicité, les conditions douces de réactions et la recyclabilité des enzymes immobilisées. La polymérisation enzymatique peut donc être considérée comme un procédé de synthèse de polymères respectueux de l'environnement en accord avec les principes de la chimie verte et du développement durable. Les catalyseurs conventionnels organo-métalliques utilisés pour la polymérisation par ouverture de cycle des lactones et des lactides sont généralement des dérivés de métaux tels que Zn, Al, Sn ou Ge qui peuvent être très toxiques. L'extraction complète de ces résidus métalliques constitue un problème important lorsqu'une application biomédicale de ces biopolyesters est envisagée. Les systèmes enzymatiques, qui sont des catalyseurs naturels, sont donc d'excellents candidats pour l'élaboration de tels biopolyesters pour des applications biomédicales.

Les lipases appartiennent à la famille des hydrolases d'esters carboxyliques. Ces enzymes, présentes chez tous les organismes vivants (microbes, animaux, végétaux), jouent un rôle clé dans la biochimie des lipides. Le rôle physiologique des lipases est d'hydrolyser les triglycérides en diglycérides, monoglycérides, acides gras et glycérol. L'hydrolyse des liaisons esters de ces substrats lipidiques, insolubles dans l'eau, se produit à l'interface entre lipide et eau. Dans certaines conditions, en milieu organique, certaines lipases ont également la capacité de réaliser des réactions de synthèse telles que l'estérification (réaction entre un acide et un alcool), la transestérification (ester et alcool) et l'interestérification (ester et ester). Les lipases sont particulièrement versatiles et s'accommodent d'une large gamme de substrats synthétiques. Elles peuvent ainsi catalyser la polymérisation par ouverture de cycle de nombreuses lactones (des petits aux larges cycles), de diesters cycliques (lactides) ou encore des carbonates cycliques pour former des polyesters ou des polycarbonates.

Les lipases, de par leur coût élevé et les problèmes de désactivation rencontrés à température élevée dans les solvants organiques, sont le plus souvent immobilisées sur un support poreux (silice, terres de diatomées, résine acrylique, etc.). Cette immobilisation peut par exemple être une simple physisorption sur le support ou bien encore un greffage covalent mono- ou multi-points. L'immobilisation de la lipase, outre sa récupération et sa réutilisation, peut également permettre d'augmenter la stabilité de l'enzyme et son activité catalytique. L'immobilisation des lipases se fait le plus souvent par adsorption via des interactions hydrophobes entre l'enzyme et le support.

Parmi les lipases, le système catalytique le plus étudié et utilisé actuellement est une lipase B de *Candida antarctica* (CALB) immobilisée sur des billes poreuses de résine acrylique. Il est commercialement disponible, notamment sous le nom de Novozym® 435 (NOV-435). D'autres types de supports tels que des silices poreuses ou des systèmes à base de polymères ont également été testés dans la littérature pour l'élaboration de systèmes catalytiques à base d'enzymes immobilisées pour la synthèse de polymères.

L'usage de phyllosilicates (argiles) comme supports poreux inorganiques pour immobiliser les enzymes a également été décrit. L'utilisation de ces nanoparticules d'argiles en tant que support pour l'immobilisation de lipases peut apporter plusieurs avantages résultant de leur grande surface spécifique, de la facilité de dispersion et de récupération en solution, et de leur excellente résistance mécanique.

Au delà de la synthèse de biopolyesters par voie enzymatique, d'importantes activités de recherche sont dédiées à l'élaboration des matériaux nano-biocomposites résultant de la combinaison de biopolyesters avec des nanoparticules inorganiques afin d'améliorer certaines propriétés en vue d'applications spécifiques (dans le domaine biomédical, par exemple). Jusqu'à présent, ce sont essentiellement l'hydroxyapatite, la wollastonite et le verre bioactif qui ont été testés et étudiés en tant que phase inorganique pour le développement de matériaux dédiés à l'ingénierie tissulaire (e.g., reconstruction osseuse). Toutes les études ont démontré que ces matériaux sont très prometteurs, la partie inorganique entraînant une bioactivité plus importante. Cependant, des études plus approfondies sont encore nécessaires afin d'améliorer et optimiser ces biomatériaux. L'utilisation de nanoparticules d'argile en tant que renfort inorganique largement disponible et peu onéreux est ainsi considérée comme particulièrement attractive.

Dans les systèmes nano-biocomposites argile/biopolyester, la nanocharge la plus communément utilisée est la montmorillonite. Il s'agit d'une argile lamellaire qui à l'état natif, est constitué d'un empilement de feuillets alumino-silicates de 1 nm d'épaisseur, séparés par un espace interfeuillets caractéristique, à la surface desquels se trouvent des cations inorganiques ( $\text{Na}^+$ ,  $\text{Ca}^{2+}$ ,...). La montmorillonite « naturelle » présente ainsi un caractère hydrophile qui, bien souvent, n'est pas en adéquation avec le caractère organophile de la plupart des polymères. Toutefois, par un simple échange cationique, l'affinité polymère/montmorillonites peut être modulée.

Parmi les autres argiles envisagées pour l'élaboration de matériaux nano-hybrides organique/inorganique à base de biopolyesters, la sépiolite présente un intérêt particuliers. La sépiolite est une argile poreuse très légère, qui ne gonfle pas dans l'eau, ayant une morphologie en bâtonnets (ou aiguilles). Il s'agit d'un silicate de magnésium hydraté qui présente la particularité d'avoir une faible surface de contact entre ses aiguilles (comparée aux autres argiles lamellaires) et une surface spécifique assez importante (environ 400 m<sup>2</sup>/g).

L'objectif de ce travail est donc de développer des catalyseurs originaux et performants à base de lipases pour des réactions de synthèse des biopolyesters. En parallèle, il s'agit d'obtenir des matériaux nanohybrides organiques/inorganiques par greffage des chaînes polyesters sur des nanoparticules d'argiles (sépiolite et montmorillonite) pouvant également servir de support pour l'immobilisation de l'enzyme. Pour cela, la polymérisation de  $\epsilon$ -caprolactone ( $\epsilon$ -CL) catalysée par *Candida antarctica* lipase B (CALB) a été réalisée en présence de montmorillonite ou de sépiolite afin d'obtenir des nanohybrides organique/inorganique par greffage et

croissance de chaînes polyesters à partir des groupements hydroxyles en surface de l'argile.

Les formes organo-modifiées et "non-modifiées" de ces deux argiles sont de bons candidats pour l'immobilisation des lipases et elles ont donc été utilisées dans les procédures d'immobilisation. Ainsi, CALB sous sa forme libre (non-immobilisée), sous sa forme immobilisée sur résine acrylique commerciale NOV-435 et sous sa forme immobilisée sur argiles ont été testés en tant que systèmes catalytiques et leur efficacité comparée. Les cinétiques de polymérisations et les polymères obtenus ont été analysés et caractérisés par analyses de RMN, CES, DSC, ATG, MEB, DRX et EDX.

Ainsi, le début de l'étude a consisté à tester et définir les techniques expérimentales et conditions opératoires les plus appropriées pour la synthèse de polycaprolactone (PCL) par polymérisation d'ouverture de cycle. Pour cela, les réactions ont été réalisées en utilisant soit le système catalytique commercial à base de CALB immobilisée sur résine acrylique (NOV-435), soit son équivalent sous la forme "libre" (CALB non-immobilisée). Une fois cette première phase de l'étude achevée, il s'est agit d'optimiser les conditions opératoires pour la synthèse de biopolyesters, en milieu solvant organique et en masse, telles que l'influence de la température, des concentrations en réactifs, de la nature du solvant. Pour cela, l'étude s'est essentiellement basée sur les suivis cinétiques de réaction de polymérisation et les caractéristiques des polyesters obtenus.

Dans un second temps, un important travail a été mené sur le développement de systèmes catalytiques originaux obtenus par immobilisation de lipases sur des supports inorganiques à base de nanoparticules d'argiles telles que les sepiolite et montmorillonite naturelles et organomodifiées. Différentes conditions d'immobilisation ont été testées et les systèmes lipase/argile obtenus ont été caractérisés, sélectionnés et optimisés en fonction de leur performances respectives vis à vis de la réaction de polymérisation envisagée. Les résultats principaux obtenus dans cette partie de l'étude concernent les différences de performances catalytiques entre les systèmes basés sur la montmorillonite et ceux à base de sepiolite ainsi que l'influence de l'organo-modification de ces argiles. En effet, il a été démontré que les lipases immobilisées sur montmorillonite présentent de meilleures performances que celles immobilisées sur sepiolite. De plus, l'organo-modification de la surface des feuillets d'argiles par des sels d'alkylammonium s'est avérée améliorer la procédure d'immobilisation des lipases et donc l'activité catalytique des systèmes correspondants. Il a notamment été suggéré que de telles disparités dans le comportement catalytique de ces systèmes, pouvaient être expliquées par des différences de forces d'interactions électrostatiques entre l'enzyme et la surface de l'argile. Enfin, les systèmes catalytiques les plus efficaces ont ensuite été testés pour l'élaboration des nanohybrides organiques/inorganiques.

L'approche choisie a donc été d'élaborer ces nanohybrides en utilisant la stratégie "grafting from" de manière à promouvoir le greffage et la croissance des chaînes de polyesters directement à partir des groupes hydroxyles présents à la surface des nanoparticules d'argile et donc au voisinage direct de la lipase immobilisée. Cette méthode originale a été comparée à celle, plus directe, qui consiste à réaliser cette polymérisation par "grafting from" en utilisant le système NOV-435 simplement mis en présence des argiles dans le milieu réactionnel. Le greffage effectif des chaînes de

PCL à partir de la surface des argiles a été démontré par des méthodes de séparation sélectives suivies d'analyses thermogravimétriques.

En parallèle, des systèmes catalytiques à base de lipases ont été aussi testés pour la polymérisation des isomères D, L et D-L du lactide, mettant en lumière la sélectivité de l'enzyme envers ces différents isomères. Finalement, des réactions de copolymérisation entre l' $\epsilon$ -caprolactone et les isomères de lactide ont également été réalisées afin d'obtenir des copolymères de PCL/PLA. Des copolyesters statistiques ont notamment été obtenus avec succès en copolymérisant le D-lactide avec l' $\epsilon$ -caprolactone.

## **1. INTRODUCTION**

Nowadays, environmental concerns represent an important issue for our society. Scientifics are pointing out that the problems of global warming, environmental pollution and decreasing availability of fossil resources as petroleum or gas, that we are recently facing, will dramatically increase in future years. Thus, sustainable development policies are implemented in order to raise public awareness and to attract the civic sense of the people on its everyday actions.

But in fact, for larger scale and long term solutions, these policies are aiming at promoting and implementing more significant and sustainable ecological solutions in particular for the energy and materials domains. These sustainable development orientations have emerged due to the decrease of fossil resources on earth, the high increase of their price and also for a large number of countries, due to a strong dependence on fossil-based raw materials.

In this context, biodegradable polymers, especially those of renewable origins, have been the subject of many studies over the past several years. They are generally derived from agro-resources and can be degraded in nature or in controlled compost. Thus, they represent a viable alternative to replace the conventional non degradable synthetic polymers in short-term applications.

In line with the Green Chemistry concept and principles, polymerizations performed under environmentally friendly reaction conditions and/or using monomers or other ingredients from renewable sources such as enzymatic catalysts, constitute an other important challenge for the synthesis of such biopolymers.

These biodegradable materials, whatever their source, can find applications in several domains such as the packaging but also in more high value added domains as biomedical. However, they often suffer from a certain number of weaknesses (e.g poor mechanical properties, crystallinity issues) limiting their usage and development for large scale industrial applications. To overcome the deficiencies of these biodegradable polymers two main strategies, namely the chemical modification



or their physical association with other components, can be considered. The elaboration of nano-biocomposites perfectly illustrates the second approach since it consists in designing hybrid materials composed of a biodegradable matrix in which nanofillers are finely dispersed to improve and/or to confer novel properties to the final material.

Thus, this study aims at developing original catalytic systems based on lipases immobilized on clays which are efficient for the synthesis of biopolyesters and allowing the preparation of organic/inorganic nanohybrids based on clay nanoparticles (sepiolite and montmorillonite) grafted with such polyesters.

This thesis was conducted under a cotutelle program between the University of Strasbourg (under supervision of Prof. Luc Avérous) and Istanbul Technical University (under supervision of Prof. Yüksel Güvenilir).

The subject of this thesis stands at the interface of the research thematic and expertise developed by the two laboratories. The BioTeam group at the Laboratoire d'Ingénierie des Polymères pour les Hautes Technologies (LIPHT-University of Strasbourg) is specialized in polymer and biopolymer synthesis as well as the elaboration and characterization of nano-biocomposites while the Biotechnology group of the Chemical Engineering Department at Istanbul Technical University (ITU) has expertise on enzymology and enzymatic catalysis.

The objective of this work perfectly fits to the research strategy of BioTeam-LIPHT which is to conduct research projects starting from biomass valorization up to the development of the final products via biotechnology and enzymatic catalysis, chemical synthesis, polymer processing and characterization of the material properties. In this context, the enzyme-catalyzed elaboration of nano-biocomposites (materials based on biodegradable polyesters and biobased fillers) is in perfect line with the research projects carried out so far within the LIPHT.

This work aiming at developing and testing enzymatic catalytic systems for biodegradable polyester synthesis differs from other studies by its context, combining a novative approach of enzyme immobilization on clays and the originality of using the resulting catalysts for polyester synthesis and nano-biocomposite elaboration.

In the first part of this thesis, a bibliographic review on biodegradable polyesters and more particularly on polycaprolactone (PCL) and polylactic acid (PLA) will be presented. Their synthesis by organo-metallic and metal-free organic catalysts will be fully described with details on the corresponding mechanisms and reaction conditions. Then, the more recently developed enzymatic catalysis and its advantages over traditional chemical catalysis routes will be stated and explained. Regarding the aforementioned biopolyesters, their synthesis by lipase-catalyzed ring opening polymerization will be discussed in details, presenting the reaction mechanisms proposed by several research groups and the various parameters affecting the polymerization kinetics and molecular weights of the final products. In addition, recent studies on lipase-catalyzed copolymerization for P(CL-co-LA) synthesis will be reported.

The benefits of immobilizing lipases and the most common preferred lipases used for the synthesis of polyesters and polycarbonates will be presented. The promising usage of inorganic clays as lipase supports in immobilization procedures and their more common and effective usage as nanofillers within polymer matrices for the elaboration of organic/inorganic nanohybrids will be described. Elaboration routes for PCL and PLA/clay nano-biocomposites and resulting improvements in final product properties will be highlighted.

In the second part of the manuscript, experiments performed to attain the objectives of the thesis will be described and the obtained results will be detailed and discussed. First, reference reactions of  $\epsilon$ -CL polymerization carried out by using a commercial immobilized lipase will be presented. Then, the development of original catalytic systems based on lipases immobilized on clays will be shown. Two different types of nanoclays and their respective surface modification will be investigated for lipase immobilization. The catalytic activities of these lipase/clays based catalytic systems and their performances for the polymerization reactions will be discussed. Finally, the enzymatically catalyzed elaboration of organic/inorganic nanohybrids will be considered. The characterization of these biopolyester/clay nano-biocomposites will be presented and the grafting of the polyesters chains at the surface of the clay nanoparticles will be evidenced.



## **2. LITERATURE REVIEW**

### **2.1 Short Introduction on Biodegradable Polymers**

In the last decades a rapid growth on the production and consumption of plastics was observed. The worldwide production was 250 millions of tons in 2010. These plastics are used for a large range of applications. The first application is now the packaging (35-40%), mainly for the food industry and often for short term uses. Most of these plastics are used in packaging industries and food packaging. These materials are mostly fabricated from permanent polymers such as polyolefins (polypropylene, polyethylene), polystyrene, poly(vinyl chloride), etc. mainly derived from fossil resources. In the world, these plastics once consumed, are often expelled into the environment and remain as undegradable wastes.

To protect the environment from the wastes, storage at landfill sites is proposed, which in turn has a limited application due to unsufficient places and environmental concerns. Incineration (heat production) and recycling appear as other approaches. The first one, producing an important mass of carbon dioxide and sometimes toxic gases such as dioxins, may cause global warming and pollution. The second one seems to be a more benign solution but even in this option there are disadvantages; removal of plastic wastes, separation, washing, drying, grinding, reprocessing to final product steps demand extensive labor and energy. In light of foregoing informations, biodegradable polymers with controlled properties, excluding toxic compounds during their manufacture or end of life are considered as green polymeric materials and constitute a wide and promising research area for the future of the world (Gross and Kalra, 2002; Sinha Ray and Bousmina, 2005; Avérous and Pollet, 2012a).

Today, there are a certain number of standards (norms) such as the ASTM D-5488-94d or the harmonised European norm EN 13432 which define the terms as biodegradable, compostable, etc., which are widely used and sometimes in a wrong way as a selling promotion of materials said "environmental" (Url-1).

The NF EN 13432 :2000 standard defines the characteristics required for a packaging material to be claimed as compostable and biodegradable. NF EN 13432 standard was accepted by the decision of the European Commission (2001/524/EC) and was published on the Official Journal of the European Communities. It constitutes a reference in Europe in this domain. It defines the compostability and biodegradability as (depending on the aerobic or anaerobic media): under the action of microorganisms in the presence of the oxygen, the decomposition of an organic chemical compound into carbon dioxide, water and mineral salts (mineralization) with the formation of a new biomass ; in the absence of the oxygen, decomposition into carbon dioxide, methane, mineral salts and production of a new biomass (Url-1,2).

It is worth noting that the packaging materials and constituents from natural origin which were not chemically modified, such as lignocellulosic materials, starch, etc. are recognized as biodegradable without being subjected to the tests foreseen by the norm. However, they have to be chemically characterized (identification of their constituents, determination of the heavy metals, organic carbon, dry solid and volatile solid contents...) and to be in accordance with desintegration and compost quality criteria, more particularly in terms of ecotoxicity of the residues.

There are other standards for biodegradable materials, some of them being equivalent like EN 14046 :2003 and ISO 14855 :1999, which deal with the determination of biodegradability in compost. A series of standards allows to define the test conditions for biodegradability depending on the media used : EN ISO 14851 :2004 (aqueous, aerobic system, measuring of consumed oxygen), 14852 :2004 (aqueous, aerobic system, measuring of released CO<sub>2</sub>), 14853 :2004 (aqueous, anaerobic), 17556 :2004 (soil) and 14855 :2005 (compost).

In order to qualify a packaging material as biodegradable, the EN 13432 :2000 standard requires that, for a test performed in a defined medium (soft water, salt water, soil) over a maximum 6 months period, (i) at least 90% of the initial mass of the material must be degraded, (ii) the residues must represent less than 10% of the initial mass of the tested material, (iii) the result of the biodegradation must not present any ecotoxic effects on the medium.

In order to qualify a packaging material as compostable, the EN 13432 :2000 standard defines that the tests must be performed in an industrial composting facility over a maximum 12 weeks period. The required results are: (i) the residues must represent less than 10% of the initial mass of the tested material, (ii) the size of the residues must be smaller than 2 mm (desintegration), (iii) the lack of negative effects (ecotoxicity) must be observed on the composting process. In all the cases, the tests include the comparison with a blank (Url-1,2).

Unfortunately, the test conditions (humidity, temperature cycle, etc.) are not the same depending on the standards used (ASTM, EN). So it is difficult to compare the results obtained according to various standards. However, some general rules allow to predict the evolution of the biodegradability. An increase in some parameter values such as hydrophobic character, molecular weights, crystallinity or size of spherulites can alter the biodegradability. On the contrary, for example, the presence of polysaccharides (in the case of mixtures) enhance the biodegradation.

It should be noted that the biodegradability or the composting is one of the possible end of life scenario for these materials. This does not mean that these materials can not be recycled (material valorisation).

Biodegradable polymers can be classified into four groups according to their synthesis pathways; (i) polymers derived from biomass, for ex. agro-resourced polymers as starch and cellulose, (ii) polymers produced by microbial organisms as polyhydroxyalkanoates, (iii) polymers produced from bio-derived monomers by conventional chemical synthesis as poly(lactic acid) (PLA), (iv) polymers produced by conventional chemical synthesis from synthetic monomers derived from fossil resources, e.g., poly(caprolactone) (PCL) (Bordes et al., 2009).

During the past decades, there were strong researches and developments on biodegradable polyesters and particularly on polycaprolactone and polylactide.

## **2.2 Biodegradable Polyesters**

### **2.2.1 Petroleum-based polyester: polycaprolactone**

Polycaprolactone (PCL) is an aliphatic polyester which is formed of hexanoate repeating units (Labet and Thielemans, 2009). It is a semicrystalline polymer and can reach a crystallinity degree of 69%. It can be synthesized by the condensation of 6-

hydroxycaproic acid and the ring opening polymerization (ROP) of  $\epsilon$ -caprolactone ( $\epsilon$ -CL) (Figure 2.1). There are only few studies describing the preparation of PCL by polycondensation, on the other hand ROP is the preferred route and studied extensively. By this method, high molecular weight polymers with lower polydispersity indexes can be obtained. Metal alkoxides are generally used as catalysts for the production of PCL starting from  $\epsilon$ -CL.

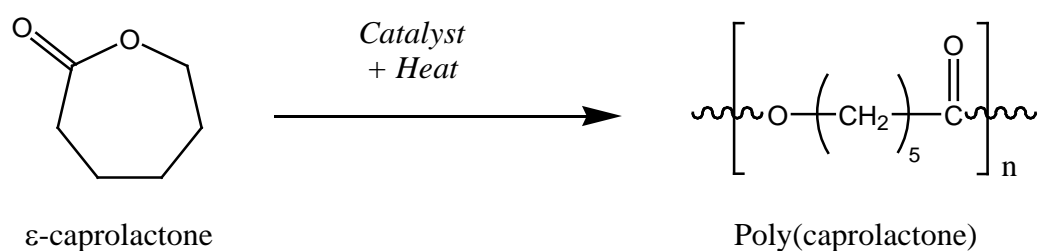


**Figure 2.1 :** Polymerization reaction of PCL from  $\epsilon$ -CL.

PCL can be used in several areas for example as PVC solid plasticizer, as polyol in polyurethane syntheses, for biomedical applications such as controlled release of drugs or as scaffold material in tissue engineering and in environmental applications for soft compostable packaging. At room temperature, PCL is in rubbery state and at body temperature it is permeable to low molecular compounds so it represents a good candidate for controlled drug release applications. PCL due to its controlled degradability, miscibility with other polymers, biocompatibility and potential to be produced from monomers derived from renewable sources finds wide usage in different application fields (Av  rous et al., 2000).

Recently, main commercial producers of PCL in the world are Perstorp, Union Carbide (subsidiary of Dow Chemical) and Daicel companies (Bordes et al., 2009). PCL has a very low glass transition ( $T_g$ ) value ( $-61\text{ }^\circ\text{C}$ ) and low melting point ( $T_m$ ) ( $65\text{ }^\circ\text{C}$ ). These values may represent a disadvantage for some applications, that is why PCL is generally blended or modified by copolymerization or crosslinking (Bastioli, 1998; Bastioli et al., 1995; Av  rous et al., 2000; Koenig and Huang, 1994).

PCL can be biodegraded within a few months to several years depending on its molecular weight, its degree of crystallinity and the conditions of degradation (Labet and Thielemans, 2009). It can be degraded hydrolytically as well as enzymatically. Abiotic degradation has been studied in phosphate buffer whereas biotic degradation has been performed in soil, lake and sea water, sewage, sludge, in compost and in

vivo. It has also been shown that PCL is easily hydrolyzed and biodegraded by fungi (Tokiwa and Suzuki, 1977).

Rutkowska and co-workers have reported a complete fragmentation of PCL samples in sea water (Baltic sea) at temperatures between 9 and 21 °C within 8 weeks (Rutkowska et al., 1989). Temperature was stated to be the major influence factor for the degradation. It has been assumed that for PCL, chemical hydrolysis and enzymatic surface erosion are responsible in parallel for the degradation of the polymer. Tsuji and Suzuyoshi (2002) have reported that PCL films of 50 mm thickness showed an erosion at a rate of 0.2 µm/week in a laboratory test with sea water at 25 °C. Honda and Osawa (2002) have shown the remarkable degradation of the PCL plates (erosion rates approximately 10-15 µm/week) using a simulation test with a synthetic waste water inoculated with mud from a lake (at 25 °C).

As far as the biodegradation trend in soil is concerned, numerous studies have been conducted on polycaprolactone. PCL shows various degrees of mineralization which, on one hand, suggest a substantial biodegradability in soil and, on the other hand, indicate a rather high variability. For instance, a PCL mass loss of 95% in 1 year has been reported (Potts et al., 1973) while other studies reported a mass loss after two years of only 32% (Sawada, 1994) or as high as 98%. For more detailed information, readers can refer to the corresponding book chapter by Degli Innocenti (2005).

PCL is a synthetic polyester, but its structure resembles the cutin which is a natural polyester originated from plants. Thus, it is likely that many organisms that exist would be able to degrade PCL. For example, Mochizuki and co-workers (1995) reported the enzymatic hydrolysis of PCL fibers by lipase (Enzyme Commission Numbers: EC 3.1.1.3). Vert (2000) has put PCL films in a mineral medium containing a mixed culture of organisms and has observed groove or crack formation at the end of degradation period. Thus, PCL can be degraded by enzymes in natural environment, but it is degraded non-enzymatically in the body (Ikada and Tsuji, 2000).

During the biodegradation process, the amorphous phase of PCL is firstly degraded, this causes the augmentation of crystallinity degree, but the molecular weight does not change significantly. In the second stage, cleavage of ester bonds occurs and this results in the weight loss of the polymer. At high temperatures, polymer degrades by



chain-end scission whereas at low temperatures random chain scission is observed (Labet and Thielemans, 2009). The degradation of PCL can be autocatalyzed by carboxylic acids liberated during hydrolysis but also by enzymes providing a faster decomposition of the product. Carboxylic acids produced during hydrolysis enter the citric acid cycle and are totally consumed.

### 2.2.2 Bio-based polyester: poly(lactic acid)

Poly(lactide) (poly (lactic acid)) (PLA) is a biodegradable and bio-based material synthesized from lactic acid, by direct condensation of lactic acid (LA) or via ROP of lactide (Figure 2.2). It has been reported that the most effective route for the polylactide preparation is ROP by anionic, cationic and coordination initiators (Löfgren et al., 1995). For a chemical approach lactic acid is an interesting monomer due to its chiral structure and two stereoisomers, L(+)-LA and D(-)-LA. Additionally, LA molecule has both carboxylic and hydroxyl functional groups that can undergo inter- and intramolecular esterification reactions in polymerization processes (Södergard and Inkinen, 2011).

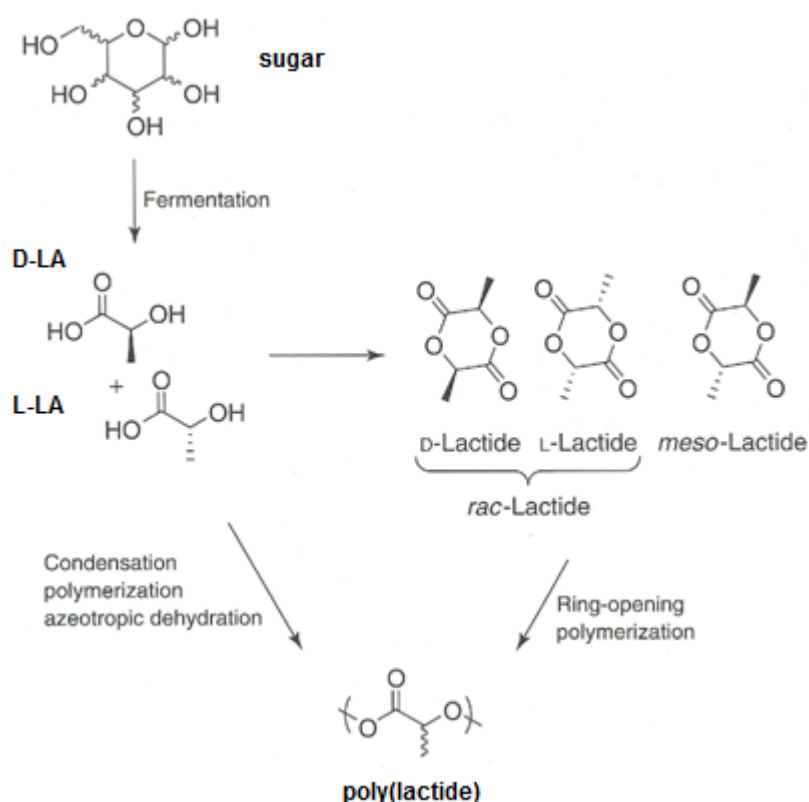


**Figure 2.2 :** Synthesis of PLA by direct condensation polymerization or by ROP of lactide (Becker and Dove, 2011).

Due to its relatively moderate price (2€/kg) and large availability on the market, today PLA is the biopolymer showing the greatest potential compared to other biodegradable polyesters. Estimated global production of PLA in 2010 is of 113 ktons according to European Bioplastics association (Url-3). Cargill-NatureWorks company, the leader on the market, has developed some processes that use corn and other raw materials to produce various grades of PLA. Other companies as Mitsui Chemicals (Japan), Mitsubishi (Japan), Shimadzu (Japan), Futerro (Total / Galactec - Belgium), Purac (Netherlands), Teijin (Japan) and Zhejiang Hisun Biomaterials (China) produce different PLAs with a broad range of L/D isomer ratios (Avérous and Pollet, 2012a).

PLA characteristics can vary depending on the type of isomers used for its synthesis. Poly(L-LA) and Poly(D-LA) are semicrystalline and stiff materials. Typical  $T_g$  values of these PLAs vary between 50-80 °C whereas PLAs synthesized from D/L-lactide or from a racemic mixture of D-and L-lactide are amorphous and show  $T_g$  values of 55-60 °C.  $T_g$  of PLA can be influenced by the molecular weight and architecture, tacticity, crystallinity and presence of plasticizers. Oligomers or low molecular weight polymers can show lower  $T_g$  values (Södergard and Inkinen, 2011). By copolymerization, incorporation of stiff monomers or by cross-linking, higher  $T_g$  values can be obtained. Poly(lactic acid) can be in both amorphous and semi-crystalline states depending on its stereochemistry, composition and thermal history. The melting point of semi-crystalline PLLA is around 180 °C but by the introduction of D-lactide units content higher than ca. 7%, the resulting PDLLA is amorphous and does not show any melting point (Avérous, 2008).

It has been also observed that an equivalent mixture (50/50) of PLLA and PDLA forms a stereo-complex displaying mechanical properties superior to those of pure PLLA or PDLA and a higher  $T_m$  equal to 230 °C.

Today, PLA provides a potential solution to replace petroleum-based and non-biodegradable polymers in several applications. Original applications of PLA were firstly seen in biomedical field as degradable sutures and fracture fixation pins. After the developments in fermentation processes from corn starch to produce lactic acid, PLA has found a wider application area due to decreased production costs. It is used as packaging materials for food and beverages, plastic bags, thin film coatings and rigid thermoforms (Becker and Dove, 2011).

Lactic acid can be yielded from renewable sources such as corn, sugar beets and other carbohydrate containing feedstocks by bacterial fermentation. As it can be seen on the Figure 2.3, starting with the fermentation of renewable sources and following with chemical reactions, polymeric products can be yielded which, after being used, will in turn break down back into carbon dioxide and water. These components will then help the growth of new crops and consequently the possible formation of a new generation of PLA products.

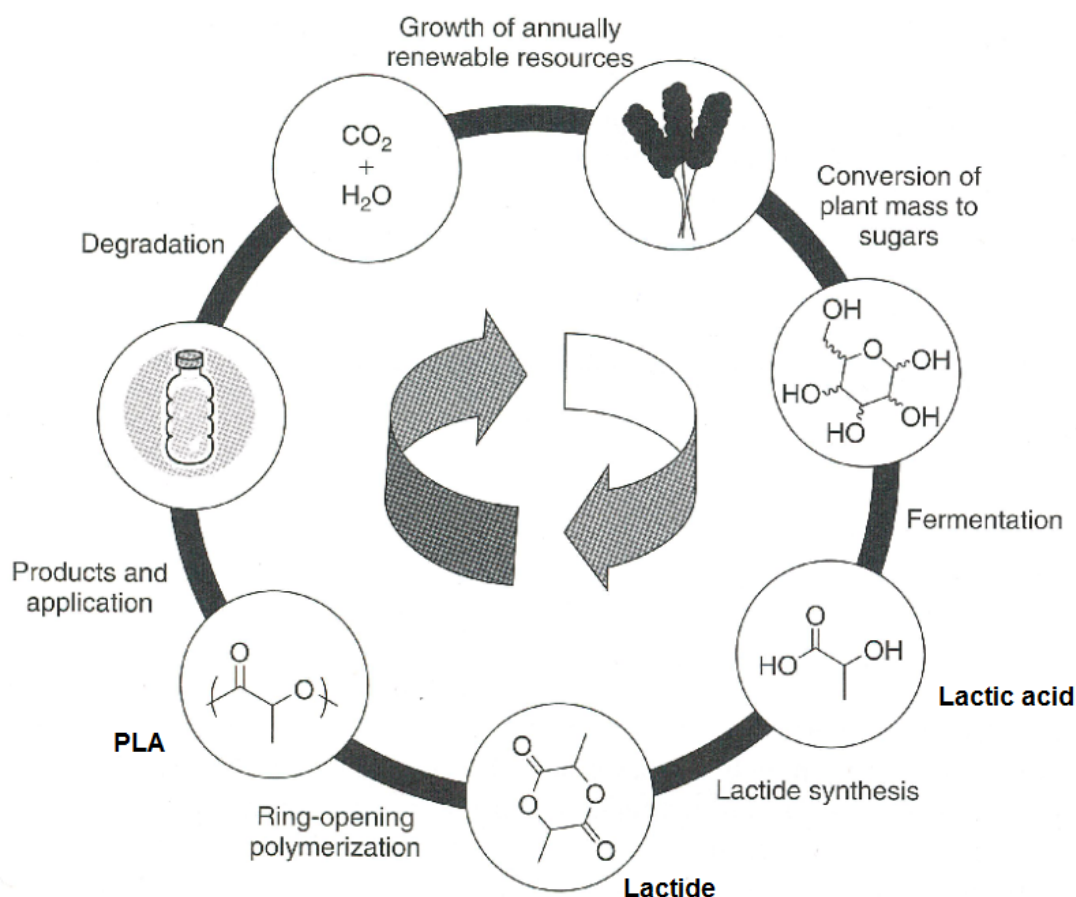


**Figure 2.3 :** The lifecycle of poly(lactide) (Becker and Dove, 2011).

PLAs are readily degradable both in the body and in bulk. Enzymatic degradation of PLA has been a subject of interest and so far, proteinase K (EC 3.4.21.64) was reported to be the only enzyme that could degrade amorphous regions of low molecular weight PLA (Reeve et al., 1994). Even though most microorganisms which have been studied thus far can utilize lactic acid and its dimer, microbial degradation of oligomers and polymers of PLA have not yet been observed at appreciable rates. Hence, compost, field and environmental degradations of PLA are primarily due to hydrolysis (Ho et al., 1999).

The rate of hydrolysis varies with many factors as physical/material characteristics i.e, molecular weight, polymer microstructure, particle size and shape and also environmental conditions i.e, temperature, pH, humidity, etc. (Becker and Dove, 2011). For instance, under dry conditions pure PLA can last more than 10 years (Huang, 2005) and the hydrolysis of PLA with smaller surface/volume ratios is much more slower and complicated. On this basis, less crystalline materials having lower molecular weight and being non-stereoregular are expected to degrade more rapidly and also harsher conditions can increase the degradation rate.

The hydrolytic degradation of PLA occurs in three steps: it starts with a random chain scission causing a decrease in the molecular weight. Then mass loss and formation of oligomers and monomers are observed. During hydrolysis, an increase in crystallinity is usually observed which can be attributed to the increase of mobility of oligomers formed which can crystallise themselves or induce the crystallization of larger PLA chains. In the final stage, resulting oligomers continue to be hydrolyzed. Lactic acid which is formed during hydrolytic degradation, is metabolized via tricarboxylic acid cycle and eliminated afterwards in the respiratory system as carbon dioxide (Albertsson and Varma, 2003).

In the degradation studies of PLA, in a biotic medium, acetic acid, propanoic acid and ethyl ester of lactoyllactic acid formation was determined while in a sterile mineral medium only lactic acid, lactide and lactoyllactic acid were formed. The PLA films in the biotic medium were transformed in fragments but they kept their original form in the abiotic medium (Hakkarainen et al., 2000)

PLLA is more slowly degraded in vitro when compared to PDLLA because of its crystalline nature. Two years is needed for its complete degradation. It is totally resorbable and cause no or very mild adverse reactions in tissues (Albertsson and Varma, 2003).

In conventional chemical polymerizations, from lactic acid or lactide, some restrictions exist such as the usage of extremely pure monomers and anhydrous conditions. Also the complete removal of metallic catalysts is needed when medical applications are concerned. These restrictions are some of the reasons why researchers then decided to investigate enzymatic polymerization route to avoid these disadvantages.

## 2.3 Ring Opening Polymerization (ROP) of Lactones and Lactides by “Chemical Catalysis”

Ring opening polymerization of cyclic esters can proceed via different mechanisms depending on the catalyst type and can be classified as anionic, coordination-insertion, cationic, organocatalytic and enzymatic polymerization. The latter will be discussed more in details in section 2.4 whereas all other mechanisms classified as “chemical-catalysis” are described hereafter.

### 2.3.1 ROP of lactones and lactides by organo-metallic compounds

#### 2.3.1.1 Anionic ROP

ROPs where nucleophilic reagents act as initiators are classified as anionic ROP. These nucleophilic reagents usually consist of organometals (alkyl lithium, alkyl magnesium bromide, alkyl aluminum, etc.), metal amides, alkoxides, phosphines, amines, alcohols and water (Endo, 2009).

First, the carbon of the carbonyl group or the alkyl-oxygen is nucleophilically attacked by a negatively charged initiator and this results in the formation of a linear polyester with carboxylate end alkoxide end groups (Figure 2.4) (Albertsson and Varma, 2003).

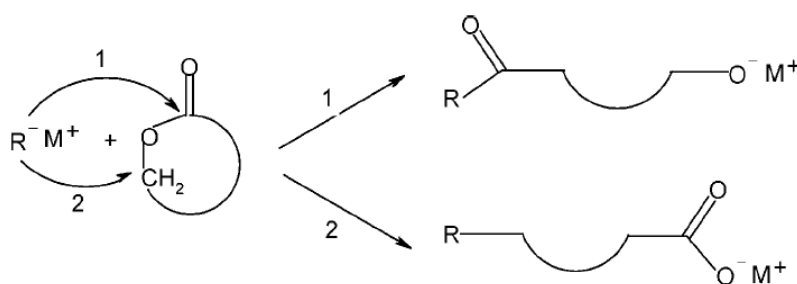


**Figure 2.4 :** Initiation of ring opening polymerization of lactones by anionic initiators (Albertsson and Varma, 2003).

In this type of ROP, important intramolecular transesterification reactions can occur in the later steps of polymerization because of the tendency of alkoxides to react not only with the ester function of the cyclic monomer but also with ester functions present along the polyester chains. This results in the formation of shorter polymer chains and also cyclic oligomers (Lecomte and Jérôme, 2012). For example in the case of  $\epsilon$ -CL polymerization by potassium tert-butoxide an important amount of cyclic oligomers has been formed, besides by the usage of lithium tert-butoxide in an

apolar solvent, this oligomer generation has been decreased (Albertsson and Varma, 2003).

### 2.3.1.2 Coordination-insertion ROP

This type of polymerization is most commonly used for the production of aliphatic polyesters. To better control the polymerization, organometallic derivatives of metals with d-orbitals of favorable energy have been chosen to replace anionic initiators. These compounds are less reactive and more selective so the control of molecular parameters can be improved by decreasing the rate of propagation (Lecomte and Jérôme, 2012). These initiators, the main ones being aluminum and tin alkoxides or carboxylates, can produce stereoregular polymers with narrow polydispersities (PDIs), controlled molar masses and well-defined end groups (Albertsson and Varma, 2003).

A general mechanism for the coordination-insertion ROP is presented in Figure 2.5 together with other types of mechanisms for the ROP. For all these types of polymerizations, there have been various mechanisms proposed by several research groups which have been subsequently changed and developed over time. For more details on these mechanisms, readers can refer to several recent and complete reviews (Endo, 2009; Labet and Thielemans, 2009; Lecomte and Jérôme, 2012).

ROPs of lactones in presence of organometallic initiators at high temperatures or long reaction times can cause inter/intramolecular transesterification reactions leading to the broadening of the polydispersities (Albertsson and Varma, 2003).

*Tin(II) bis-(2-ethylhexanoate)* referred as tin octoate [ $\text{Sn}(\text{Oct})_2$ ] is the most widely used catalyst for ROP of lactones. It is versatile and soluble in common organic solvents. Its usage in the polymer coatings in contact with food is approved by Food and Drug Administration (FDA).

For the ROP of lactones by  $\text{Sn}(\text{Oct})_2$  several mechanisms have been proposed but in 1998, Kowalski and coworkers proposed a different mechanism. They suggested that when  $\text{Sn}(\text{Oct})_2$  is mixed with an alcohol added intentionally into the reaction medium or with a protic impurity present in the medium, it is converted to tin alkoxide due to the liberation of acid from catalyst structure. And this tin alkoxide is the real initiator of the polymerization (Figure 2.6). This assumption has been

supported in further studies where the addition of butanol increased ROP rate and the presence of alkoxides were reported (Kowalski et al., 2000a-b).

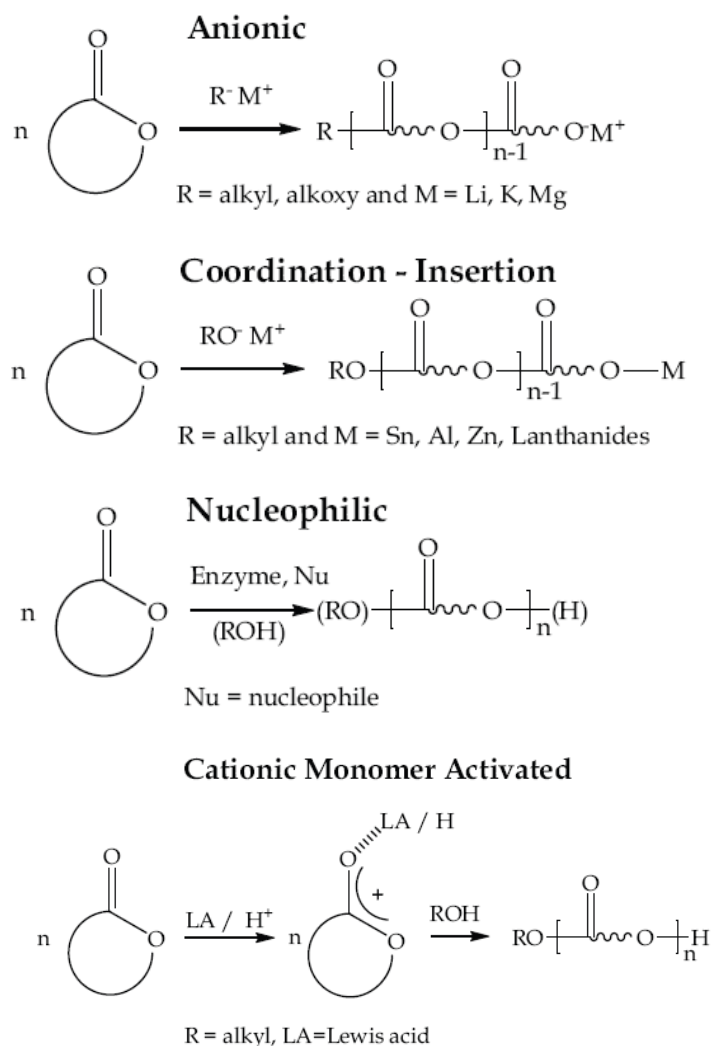


**Figure 2.5 :** Ring-opening polymerization mechanisms (Zinck, 2011).

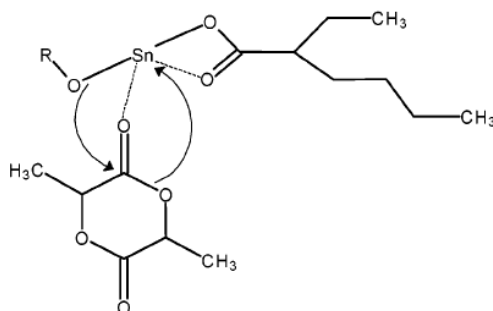


**Figure 2.6 :** Tin alkoxide complex initiated polymerization of lactones (Albertsson and Varma, 2003).

In the study of Kricheldorf et al. (2000), it has been reported that by the heating of  $\text{Sn}(\text{Oct})_2$  to temperatures above 100 °C, octanoic acid is formed in the reaction medium. This acid may cause the esterification of alcohol and form water which can in turn react with  $\text{Sn}(\text{Oct})_2$  and produce stannoxanes and tin hydroxides. By the presence of water and other hydroxyl compounds, molar masses of products would diminish and side reactions would take place.

The ROP of lactides by  $\text{Sn}(\text{Oct})_2$  proceeds quite slowly. By the addition of triphenyl phosphine, this rate could be increased and intramolecular side reactions could be restrained (Degee et al., 1999).

Among tin alkoxides, tin (II) butoxide [ $\text{Sn}(\text{OBu})_2$ ] is highly effective and can reach reaction rates similar to those catalyzed by rare earth metal alkoxides (Kowalski et al., 2000b). Tin alkoxides provide better control of the polymerization when compared with  $\text{Sn}(\text{Oct})_2$ . At relatively low temperature (80 °C), 100% of  $\epsilon$ -CL conversion was reached in bulk with 2,2-dibutyl-2-stanna-1,3-dioxepane initiator (Kricheldorf and Eggerstedt, 1998).

Cyclic tin initiators, which have been rarely studied, show more hydrolytic stability compared to aluminum derivatives and can be easily handled and used in polymerizations.

Aluminum alkoxides have also been widely explored for ROPs of lactones and lactides. Teyssié and co-workers have first reported in 1994, the favorable usage of these initiators (aluminum trialkoxides and aluminum alkyl dialkoxides) for ROP (Löfgren et al., 1994). It has been observed that the polymerization of lactones initiated by aluminum alkoxide proceeds according to a coordination-insertion mechanism where aluminum isopropoxide first coordinates to the exocyclic carbonyl oxygen and then the cleavage of acyl-oxygen bond forms an isopropyl ester end group. The living character of this polymerization has been confirmed by a narrow molecular mass distribution and an increase in  $\text{DP}_n$  with an increase in monomer/initiator ratio. In the propagation step, very high conversion percentage has been reached indicating almost complete absence of transesterification reactions.

It has been reported that most of the metal alkoxides form aggregates in solution at low temperatures, thus sometimes for the rearrangement of the initiator to form active species for the polymerization, an induction period is needed. The groups



which have been identified to be involved in coordinative aggregation were not available for the propagation step. The type and size of these aggregates were proclaimed to depend on the solvent polarity, the nature of the substituents and the presence of coordinative ligands such as amines and alcohols (Duda and Penczek, 1994; Duda, 1996). Dubois et al. (1991) have reported that these agglomerates are solvated in polar and nucleophilic solvents and in this way the reaction can be fully controlled.

Freshly distilled aluminum isopropoxide consisting mainly of trimers is cited to be more reactive initiator for ROP since three chains can grow per aluminum atom. In the kinetic studies conducted by several research groups on ROP of lactones and lactides using aluminum alkoxide as an initiator, first order kinetics with respect to monomer and initiator was observed (Löfgren et al., 1994; Duda and Penczek, 1994).

Lanthanide alkoxides such as yttrium isopropoxide and yttrium 3-oxapentoxide can be cited as "new" initiators for ROP of  $\epsilon$ -CL and lactides. Their performance on yield, molecular weight, polydispersity and regularity of the final product depend on the ligands and the oxidation state of respective rare earth metals. Especially in lactide polymerizations these catalysts (yttrium, lanthanum, samarium, lutetium complexes) show higher activities than aluminum alkoxides; under mild conditions higher molecular weight polyesters can be obtained (Stevens et al., 1997). Rapid polymerization of  $\epsilon$ -CL by yttrium alkoxide has been observed at room temperature (Shen et al., 1995).

Miola-Delaite and coworkers (1999; 2000) have studied the kinetics of the polymerization of  $\epsilon$ -CL initiated by rare earths such as Y, Sm, Nd in the presence of excess alcohol and compared the efficiency of these rare earths to aluminum and zirconium alkoxides. The polymerization was described according to a living process where a fast transfer reaction takes place, providing the control of the molecular weight by the monomer/alcohol ratio. It has been reported that rare earth alkoxides resulted in higher activities; functionalized oligomers were obtained within less than 5 min with yttrium or samarium isopropoxide initiators and benzyl alcohol in excess even if some transesterification reactions were observed when polymer chains remained in contact with the active centers.

### 2.3.1.3 Cationic ROP

In cationic ROPs, initiators having electrophilic nature as Brønsten acid, Lewis acid and alkyl esters of strong organic acids are used (Endo, 2009). General mechanism for cationic ROP is shown in Figure 2.5.

This type of polymerization is not preferred because of the bare control of molecular parameters. A first example of controlled cationic ROP of  $\epsilon$ -CL and  $\delta$ -VL (valerolactone) by an alcohol initiator and HCl.Et<sub>2</sub>O catalyst was reported by Shibasaki et al. (2000). A PCL having a molar mass of 15000 g/mol was obtained, PVL had a higher molar mass of 50000 g/mol. Controlled cationic ROPs mechanism was described by Penczek (2000). It has been suggested that the acid activates the cyclic ester monomer and the alcohol acts as the initiator of the polymerization.

Basko and Kubisa (2006) have shown that when trifluoromethanesulfonic was used as catalyst, cationic ROP was controlled and  $M_n$  values of 20000 for PCL could be reached. Then Bourissou and coworkers showed that trifluoromethanesulfonic acid could be replaced by the less acidic methanesulfonic acid (Gazeau-Bureau et al., 2008).

Recently, Takasu et al. investigated perfluoroalkanesulfonates and perfluoroalkanesulfonimides to perform fast ROP. Nonafluorobutanesulfonimide was reported to be the fastest catalyst for ROP of  $\epsilon$ -CL (Oshimura et al., 2011).

Besides, organic compounds as lactic acid, citric acid, fumaric acid and amino acids were found to be effective for ROP of lactones in presence of alcohol and amine initiators (Lecomte and Jérôme, 2012).

### 2.3.1.4 Organo-metallic catalyst concerns

Today, the preferred route for polyester synthesis by ROP is the use of organo-metallic catalysts such as tin or aluminum alkoxides. The major restraint of the coordination ROP of lactones is the toxicity of these metals. Aluminum derivatives are assumed to be involved in Alzheimer's disease and Sn(Oct)<sub>2</sub> is known to be cytotoxic. So this could limit the usage of polyesters synthesized by these catalysts in biomedical applications. In the report published by Schwach et al. (1996), a residue of 306 ppm of Sn in PLA catalyzed by Sn(II)-ethyl hexanoate was determined even after the application of a purification step. It has been demonstrated that it is not possible to entirely remove tin compounds from polyesters.

For this, many researches have made efforts to replace tin and aluminum alkoxides by initiators with less toxic metals that take part in the metabolic processes as magnesium, calcium, ferrum alkoxides (Lecomte and Jérôme, 2012). Zinc based catalysts are regarded as less toxic so zinc metal and salts as zinc octoate, zinc stearate, zinc salicylate, zinc lactate are used in pharmaceutical and biomedical applications. Regarding the polymerization kinetics, it can be said that polymerizations mediated by these catalysts proceed slower compared to  $\text{Sn}(\text{Oct})_2$  mediated polymerizations and lower molar masses for final polymers are obtained but the residual level of Zn in the polylactide is in the range of 20-40 ppm while the tin level remains between 300-400 ppm.

As an alternative issue, the initiators were immobilized onto insoluble supports by different research groups; yttrium isopropoxide on a porous silica (Martin et al, 2003a-b) and Al, Zr, Y, Sm, Nd alkoxides onto silica and alumina (Miola-Delaite et al., 1999 and 2000).

More recently, promising alternative routes based on non-metallic catalysts for the polyester synthesis have emerged. The usage of organocatalysts as tertiary amines (pyridines), phosphines, N-heterocyclic carbenes, amidines, guanidines, phosphazenes, etc. and enzymes especially lipases has been developed opening a more green way for the future.

### **2.3.2 ROP of lactones and lactides by “metal-free” organic catalysts**

Synthesis of polymers by metal-free strategies shows advantages over processes catalyzed by metal derivatives. One of the major advantage is the lack of high cost separation step of metal impurities which remain in the final polymeric product and which may cause severe problems for targeted applications (Dove, 2009).

#### ***Tertiary amines (pyridines)- Phosphines***

Among the basic metal-free catalysts, tertiary amines and phosphines can be cited. The ROP of lactide by 4-(dimethylamino)pyridine (DMAP) and 4-pyrrolidinopyridine (PPY) has been reported by the research group of Hedrick (Nederberg et al., 2001). They have performed the polymerization of D/L- and L-lactide in dichloromethane at 35 °C and in the melt at 135 and 185 °C. The catalyst was proven to be highly effective. Polymerization kinetics followed living

polymerization trends and PLAs produced had a narrow PDI range. Even in high monomer conversions PDI values did not change. This feature was contrary to the polymerizations promoted by organometallic compounds and thus showed that there aren't any transesterificative side-reactions taking place.

The proposed mechanism of the ROP of lactide by DMAP is based on a monomer-activated mechanism where the lactide monomer is first subjected to the nucleophilic attack of amine. This results in the formation of zwitterionic species which then undergo an attack by the initiating or propagating alcohol chain-end (Figure 2.7).

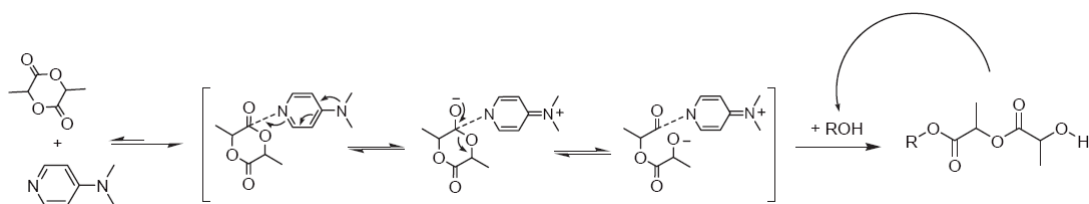


**Figure 2.7 :** Proposed mechanism for the ROP of lactide by DMAP.

DMAP has been also used as catalyst in the ROP of  $\epsilon$ -CL for the synthesis of chitosan-graft-PCL in the presence of water as swelling agent (Feng and Dong, 2006).

Phosphines are generally known as ligands in organometallic chemistry and homogeneous catalysis areas. They are also able to mediate organic transformations, acylation reactions (Kamber et al., 2007).

Nucleophilic phosphines have been also described to be effective catalysts for ROP of lactides by Hedrick and co-workers (Myers et al., 2002). Polymerization conducted in toluene solution required higher temperatures than those with DMAP and in bulk state but polydispersities were broadened due to adverse transesterification. Effective lactide polymerization was performed in bulk by phosphines in the presence of benzyl alcohol initiator generating PLA of narrow PDI.

Phosphine catalyst activity toward lactide polymerization decreased according to the following order:  $P(n\text{-Bu})_3 > P(\text{tert-Bu})_3 > \text{PhPMe}_2 > \text{Ph}_2\text{PMe} > \text{PPh}_3 > \text{P}(\text{MeO})_3$  (unreactive). As expected from the proposed nucleophilic mechanism, the more basic and nucleophilic alkyl-substituted phosphines showed higher activity toward lactide polymerization than phosphines with one or more aryl groups.

### *N-Heterocyclic carbenes*

Recently, the usage of N-heterocyclic carbenes (NHCs) as organic catalysts for transesterification reactions has attracted attention due to their high nucleophilic characteristic (Dove et al., 2006). ROP of lactide,  $\epsilon$ -CL and  $\beta$ -butyrolactone has been performed by 1,3-bis-(2,4,6-trimethylphenyl)imidazol-2-ylidene (IMes). For each monomer the IMes was highly active leading to polymers with predictable molecular weights, based on the monomer-to-initiator ratio, and narrow polydispersities. As an example, lactide was polymerized reaching  $M_n$  values of 25000 g/mol in 10 min. The electronic nature of carbene substituents was proven to affect the polymerization kinetics; catalysts with more electron-withdrawing backbone showed lower reactivities for ROP mechanism (Nyce et al., 2003).

The ROP mechanism of lactide by IMes was proposed by the Hedrick's group to proceed through a monomer-activated mechanism in which the monomer is nucleophilically attacked and forms a complex with carbene (Figure 2.8). This complex is initiated or propagated esterificatively with the initiating alcohol or propagating chain-end (Connor et al., 2002).

By deprotonation of imidazolium, imidazolinium and thiazolium salts, carbene can be produced. These compounds have been described to be efficient precatalysts for the ROP of lactide and other cyclic esters.

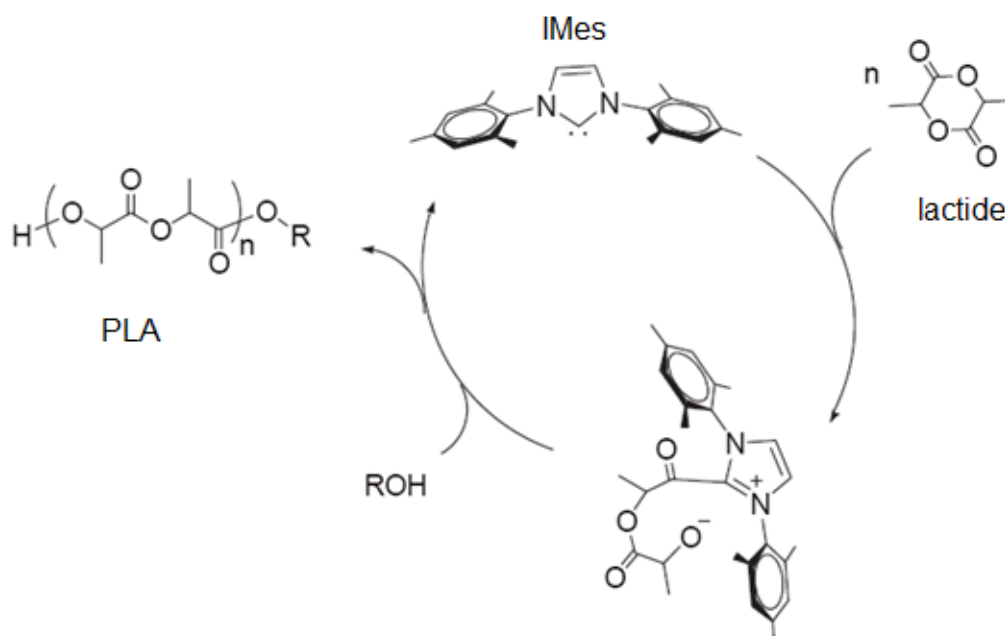


**Figure 2.8 :** Proposed monomer-activated mechanism for the ROP of lactide by IMes (Dove, 2009).

Developing the strategy of one pot routes as the releasing of free carbenes from their silver salts, one-component catalyst/initiator adducts have been discovered (Coulembier et al., 2005; Csihony et al., 2005). These adducts can be obtained by the reaction of free carbene with the corresponding alcohol or by the liberation of imidazolinium salt with the appropriate alkali metal alkoxide. It has been determined that these adducts easily eliminate alcohol at ambient temperature to form free carbene. So they can function as single component catalyst/initiator for the ROP of lactide.

More thermally stable adducts from commercially available 1,3,4-triphenyl-4,5-dihydro-1H-1,2-triazol-5-ylidene have been developed by Dubois-Hedrick-Waymouth (Coulembier et al., 2005). The polymerization of L-lactide was performed in toluene at 90°C and polymers with good control of molecular weight and end-group were produced. However, the ROP proceeded slowly and polymers had a broad range of  $M_n$  values. Due to the formation of a strong adduct at room temperature, reversible termination of ROP could be obtained by just changing the reaction temperature. In addition, transesterification side reactions were prevented at low temperature with this slow system.

### ***Bifunctional thiourea catalysts***

It has been reported that the superiority of NHCs over DMAP for ROP of lactones is due to their increased nucleophilicity and basicity. Normally, in a ROP mechanism there is a nucleophilic species in the form of initiating or propagating alcohol and an electrophilic compound in the form of cyclic monomer. Besides, in a conventional coordination-insertion mechanism, an electrophilic activation of a monomer by Lewis acidic metal cations such as Sn(II) occurs. So by the addition of organic Lewis acids in organocatalysts, improvements in accelerating or controlling the ROP kinetics can be achieved. For this, ureas and thioureas have been studied as alternative organocatalysts for small-molecule transformations (Kamber et al., 2007). Dove et al. (2005) tested a bifunctional thiourea-amine for the ROP of lactide. Polymerization kinetics were slower compared to NHCs, but even at total conversion values, at prolonged reaction times (48-72 h) broadening of PDI was very low proving that linear polymer chains were resistant to any transesterification. So chain extension of PLAs could be achieved by adding more monomer.

### ***Amidines, guanidines and phosphazenes***

They are also called superbases and can be used as cocatalysts for the transesterification of small molecules. Superbasic guanidine 1,4,7-triazabicyclodecene (TBD) was able to polymerize under melt conditions various lactones and products with variable molecular weights and high PDIs were obtained. Amidine 1,8-diazabicycloundec-7-ene (DBU) was used for the ROP of cyclic carbonates and lactone monomers in melt (Parzuchowski et al., 2006).

TBD, DBU and N-methyl TBD (MTBD) showed high activity for the ROP of lactide in non polar solvents reaching a DP of 500 for PLAs in few minutes of polymerization at ambient temperature and with 1 mol% catalyst loadings. Cyclic esters as  $\delta$ -VL and  $\epsilon$ -CL could be polymerized by TBD and BEMP (2-*tert*-butylimino-2-diethylamino-1,3-dimethylperhydro-1,3,2-diazaphosphorine) alone, whereas the polymerization could proceed only in the presence of thiourea cocatalyst when it was catalyzed by DBU and MTBD (Lohmeijer et al., 2006; Zhang et al., 2007). The kinetics with BEMP catalyst, in presence of 1-pyrernebutanol as initiator, were quite low, only 14% of  $\epsilon$ -CL conversion could be reached in 10 days.

For more details and additional results on similar studies, readers can refer to recent reviews (Kamber et al., 2007; Dove, 2009).

### ***Organocatalysts for copolymerizations***

The usage of organocatalysts, avoiding any presence of metallic derivatives, is also very promising for the synthesis of block copolyesters that will be used in biomedical and microelectronics applications. In the work of Hedrick's group, various cyclic esters were homopolymerized and polymerization rates varied depending on the monomer type (*lactide* >>  $\delta$ -VL >  $\epsilon$ -CL) (Pratt et al., 2006). A superbasic organocatalyst was used for the ROP of lactide and CL mixture found in equimolar proportion, at ambient temperature. Lactide monomer was firstly polymerized reaching 95% of conversion. Then preformed PLA chains started to transesterify and during this time ROP of  $\epsilon$ -CL was very low. In an other reaction, first PLA was synthesized and  $\epsilon$ -CL was then added to the reaction medium. Again, PDI values increased and polymerization of  $\epsilon$ -CL was low. It has been concluded that organocatalysts are not appropriate for random copolymerization of polyesters except

for the cases where transesterification of copolymer chains leading to high PDIs are acceptable.

Block copolyesters of LA-VL/CL have been prepared by sequential ROP catalyzed by superbasic organocatalysts. The slow-propagating monomer (CL or VL) was first polymerized and when 70% conversion was reached, the other fast-propagating monomer (lactide or CL) was added and the reaction was stopped by the 95% of conversion of this second monomer. By this way, clean chain extensions were obtained and final block copolymers had narrow PDIs. This point showed that efficient crossover reactions took place. Similar copolymerization trends were observed when TBD alone, DBU and MTBD with thiourea were used as catalysts for the same system (Pratt et al., 2006; Lohmeijer et al., 2006).

## **2.4 Enzyme Catalysis**

### **2.4.1 Introduction**

The use of enzymes by mankind dates back to earliest civilizations. In 19<sup>th</sup> century, their nature and functioning have been elucidated by the developments in biochemistry. The recognition of their structure by new purification techniques and analytic tools in 20<sup>th</sup> century, opened the way for the innovation of processes for industrial production and usage of the enzymes.

Enzymes are considered as the catalytic apparatus of living systems. Their introduction to industry started by microbial proteases used in detergents. So far more than 3000 types of enzymes have been isolated and classified but only a small number of these known enzymes are commercially available. More than 75% of industrial enzymes are hydrolases, while protein-degrading enzymes constitute about 40% of all enzyme sales (Sharma et al., 2001).

Besides, the increasing concern on environmental pollution caused by the production and the disposal of petrochemical- derived plastics has recently opened the way to alternative environmentally benign approaches to synthesize plastics. In this context, enzymes belong to a sustainable approach since they come from natural systems, and when they are degraded, the amino acids which are formed, can be readily recycled back into natural substances. Their wide usage in aqueous or solventless systems has



made them particularly attractive to replace potentially toxic heavy metal catalysts for polymer synthesis.

The distinctive feature of the enzyme catalysis stands on its superior catalytic activity and high selectivity under mild reaction conditions. By this way, enzyme catalysis in polymer synthesis offers several advantages over chemical synthesis routes. Well-defined polymeric structures have been prepared so far by using in vitro enzyme catalysis and some examples of them are: (i) enantio enriched polyesters synthesized by lipase-catalyzed stereoselective ring opening polymerization, (ii) cellulase-catalyzed cellulose synthesis, (iii) horseradish peroxidase (HRP)-catalyzed polymerization of aromatic substrates (e.g., phenols, aniline, and their derivatives).

By the recent advances in non-aqueous enzymology, potential conditions for the polymerization reactions have been significantly expanded. Various organic solvents, biphasic organic solvent-aqueous mixtures, reversed micelle systems, and supercritical fluids can be used as new alternative reaction environments. Besides, these non-traditional reaction media have allowed the control of polymer molecular weight as well as the morphology and architecture of polymer products. Additionally, diversity in reaction environments facilitated the downstreaming processes for the product separation and enzyme reuse.

Furthermore, the products derived from enzyme catalysis, whether polyesters, polyphenols, polysaccharides, proteins, or other polymers, are in most cases biodegradable. Thus, taking into consideration all formentioned advantages of the enzymatic catalysis, it is not surprising that the research activity in this field has flourished (grown) in recent years.

#### **2.4.2 Advantages of enzyme catalyzed polymerization over chemical polymerization for the synthesis of biopolyesters**

The enzymatic polymerization is considered as an environment-friendly synthetic process for polymeric materials. It serves a good example for “green polymer chemistry” which is defined as polymerizations carried out in environmentally friendly reaction conditions or using monomers and catalysts derived from renewable resources (Puskas et al., 2011). As previously described, the organo-metallic catalysts used for the ROP of lactones or lactides are based on derivatives of metals such as Zn, Al, Sn or Ge, which may be very toxic (Albertsson and Varma, 2003).

Thus, it is required to completely remove these metallic residues when biomedical applications of these biopolyesters are in concern, since these toxic impurities may become concentrated within matrix remnants after polymer degradation (Schwach et al., 1996). Besides, it is very well known that traditional catalyst residues can also catalyze the hydrolysis of polyesters and increase their degradation rate. Enzymes are natural catalysts and can be better candidates for the elaboration of such biopolyesters for biomedical applications.

The advantages of enzyme-catalyzed polymerization can be stated as below (Albertsson and Srivastava, 2008):

- Reactions can take place under mild reaction conditions in terms of temperature, pressure and pH by the catalysis of enzymes showing high enantio- and regio-selectivity.
- Enzymes are derived from renewable resources, they are recyclable eco-friendly materials and their separation from the final products is very simple.
- Enzymes can be active in bulk, organic media and at various interfaces.
- Enzyme-catalyzed processes result in polymers with well-defined structures.
- The total exclusion of water and air is not required when lipases are used as catalysts for polyester synthesis which is not the case for traditional organometallic catalysts where there are strict precautions to exclude air and water from the system.
- Organometallic catalysts can easily polymerize small (4–7 member) cyclic lactones which have important ring strain, whereas the polymerization of larger ring lactones (macrolides) is slow and only low molecular weight products are obtained. Enzymes have shown the capability to polymerize macrolides under normal polymerization conditions.

#### **2.4.3 Lipases for polyester and polycarbonate synthesis**

Enzymes are classified into six groups (E.C groups 1 to 6) depending on the specific reactions they catalyze. Three groups among them: oxidoreductases (E.C group 1), transferases (E.C group 2) and hydrolases (E.C group 3) have shown the ability to catalyze or induce polymerization *in vitro*. Lipases (E.C 3.1.1.3), which are members of the hydrolase family, are ubiquitous enzymes and are found in most organisms from microbial, plant and animal kingdom (Schmid and Verger, 1998). Lipases are esterases which can hydrolyze triglycerides (or esters) to glycerol and fatty acids at

water–oil interface. In nature these enzymes take part in the degradation of food and fats by their hydrolytic capability. They also find applications as valuable drugs against digestive disorders and diseases of the pancreas, as detergent additive for removal of fat stains and as catalysts for the manufacture of special chemicals and for organic synthesis (Varma et al., 2005).

All lipases show an exceptional structural and functional similarity even if they are isolated from different organisms or their molecular masses are different. In 1958 Sarda and Desnuelle (1958) defined lipases in kinetic terms and proposed the phenomenon of “interfacial activation”. This fact means that the activity of lipases is low on dissolved monomeric substrates but strongly enhanced when the substrate concentration is above its saturation limit (critical micelle concentration or CMC) and forms a lipophilic phase. This property is totally different from usual esterases which act on water-soluble carboxylic ester molecules, and for a long time lipases were considered as a special category of esterases which are highly efficient at hydrolyzing molecules aggregated in water (Jaeger et al., 1999).

In 1990, two lipase structures were solved by X-ray crystallography for the first time (Winkler et al., 1990; Brady et al., 1990). A unique structural feature that is typical to most lipases was revealed. That is a lid or flap, an amphiphilic peptidic loop that covers the active site of the enzyme in solution and prevents the access of the substrate. It was suggested that interfacial activation might be due to the presence of this lid. When a contact occurs with a lipid/water interface, this lid undergoes a conformational rearrangement which renders the active site accessible to the substrate (Brzozowski et al., 1991). But to the contrary, the lipases from *Pseudomonas glumae* and *Candida antarctica* (type B), whose tertiary structure is known and both having an amphiphilic lid covering the active site do not show any interfacial activation (Uppenberg et al., 1994). After the lid is opened, a large hydrophobic surface is created to which the hydrophobic supersubstrate (oil drop) binds. The active site is composed of a nucleophilic serine (Ser) residue activated by a hydrogen bond in relay with histidine (His) and aspartate (Asp) or glutamate (Ser105–His224–Asp187) as the catalytic triad.

The serine residue is situated at the bottom of a deep and narrow pocket having dimensions of 10×4×12 Å. This region is markedly polar but the inner walls of the pocket are very hydrophobic. The more capacious channel of this pocket receives the

acyl- and the other channel receives the alcohol-moiety of ester substrate (Figure 2.9) (Uppenberg et al., 1995).

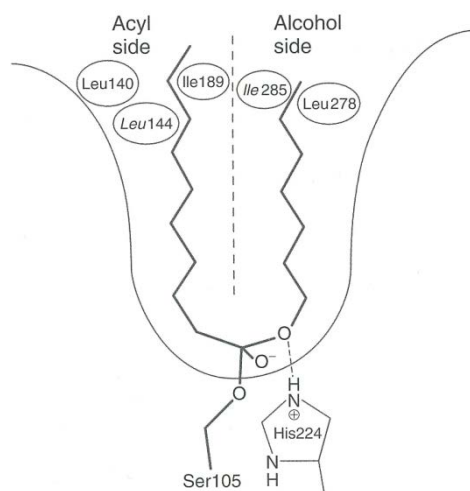


**Figure 2.9 :** The active site pocket of CALB partitioned into two sides: an acyl and an alcohol side (Uppenberg et al., 1995).

*Candida antarctica* lipase B (CALB), is a globular  $\alpha/\beta$  type protein with a molecular weight of 33 kDa and an isoelectric point of 6.0 (Figure 2.10). CALB is not as efficient as other lipases in hydrolyzing triglycerides; but, it is highly stereospecific towards both ester hydrolysis and synthesis. This phenomenon is said to be probably related to a limited space available in its hydrophobic pocket (Uppenberg et al., 1994). It is used in many industrial applications due to its high enantioselectivity, wide range of substrates, thermal stability and stability in organic solvents (Trodler and Pleiss, 2008).



**Figure 2.10 :** 3D-structure of CALB (Uppenberg et al., 1994).

Interestingly, in some cases, the lipase-catalyzed hydrolysis in water can be easily reversed in non-aqueous media into ester synthesis or transesterification (Albertsson and Srivastava, 2008). This specific behavior paved the way for the development of lipase-catalyzed polymerization reactions such as polyester synthesis. Lipases catalyze the ring-opening polymerization (ROP) of lactones (small to large rings), cyclic diesters (lactides) and cyclic carbonates to produce aliphatic polyesters or polycarbonates (Varma et al., 2005).

In spite of the advantages of organic solvents, most of the time the enzymatic catalytic activity is much lower than in aqueous systems. This is explained by diffusional limitations, changes in protein flexibility or destabilization of the protein (Klibanov, 1997). In some studies enzymatic activity in organic solvents has been correlated with solvent polarity whereas in some others the effect of the solvent was independent of its  $\log P$  value (parameter defining its hydrophobicity) (Lee et al., 2004; Degn and Zimmermann, 2001).

It has been revealed that enzymes when transferred from water to organic solvents, retain their native structures. In this phenomenon, enzyme-bound water is essential for the catalytic activity of the enzyme and serves as a lubricant. (Zaks and Klibanov, 1988). Besides, it has been proved that enzymes become inactive when they are totally dried and they show denaturation in organic solvents in the presence of high amounts of water (Griebenow and Klibanov, 1996).

Trodler and Pleiss (2008), aimed to expose the structure and flexibility of CALB in water and five different organic solvents using multiple molecular dynamics simulations. They examined the interactions of solvents with the protein and distribution of water molecules at the protein surface. They concluded that the cause of CALB reduced flexibility in organic solvents is a spanning water network which is formed at the protein surface by less mobile and slowly exchanging water molecules (Figure 2.11). This reduced flexibility is rather due to the spanning water network formation than interactions between the solvent and the protein.

Enzymatic catalysis in non-aqueous media has attracted an important attention in the preparation of a wide range of natural products, pharmaceuticals, and food ingredients. For that reason, several studies focused on defining reaction conditions to provide higher rates in low water media and with a minimum inactivation of

biocatalysts to obtain improved production in industrial scale (Turner and Vulfson, 2000).

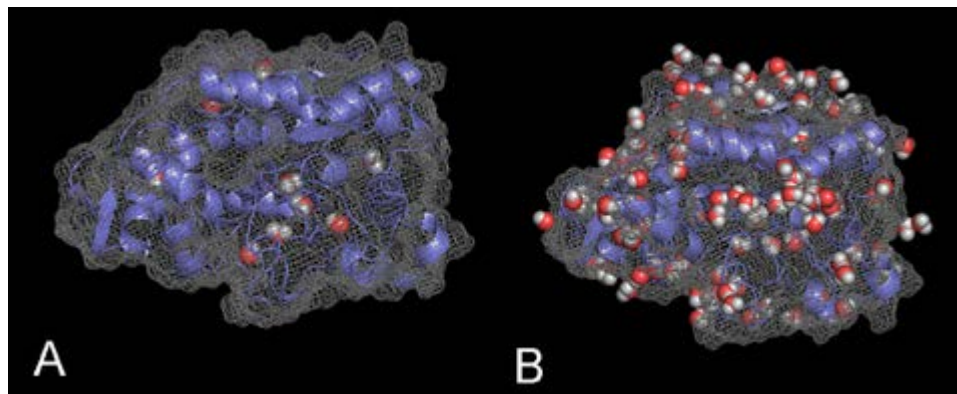


**Figure 2.11 :** Less mobile water molecules at the surface of CALB. Location of less mobile water molecules, with a B-factor lower than  $40 \text{ \AA}^2$ , at the surface of the last snapshot of CALB during the simulation (A) in water and (B) in cyclohexane; water molecules are displayed as red and white spheres (Trodler and Pleiss, 2008).

The effect of water associated to the enzymes has been studied so far. It has been demonstrated that different types of enzymes show different requirements in terms of bound water which provides them to keep an important catalytic activity in non-aqueous media (Zaks and Klivanov, 1988). It has been also shown that the enzyme stability is increased under low water conditions (Turner et al., 1995). This feature provides the catalysis of biotransformation reactions at higher temperatures than those used in conventional methods in aqueous media. It is cited that the most common reason for enzyme inactivation at high temperatures is the loss of native, catalytically competent structural conformation, called thermodenaturation.

Turner et al. (1995) has proved that the temperature at which a protein undergoes thermal denaturation ( $T_d$ ) depends on the amount of water associated with the protein. For instance, under relatively dry conditions chymotrypsin and *Candida rugosa* lipase denatured at 111 and 118 °C respectively, while the denaturation of these enzymes were at 53 and 61 °C in water. Similar behavior was observed for *Mucor miehei* lipase providing to suggest that at temperatures of around 90–120 °C and at low water activity, enzymes should be catalytically active.

Turner and Vulfson (2000) tried to find out how tightly water molecules are bound to enzymes at high temperatures and also to determine if there is any chemical alteration occurring in the primary structures of proteins under these conditions. They

showed that to remove tightly bound water from enzymes, temperatures around 200 °C are needed and heating process to that temperature region does not cause any cleavage of polypeptide chains but causes some little chemical degradation of particular amino acid residues if there are any. They concluded that at elevated temperatures, enzymes which need a small amount of water for their catalytic action, can keep their activity if they are stabilized against thermodenaturation. They proved this theory with the case of immobilized *Candida antarctica* lipase which catalyzed the transesterification of octadecanol with palmityl stearate at 130 °C for a considerable time.

#### **2.4.4 Lipase catalyzed ROP of lactones and lactides into polyesters**

##### **2.4.4.1 Proposed mechanisms**

Lipases can catalyze the ROP of lactones (small to large rings), cyclic diesters (lactides) and cyclic carbonates to produce polyesters or polycarbonates (Varma et al., 2005).

Lipase catalysis induces ring opening polymerization of non-substituted lactones with various ring-sizes. Lipase-catalyzed ROP of lactones was first presented by two independent groups, Uyama and Kobayashi and Knani et al. (1993) for  $\epsilon$ -CL and  $\delta$ -VL and the technique has rapidly developed as a novel methodology for polymer synthesis since then. The mechanism for the lipase-catalyzed polymerization of lactones was first presented by Uyama et al. (1995) (Figure 2.12).

In Figure 2.13, a detailed proposed mechanism can be observed where the carbonyl groups of lactone are first subjected to the nucleophilic attack of the -CH<sub>2</sub>OH group of lipase serine residues which are situated on the active center of the enzyme. This results in the formation of an acyl-enzyme complex. Then water, probably present in small amount in the enzyme, or an alcohol present in the reaction mixture acts as a nucleophile and reacts with the enzyme activated monomer complex (EAM) yielding an oxyacid which is considered as the basic propagation species.

In the propagation step, the terminal hydroxyl group of the growing polymer chains attack the EAM to give a product that is elongated by one repeat unit.

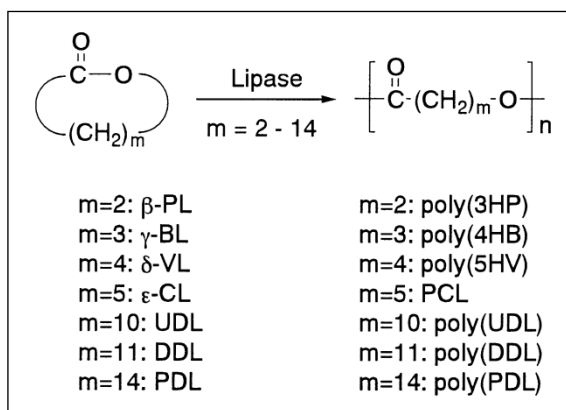


**Figure 2.12 :** Lipase catalyzed ring-opening polymerization of lactones (Matsumura, 2006).

It is supposed that the polymerization proceeds via a “monomer activated mechanism”, the rate-determining step is the formation of the EAM intermediate (Figure 2.13) (Matsumura, 2006; Gross et al., 2001; Kobayashi et al., 1998b).

This is different from the “active chain-end mechanism” observed in many other polymerizations. In that situation, active propagating chain end reacts with a monomer to give a propagating polymer elongated by one more monomer unit (Kobayashi, 2006).

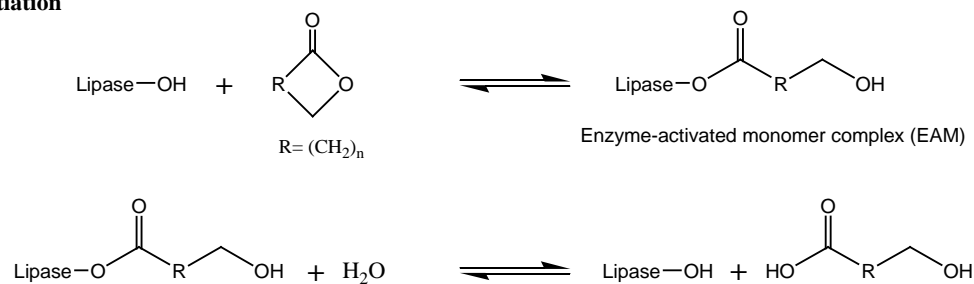
Mei et al. (2003a) have reported that CALB which was inhibited irreversibly at the serine (Ser105) residue with diethyl p-nitrophenyl phosphate, could not initiate the ROP of CL. So they confirmed that the lipase catalyzed polymerization proceeds by the catalysis at the active serine residue of the enzyme and not by other chemical or non-specific protein mediated process.

Puskas et al. (2011) proposed the representation of this catalytic cycle based on the involvement of ionic intermediates at the enzyme active site (Figure 2.14).

After the observations made on lipase catalyzed copolymerization of racemic  $\delta$ -CL with achiral lactones, it was suggested that the formation of the acyl-enzyme intermediate (EAM) is not always the rate determining step (Kikuchi et al., 2000; Kobayashi, 2006). They considered a mechanism where the formation of EAM (acylation of lipase) is operative with the subsequent reaction of EAM with monomer (deacylation of lipase) depending on the monomer structure.



### Initiation



### Propagation

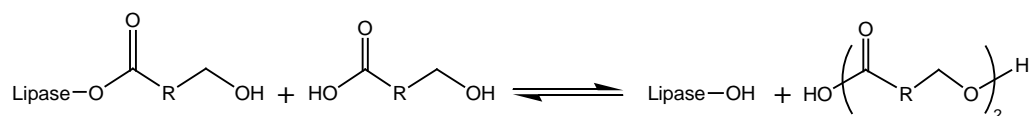


**Figure 2.13 :** Postulated mechanism of lipase-catalyzed ring-opening polymerization of lactones (Albertsson and Srivastava, 2008).

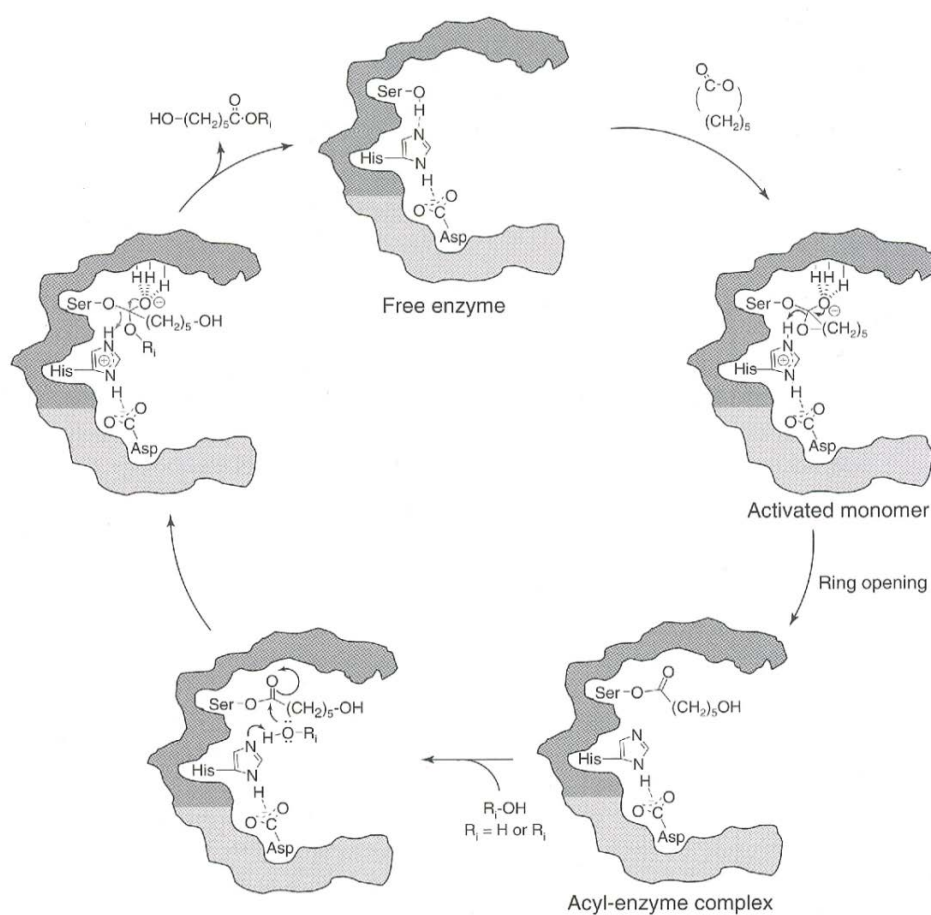


**Figure 2.14 :** Illustration of suggested mechanism for the lipase catalyzed ROP of lactones showing the involvement of ionic intermediates at the enzyme active site (Puskas et al., 2011).

They pointed out that when the propagating alcohol end is of sterically bulky nucleophile, the deacylation step determines the overall rate of reaction. The enantioselectivity plays an important role for both acylation and deacylation steps (Kobayashi, 2006). The proposed mechanism was illustrated in Figure 2.15.

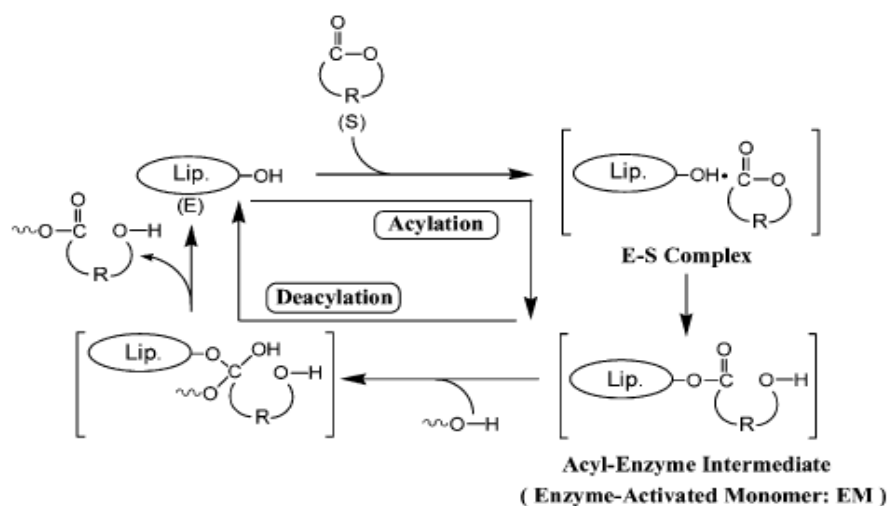


**Figure 2.15 :** A general illustrative mechanism of lipase-catalyzed ROP of lactones involving the acylation step and/or the deacylation step as rate-determining step, depending on the structure of R in monomer (Kobayashi, 2006).

Different types of commercial lipases from various species as *Aspergillus niger* (lipase A), *Candida antarctica* (lipase B, Nov-435), *Candida rugosa* (lipase AYS), *Mucor javanicus* (lipase M), *Mucor miehei* (lipozyme), porcine pancreatic lipase (PPL), *Pseudomonas aeruginosa* (lipase PA), *Pseudomonas cepacia* (lipase PS), *Pseudomonas fluorescens* (lipase PF), *Pseudomonas* sp. lipase (PSL), *Rhizopus delemar* (lipase RD), and *Rhizopus oryzae* (lipase RO), etc. have been reported to catalyze the ROP of lactones, lactides, cyclic carbonates of ring sizes differing from 4 to 17 in the presence or absence of organic solvents.

As a difference from chemical ROP, enzymatic ROPs are not dependent of ring strains of the monomers. It has been shown that macrolides (e.g. 12-dodecanolide, 15-pentadecanolide) can be polymerized more faster than the smaller ring lactones (e.g.  $\epsilon$ -CL) by the catalysis of lipases (Namekawa et al., 1999). This is due to high dipole moment of macrolides showing more hydrophobicity compared to smaller ring lactones.

The lipase-catalyzed ROP of lactones, lactides, cyclic carbonates and cyclic depsipeptides are being actively pursued in several laboratories aiming to produce high molecular weight polymers. Most of the studies performed and reported so far concerned the polymerization of  $\epsilon$ -caprolactone ( $\epsilon$ -CL).

The preferred lipase system used is generally a physically immobilized form of *C. Antarctica* lipase B known as commercially available Novozym<sup>®</sup>-435. The influence of enzyme immobilization and the different strategies will be discussed later on in section 2.4.6.

#### **2.4.4.2 Lipase catalyzed ROP of $\epsilon$ -CL**

Reaction parameters as solvent type, temperature, enzyme concentration and type of enzymes have been studied by different research groups with the aim to obtain high molecular weight polymers and fast kinetics via enzymatic catalysis.

As far as  $\epsilon$ -CL is concerned, various enzymes have been tested and the main results are reported in Table 2.1 together with the specific conditions of the corresponding reactions.

From the table it can be seen that, in terms of reaction kinetics and molecular weights of PCLs, most performant enzymes are CALB and its commercially immobilized form NOV-435.

With CALB, higher monomer conversion percentages and final molar masses can be reached in shorter periods compared to other types of free lipases. For the cases where CALB and NOV-435 are used as catalysts, it is observed that polymerizations proceed better in toluene compared to the reactions performed in bulk with the same enzymes.

Interestingly when the ROP of  $\epsilon$ -CL is carried out in supercritical liquids as  $\text{scCO}_2$  very promising results can be obtained at moderate temperatures and in one day; by the catalysis of CALB at 35 °C, a PCL having a  $M_n$  of 50000 g/mol can be obtained (Thurecht et al., 2006), in addition to this a PCL with a  $M_n$  of 35000 g/mol can be synthesized by NOV-435 at 65 °C (Loecker et al., 2004).

**Table 2.1 :** Lipase catalyzed ROP of  $\epsilon$ -CL at various temperatures and media with corresponding monomer conversion rates (C) and molecular weights ( $M_n$ ) of PCL chains.

Monomer	Enzyme	T (°C)	Time (h)	Medium	$M_n$ (g/mol)	C (%)	Reference
$\epsilon$ -CL	CALB	60	4	Bulk	5200	72	Uyama et al., 1997
		60	24	Toluene	15600	55	Marcilla et al., 2006
		60	24	scCO <sub>2</sub>	17000	97	Takamoto et al., 2001
		20	7	Toluene-d8	17800	97	Mei et al., 2002
		35	24	scCO <sub>2</sub>	50000	100	Thurect et al., 2006
	NOV-435	116	1.5	Toluene	3200	41	MacDonald et al., 1995
		45	24	Bulk	4100	95	Peeters et al., 2005
		60	4	Bulk	22000	47	Srivastava et al., 2005
		65	24	scCO <sub>2</sub>	35000	98	Loeker et al., 2004
		70	24	Toluene	44800	85	Kumar and Gross, 2000a
	PPL	75	75	Bulk	2300	99	Kobayashi et al., 1998a
		65	96	Heptane	2700	100	MacDonald et al., 1995
		65	96	Heptane	7600	85	Henderson et al., 1996
	CCL	75	480	Bulk	3100	100	Kobayashi et al., 1998a
		45	240	Heptane	3200	97	Kobayashi et al., 1998a
	PFL	45	240	Isooctane	1800	52	Kobayashi et al., 1998a
		75	480	Bulk	12000	99	Kobayashi et al., 1998a

In 1998, Kobayashi et al. reported the polymerization of  $\epsilon$ -CL by using *Pseudomonas fluorescens* (PFL), *Candida cylindracea* (CCL), *Pseudomonas cepacia* (PCL) and porcine pancreatic (PPL) lipases as catalysts. Among the tested lipases, PFL showed the best activity by converting 71% of the  $\epsilon$ -CL in bulk at 60 °C at the end of 10 days (50 mg lipase:1 mmol monomer). A PCL having carboxyl and hydroxyl end groups with a molecular weight of 7000 g/mol was obtained. With a prolonged reaction time (20 days), and at 75 °C, 99% of conversion and  $M_n$  value of 12000 g/mol was reached with the same enzyme (Table 2.1). Molecular weights of obtained PCLs fully depended on the type of enzyme.

In another study, PPL has been tested for  $\epsilon$ -CL polymerization in dioxane, toluene and heptane with the addition of butanol as initiator. Low molecular weight ( $M_n$ =2700 g/mol) PCL was formed at the end of 4 days at 65 °C (MacDonald et al., 1995). Later on, Henderson et al. (1996) could reach a higher  $M_n$ =7600 g/mol in similar conditions.

As it can be seen, with other free lipases very long reaction times were required to attain considerable monomer conversion percentages and PCL molecular weights, whereas with CALB these targets can be obtained within shorter periods of time.

In an effort to improve  $\epsilon$ -CL polymerization kinetics and increase product molecular weights, parameters such as solvent, reaction temperature, monomer to solvent ratio, enzyme concentration, enzyme source, and water content in the reaction medium were studied (Kumar and Gross, 2000a; Deng and Gross, 1999).

### ***Influence of water content***

Gross and coworkers have reported the increase in  $M_n$  values of PCL chains depending on the enzyme water content decrease in the reaction media (Mei et al, 2003a). It has been also admitted that water functions as an initiator and reacts with the enzyme activated monomer complex. So an increase in water concentration may lead to the initiation of a greater number of chains and hence polymers with lower  $M_n$ . It is suggested that in bulk polymerizations there is a restricted diffusion phenomenon of propagating chains and monomer which can limit the further growth of higher molecular weight chains. Contrary to this situation, in polymerizations conducted in solvent media, diffusion limitations are unlikely to occur so an increase in the reaction temperature would liberate water and reduce  $M_n$  values. Additional considerations have been also made on relationship between  $M_n$  and reaction temperature, stating that for some enzyme-monomer systems an enzyme-catalyzed chain hydrolysis may occur due to an increase in water content.

### ***Effect of solvent type***

The relationship between the type of solvent and polymerization behavior has been investigated by Kobayashi et al. (1998a) for the polymerization of  $\epsilon$ -CL and  $\delta$ -VL by *Candida cylindracea* lipase. Log $P$  value of these solvents which is often used as a hydrophobicity parameter was taken into consideration. Log $P$  is defined as the logarithm of the partition coefficient  $P$  of a given solvent between 1-octanol and water and the hydrophobicity increases as this value gets larger. They concluded that larger conversion percentages and polymer molecular weights could be obtained with solvents with larger log $P$ .

Later on, Kumar and Gross (2000a) have performed  $\epsilon$ -CL polymerizations catalyzed by NOV-435 at 70 °C in different solvents as dioxane ( $\log P:-1.1$ ), acetonitrile ( $\log P:0.33$ ), tetrahydrofuran ( $\log P:0.49$ ), chloroform ( $\log P:1.9$ ), isopropyl ether ( $\log P:1.9$ ), butyl ether ( $\log P:2.9$ ), isooctane ( $\log P:4.5$ ) and toluene ( $\log P:2.5$ ). Polymerization rates and molar masses of products were analyzed versus  $\log P$  values of tested solvents. Two distinct data regions were observed: low propagation rates ( $\epsilon$ -CL conversion  $\leq 30\%$  in 4 h) and low chain lengths ( $M_n \leq 5200$  g/mol) were obtained when solvents having  $\log P$  values from -1.1 to 0.49 were used and better propagation rates and higher molecular weights ( $M_n=11500-17000$  g/mol) were attained when solvents with higher  $\log P$  values were used.

In toluene, best conditions were obtained with about 80% of monomer conversion and  $M_n=15000$  g/mol. Interestingly with buthyl ether which has a higher  $\log P$  value than toluene, relatively lower results were reached (60% conversion,  $M_n=12900$  g/mol). So this trend could not be explained only by the differences of the  $\log P$  values of solvents. Other physicochemical factors as solvent geometry, dipole moments, solubility of monomers and polymers are to be considered. For example produced PCLs were hardly soluble in isopropyl and butyl ethers and  $\epsilon$ -CL formed two separate phases with isooctane in related reaction conditions. Toluene providing a good solubility for both monomer and formed PCL and high polymerization rate and molar masses for products, was thus chosen as the best solvent for this system.

#### ***Influence of the monomer: solvent ratio***

Once toluene has been selected as the best solvent for  $\epsilon$ -CL polymerization, Kumar and Gross (2000a) also studied the influence of the monomer concentration on the polymerization reaction. At toluene: $\epsilon$ -CL ratios (vol/vol) varying from 1.5 to 3, highest monomer conversion rates and high molecular weight PCLs have been obtained at 70 °C by the catalysis of NOV-435 (10%w/w, enzyme relative to monomer). Optimal toluene: $\epsilon$ -CL ratio was determined to be 2:1 leading to monomer conversion of 85% and final product molar mass of 17200 g/mol (Kumar and Gross, 2000a).

#### ***Influence of the reaction temperature***

Even if the fastest polymerization rate was obtained at 90 °C, highest  $M_n$  values have been reached at 60 °C. This was explained by the low  $N_p$  (total number of chains)

value at 60 °C indicating the formation of just few chains. It was suggested that the thermal energy at 60 °C was insufficient to break the interactions between some water molecules and the catalytic matrix. As a result, the release of water molecules in the medium at 90 °C led to higher number of propagating chains and thus lower  $M_n$  values. Then, an important decrease in  $N_p$  was observed when temperature was increased from 90 °C to 100-105 °C. It has been assumed that the protein denatured at these temperatures and some condensation reactions took place between chains leading to a loss in the total number of chains. It has been concluded that at temperatures between 60-85 °C at a 55% of monomer conversion,  $N_p$  did not change and linear slopes were observed for  $\ln [Mo/Mt]$  vs time and  $M_n$  vs monomer conversion percentage graphics indicating the absence of termination and chain transfer during these reactions (Kumar and Gross, 2000a).

#### ***Impact of enzyme concentration***

The effect of catalyst concentration on the polymerization and molecular weights has been studied for  $\epsilon$ -CL polymerization at 70 °C by NOV-435 in bulk (Deng and Gross, 1999). Initial conversion rates increased with increasing lipase content but  $M_n$  values decreased for same conversion percentages. When enzyme concentration was increased five times, a three times increase was observed for  $\epsilon$ -CL conversion and total chain number most probably due to higher amounts of water molecules present within the enzyme. When this water was totally consumed during the initiation step, further monomer conversion did not vary the total chain number ( $N_p$ ) even at higher enzyme concentrations. Monomer consumption after this period was rather due to propagation steps. No significant differences were observed in polydispersity of products by different enzyme concentrations.

These aforementioned, important and sound studies performed by Kumar and Gross's research group on the parameters influencing the  $\epsilon$ -CL polymerization allowed to determine the key parameters and some optimized conditions which usually are a good starting point for studies on different systems, such as alternative enzymes or other lactone monomers.

#### **2.4.4.3 Lipase catalyzed ROP of lactides**

The number of publications dealing with the ROP of lactides by enzyme catalysis has remained markedly low so far and the mechanism has not been well described.

Enzymatic polymerization of lactides has some restraints as the poor solubility of the substrate in non-polar, hydrophobic solvents and relatively high temperatures needed to reach the melting point of lactide monomers which may affect the enzymatic activity during the reactions (Hakkarainen and Wistrand, 2011).

First studies concerning enzymatic ROP of lactide was started by the research group of Matsumura in 1997. They succeeded in polymerizing the different lactide isomers (D-, L-, D/L- lactides) by the catalysis of different lipases (PPL, CCL, *Burkholderia cepacia* lipase -called Amano lipase PS) at a temperature range of 80-130 °C and announced having reached average molecular weights in the range of 6000-115000 g/mol (Matsumura et al., 1997). The polymerization occurred with all types of lipases they used, except for NOV-435. Among the lipases tested, lipase PS showed the highest catalytic activity in terms of polymerization of lactide.

In the Table 2.2 below, are listed some of the main results reported so far for the polymerization of lactides with different enzymes that have been tested together with the corresponding reactions conditions.

**Table 2.2 :** Lipase catalyzed ROP of lactide isomers at various temperatures and media with corresponding monomer conversion rates (C) and molecular weights ( $M_n$ ) of poly(lactide) chains.

Monomer (lactide)	Enzyme	T (°C)	Time (days)	Medium	$M_n$ (g/mol)	C (%)	Reference
D/L-	NOV-435	80	7	Bulk	-	0	Matsumura et al., 1997
	PPL	80	7	Bulk	6250	37	"
	CCL	80	7	Bulk	6700	30	"
	PS	80	7	Bulk	22500	7	"
	PS	130	7	Bulk	115000	100	"
	NOV-435	60	4	Solvent	446	58	Lasalle&Ferreira, 2008
	PPL	60	4	Solvent	768	96	"
	PCL	60	4	Solvent	400	88	"
L-	PS	100	7	Bulk	40000	82	Matsumura et al., 1997
	CALB	120	1	Bulk	26600	99	Yoshizawa et al., 2008
	CALB	120	1	Toluene	42600	100	"
	PS	125	7	Bulk	78000	98	Malberg et al, 2010
	NOV-435	70	3	Toluene	-	0	Hans et al., 2009
D-	PS	100	7	Bulk	49000	96	Matsumura et al., 1997
	NOV-435	70	3	Toluene	3300	33	Hans et al., 2009



Lasalle and Ferreira (2008), have tried to analyze the subject from a different approach, taking into account all factors in the reaction conditions as nature of lipase, solvent and time. Three lipases (PPL, PC (*Pseudomonas cepacia* lipase), NOV-435) were evaluated in terms of lactide (D/L-lactide) conversion. After 96 h of polymerization at 60 °C in solvent, PPL was the best catalytic system with 96% of conversion, followed by PC (88%) and NOV-435 having shown rather poor activity (58%).

It has been highlighted that in the case of bulk reactions, NOV-435 caused some problems for the recovery of PLA. A rubbery resin was recovered from the reaction mixture not depending on enzyme concentration and lactide conversion values. This phenomenon could not be explained clearly but, it has been suggested that low molecular weight oligomers are formed because of the possible deactivation of NOV-435 in strong polar media such as lactide monomer. Thus solution reaction was considered as the most effective route to obtain PLA by this enzyme.

To explain the low catalytic activity of CALB for polymerization and copolymerization of L-lactide and D/L-lactide, the high enantioselectivity of CALB for R-configured secondary alcohols was assumed by Zhou et al. (2006). Hans et al. (2009) have hypothesized that CALB can not polymerize L-lactide and D/L-lactide because of the S-configured secondary alcohol formed after the ring-opening of the lactide. On the other hand, when D-lactide is ring-opened, resulting secondary alcohol has R-configuration and can react with an enzyme activated monomer (EAM) and thus propagation step can continue and polymerization can occur (Figure 2.16).

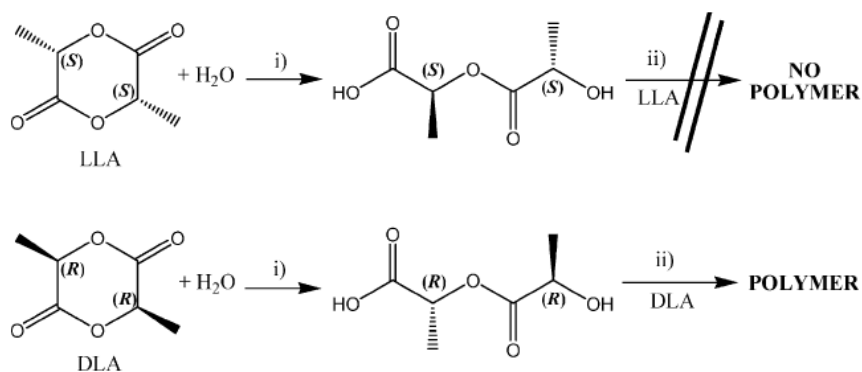


**Figure 2.16 :** Hypothesis concerning the enzymatic ROP of L- lactide (LLA) and D- lactide (DLA) by Novozym<sup>®</sup>-435, (i) initiation and (ii) chain propagation step (Hans et al., 2009).

To support their hypothesis, polymerization reactions of L- and D-lactide were performed at 70 °C, by NOV-435, in toluene. After 3 days of reaction no conversion was observed with L-lactide, but 33% of conversion was detected for D-lactide and resulting polymer had a  $M_n$  value of 3300 g/mol with a PDI of 1.2 (Table 2.2). They studied several factors effecting reaction kinetics as enzyme and monomer concentration, temperature. They have concluded that an increase in the enzyme concentration results in higher conversions and higher number of polymer chains but naturally in the formation of lower molecular weight products. This fact has been explained by the introduction of higher amounts of water, found in the structure of the enzyme.

During these reactions, after certain conversion values, loss of activity of the enzyme has been observed which might be due to the bulkiness of lactide chain ends (secondary alcohol), which in turn leads to the depletion of water from the enzyme causing the destruction of its tertiary structure.

More clearly, during the lactide polymerization, the secondary alcohol has to penetrate the active site of the enzyme in a way that the conformational stress implied to the enzyme is much more higher compared to the polymerization of  $\epsilon$ -CL where the primary alcohol is at the chain-end. It has been assumed that because of the impeded entrance of the bulky chain-end to the active site and the implied strain to the enzyme conformation, loosely bound water is more likely to react with the activated species. The depletion of free and loosely bound water from the enzyme leads to a reduced flexibility of the tertiary protein structure and thus a loss of activity.

The optimal conditions were estimated to be 1:2 (g:ml) monomer to toluene ratio at 70 °C. At lower temperature (60 °C), a polymer (PDLA) with a molecular weight of 12000 g/mol has been synthesized starting from D-lactide as monomer (Hans et al, 2009).

Albertsson and co-workers (2010), have performed L-lactide polymerizations by different lipases as lipase PS, lipase PS-immob, lipase AK from *Pseudomonas fluorescens* and CALB with and without the addition of ethylene glycol (Malberg et al., 2010). Highest molecular weight (78000 g/mol) and reaction rate was obtained with lipase PS at 125 °C without ethylene glycol as co-initiator. CALB reached its

maximum in terms of conversion (94%) at the end of 7 days at 125 °C with an monomer:initiator ratio of 100, but related molar masses ( $M_n=9400$  g/mol) did not increase according to the conversion.

It can be clearly seen that the results from different research groups still remain contradictory to each other in terms of polymerizability of lactide isomers. The main issue concerns the polymerizability of the L-lactide, which is assumed to be impossible to polymerize by some authors while others report experimental results showing its good polymerizability by other enzymes and in different reaction conditions. In addition, many of the reported results concern the polymerization reactions performed at relatively high temperatures (100 to 130 °C) for which the issue of enzyme denaturation and deactivation as well as non-enzymatic initiation could arise but are not often discussed.

Thus, a more systematic investigation on the enzymatic polymerization of lactide still seems necessary to confirm or invalidate some of the hypotheses and conclusions advanced so far.

#### **2.4.5 PCL/PLA copolymerizations by lipase catalysis**

Polymer blending process appears to be an attractive and simple route for the improvement of polymer properties. Nonetheless, resulting materials show often poor mechanical properties due to limited miscibility and weak adhesion between phases. Copolymerization in this case, can be regarded as an alternative to increase the compatibility between the different phases. Polymer properties as degradation rate, hydrophilicity and mechanical characteristics can be modified by copolymerization since the resulting materials inherit the properties of the corresponding homopolymers.

Kumar and coworkers, after having extensively studied  $\epsilon$ -caprolactone polymerizations catalyzed by enzymes in toluene, were interested in lipase-catalyzed copolymerizations which have received only little attention in the literature. They assumed that copolymerizations by lipase catalysis may create highly ordered repeat-unit chain sequences and may be conducted more easily compared to more traditional methods. They studied the Novozym<sup>®</sup>-435/toluene system for the copolymerization of  $\omega$ -pentadecalactone/  $\epsilon$ -caprolactone at 70 °C (Kumar et al., 2000c; Ceccorulli et al., 2005).

They experimentally determined that  $\omega$ -pentadecalactone enzymatic polymerization was 13 times faster than  $\epsilon$ -caprolactone polymerization. But in spite of this great difference in reactivities of these monomers, random copolymers were obtained by the transesterificative activity of NOV-435 between the chains. This result is also interesting for the reason that for transesterification to occur between the homopolymer chains, both large macromolecules have to be close to the active site of the lipase enzyme. Another promising feature was that lipase enzyme catalyzed low temperature transesterification reactions and the repeating unit distribution changed with reaction time from block to close to random. In 45 minutes, a copolymer having a  $M_n$  of 20000 g/mol was obtained with a 88% yield.

Kumar and Gross (2000b), Namekawa et al. (2001) have also studied similar systems to obtain close-to-random distributions starting from presynthesized PCL and adding PDL monomer or from two homopolymers and continuing the reaction for a longer time.

PCL is highly flexible polymer, shows good biodegradability but its strength is relatively low and its low melting point at 60 °C limits its usage in many applications. PLA shows good biocompatibility and high strength but its brittleness remains a major drawback (Wang et al., 1998). As far as medical and pharmaceutical applications are concerned, PCL and PLA show complementary properties. PLA has a shorter half-time in vivo (a few weeks) than PCL (1 year). PCL is permeable to many drugs with low molecular weights, whereas PLA because of its hydrophilicity is not. Thus, among their other interesting properties, copolymers synthesized from  $\epsilon$ -caprolactone (CL) and D/L-lactides would be more permeable to drugs than PLA and they would be advantageous in biodegradable devices due to their shorter lifetime relative to PCL (Nomura et al., 2010).

PCL, PLA and their block copolymers are usually synthesized by the catalysis of organometallic compounds as tin(II) 2-ethylhexanoate via ROP of related cyclic esters. Even if this catalyst is considered safe for the production of biomedical grade polymers, there are still some possible toxicity arguments on its usage. So there is a big interest for the development of organometallic-free catalysts such as enzymes.

Basing on the facts that CALB is highly reactive for  $\epsilon$ -CL but not for D/L-lactide and that D/L-lactide inhibits reversibly this enzyme, Wahlberg et al. (2003) have

performed series of PCL/PLA copolymerizations to see how the lactide slows down the reaction kinetics.

Lactide being the cyclic dimer of lactic acid, the reaction between one molecule of  $\epsilon$ -CL and one molecule of lactide yields a copolymer with CL unit connected to two lactic acid (LA) units (Figure 2.17). Targeted copolymer composition was based on this CL to LA ratio.

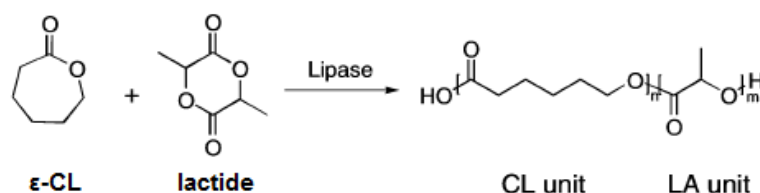


**Figure 2.17** : Lipase catalyzed copolymerization of  $\epsilon$ -CL and lactide.

Two types of copolymerization have been conducted: high lactide content copolymerization where a ratio of CL:LA (1:1) was employed (70 °C; 15 mg lipase) and low lactide content copolymerization with ratios of CL:LA of (5:1 and 10:1), (60 °C; 5 mg lipase). Oligomeric products of 1:1 CL:LA reaction, formed after one week, contained copolymers mostly composed of LA units and no PCL homopolymer was detected in the product mixture. This result was quite interesting for CALB which is known to be active for  $\epsilon$ -CL and inactive for lactide. After 3 and 8 weeks of copolymerization, higher quantities of CL units were observed in the product. According to MALDI-TOF analysis, it has been suggested that lipase catalyzed ring-opening copolymerization represents a non-random behavior at initial state, then at prolonged reaction times intermolecular transesterification destroys this pattern and provides a random mixture. SEC and <sup>1</sup>H NMR analyses demonstrated that all monomers have been polymerized at the end of 8<sup>th</sup> week and this polymerization is not due to non-enzymatic reactions. This was confirmed by reactions carried out in the absence of lipase and no polymer formation was detected at the end of the same period.

In the low lactide content polymerizations, lactide was rapidly consumed within 2 h, and a few CL units incorporated the product. After this initial stage, both monomers were polymerized at equal rates. These observations revealed that even if lactide decreases the overall polymerization rate of the reaction, during the initial stage it seems to be more reactive. It has been also observed that after the total consumption

of lactide, the polymerization rate of  $\epsilon$ -CL did not increase. This point could not be attributed to the deactivation of enzyme since the molecular weights continued to increase. It has been shown that during polymerizations with low lactide proportion, macrocyclic products were firstly formed, these products being possibly cyclic PCL or cyclic copolyesters having one or two LA units within their structures and as the reaction proceeded further, these cyclic products gradually transformed into linear polymers.

Even if a very limited number of studies were reported on the enzymatic copolymerization of  $\epsilon$ -CL and lactides, the main and logical result observed is the formation of a random copolyester due to the high transesterification activity of the lipase catalyst.

Interestingly, in a recent study by Xiao et al. (2009), chemoenzymatic combination of both enzymatic and carbene catalysts to be used for the formation of (L-lactide and  $\epsilon$ -caprolactone) copolymers was investigated. By this way, it was aimed to overcome the deficiencies of each catalyst and produce degradable aliphatic block copolyesters by completely metal-free ROP (Figure 2.18).

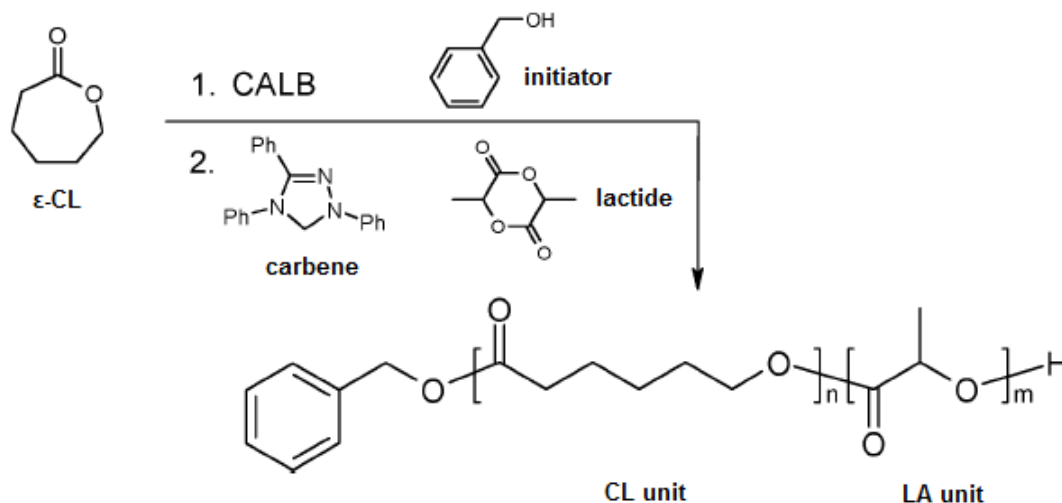


**Figure 2.18 :**  $\epsilon$ -CL and lactide copolymerization initiated from benzyl alcohol using enzymatic (CALB) and/or carbene catalysis (Xiao et al., 2009).

As previously mentioned, CALB is well known to polymerize by ring-opening, lactones of all sizes. Besides, it shows lower catalytic activity towards L-lactides likely due to the formation of a chiral secondary alcohol end-group by the ring opening of the monomer which inhibits the active site of the enzyme and

prevents further propagation. Carbene, on its side, is highly active for the polymerization of lactides but not for lactones.

First, the results obtained for the one-pot copolymerization reactions showed that ROP of  $\epsilon$ -CL by immobilized CALB is inhibited in the presence of carbene. Authors then put the two monomers and two catalysts in the same reaction pot and reactions proceeded into two steps; starting first at low temperatures to allow the enzymatic polymerization of  $\epsilon$ -CL and then initiating carbene catalyzed L-lactide polymerization by increasing the temperature. By this procedure they could not obtain copolymers but just PLA homopolymers. They decided to put the reactants consecutively to the reaction flask. First, polymerization of  $\epsilon$ -CL at 60 °C for 6 h was performed and a PCL with a molecular weight of 5300 g/mol was obtained. Secondly, L-lactide and carbene were introduced to the reaction medium and after further polymerization at 90 °C for 6 h formed the expected copolymer having a  $M_n$  value of 10500 g/mol. By this method, the inhibition of the enzyme has been provided by the introduction of carbene which is itself an internal inhibitor for that enzyme and so the possible enzyme catalyzed transesterification reactions that might cause the random restructuring of the copolymer have been prevented.

As it was previously highlighted, enzymatic polymerization must often be carried out at rather elevated temperatures to provide faster kinetics and/or to allow monomer solubilization or melting in the reaction medium (e.g., for the lactide polymerization). Such elevated temperatures may result in the enzyme denaturation and deactivation and thus it is of great importance to increase the thermal resistance and stability of the enzymes. Among the possibilities to increase such lipase stability, their immobilization on solid supports is of prime interest.

#### **2.4.6 Immobilization of lipases**

Various process parameters of enzyme catalyzed reactions such as: operational and thermal stability and easier separation from the reaction mixture can be modified by enzyme immobilization (Gitlesen et al., 1997). Especially, soluble enzymes must be immobilized to provide their reuse for longer times in industrial scale processes. The ideal immobilization procedures should not use toxic or unstable reagents, should be very simple and robust (Mateo et al., 2007). There are many advantages of enzyme immobilization: (i) a single batch of enzyme can be used several times, (ii)

the reaction can be easily stopped by just removing the enzyme from the reaction mixture, (iii) denaturing effects can be limited by stabilizing the enzyme, (iv) in food, pharmaceutical or biomedical applications, product contamination can be avoided, (v) catalyst can be easily separated (Ghiaci et al., 2009a).

Enzyme immobilization can be performed either by simple physical adsorption on the support or by covalent bonding between the enzyme proteins and the carrier surface. However, covalent anchoring of the enzyme on the support may affect the enzyme activity due to possible loss of mobility of the enzyme and thus impossibility for the substrate to reach the active site or difficulty for the enzyme to change its structure to accommodate the specific organic substrate.

Immobilization of lipases is thus often performed by adsorption through hydrophobic interactions between the enzyme and the support (Blanco et al., 2004). The enzyme binding depends on the nature of the surface and may be the result of ionic interactions, physical adsorption, hydrophobic bonding, Van der Waals attractive forces, or a combination of these interactions. The non-covalent nature of this linking does not usually cause an abstraction of the enzyme when anhydrous media is used for the reaction because it is not probable that lipase desorption occurs under such conditions (Kennedy et al., 1988).

#### **2.4.6.1 CALB immobilization and Novozym<sup>®</sup>-435 commercial catalyst**

Among the immobilized lipases, the most common and preferred system used is a physically immobilized form of CALB commercially available and known as Novozym<sup>®</sup>-435. This efficient and versatile catalyst is based on a macroporous acrylic resin (Lewatit VP OC 1600) of poly(methyl methacrylate-*co*-divinylbenzene) as the enzyme carrier. The polymeric resin has an average particle size of 315-1000  $\mu\text{m}$ , a surface area of 130  $\text{m}^2/\text{g}$  and a pore diameter of  $\sim 150 \text{ \AA}$  (Chen et al., 2008). Its water and protein contents are estimated to be 1.3% (w/w) and 10% (w/w), respectively. It shows high regioselectivity during esterification and transesterification of sugars, nucleosides and steroids and high enantioselectivity for the resolution of secondary alcohols via hydrolysis or esterification reactions in organic solvents (Qian, 2007).

Mei et al. (2003b) have used an IR microspectroscopy method to show the enzyme distribution within NOV-435 and its structure (Figure 2.19). The results revealed that



the CALB formed an external shell on the Lewatit beads with a thickness of 80-100  $\mu\text{m}$ . The average pore size for the NOV-435 beads was determined to be about 100 nm by SEM analysis, and this value is 10 times larger than the size of a CALB molecule. On the basis of this information, it has been concluded that the diffusion of the enzyme into the core of the bead can not be prevented just with a simple physical barrier. So the research group suggested that the strong affinity of CALB for the matrix and low affinity or even repulsion between immobilized CALB molecules at the resin surface and soluble free CALB has limited the further diffusion and adsorption of soluble free CALB to the internal portions of the bead.

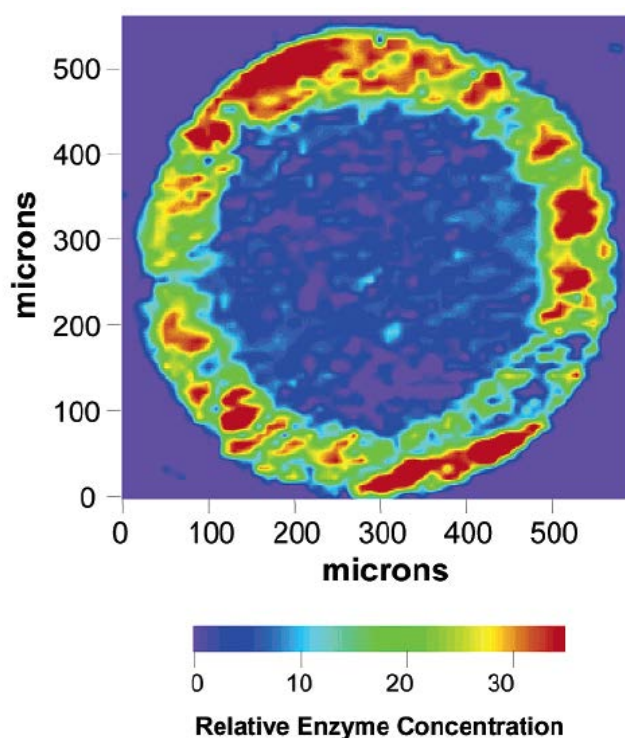


**Figure 2.19 :** The enzyme distribution throughout the center section of the NOV-435 bead (Mei et al., 2003b).

It has been suggested that the high catalytic activity of NOV-435 at high temperatures, may be due to this thick layer of CALB on the surface of resin beads. Another explication for this high activity was the swelling of the resin in toluene, ~350% by dry weight which led to a surface area increase in the particles and thus an augmentation in the number of available catalytic active sites of enzymes. New active sites, which are normally buried deep inside this thick layer are exposed by swelling phenomenon and enhance the overall catalytic activity of NOV-435 beads.

It has been concluded that the immobilization of CALB on the Lewatit polymer matrix consists of strong affinity of the enzyme for the matrix or strong protein-protein interactions between CALB molecules or a combination of both. After incubation in detergents and organic solvents, desorption of CALB from the surface of NOV-435 was observed. This indicated that the lipase may be adsorbed physically onto the support through hydrophobic interactions.

Some studies revealed the physical desorption or leaching of CALB during reactions as a disadvantage of NOV-435. This instable state was related to high mechanical shear used for mixing the reaction components (Chen et al., 2008; Poojari et al., 2008).

Qian (2007) has incubated free CALB and NOV-435 in toluene for 24 h in the temperature range of 40 to 100 °C. NOV 435 showed superior thermal stability at 70 °C keeping 70% of its initial activity while CALB has just kept about 40% of it. At 90 °C, CALB lost all its catalytic activity and NOV-435 still kept 60% of its activity at 100 °C. This simple study clearly shows and confirms the benefits obtained from enzyme immobilization on the catalytic activity.

Additionally, the reuse of NOV-435 beads has been analyzed. Interestingly, results indicated that the activity of the immobilized lipase has increased after the first cycle allowing to obtain PCL of higher molecular weight and lower PDI in the next cycles. This phenomenon was attributed to the formation of a new equilibrium state which was resulted from the swelling of acrylic resins in organic media.

Alternative enzyme supports such as porous ceramic (silica) or other polymer-based supports for the development of immobilized lipase catalyst for efficient production of polymers have also been investigated (Matsumura, 2006).

Sun et al. (2010) have performed the adsorption of CALB onto different supports (diatomite and various macroporous resins) by three different techniques: adsorption in aqueous media, precipitation by vacuum-drying and adsorption in organic media. Better results obtained for the organic media immobilization were in agreement with the study of Xin et al. (1999) who have reported that lipases, which are insoluble in organic solvents, can only exist in the aqueous film surrounding the support which is formed by a small amount of buffer solution and this fact can lead to higher immobilization efficiencies. While in the aqueous media an important quantity of

lipase remains in the supernatant and in vacuum drying in the walls of the flask. As another point, organic solvent may have an interaction with hydrophobic regions in the active sites of the lipase and this can enhance the catalytic activity of the enzyme at the hydrophobic interface (Lafuente et al., 1998).

It has been reported that higher activity and stability were observed in more hydrophobic solvents as heptane or isooctane. In contrast, hydrophilic solvents may compete with small amount of water within the enzyme during the adsorption onto the supports and this can affect the immobilization rate. A 2 hours adsorption time, 1:80 (w/w) lipase/support ratio and 30 °C were determined as optimal conditions for CALB immobilization on polar resin (NKA-9) in isooctane.

So far, CALB has been immobilized by different research groups onto various types of supports as PS nanoparticles, chitosan, chitosan-alginate complex, epoxy-activated macroporous poly(methyl methacrylate) (PMMA), Amberzyme beads, hydrophobic (Accurel), hydrophilic (Duolite) carriers, fumed silica, green coconut fiber, modified silicon wafers, diatomaceous earth, etc. (Brigida et al., 2008; Cruz et al., 2009)

#### **2.4.6.2 Clays as enzyme supports**

In parallel, the use of phyllosilicates (see section 2.5.1) as inorganic porous supports to immobilize enzymes has also been reported. Interestingly, the use of such nanoclays as lipase carriers can bring numerous advantages such as the high specific surface availability, the facility of water dispersion/recuperation, the high water uptake capacity, and the excellent mechanical resistance of these materials (Fuentes et al., 2001).

Fuentes et al. (2001), have performed immobilization of *Rhizomucor mihei* lipase (RML) and *Candida cylindracea* lipase (CCL) by physical adsorption onto different phyllosilicates as sepiolite, palygorskite and montmorillonite and compared the hydrolytic activities of resulting derivatives to those of immobilized onto Duolite A-568 which is a widely used anionic exchange resin.

They have supposed that the ionic adsorption of the enzyme onto silicate supports would be done through silanol groups of silicates and protonated lysines of the protein which are positively charged whereas for duolite this interaction would take place between the carboxylic groups of the enzyme and the positive charges on the carrier. But they also stated that steric factors related to the textural structures of the

supports must have been considered to describe the differences in hydrolytic activities of these derivatives.

It has been demonstrated that tested clays were more appropriate for the immobilization of low molecular weight proteins as RML rather than larger enzymes as CCL. Fibrous structures of sepiolite and palygorskite seem to enhance the activity due to better geometrical coherence with the protein.

Immobilization of CALB on three organomodified smectite nanoclays (laponite-synthetic trioctahedral hectorite, SWy-2, kunipia- dioctahedral montmorillonites) has been performed (Tzialla et al., 2010). Adsorptions have been carried out at the isoelectric point of the enzyme (pH 6.0), to prevent the possible electrostatic interactions between the enzyme and negatively charged clay surfaces. XRD results revealed the total exfoliation of the ordered structure of the layered mineral after the adsorption of enzyme molecules onto natural and organomodified laponite. On this basis, it has been assumed that a small part of the enzyme was located in the interlamellar spacing while the rest is immobilized either on the external surfaces of the edges of clay sheets since the CALB molecule is not expected to intercalate between clay nanosheets due to its dimensions ( $30\text{\AA} \times 40\text{\AA} \times 50\text{\AA}$ ) which are greater than the size of the clay basal spacing.

It has been already reported that in the case of montmorillonite K10, adsorption takes place on the external surface of organomodified clay; polypeptide backbone of the enzyme remaining on the external surface while the side chains of different amino acid residues take part in the intercalation and enters the interlayer spacing (Gopinath and Sugunan, 2007).

The derivatives were tested for terpene oxidation reactions and it has been concluded that with CALB immobilized on organomodified clays (OMCs), especially laponite, 20% of higher oxidation product concentration compared to NOV-435 can be obtained due to higher stability of these derivatives (Tzialla et al., 2009).

Alkaline phosphatase has been immobilized on both natural and organomodified forms of sepiolite and bentonite and *Candida rugosa* lipase on modified bentonite by the research group of Ghiaci (2009a-b) and Sedaghat (2009).

Adsorption of phosphatase onto Na-bentonite and organobentonite was declared to be on the external surface of the clays and was in the same order of magnitude. In the

case of sepiolite having a greater specific surface area compared to bentonite, no significant improvement in terms of the adsorption of the enzyme was observed. A loss in the activity of enzyme compared to its free form has been observed after its immobilization onto clays (Carrasco et al., 2005; Ghiaci et al., 2009a; Sedaghat et al., 2009).

In the case of the immobilization of *Candida rugosa* lipase onto bentonite modified with double layer of surfactant, enzymatic activity value was approximately 10 times higher than the activity of enzyme immobilized on Na-bentonite or single layered modified bentonite. This point was related to the possible formation of enzyme aggregates on the surface of natural and slightly modified bentonite which leads the distortion of the tertiary structure of the enzyme molecule (Ghiaci et al., 2009b).

As previously described, nanoclays are interesting solid supports and they have recently gained increased interest for lipase immobilization. This is not surprising since research and studies on nanoclay-based materials have increased exponentially during the last decade, more particularly driven by the intensive works on polymer/clay nanocomposites and other organic/inorganic nanohybrids as innovative materials.

## **2.5 Organic/Inorganic Nanohybrids**

Recently there have been many researches focused on polymer nanocomposites from scientific and technological views. Among organic/inorganic nanohybrids, polymers filled with inorganic nanoparticles have attracted great attention. The presence of these nanofillers in polymer matrices provides new characteristics to the final product and betterments in terms of thermal, mechanical and barrier properties. Even with  $\leq 5\text{wt}\%$  content of nanofiller, high aspect ratios and surface areas can be reached whereas with conventional composites, 40-50% of conventional filler content must be present within the matrix to provide similar reinforcement efficiencies (Sinha Ray and Bousmina, 2005).

Nanocomposites were defined as a newer category of composites filled with particles having at least one dimension at nanometer scale. Basing on this criterion, nanocomposites can be divided into three groups according to the dispersed particle dimension number at nanometer scale: (i) isodimensional nanocomposites, such as

spherical silica nanoparticles having three dimensions in order of nanometers, (ii) nanocomposites based on elongated particles like nanotubes or whiskers of which two dimensions are in nanometer scale and the third dimension forms an elongated structure, (iii) polymer-layered crystal nanocomposites in which the filler has the form of sheets with one dimension in the nanometer range; one to few nanometer thick to hundreds to thousands nanometers long (Alexandre and Dubois, 2000).

Typical nanomaterials which are currently investigated include: nanoparticles, nanotubes, nanofibers, fullerenes, and nanowires. They are commonly represented by their structural geometries (Figure 2.20); particle, fibrous and layered materials (Thostenson et al., 2005). Carbon black, silica nanoparticle, polyhedral oligomeric silsesquioxanes (POSS) can be classified as nanoparticle reinforcing agents while nanofibers and carbon nanotubes are examples of fibrous materials (Schmidt et al., 2002).

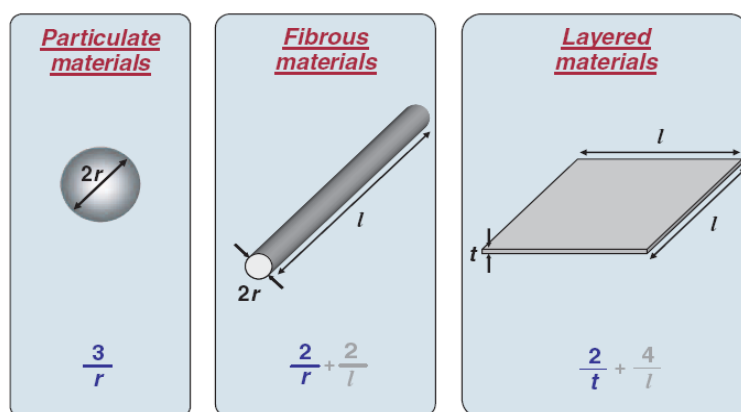


**Figure 2.20 :** Common particle reinforcements/geometries and their respective surface area-to-volume ratios (Thostenson et al., 2005).

The intrinsic properties of the constituents, the amount of nanofiller and the dispersion state strongly affect the properties of these nanomaterials (Alexandre and Dubois, 2000; Sinha Ray and Okamoto, 2003b). Depending on the size and shape of the particles, fillers may be more or less effective on the properties of the nanocomposite (Chow, 1978). The effect of highly anisotropic particles such as needles or nanoplatelets on composite polymer properties can be entirely different than of spherical fillers. Physical properties can completely change by the transition from microparticles to nanoparticles. For particles and fibers, the surface area per unit volume is inversely proportional to the diameter; the smaller the diameter, the greater the surface area per unit volume.

Clays (layered silicates), such as montmorillonite, have been widely investigated for the elaboration of polymer-based nanocomposites using various techniques (Alexandre and Dubois, 2000; Ray and Okamoto, 2003). Important features to be considered in these syntheses are the hydrophilic nature of clays and the strong solid-solid interactions that take place in-between the clay layers because they can prevent their dispersion in the polymer (Bordes et al., 2009).

### 2.5.1 Clays

Natural clays are available in large quantities in nature, spread all over the world (North Africa, Europe, Russia, China, USA...) and most deposits are exploited and commercialized. Clay minerals are mainly formed by dissolution and reprecipitation of preexisting minerals. The type of clay mineral which is formed, depends on the soil solution concentration of Si and Al resulting from the weathering of volcanic rock. In addition to the weathering process, some clay minerals are formed by hydrothermal activity. Thick clay deposits are usually formed as the result of a secondary sedimentary deposition process after they have been eroded and transported from their original location of formation. The commercially available products are often raw clays that usually contain impurities such as carbonates, cristobalite, feldspars, quartz, organic matter, iron hydroxides, etc. (Bergaya et al., 2012).

As previously mentioned, polymer nanocomposites are mainly elaborated from clay minerals which are a particular variety of silicates. Silicates constitute the largest class of natural minerals (about 30 % of all known minerals) and form the lithosphere, which is the crust of the Earth. The basic chemical unit of silicates is the  $(\text{SiO}_4)$ -based tetrahedra. Silicates are classified according to the connectivity of these arrangements of tetrahedra. In phyllosilicates (from the Greek word "phullon", which means "leaf"), condensation occurs in two directions to give infinite sheets of tetrahedra, but is limited in the direction perpendicular to the sheets (Bergaya et al., 2012).

In addition to the tetrahedra sheets which are denoted as "T" sheets, phyllosilicates contain octahedral, or "O" sheets, formed by the juxtaposition of  $(\text{MO}_4(\text{OH})_2)$  or  $(\text{MO}_2(\text{OH})_4)$  polyhedra, where the central cation can be  $\text{Li}^+$ ,  $\text{Mg}^{2+}$ ,  $\text{Fe}^{2+}$ ,  $\text{Fe}^{3+}$ ,  $\text{Al}^{3+}$ , etc.

Since the oxygens exposed on the surface of an octahedral (O) sheet are close to the terminal Si-O exposed by a tetrahedral (T) sheet, T-O condensation can occur. The result of this condensation is called a “layer”. All the clay minerals are composed of either TO or TOT layers. These TO and TOT layers are also called “1:1” and “2:1” types because one octahedral sheet is linked to one tetrahedral sheet, or sandwiched between two tetrahedral sheets, respectively (Brigatti et al., 2006).

Within this general structural framework, the phyllosilicates are subdivided in nine clay minerals groups which are listed below (Table 2.3). This classification in groups is based on the molecular-level order and does not allow predicting the larger-scale morphologies.

**Table 2.3 :** The nine groups of phyllosilicates (Bergaya et al., 2012).

<b>Group</b>	<b>Name</b>
I	The TO kaolinite and serpentine group
II	The TOT pyrophyllite and talc group
III	The TOT smectite group
IV	The TOT vermiculite group
V	The TOT true (flexible) micas and brittle micas group
VI	The TOT chlorite group
VII	The interstratified clay minerals group
VIII	The TOT sepiolite and palygorskite group
IX	The TO allophane and imogolite group

A specific feature of silicates is the easy substitution of the  $\text{Si}^{4+}$  by the  $\text{Al}^{3+}$  cation since both are similar in size. If one  $\text{Al}^{3+}$  occupies the place of one  $\text{Si}^{4+}$ , the structure will lack one positive charge to compensate the negative charges of the  $\text{O}^{2-}$  anions, leading to a localized negative charge at the point of substitution. These localized charges play a key role in the chemistry of aluminosilicates.

The pyrophyllite and talc groups, considered as the “leaders” of the TOT family, have neutral layers. But for the other clay mineral groups, high degrees of isomorphic substitutions can occur in the T and/or O sheets of the layers.

To maintain global electric neutrality, the negative charges of the layer are counterbalanced by an equal amount of positive charges provided by cations located between the layers. The variable negative charge amount from 0 (neutral) up to 2 per formula unit of the layers is a criterion for the phyllosilicates groups classification.



The negative layers, and compensating cations, alternate in a stacking in the c crystallographic direction. This means that the 2D layers can be separated from each other relatively easily and the volume between two successive layers is called the “interlayer space”. The different groups can be more or less recognized using their basal distances ( $d_{001}$ ) as a criterion. Although it is a rough method, it is often used due to its ease of implementation (Brigatti et al., 2006).

The table below (Table 2.4) presents the main clay minerals used for polymer nanocomposites elaboration with their typical composition and average basal spacing.

**Table 2.4 :** Classification and examples of clay minerals  
(Alexandre and Dubois, 2000).

Structure type	Group	Mineral examples	Ideal composition	Basal spacing (Å)
2:1 (TOT)	Smectite	Montmorillonite	$[(Al_{3.5-2.8}Mg_{0.5-0.2})(Si_8)O_{20}(OH)_4] Ex_{0.5-1.2}$	12.4 - 17
		Hectorite	$[(Mg_{5.5-4.8}Li_{0.5-1.2})(Si_8)O_{20}(OH)_4] Ex_{0.5-1.2}$	
		Saponite	$[(Mg_6)(Si_{7.5-6.8}Al_{0.5-1.2})O_{20}(OH)_4] Ex_{0.5-1.2}$	
2:1 (TOT)	Illite	Illite	$[(Al_4)(Si_{7.5-6.5}Al_{0.5-1.5})O_{20}(OH)_4] K_{0.5-1.5}$	10
2:1 (TOT)	Vermiculite	Vermiculite	$[(Al_4)(Si_{6.8-6.2}Al_{1.2-1.8})O_{20}(OH)_4] Ex_{1.2-1.8}$	9.3 - 14
1:1 (TO)	Kaolin-serpentine	Kaolinite, dickite, nacrite	$Al_4Si_4O_{10}(OH)_8$	7.14

In the case of smectites the basal distances are variable according to the hydration state. The most typical value is a little over 1.2 nm corresponding to one water layer between the clay mineral layers but the observed value depends on several factors; i) the nature of the interlayer cation which can have a higher or lower affinity for water; ii) the water activity, i.e. the relative water pressure and iii) the pretreatment to which the sample has been submitted (Bergaya et al., 2012).

Among the nine classically recognized groups (see Table 2.3), only three different clay minerals groups (kaolinite, smectite and sepiolite) are usually considered and reported for the elaboration of polymer/clay composites. Since the clay minerals from the kaolinite group are usually not considered as nanosized fillers (these non-swelling clays remain as aggregates of average dimension up to several microns), only members of the sepiolite-palygorskite and smectite groups will be discussed hereafter. From these two groups, sepiolite and montmorillonite clays will be considered more in details because of their widespread occurrence and/or frequent use in polymer/clay nanocomposite studies.

### 2.5.1.1 Sepiolite

Sepiolite is a non swelling, lightweight, porous clay with a large specific surface area and having particles of needle-like morphology.

Sepiolite is a hydrated magnesium silicate with the structural formula of  $\text{Si}_{12}\text{Mg}_8\text{O}_{30}(\text{OH})_4 \cdot (\text{OH}_2)_4 \cdot 8\text{H}_2\text{O}$ . Sepiolite has a higher surface area ( $384 \pm 7 \text{ m}^2/\text{g}$ ) carrying a high density of silanol groups ( $-\text{SiOH}$ ) and lower contact area between needles when it is compared to layered phyllosilicates. Since connections in the direction perpendicular to the layers are assured in part by covalent bonds ( $\text{Si-O-Si}$ ), sepiolite does not present swelling ability. The fibers of sepiolite have an average length of 1-2  $\mu\text{m}$ , a width of 0.01  $\mu\text{m}$  and contain open channels of dimensions  $3.6 \times 10.6 \text{ \AA}$  running parallel to the axis of the fibers (Figure 2.21).

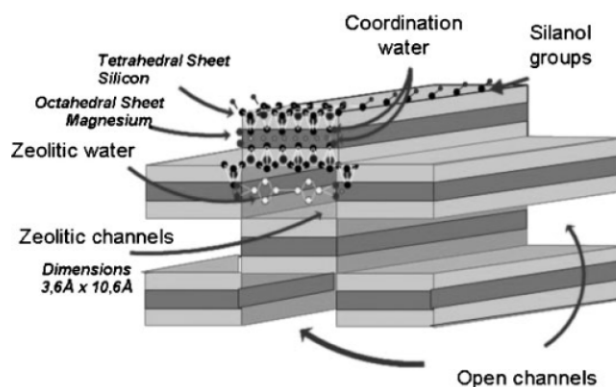


**Figure 2.21 :** Structure of sepiolite (Duquesne et al., 2007).

These nanostructured tunnels are filled of *zeolitic water* bonded by hydrogen bonds at the external surface or within the channels under ambient conditions. The terminal  $\text{Mg}^{2+}$  cations located at the edges of the octahedral sheets provide their coordination with the two other structural water molecules. These structural water molecules called as *coordination water* are in turn hydrogen-bonded to zeolitic water molecules (Duquesne et al., 2007; Tartaglione et al., 2008; Chivrac et al., 2010).

Palygorskite belongs to the same clay group and differs by its unit cell dimension, smaller for palygorskite than for sepiolite, leading to smaller channels. The name “attapulgite” which was given to a clay mineral discovered in fullers’ earth from Attapulgis (Georgia, USA), is often used as synonymous with palygorskite and is still largely used in industry (Wang and Sheng, 2005). Among the phyllosilicates, sepiolite shows the highest external surface area as it can reach about  $300 \text{ m}^2/\text{g}$ , and this explains why they are often used as industrial adsorbents. Due to these specific

properties, sepiolite is mainly used as a bleaching agent, filter aid, industrial absorbent, catalyst carrier and for clarification of beer and wine.

Despite the scarce occurrence of commercial deposits and the absence of swelling properties, sepiolites were recently used and are drawing increased attention as nanofillers in polymer nanocomposites because their particular morphology allows obtaining materials with interesting properties and performances (Bokobza and Chauvin, 2005; Duquesne et al., 2007; Chivrac et al., 2010).

### 2.5.1.2 Montmorillonite

In the smectite group, the layer charge varies from 0.2 to 0.6 per half unit cell. The morphology of TOT planar layers of smectites is 2-dimensional and the name comes from the Greek word "smektikos", whose initial meaning is “cleaning earth”. Smectites are also known as “swelling clays” because of their behavior in water. Montmorillonite (MMT) which is the most widely used filler in polymer clay nanocomposites, belongs to this group. MMT is the major component of the commercial bentonites.

Montmorillonite is a crystalline 2:1 layered silicate mineral with the general formula of  $(\text{Na,Ca})_{0.33}(\text{Al,Mg})_2(\text{Si}_4\text{O}_{10})(\text{OH})_2 \cdot n\text{H}_2\text{O}$ . It is composed of platelets formed of a central alumina octahedral sheet sandwiched between two silica tetrahedral sheets (Figure 2.22). The isomorphous substitutions found inside these clay platelets generate a negative charge which is naturally counterbalanced by inorganic cations ( $\text{Na}^+$ ,  $\text{Ca}^{2+} \dots$ ) located into the inter-layer spacing. This feature gives a hydrophilic character to the clay (Alexandre and Dubois, 2000).

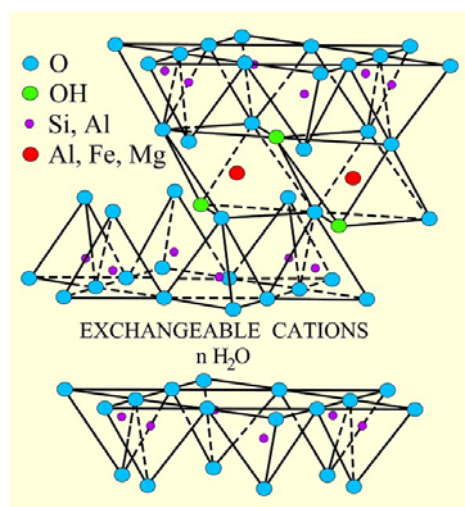


**Figure 2.22 :** Structure of montmorillonite.

Montmorillonite is proven to be effective as an adsorbent of heavy metals, toxins, and hazardous chemicals. It is also widely used in pharmacology for a variety of application, such as stabilization of suspensions and emulsions, viscosizing, adhesion to the skin, and tablet making. It is also used as drug carrier, or as part of a drug delivery system, such as for controlled drug release; including for gene delivery, and for drug targeting to specific tissues. It has shown itself useful in tissue engineering. It is also used for stability enhancement in drug and nutrient application, in the production of pharmaceuticals, e.g. as a catalyst (Malachová et al., 2009).

Smectites such as montmorillonites are particularly important in the nanocomposites technology, and the intercalation properties of the clay minerals have been mostly assessed on this group (see hereafter).

### **2.5.1.3 Organomodification of clays**

As previously mentioned, phyllosilicates, also called cationic clays, consist in 2-dimensional layers bearing a net negative charge which is compensated by an equivalent number of “exchangeable cations” located between the layers. The cationic exchange capacity (CEC) is defined as the number of cationic charges retained by a fixed mass of the clay mineral sample, generally either 1 g or 100 g. Therefore it is commonly expressed as (meq/g) or (meq/100 g), where “meq” stands for “milliequivalents”. The CEC is an important parameter of clay minerals and typical values are 80 to 120 meq/100g for smectites, 150 meq/100 g for vermiculites, 3 to 15 meq/100 g for kaolinites and 20 to 30 meq/100 g for palygorskite.

As the forces that hold together the platelet stacks are relatively weak, the intercalation of small molecules between the layers is rather easy. Intercalation in clay minerals can involve both inorganic and organic species and can occur from vapor, solutions, polymer melts or even in the solid state (from solid mixtures of the clay mineral and the intercalating species). It is quite obvious that intercalation phenomena are of primordial importance when studying clay mineral/polymers nanocomposites. In order to render these hydrophilic clays more organophilic, the hydrated cations of the gallery can be replaced by organic cations (Figure 2.23). The surface energy of the modified clay (called "organoclay") is lowered and becomes more compatible with organic molecules such as polymers.

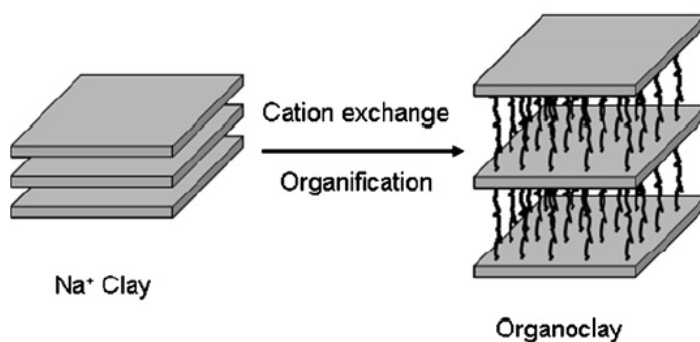


**Figure 2.23 :** Organoclay preparation (Chen and Yoon, 2005).

Modified bentonites called bentones are marketed in large amounts and they constitute an example of “organoclays”. Bentones are in fact clay minerals intercalated with different alkylammonium cations, generally from water solutions, and in this case the main adsorption mechanism is ion exchange.

Alkylammonium-intercalated clay minerals are composite materials in which the intercalation of organic molecules into clay minerals strongly modifies their properties, for instance changing them from hydrophilic to hydrophobic. There are several recent reviews in the field of organoclays (Lagaly et al., 2006; De Paiva et al., 2008; Bergaya et al., 2011).

For the elaboration of polymer/clay nanocomposites, various types of organo-modified montmorillonites (OMMT), either "home-made or commercially available", have been investigated. As previously mentioned, these clays are usually organo-modified with alkylammonium salts. Table 2.5 presents the characteristics of the main commercially available organoclays used for the preparation of polymer nanocomposites.

By changing the alkylammonium surfactant (number, length and type of alkyl chains and/or additional functional groups) it is possible to tune the organophilicity or polarity of the clay and thus its affinity towards the polymer matrix. Then, under appropriate experimental conditions, the polymer chains may be able to intercalate the interlayer space of the organoclay leading to polymer/clay nanocomposites.

**Table 2.5** : Commercial organomodified clays (Bordes et al., 2009).

Commercial clays	Clay type	Organomodifier type
Supplier/trade name/designation		
Southern Clay Products (USA)		
Cloisite <sup>®</sup> Na	CNa	MMT
Cloisite <sup>®</sup> 15A	C15A	MMT
Cloisite <sup>®</sup> 20A	C20A	MMT
Cloisite <sup>®</sup> 25A	C25A	MMT
Cloisite <sup>®</sup> 93A	C93A	MMT
Cloisite <sup>®</sup> 30B	C30B	MMT
Süd-Chemie (Germany)		
Nanofil <sup>®</sup> 804	N804	MMT
Laviosa Chimica Mineraria (Italy)		
Dellite <sup>®</sup> LVF	LVF	MMT
Dellite <sup>®</sup> 43B	D43B	MMT
CBC Co. (Japan)		
Somasif	MEE	SFM
	MAE	SFM

Tallow: ~65% C<sub>18</sub>; ~30% C<sub>16</sub>; ~5% C<sub>14</sub>

### 2.5.2 Polymer/clay nanocomposites

As already mentioned, among the different types of clays, the 2:1 phyllosilicates from the smectites family are the minerals most widely used for the preparation of nanocomposites. However, fibrous clay minerals such as sepiolite and palygorskite can also constitute the inorganic nanofiller dispersed in the polymeric matrix.

Historically, the first reason to add nanoclay fillers to polymers was to reduce costs as compared to other commonly used fillers such as calcium carbonates. It took some time before realizing that clays, these cheap materials, could also be smart materials.

It has appeared many times that the addition of a few percent of incorporated clay minerals can provide spectacular improvements as compared to the properties of the raw polymer, or to gain new properties not observed for the neat polymer alone. Since then it has also been demonstrated that the final material properties highly depend on the nanocomposite morphology and thus on the elaboration route.

### 2.5.3 Elaboration routes and morphologies of polymer/clay nanohybrids

For the preparation of nanocomposites three main methods can be mentioned: (i) the solvent intercalation route where layered silicates are swollen in a polymer solvent to enhance the diffusion of macromolecules in the clay interlayer spacing (ii) the in-situ intercalation method for which the layered silicates are swollen in the monomer or monomer solution before polymerization, and (iii) the melt intercalation process consisting in polymer processing in the molten state, such as extrusion, to disperse the clay particles (Bordes et al., 2009).

Different nanocomposite structures (Figure 2.24) can be formed: (i) a microcomposite where the clay layers remain stacked onto each other and the polymer is not intercalated within the (O)MMT's layers due to poor polymer-clay affinity, a material presenting a phase separation; (ii) an intercalated nanocomposite where the polymer is partially intercalated between the silicate layers which still remain stacked but the interlayer spacing has increased; (iii) an exfoliated nanocomposite showing individual and well-dispersed clay platelets within the matrix, the layered structure is not observed anymore (Bordes et al., 2009).

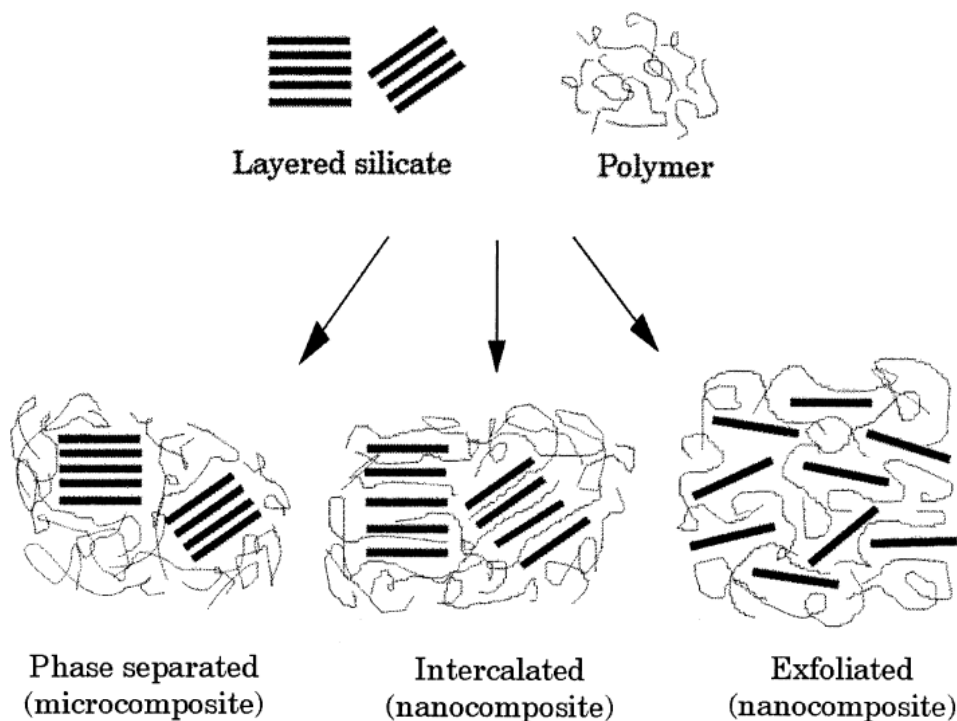


**Figure 2.24 :** Scheme of the three main different types of polymer/layered silicate composite structures : (a) phase separated microcomposite; (b) intercalated nanocomposite and (c) exfoliated nanocomposite (Alexandre and Dubois, 2000).

#### **2.5.4 Biopolyester/clay nanohybrids**

In the last 25 years, an important development in polymeric nanocomposites has been observed. In the early 1990s, Toyota Central Research Laboratories in Japan has reported a work on a Nylon-6 nanocomposite in which an important improvement in thermal and mechanical properties has been reached by a very small amount of nano filler loading. There has been since a large variety of polymer systems used for the preparation of nanocomposites.

Polystyrene (PS), polyamides (PA), polycarbonate (PC), polyesters, polyethylene oxide (PEO) and ethylene oxide copolymers, polyolefins such as polypropylene (PP), polyethylene (PE), copolymers such as poly(ethylene-co-vinylacetate) (EVA), ethylene propylene diene rubber (EPDM), poly(1-butene), polybutadiene, butadiene copolymers, epoxidized natural rubber, polyurethanes (PU), epoxy polymer resins (EPR), phenolic resins, etc. have been used to obtain nanocomposites (Sinha Ray and Okamoto, 2003b).

Nowadays, due to environmental concerns researchers tend to work with biodegradable polymers instead of polyolefins, polystyrene and poly (vinyl chloride) produced from fossil fuels. Several studies deal with the preparation and characterization of biodegradable polymers/layered silicate nanocomposites having properties suitable for a wide range of applications (Nikolic et al., 2012).

So far, the preparation of nanocomposites based on biodegradable polymers also called nanobiocomposites has been reported for polylactide (PLA), polycaprolactone (PCL), poly(hydroxybutyrate) (PHB) and poly(hydroxybutyrate-co-valerate) (PHBV), poly(butylene succinate) (PBS), poly(butylene succinate-co-adipate) (PBSA), aromatic copolyesters, polysaccharides, proteins, etc. (Bordes et al., 2009; Chivrac et al., 2009; Avérous and Pollet, 2011; Avérous and Pollet, 2012b).

Among these polymers, a great number of the published studies concern polylactide (PLA) and polycaprolactone (PCL).

##### **2.5.4.1 PCL/clay nanobiocomposites**

First studies on biopolymer/clay nanocomposites were conducted by Giannelis' group from Cornell University (USA) who worked on the elaboration of PCL-based nanocomposites by intercalative polymerization (Messersmith and Giannelis, 1993).



They have proved that polymer–clay chemical interactions at the interface were strong and the intercalation of the polymer was irreversible. A phenomenon revealing a decrease in the *d*-spacing was observed after polymerization which was further attributed to the reorganization of intercalated molecules during the transition from monomer to polymer structure. Parallel observations have been declared later by Kiersnowski's group for the PCL-based composites prepared by in-situ polymerization catalyzed by water (Kiersnowski and Piglowski, 2004; Kiersnowski et al., 2004).

Messersmith and Giannelis (1995) have also worked on PCL-based nanocomposites by in-situ polymerization, dealing this time by thermal activation and initiation by an organic acid. The protonated form of 12-aminododecanoic acid ( $\text{NH}_3^+(\text{C}_{11}\text{COOH})$ ) was used as the organomodifier at the surface of the OMMT. By its nucleophilic attack to the carbonyl group of  $\epsilon$ -CL, ROP was initiated. Synthesized PCL was by this way ionically bound to the silicate layers through the protonated amine chain-end. XRD results confirmed the dispersion of individual silicate layers within the polymer matrix, contrary to this, in the case where less polar ammoniums were used as organomodifier at the clay surface, no dispersion was observed in CL or PCL.

Research groups then investigated possible interactions occurring at the interface of a PCL/OMMT exfoliated nanocomposite (Messersmith and Giannelis, 1995; Pucciariello et al., 2004). The crystallinity, permeability and the rheological behavior of such structures were examined. It has been reported that both crystallinity and crystal size decreased due to dispersed silicate layers which act as physical barriers and hinder the PCL crystal growth. By the dispersion of 4.8 vol% of silicate, water permeability of the nanocomposite has also been reduced.

Dubois' group (Mons, Belgium) has developed different studies on the in-situ ROP of  $\epsilon$ -CL and in the melt intercalation route (Benali and Dubois, 2012). They correlated the formation of PCL-based nanocomposites with not only by the presence of ammonium cations and related functionalities, but also with the elaboration route. They prepared PCL-based nanocomposites by in-situ ROP according to a “coordination-insertion” mechanism (Kubies et al., 2002; Viville et al., 2003). The OMMT organomodified by alkylammonium bearing hydroxyl groups ( $\text{MMT-N}^+(\text{Me})_2(\text{EtOH})(\text{C}_{16})$  or  $\text{MMT-N}^+(\text{Me})(\text{EtOH})_2(\text{tallow})$ ) was swollen and then an

initiator/ activator such as tin(II) octoate ( $\text{Sn}(\text{Oct})_2$ ), dibutyltin- (IV) dimethoxide ( $\text{Bu}_2\text{Sn}(\text{OMe})_2$ ) or triethylaluminium ( $\text{AlEt}_3$ ) was added.

By this way the ammonium is activated and surface grafted PCL chains can be obtained. From each hydroxyl function a PCL generation can be expected (Figure 2.25).

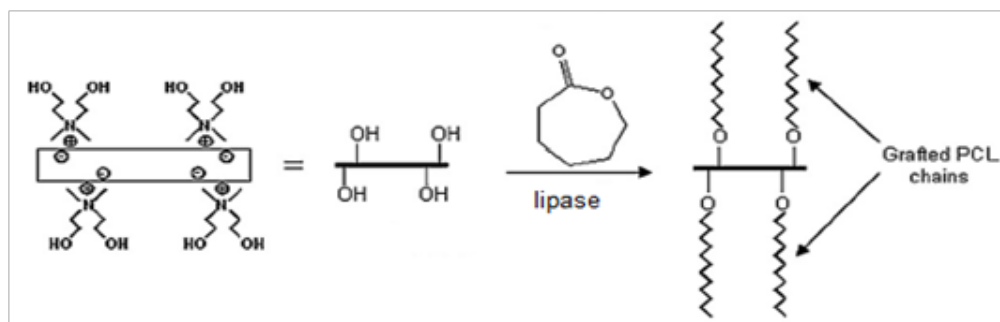


**Figure 2.25 :** Illustration of PCL chain grafting on clay, for the case of organomodified montmorillonite.

So in the presence of high hydroxyl groups content, average molar masses of PCL chains would be lower. In the presence of tin(IV) catalysts which are more efficient towards  $\epsilon$ -CL ROP, the procedure takes place in milder conditions compared to  $\text{Sn}(\text{Oct})_2$  (Pantoustier et al., 2002). In both cases, a continuous decrease in molar masses of nanocomposites is observed with clay concentration. This phenomenon is explained by the presence of -OH functions, which can act both as co-initiator and chain transfer agent. At the end of this in-situ polymerization process, well-exfoliated PCL based nanocomposites with 3 wt% of clay content and partially exfoliated/partially intercalated structures with higher clay content (10 wt%) were observed. Besides, nanocomposites which were filled with non-hydroxyl functional clays showed only intercalated structures (Pantoustier et al., 2003).

Polymer chain lengths can be estimated and controlled by clay loading considering that  $\epsilon$ -CL polymerization is initiated by -OH groups. But the clay content must be limited to some extent not to obtain too short PCL chains. This problem can be avoided by adjusting the number of -OH groups, e.g by modifying the clay surface by a mixture of non-functional alkylammonium and monohydroxylated ammonium cations (Lepoittevin et al., 2002b-c, Viville et al., 2004). By this way, Dubois and coworkers succeeded to control the inorganic content, the quantitative surface grafting, the number of polyester chains per clay surface as well as the polymer chain length and molecular weight distribution using this in-situ intercalative method.

Viville et al. (2004) have also focused on the morphology of PCL grafted chains on the silicate layer surface depending on the OH content. They have demonstrated that the grafting density has drastically increased as the proportion of OH-substituted alkylammonium cations used to organomodify the clay have increased. It was assumed that a phase separation process occurred between the ammonium ions induced by the polymerization reaction because of the formation of separate polymer islands in the low OH systems. Starting only from 50% OH content that a homogeneous coverage and a subsequent thickening were reached. Adjacent platelets became then fully independent of each other, favoring exfoliation.

Eventually, when PCL was associated by the melt intercalation route to OMMT bearing quaternary ammonium salts, intercalated or intercalated/exfoliated structures could be obtained (Lepoittevin et al., 2002a). Contrarily, with the usage of MMT- $\text{Na}^+$ , just microcomposite structures could be formed since no interlayer gap was observed. Thus, contrary to the in-situ intercalative process, complete exfoliation could not be reached by the melt intercalation route whatever the OMMT considered.

Nonetheless, with 3 wt% of clay, the tensile and thermal properties of the nanocomposites were improved. In the presence of higher than 5 wt% of OMMT content, the elongation break of the composite materials dropped off due to the aggregation of clays (Pantoustier et al., 2001; Lepoittevin et al., 2002a). Kwak and Oh (2003) have reported a shift of 60 °C on the degradation temperature towards higher temperatures with the addition of 1 wt% of clay, while this temperature shift was only of 30 °C in the case of 10 wt% of clay. It has been concluded that at low clay content (<5 wt%), PCL nanocomposites can show high stiffness, good ductility and improved stability.

Afterwards, Di et al. (2003) were the lonely ones having declared reaching an exfoliated state with PCL/Cloisite30B systems prepared by direct melt intercalation in the presence of 2 to 5 wt% of clay. Besides great enhancements in thermal and mechanical properties, isothermal crystallization results indicated that the well dispersed organoclay platelets have acted as nucleating agents, also affecting the crystal quality by the restricted chain mobility.

In light of these studies, an elaboration route combining in-situ  $\epsilon$ -CL polymerization and material redispersion by melt intercalation was aimed to overcome the deficiency

of the direct melt intercalation towards effective clay dispersion. These types of masterbatch processes allowed yielding intercalated/exfoliated structures which are difficult to obtain by direct melt blending (Lepoittevin et al., 2003, Shibata et al., 2007).

As it can be seen from the mentioned studies, PCL based nanocomposites have been widely studied and several well controlled mechanisms have been settled to reach the exfoliated state. Among them, the solvent intercalation route did not seem to provide satisfactory results in terms of structure (Jimenez et al., 1997). Aside from this exception, the elaboration of such nanocomposite materials assumes to be very useful not only for the enhancement of PCL properties but also for other thermoplastic materials.

In contrast to all these works, few studies have been reported related to sepiolite/biopolyesters nanocomposites. However, Duquesne and coworkers, recently reported the dispersion of sepiolite in PCL as biodegradable aliphatic polyester matrix. Since PCL is known to show high ductility but also rather low intrinsic rigidity, it is expected that by finely dispersing a needle-like nanoclay as sepiolite within this polyester a better stiffness/toughness performance can be attained (Duquesne et al., 2007).

$\epsilon$ -CL ROP was catalyzed by  $\text{Sn}(\text{Oct})_2$  in toluene at 100 °C in the presence of amino modified sepiolite. At the end of the reaction, PCL/sepiolite crude nanohybrids were recovered and non-grafted PCL chains were removed by selective solubilization. Parallel to this, PCL/sepiolite nanocomposites were also prepared by melt blending. PCL/sepiolite nanohybrids containing around 58 wt% of grafted PCL chains have been redispersed within PCL in order to reach 3 wt% of organic filler in the final PCL/sepiolite nanocomposite product.

The addition of the PCL/Sep nanohybrids allowed an increase in the stress measured at the yield point to about 22-23 MPa (18.4 MPa for the neat PCL). Besides, the Young's modulus increased from 383 MPa (for unfilled neat PCL) to 510 MPa. This increase in stiffness could not have been explained by the finer dispersion of the nanofillers because a same trend and quality of dispersion have been observed from the SEM images for both PCL/Sep nanocomposites and PCL/Sep nanohybrids/Sep nanocomposites. It has been assumed that for the nanocomposites with dispersed

PCL/Sep nanohybrids, strong interactions such as chain entanglements or co-crystallization of grafted PCL chains with the PCL matrix could strengthen the nanoparticle/matrix interphase and thus the stiffness of the material (Duquesne et al., 2007).

#### **2.5.4.2 PLA/clay nanobiocomposites**

With its good mechanical properties, thermal plasticity and biocompatibility, PLA is a very promising material. But, its flexural properties, gas permeability and heat distortion temperature remain low, limiting its widespread usage for several applications. With an effort to reach exfoliation state in PLA/ clay nanobiocomposites, various organoclays with different modifier groups have been selected and several elaboration routes have been tested by a lot of research groups (Okamoto, 2012).

Ogata et al. (1997) have first tried to elaborate PLA-based nano-biocomposites by the solvent intercalation method but rather than obtaining individual well dispersed layered silicates they observed tactoids consisting of several stacked silicate monolayers. Even though an increase in the material's Young's modulus was reported with increasing clay content, this augmentation remained small compared to conventional nanocomposites.

Later on, Chang et al. (2003) dealt with the influence of the layered silicate aspect ratio (montmorillonite, fluorinated synthetic mica) of the organomodifier and of the clay content on the nanofiller dispersion into PLA matrix. It has been demonstrated that with only a small amount of nanofiller, intercalated structures leading to better mechanical and barrier properties can be obtained. Ultimate strength increase compared to neat PLA was recorded for the nanocomposite. Nevertheless, this mechanical enhancement was limited to a small range of clay content up to 4-6 wt% depending on the organomodifier type. Above these clay contents, a decrease in properties was observed due to the formation of silicate agglomerates.

Krikorian and Pochan (2003) were finally successful in the preparation of exfoliated materials with randomly distributed clay platelets (Cloisite<sup>®</sup> 30B) by the solvent intercalation method. It has been assumed that hydroxyl groups present at the long alkyl chain ends of the organomodifier at the surface of Cloisite<sup>®</sup> 30B interact with

the C=O moieties of PLA backbone and this interaction favors the exfoliation. A significant improvement in mechanical properties was also reported.

Okamoto and his group at Toyota Technological Institute (Japan) widely described the elaboration of PLA/clay nanocomposites by melt intercalation (Sinha Ray et al., 2002a-c; 2003a-e; Sinha Ray and Okamoto, 2003a-b; Okamoto, 2012). Different systems were tested by changing the aspect ratio of the inorganic platelets, the nature of the organomodifier and the clay content. Various systems composed of intercalated, intercalated-and-flocculated, nearly exfoliated, coexistence of intercalated and exfoliated states were obtained depending on the parameters. In spite of the fact that the total exfoliation could not be reached, all elaborated nanobiocomposites showed betterments in various material properties as mechanical and flexural properties, heat distortion temperature, O<sub>2</sub> gas permeability.

In order to reduce the brittleness and to provide the flowability during the process, research groups were interested in developing plasticized PLA-based nanocomposites. For this, PLA plasticized with PEG (Paul et al., 2003b) or diglycerine tetraacetate (Shibata et al., 2006) were melted and mixed with different organoclays leading to intercalated structures. It has been showed that there is a real competition between PEG and PLA to intercalate into the clay interlayer (Paul et al., 2003b; Pluta et al., 2006).

Paul et al. (2005) have settled a protocol describing the in-situ polymerization of lactide from end-hydroxylated PEG in presence of Cloisite<sup>®</sup> 30B with the initiation of the Sn(Oct)<sub>2</sub>. This coordination-insertion method led to PLA chains grafted onto the clay surface via hydroxylated ammonium organomodifier and to PLA-b-PEG-b-PLA triblock copolymer intercalated into the clay gallery. The plasticizing effect was ensured by PEG sequence in the triblock without any phase separation.

This mechanism allows the complete exfoliation by ROP of lactide after adequate activation (Paul et al., 2003a). In the case where the reaction was activated by triethyl aluminium (AlEt<sub>3</sub>), the polymerization was initiated by the hydroxyl groups of the organomodifier of the clay. PLA/OMMT nanocomposites synthesized by this way exhibited enhanced thermal properties; T<sub>g</sub> and T<sub>m</sub> values were not affected by the presence of the clay but the crystallinity was affected due to restricted mobility of the resulting grafted chains.

Many other studies can be found in literature reporting application of PLA-based nanocomposites for preparation of porous ceramic materials or for scaffolds as supports for tissue regeneration (Lee et al., 2005). Foams elaborated from PLA/OMMT nano-biocomposites are also reported with the aim to obtain high cell density and controlled morphology for growing cells (Ema et al., 2006). Different multiphased systems have been tested, such as plasticized PLA, to modify the behavior of the matrix and to develop new properties (Martino et al., 2010; Martino et al., 2011).

Literature offers a wide diversity about the applications of PLA/clay based nanocomposites as well as strategies to improve material properties since PLA is commercially and largely available (Okamoto, 2012).

## **2.6 Main Conclusions of The Bibliographic Review and Objectives of The Present Study**

It can be observed from the literature review presented here that there is a marked and growing interest on bio-based and biodegradable polymers to respond to the sustainable development approaches. In recent years, important researches have been conducted on the development of new synthesis routes for polyesters, such as PCL and PLA, to render these materials “greener”, more sustainable and environmentally friendly by replacing the organo-metallic catalysts by organic systems or even enzymatic catalysts.

It has been seen that CALB and its immobilized forms are regarded as the best enzymatic catalytic systems for esterification reactions for PCL synthesis in non aqueous media. On the other hand, for the synthesis of PLA, CALB does not show the same performant activity and more generally lipases display marked selectivity depending on the lactide isomer and thus important differences of activity. Contrary to PCL, only a few studies have been published on PLA synthesis by enzymatic ROP and contradictory results are often reported for the different types of lactide isomers.

Recent researches are conducted to find alternative enzymatic systems which could compete with CALB or to improve the catalytic systems by working on CALB immobilization using different types of supports. In this context, the use of inorganic supports such as clays, providing large specific surface area for enzyme adsorption,

appears as a promising way to improve the thermal and mechanical stability of the enzymatic catalysts. In addition, these clays are widely studied and used as nanofillers for the elaboration of nano-biocomposites based on biopolymers. Especially, the production of organic/inorganic nanohybrid systems involving PCL, PLA and clays is of growing interest.

The objective of this thesis is to use and develop original catalytic systems based on lipases which are efficient for the synthesis of biopolyesters and allowing the preparation of organic/inorganic nanohybrids based on clay nanoparticles grafted with such polyesters.

For this,  $\epsilon$ -caprolactone ( $\epsilon$ -CL) polymerization catalyzed by *Candida antarctica* lipase B (CALB) will be carried out in the presence of montmorillonite and sepiolite clay to obtain organic/inorganic nanohybrids through polymer chain grafting and growth from the surface of the clay. The natural and organomodified forms of these clays will be also used as lipase supports. Free form, commercial resin-immobilized form (NOV-435) and clay-immobilized forms of CALB will be tested as catalytic systems and their efficiency compared. The polymerization kinetics and resulting products will be fully characterized with NMR, SEC, DSC, TGA, SEM and FRX analyses.

The first steps of the study will consist in testing and defining the most appropriate experimental techniques and operational conditions proper to the synthesis of polycaprolactone (PCL) by enzymatic ROP. Polymerization reactions will be catalyzed by commercial enzymatic systems as CALB immobilized on acrylic resin (NOV-435) and its equivalent free lipase. Once this step will be achieved, optimization of operational conditions for the synthesis of biopolyesters in organic solvent and in bulk will be performed by analyzing the effect of temperature, concentration of the reactants and reaction time. This part will be essentially based on the determination of the polymerization reactions' kinetics and characterization of the obtained polyesters in terms of molecular weights.

As a second task, an important work will be carried out on the development of original catalytic systems obtained by immobilization of lipases on inorganic clay nanoparticles, i.e natural and modified forms of sepiolite and montmorillonite. Different conditions for immobilization will be tested and resulting lipase/clay



systems characterized, selected and optimized in function of their performances with respect to the planned polymerization reaction. Finally, the more efficient catalytic systems identified will be tested for the elaboration of organic/inorganic nanohybrids.

The global strategy of the study is schematized as follows in Figure 2.26:

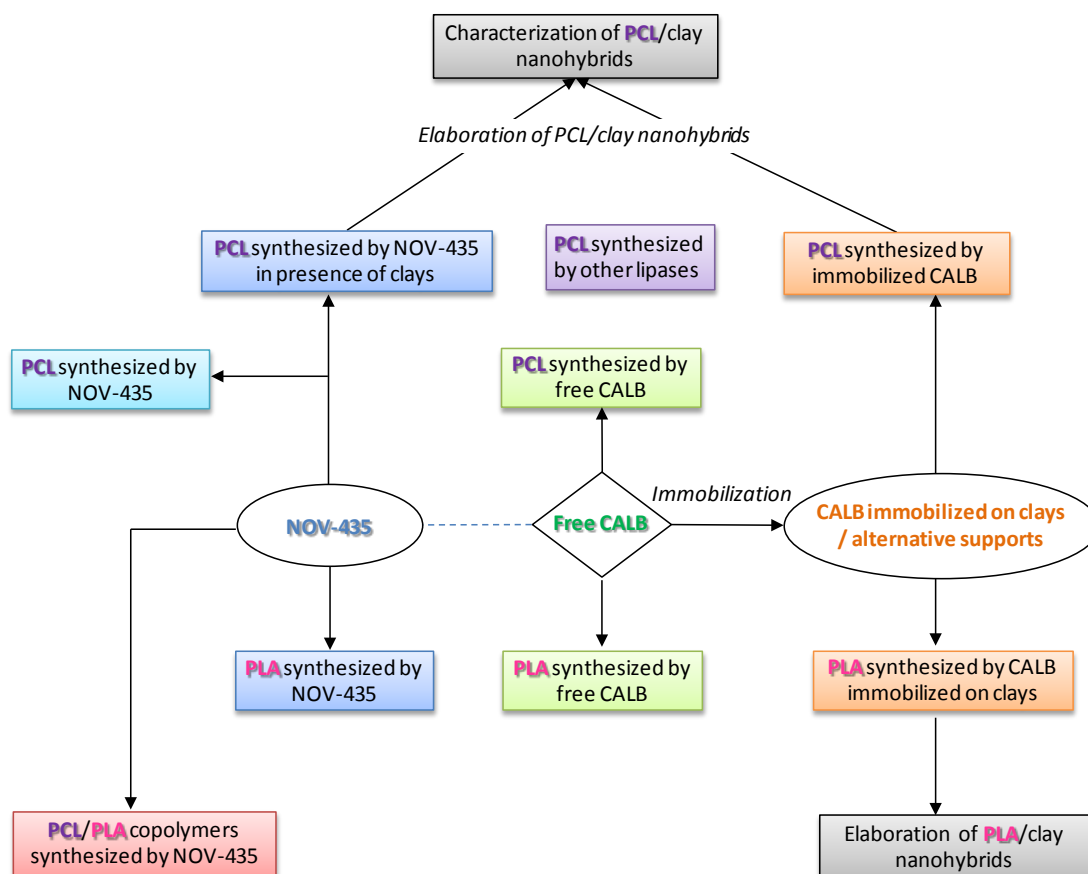


**Figure 2.26 :** Schematic representation of the performed studies.

The chosen approach is thus to elaborate such nanohybrids using the "grafting from" strategy by promoting the polyesters chain anchoring and growth directly from the hydroxyl groups present at the surface of clay nanoparticles and thus in direct vicinity of the immobilized lipase. This original route will be compared to the more direct one performed by conducting the "grafting from" polymerization using the NOV-435 catalyst in presence of corresponding clays in the reaction medium. With the intention of evidencing the effective grafting of PCL chains at the clay surface, thermogravimetric analyses will be performed on the selectively separated fractions of the obtained nanohybrids.

In parallel, lipase-based catalytic systems will be also tested for the polymerization of the lactide D-, L- and D/L- isomers, focusing on the possible selectivity of the enzyme toward the different types of isomers. Finally, copolymerization reactions between  $\epsilon$ -caprolactone and the lactide isomers will be performed using the NOV-435 catalytic system with the aim to obtain PCL/PLA copolymers.



### 3. MATERIALS AND METHODS

#### 3.1 Materials

Sepiolite (SEP) used in this study is a commercial clay (non organo-modified) supplied by Tolsa (Spain) under the tradename Pangel<sup>®</sup> S9. MMT-Na<sup>+</sup> is a commercial sodium montmorillonite clay supplied by Southern Clay Products (Texas, USA). Cloisite<sup>®</sup> 30B is a commercial montmorillonite clay organo-modified by methyl bis(2-hydroxyethyl) (tallow alkyl) ammonium salts and supplied by Southern Clay Products (Texas, USA). The organo-modifier content of this clay is approximately 20 wt% as attested by thermogravimetry analysis. Each organo-modifier molecule bears two hydroxyl groups. A "home-made" organo-modified sepiolite with methyl bis(2-hydroxyethyl) (tallow alkyl) ammonium was prepared from the non-modified sepiolite as described in section 3.2.4.

Novozym<sup>®</sup> 435 (NOV-435), immobilized form of *Candida antarctica* lipase B (CALB) was purchased from Aldrich. The free form (not immobilized) of CALB, received as an aqueous solution, was kindly provided by Novozymes and was used after dialysis and lyophilization. Lipase basic kit (Sigma-Aldrich) containing lipases isolated from *Rhizopus arrhizus*, *Rhizopus niveus*, porcine pancreas, *Pseudomonas cepacia*, *Aspergillus species*, *Candida antarctica*, *Candida rugosa*, *Mucor mihei*, *Pseudomonas fluorescens* was used to test various types of lipases.

$\epsilon$ -caprolactone ( $\epsilon$ -CL) (99%, Acros) was dried and stored over molecular sieves before polymerization. Anhydrous toluene was freshly distilled over sodium under nitrogen atmosphere. The isomers of lactide; D-lactide, L-lactide and D/L-lactide were obtained from Purac with the commercial name of Purasorb<sup>®</sup>.

Bovine serum albumin (BSA) and *p*-nitrophenyl butyrate (*p*NPB) both from Sigma Aldrich and dye reagent from Bio-Rad were used for protein assay measurements and lipase hydrolytic activity determinations.

## 3.2 Methods

### 3.2.1 Measurement of lipase activity

The assay was performed by measuring the increase in absorbance at 410 nm, produced by the release of *p*-nitrophenol (*p*NP) resulting from the hydrolysis of the *p*-nitrophenyl butyrate (*p*NPB) substrate. To start the test, 100 µl of enzyme solution was added into 900 µl of substrate solution (5mM *p*NPB in 25 mM sodium phosphate buffer; pH 7.0) found in a spectrophotometer cuvette. Absorbance values were recorded at 410 nm, with Genesys10 Bio UV-Visible spectrophotometer at determined time intervals. The enzymatic activity is deducted from the slope of the linearized curve of absorbance vs. time graphic and molar extinction coefficient of *p*NP.

One unit of enzyme activity (A) was defined as 1µmol of *p*NP liberated in one minute by 1 ml of enzyme solution at ambient temperature (1U/ml= 1µmol *p*NP /min.ml). Enzyme activity was calculated according Equation 3.1.

$$A \text{ (U/ml)} = [(\Delta \times 1000 \times V_{\text{total}}) / (\epsilon \times V_{\text{enzyme}})] \times \text{dilution coefficient} \quad (3.1)$$

where

$\Delta$ : slope of the liberation kinetics of *p*NP (absorbance unit at 410 nm/min)

$V_{\text{total}}$ : total volume of reaction (1 ml)

$\epsilon$ : molar extinction coefficient of *p*NP in reaction conditions = 2126

(absorbance unit at 410 nm.l.mol<sup>-1</sup>.cm<sup>-1</sup>)

$V_{\text{enzyme}}$ : volume of enzyme solution (0.1 ml)

dilution coefficient: dilution factor of the enzyme solution.

### 3.2.2 Determination of the protein content

To determine the efficiency of lipase immobilization on the clay supports, protein content in each step was analyzed. Protein content was estimated according to Bradford's method using Bio-Rad protein dye reagent and bovine serum albumin (BSA) as a standard (Bradford, 1976). The amount of bound protein was calculated from the difference between the loaded protein amount and the protein amount present in the supernatants determined by Bio-Rad protein assay procedure.

The Bradford's method is a colorimetric protein assay which is based on the absorbance shift of Coomassie Brilliant Blue G-250 dye. In acidic conditions, by binding to the protein which is assayed, the red form of this dye is converted into its blue form. During the formation of this complex, the red form of Coomassie dye first donates its free electron to the ionizable groups on the protein, which causes a disruption of the protein's native state, by this way hydrophobic pockets of the enzyme become exposed. These pockets then bind non-covalently to the non-polar region of the dye via Van der Waals forces, positioning the positive amine groups in proximity with the negative charge of the dye. The bond is further strengthened by the ionic interaction between the two charges.

The bound form of the dye has an absorption spectrum maximum at 595 nm. While the cationic (unbound) forms of the dye are green or red, the binding of the dye to the protein stabilizes the blue anionic form. The increase of absorbance at 595 nm is proportional to the amount of bound dye, and thus to the amount (concentration) of protein present in the sample.

Microassay procedure proposed by Bio-Rad was used to determine protein concentrations in a range of 5-25 µg/ml. 800 µl of each sample solution were put into spectrophotometer cuvettes and 200 µl of dye reagent concentrate were then added to each cuvette. Mixtures were incubated at room temperature for at least 5 min for color development. Absorbance values were measured at 595 nm. All readings were carried out in duplicate. Protein concentration for each sample was calculated using Equation (3.2) obtained from the plotted BSA standard curve (Figure 3.1).

$$\text{Protein concentration (}\mu\text{g/ml)} = (\text{OD}_{595} - 0.0053) / 0.0432 \quad (3.2)$$

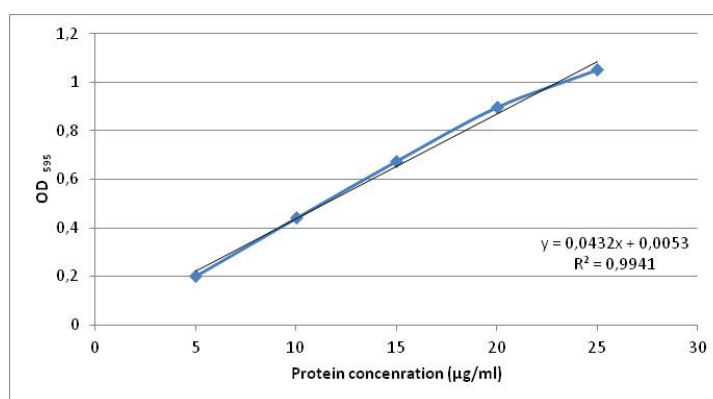


**Figure 3.1 : BSA standard curve.**

### 3.2.3 Immobilization of lipase

Both non-modified and organo-modified forms of sepiolite and montmorillonite were used as inorganic supports. Determined amounts of dialyzed CALB enzyme solution were added onto previously weighted supports prepared as suspensions in 0.1 M sodium phosphate buffer solution (pH 7.0). Mixtures were stirred for 2 h at 4 °C. At the end of this procedure, clay-enzyme suspensions were centrifuged at 6000 rpm for 20 min (at 4 °C) with Beckman-Coulter Avanti series centrifuge. The centrifugation pellets were washed two times by the buffer solution to remove loosely-bound enzymes. The supernatants were tested for their protein content and enzymatic activity. The collected solid composed of CALB adsorbed on inorganic support was lyophilized for 48 h and the resulting immobilized enzyme derivatives were stored at 4 °C, under vacuum in a desiccator.

The efficiency of immobilization was evaluated in terms of protein loading as follows (Equation 3.3):

$$\text{Immobilization (\%)} = \left( \frac{\text{amount of fixed protein}}{\text{amount of loaded protein}} \right) \times 100\% \quad (3.3)$$

In order to obtain powdery catalysts, the derivatives (CALB immobilized onto clay) recovered as a paste after immobilization, due to the swelling of clays in the buffer solution, were subjected to a lyophilization step. They were firstly frozen at -80 °C for three hours. Resulting frozen samples were immediately lyophilized in Christ-Alpha 2-4 LD plus lyophilizator for one or two days, depending on the sublimation rate of the aqueous buffer, prior to their usage as catalyst in polymerization reactions.

### 3.2.4 Surface modification of clays

To modify the natural sepiolite surface by the same organo-modifier (methyl bis(2-hydroxyethyl) (tallow alkyl) ammonium salts) of Cloisite 30B, the procedure described below was used.

5 g of sepiolite “Pangel<sup>®</sup> S9” was suspended in 250 ml of deionized water and dispersed in an ultrasonic bath for 4 h at 60 °C. Calculated amount of Ethoquad O/12 (methyl bis(2-hydroxyethyl) (tallow alkyl) ammonium salt) commercial solution was added to the sepiolite suspension and the mixture was left in the ultrasonic bath for one day at 60 °C. At the end of this time, the mixture was filtered and washed with 2 L of distilled water at 60 °C to remove the formed NaCl salt and excess

ammonium. Finally, resulting sludge was lyophilized to get powdered organomodified-sepiolite.

### **3.2.5 Polymerization reactions**

#### ***$\epsilon$ -CL polymerization setup***

All reactions were carried out in dry toluene at 70 °C. Predetermined amounts of catalysts, NOV-435, lyophilized free CALB or immobilized CALB derivatives (i.e CALB immobilized on nanoclays) were introduced into previously dried Schlenk tube under an inert dry nitrogen atmosphere. The tube was immediately capped with a rubber septum. Toluene and  $\epsilon$ -CL were transferred with a syringe through rubber septum caps. The reaction tube was then immersed in a heated oil bath and the polymerization reaction was allowed to proceed. An aliquot was withdrawn at specified time intervals to monitor the polymerization reaction progress. Reactions were terminated by dissolving the reaction mixture in chloroform and removing the catalyst by filtration. Chloroform in the filtrate was then stripped by rotary evaporation at 35 °C. The polymer in the resulting concentrated solution was precipitated in cold methanol (previously stored at -20 °C). The polymer precipitate was separated by filtration and dried overnight at 30 °C under vacuum.

#### ***Lactide polymerization setup***

In a typical experiment, 1 g of lactide was first heated in a capped reaction tube under inert dry nitrogen atmosphere, to ensure the total melting of the monomer, to respectively 115 °C for D- or L-lactide and 130 °C for D/L-lactide. Once the powdery form of the lactide became liquid, freshly distilled toluene was added into the tube connected to a cooling unit refrigerated by water. The temperature was subsequently decreased to the reaction temperature (70 °C). When 70 °C was reached, a determined amount of enzyme was introduced and the polymerization was started. At the end of the polymerization, the resulting highly viscous mixture is dissolved in chloroform and the catalyst is removed by filtration. Chloroform in the filtrate was then stripped by rotary evaporation at 30 °C. The polymer in the resulting concentrated solution was precipitated in cold methanol to ensure the recovery of the shortest PLA chains. The polymer precipitate was separated by filtration and dried overnight at 25 °C under vacuum.



### ***Copolymerization reactions setup***

In the first type of copolymerization reaction, where 1 g of  $\epsilon$ -CL and 1 g of lactide were reacted at the same time, lactide monomer was first melted, then freshly distilled toluene was added into the tube and the temperature was subsequently decreased to the reaction temperature (70 °C). When 70 °C was reached, determined amount of enzyme and  $\epsilon$ -CL was introduced and the copolymerization was started. In the second type of reaction,  $\epsilon$ -CL was first polymerized for 2 hours with typical reaction conditions and procedures, then premelted lactide monomer solution in toluene was transferred to the reaction tube. By this way the copolymerization with previously formed PCL chain was carried out.

### **3.2.6 Nanohybrid synthesis**

Reactions were performed with the same procedure described above except that a desired amount of sepiolite or montmorillonite clay (10 to 100 mg) , previously dried overnight under vacuum at 80 or 60 °C, respectively, was added in the reaction tube prior to the solvent and monomer addition. After the reaction, in order to evidence the polymer grafting at the clay surface, the final product mixture recovered was dissolved in chloroform and then separated into a clay-rich fraction and a PCL-rich fraction by three successive chloroform washing/centrifugation steps. The solid clay-rich phase, collected as a pellet after each centrifugation was washed with chloroform and after three successive washing/ centrifugation repeats, it was dried. Whereas the non-grafted PCL was recovered from the supernatant solution by precipitation in methanol and further dried to obtain the PCL-rich phase as a fine white powder. Both fractions were characterized by thermogravimetric analysis (TGA).

The grafting efficiency was assessed by TGA by measuring the amount of organic polymeric material in the solid clay-rich fraction and by measuring the residual amount of inorganic clay after complete thermal degradation of the polymer-rich organic fraction.

### 3.3 Characterization Techniques

#### 3.3.1 Nuclear magnetic resonance (NMR)

$\epsilon$ -CL and lactide polymerizations were monitored by proton nuclear magnetic resonance ( $^1\text{H}$  NMR) to determine monomer conversion and the number average degree of polymerization.  $^1\text{H}$  NMR spectra were recorded in  $\text{CDCl}_3$  on a Bruker NMR spectrometer at 300 MHz. Monomer conversion percentages were determined according to the polymer to monomer characteristic peaks integral ratios (Equation 3.4).

$$\text{Monomer conversion (\%)} = \frac{I_{\text{polymer}}}{I_{\text{polymer}} + I_{\text{monomer}}} \times 100 \quad (3.4)$$

Molecular weights of polymers were calculated according to the degree of polymerization ( $\text{DP}_n$ ) determined from integral values ratio of characteristic peaks of the polymer chains and chain-ends (Equation 3.5).

$$(M_n \text{ PCL} = \text{DP}_n \times 114 \text{ g/mol}; M_n \text{ PLA} = \text{DP}_n \times 144 \text{ g/mol})$$

$$\text{DP}_n = \frac{I_{\text{polymer}} + I_{\text{chain-end}}}{I_{\text{chain-end}}} \quad (3.5)$$

Carbon nuclear magnetic resonance ( $^{13}\text{C}$  NMR) was also utilized to analyze the structures of synthesized copolymers and confirm the  $^1\text{H}$  NMR spectral data.

#### 3.3.2 Size exclusion chromatography (SEC)

The molecular weight and polydispersity of the polymer samples were determined by size exclusion chromatography (SEC) using a Shimadzu apparatus equipped with a RID-10A refractive index detector and an SPD-M10A UV detector. The columns used were PLGel Mixed-B 10  $\mu\text{m}$ . The calibration was realized with PS standards ranging from 580 to 1 650 000 g/mol. Chloroform (puriss p.a. Riedel-de Haën) was used as the mobile phase and the analyses were carried out at 30  $^\circ\text{C}$  with a solvent flow rate of 1 ml/min.

Molecular weights of samples are given as PS standards equivalent molecular weights.

### 3.3.3 Thermogravimetric analysis (TGA)

Thermal characterization of the materials was carried out by thermogravimetric analysis (TGA) on 10-20 mg samples by heating from room temperature to 700 °C at 10 °C/min under He or air flow using a TGA Q5000IR apparatus from TA Instruments.

### 3.3.4 Scanning electron microscopy (SEM)

The surface morphology of the derivatives and clays were characterized by Scanning Electron Microscopy (SEM). Samples were previously coated with a layer of gold to minimize charging effects. Analyses were performed on a Philips XL30 SEM apparatus with accelerating voltage of 20 kV or 25 kV and images were recorded at different magnifications.

### 3.3.5 Differential scanning calorimetry (DSC)

Differential Scanning Calorimetry (DSC) was conducted on a TA Instruments DSC Q200 (USA) under inert atmosphere on 2-3 mg samples placed in aluminium pans. The materials were exposed to successive thermal cycles (heat-cool-heat) with the first heating scan allowing to erase the thermal or thermomechanical history of the materials. Thermal characterization was carried out between -80 and 100 °C for PCL (or 200 °C for PLA) at 10 °C/min. DSC was used to determine the thermal properties of polymers such as glass transition temperature ( $T_g$ ), crystallization temperature ( $T_c$ ) and melting temperature ( $T_m$ ).

Crystallinity percentages were calculated by taking the ratio of fusion enthalpy of the sample to the fusion enthalpy of purely crystalline polymer ( $\Delta H_f^0$ ) reported in the literature (Equation 3.6).

$$\chi (\%) = [\Delta H_{f\text{sample}} (\text{J/g}) / \Delta H_f^0 (\text{J/g})] \times 100 \quad (3.6)$$

where  $\Delta H_f^0 \text{ PCL} = 139 \text{ J/g}$  and  $\Delta H_f^0 \text{ PLA} = 93 \text{ J/g}$  (theoretical values for 100% of crystallinity)

### 3.3.6 X-Ray diffraction analysis (XRD)

X-Ray Diffraction (XRD) patterns of samples were recorded with a powder diffractometer Siemens D-5000 (Munich, Germany) with  $\text{CuK}\alpha$  radiation source ( $\lambda = 0.1546 \text{ nm}$ ). The incidence angle was varied between 2° and 9° with step size of 0.010°

and step time of 4 s (scanning rate  $0.15^{\circ} \text{ min}^{-1}$ ). Basal spacing of natural, modified clays and nanoclays within nanohybrid structures was calculated according to Bragg's equation (Equation 3.7).

$$\lambda = 2 \times d_{001} \times \sin \theta \quad (3.7)$$

$\lambda$ : wavelength

$d_{001}$ : interplanar distance of 001 diffraction phase

$\theta$ : diffraction angle

### 3.3.7 Energy dispersive X-ray fluorescence spectroscopy (EDX)

The elemental analyses of powder samples were performed on a Shimadzu EDX 720 apparatus. In this method, the material which is excited by bombarding of high-energy X-rays or gamma rays, emits secondary (or fluorescent) X-rays specific to its configuration, by this way its chemical composition can be determined. Using this technique, elemental analysis of the polymer/clay nanohybrids can be assessed.

### 3.3.8 Transmission electron microscopy (TEM)

TEM analyses were performed to determine the morphology of polymer/clay nanohybrids on a Philips CM 120 TEM apparatus. Observations were made on very thin films (nanometric scale) obtained by solvent casting of diluted sample solution on TEM grids.



## 4. RESULTS AND DISCUSSION

### 4.1 PCL Synthesis by ROP Catalyzed by NOV-435 and Free CALB

In a first step, reference polymerization reactions of  $\epsilon$ -CL were conducted with both, free and immobilized lipase with the aim to determine the catalyst efficiency from the reaction kinetics and to characterize the obtained PCL. For that, aliquots of the reaction mixture were taken at specific time intervals, placed in NMR tubes and dissolved in  $\text{CDCl}_3$  for  $^1\text{H}$  NMR analyses to monitor the polymerization reaction progress.

A typical  $^1\text{H}$  NMR spectrum of PCL with the peak assignments is presented in Figure 4.1.

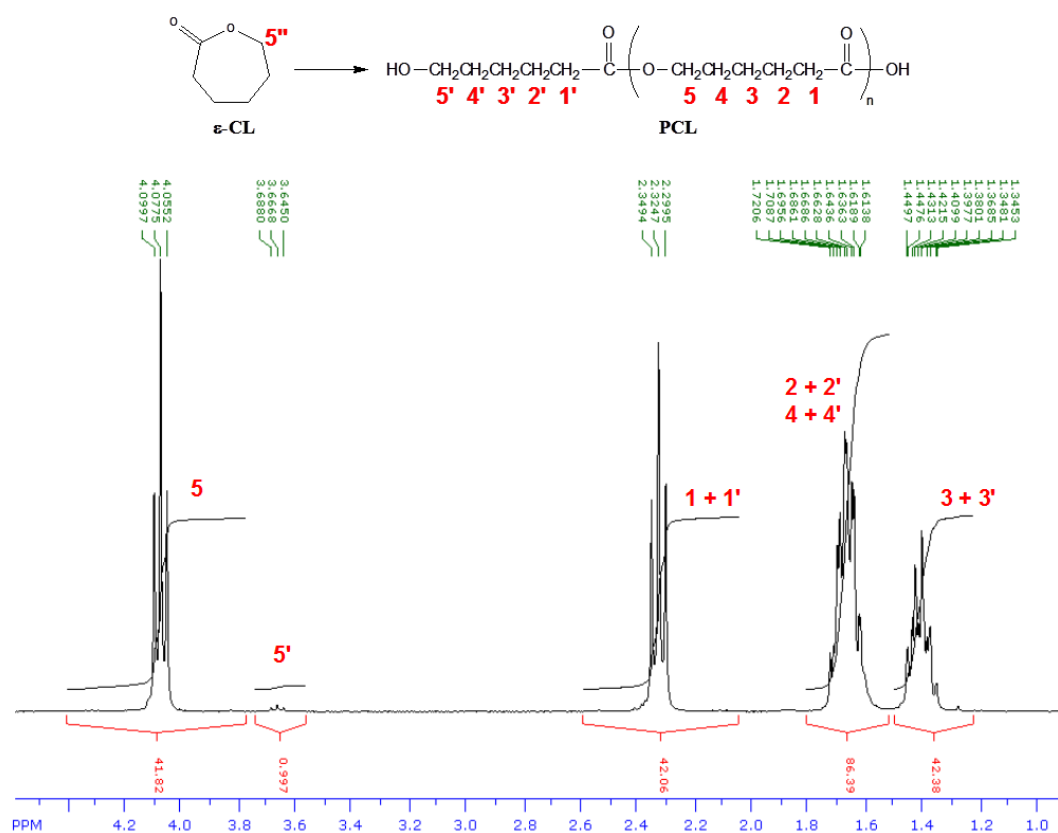


**Figure 4.1 :** Typical  $^1\text{H}$  NMR spectrum of PCL synthesized by lipase catalyzed ROP of  $\epsilon$ -CL at 70 °C. The proton assignments and corresponding peaks integral areas are shown in the spectrum.

The chemical shifts in parts per million (ppm) are given relative to tetramethylsilane (TMS, 0.00 ppm) as the internal reference and are as follow: 4.05 ppm (t, CH<sub>2</sub>O), 3.65 ppm (t, CH<sub>2</sub>OH, end group), 2.3 ppm (t, CH<sub>2</sub>CO), 1.6-1.7 ppm (m, 2xCH<sub>2</sub>), 1.35-1.45 ppm (m, CH<sub>2</sub>).

Figure 4.2 presents a zoomed view on the 3.5 to 4.4 ppm range which allows the determination of the monomer conversion and estimation of the degree of polymerization versus time.

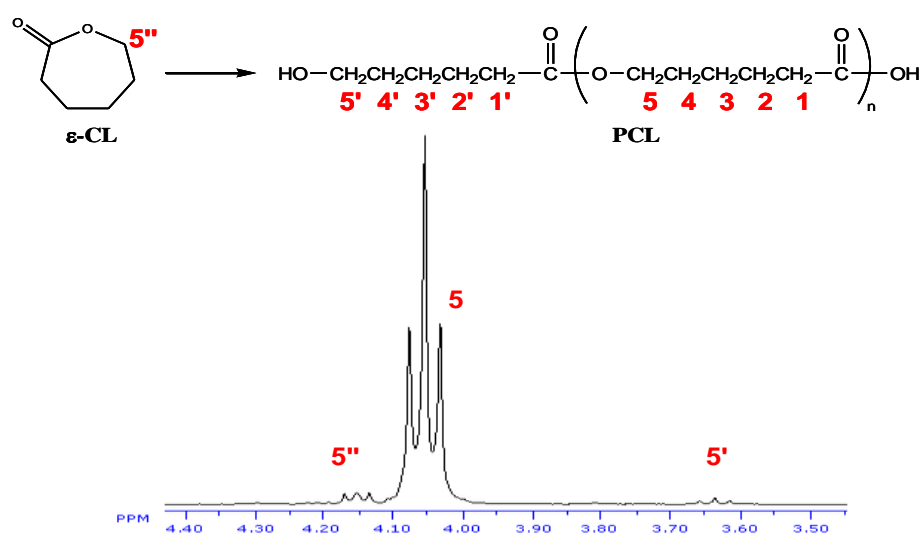


**Figure 4.2 :** Zoomed view of <sup>1</sup>H NMR spectrum of a reaction mixture showing the methylene signals of monomer, polymer and chain-end.

Indeed, since the signal at 4.15 ppm (t, CH<sub>2</sub>O) is assigned to the protons of CL monomer, comparing its integral value (I<sub>5''</sub>) to the integral of the corresponding signal of the polymer (I<sub>5</sub>) at 4.05 ppm allows the calculation of the monomer conversion. In addition, the degree of polymerization can be estimated from the ratio of integrals of the signals 5 and 5' at 4.05 and 3.65 ppm which are assigned to the CH<sub>2</sub>O groups of respectively the PCL main chain and the chain-end. These NMR analyses of aliquots from the reaction mixture allowed us to monitor the polymerization kinetics.

Synthesis of PCL was firstly carried out with the immobilized form (NOV-435) and free form (CALB) of *Candida Antarctica* lipase, in absence of clay, as reference polymerization reactions. Then, polymerizations were performed in presence of nanoclay, and compared to the reference results obtained without clay. In all these

cases, the monomer to solvent ratio was the same, with the polymerization reactions starting with 1 ml of  $\epsilon$ -CL in 2 ml of toluene.

In the case of  $\epsilon$ -CL polymerization catalyzed by immobilized lipase NOV-435, the reaction proceeds fast with a monomer conversion greater than 95% within two hours (Figure 4.3a). Interestingly, the degree of polymerization and thus the number average molecular weight of the obtained PCL chains initially increase with monomer conversion and then reach a maximum value (around 7500 g/mol), after ca. 1 hour of polymerization time, before starting to decrease. Such a decrease in molecular weight observed at high monomer conversion and for long polymerization time is not surprising and is more likely due to the well known inter- and/or intra-molecular transesterification reactions taking place in such conditions (Stridsberg et al., 2001).

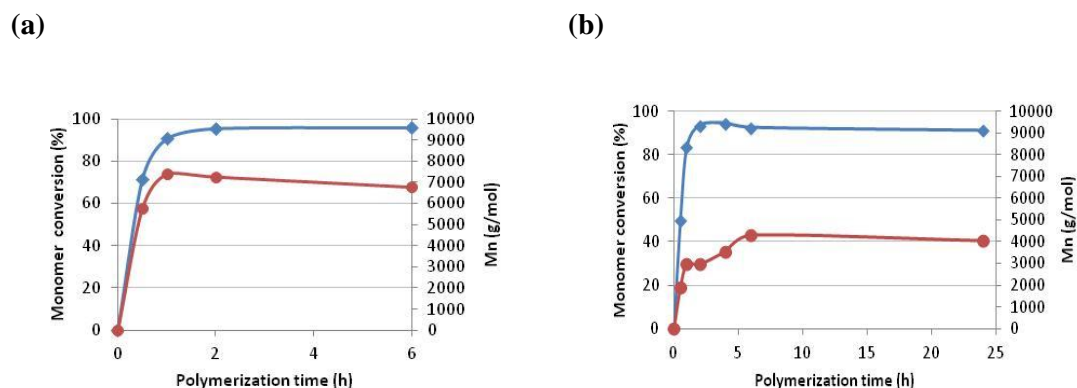


**Figure 4.3 :** Time-evolution curves of  $\epsilon$ -CL conversion ( $\blacklozenge$ ) and molecular weight ( $M_n$ ) of obtained PCL ( $\bullet$ ), as determined by  $^1\text{H}$  NMR analyses, for polymerizations carried out with (a) **NOV-435** (100 mg) catalyst and (b) **"free" CALB** (50 mg) catalyst.

Regarding the polymerization of  $\epsilon$ -CL catalyzed by "free" CALB previously dialyzed and lyophilized, a similar or slightly slower reaction rate is observed (Figure 4.3b) compared to the NOV-435 immobilized lipase. Besides, PCL chains of significantly lower molecular weights (around 4000 g/mol) are recovered from the free CALB catalyzed polymerization when compared to the ones carried out with NOV-435. Nevertheless, a similar behavior is observed with the slight decrease in molecular weights for long polymerization times, due to transesterification reactions.

It is worth pointing out that even if the added amount of NOV-435 catalyst is of 100 mg, the estimated lipase content is of ca. 10 mg only (10 wt% immobilized lipase) and thus this amount is much lower than for the free CALB catalyzed reaction (50



mg). Thus, taking into consideration the catalytic activity with the effective amount of enzyme, the NOV-435 immobilized system is much more efficient than the non-immobilized counterpart. This confirms the benefits of CALB immobilization and reported results on the high activity of NOV-435. Regarding the lower molecular weights obtained with "free" CALB, this can be explained by the greater amount of enzyme involved in the reaction which could also result in a slightly higher amount of water (bound to the enzyme) in the reaction medium and thus a higher number of propagating chains in the case of the free CALB and thus lower molecular weights.

## 4.2 PCL Synthesis by ROP Catalyzed by NOV-435 and Free CALB in Presence of Clays

### 4.2.1 PCL synthesis in presence of sepiolite

To determine the possible influence of different clays, polymerizations were first carried out in presence of various amounts of non-modified sepiolite clay in the medium (Figures 4.4 and 4.5). Figures 4.4b and 4.5a present respectively the characteristics of the free CALB and NOV-435 catalyzed polymerization reactions, which are performed in presence of 10 mg of sepiolite clay. With the addition of sepiolite in the reaction medium, one can see that the polymerization rate is not significantly affected since the monomer conversion is still higher than 95% after ca. 3 hours of polymerization for all cases.

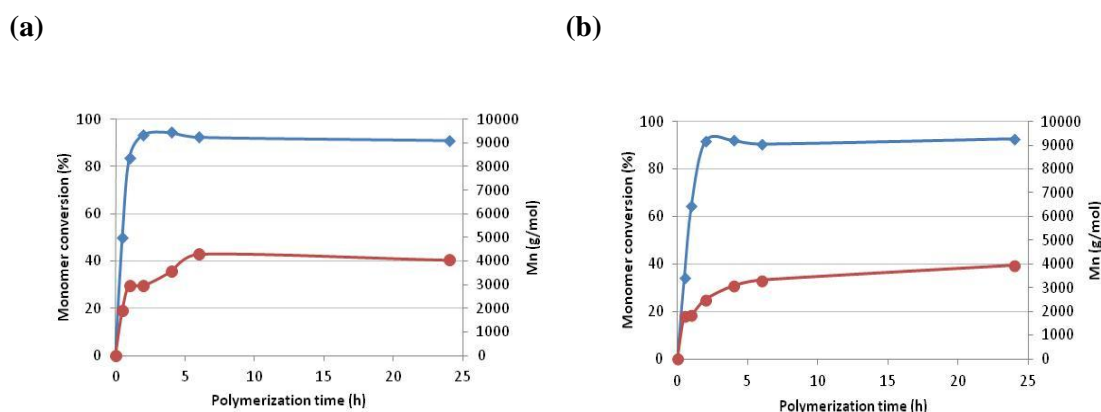


**Figure 4.4 :** Time-evolution curves of  $\epsilon$ -CL conversion ( $\blacklozenge$ ) and molecular weight ( $M_n$ ) of obtained PCL ( $\bullet$ ), as determined by  $^1\text{H}$  NMR analyses, for **free CALB** (50mg) catalyzed polymerizations carried out (a) *in absence of clay* and (b) *in the presence of 10 mg of sepiolite*.

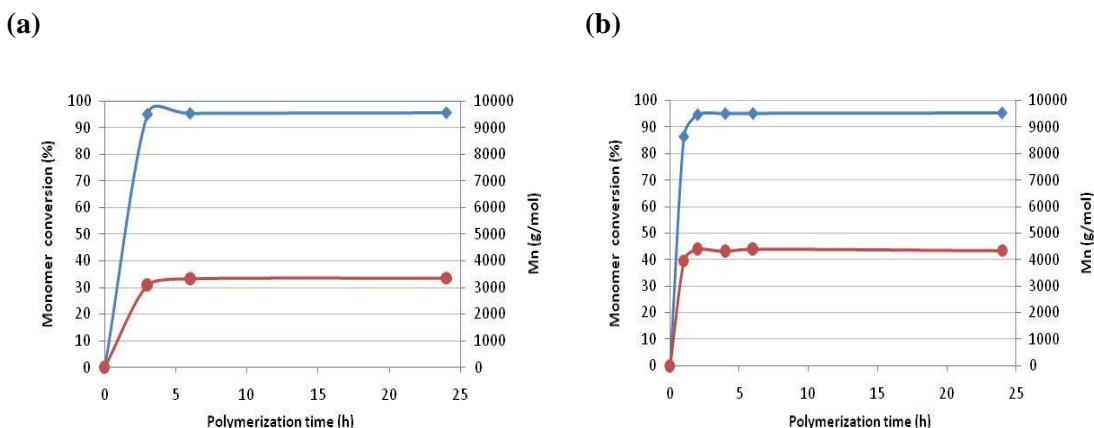


**Figure 4.5 :** Time-evolution curves of  $\epsilon$ -CL conversion ( $\blacklozenge$ ) and molecular weight ( $M_n$ ) of obtained PCL ( $\bullet$ ), as determined by  $^1\text{H}$  NMR analyses, for **NOV-435** (100 mg) catalyzed polymerizations carried out in the presence of (a) 10 mg of sepiolite and (b) 100 mg of sepiolite.

Nevertheless, a decrease in the PCL molecular weight ( $M_n$ ) is observed when sepiolite clay is added in the reaction medium. This decrease is more markedly observed for the NOV-435 catalyzed reaction (Figure 4.5a), compared to the “no clay” case (Figure 4.3a). Shorter PCL chains were expected and this can be explained by two main reasons. First, the addition of such hydrophilic clay may result in a higher water content in the reaction medium which may lead to the initiation of more numerous PCL chains having thus lower average molecular weights. The second possible reason relies on the presence of numerous hydroxyl groups at the sepiolite surface acting as a co-initiator in the polymerization reaction. Here again, this results in a higher number of growing chains and thus lower molecular weights for the obtained PCL. However, since no marked difference is observed when increasing the clay content (Figure 4.5a and 4.5b), it is more likely that a combined effect of both facts is occurring with predominant impact from the water content brought by the clay.

Interestingly, the participation of the clay hydroxyl groups to the polymerization reaction may also induce the grafting and growth of some polyester chains from the clay surface resulting in the formation of organic/inorganic nanohybrids.

#### 4.2.2 PCL synthesis in presence of montmorillonite

In a second step,  $\epsilon$ -CL polymerizations, catalyzed by NOV-435, were carried out in presence of the montmorillonite ( $\text{MMT-Na}^+$ ) non-modified clay, which has a much lower amount of hydroxyl groups at the surface of the platelets compared to

sepiolite. Here again, the polymerization rate is not significantly affected since the monomer conversion reaches 95% within 2 hours of polymerization (Figure 4.6).

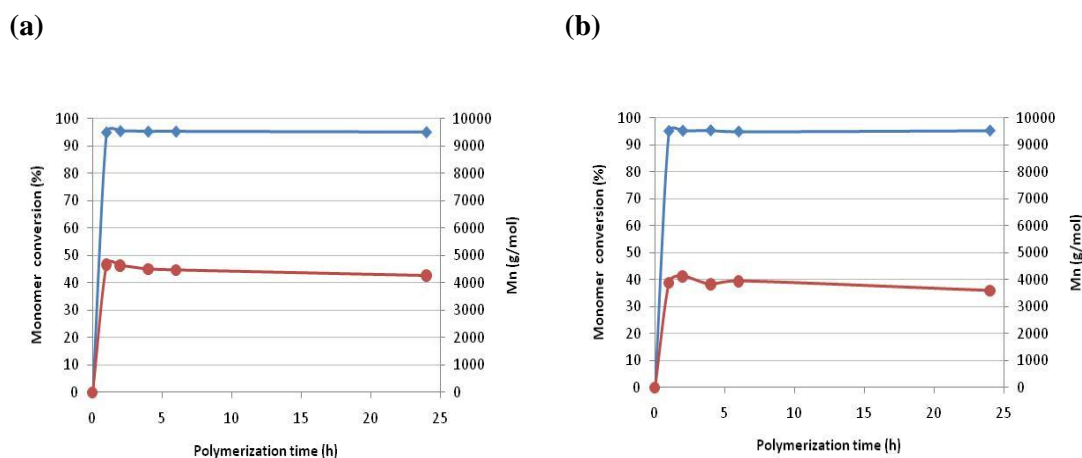


**Figure 4.6 :** Time-evolution curves of  $\epsilon$ -CL conversion ( $\blacklozenge$ ) and molecular weight ( $M_n$ ) of obtained PCL ( $\bullet$ ), as determined by  $^1\text{H}$  NMR analyses, for **NOV-435** (100 mg) catalyzed polymerizations carried out (a) in the presence of 10 mg of  $\text{MMT-Na}^+$  and (b) in the presence of 100 mg of  $\text{MMT-Na}^+$ .

As previously observed for the polymerization carried out in the presence of sepiolite, the addition of montmorillonite clay to the reaction medium induces a marked decrease in the PCL average molecular weights. As already described for sepiolite, it seems that increasing amounts of montmorillonite do not have a significant impact on the polymerization kinetics and on the PCL chains average length, at least for the clay amount range studied here. This behavior seems to indicate that for the polymerization performed in presence of the non-modified forms of both sepiolite and montmorillonite, the decrease in the PCL chain length is more likely due to a low, and almost fixed, amount of water brought by these hydrophilic clay which participate in the reaction as a co-initiator.

#### 4.2.3 PCL synthesis in presence of organomodified montmorillonite (Cloisite<sup>®</sup> 30B)

The hypothesis of the hydroxyl groups participating in the polymerization reaction is well supported by the results obtained when introducing various contents of the organophilic modified montmorillonite (Cloisite<sup>®</sup> 30B) in the reaction medium. Figure 4.7 presents the characteristics of the NOV-435 catalyzed polymerization

reactions performed in presence of, respectively, 10 mg and 100 mg of organo-modified montmorillonite clay (Cloisite<sup>®</sup> 30B).

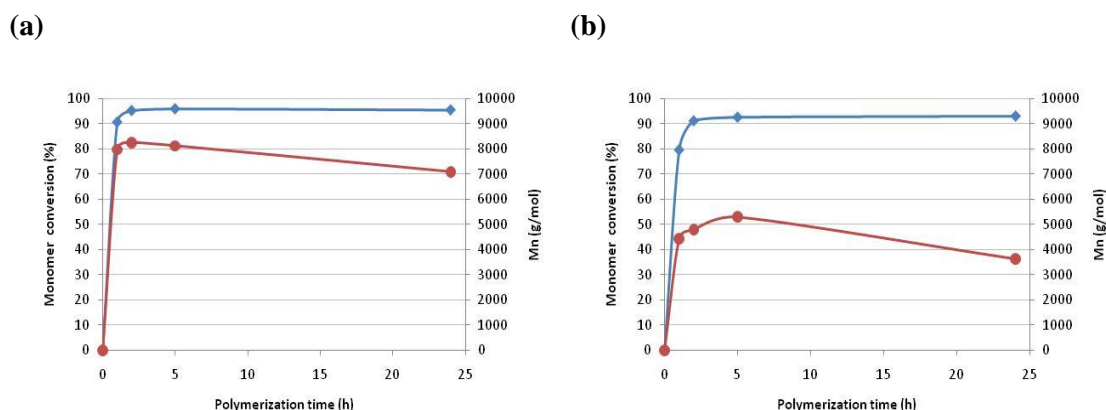


**Figure 4.7 :** Time-evolution curves of  $\epsilon$ -CL conversion ( $\blacklozenge$ ) and molecular weight ( $M_n$ ) of obtained PCL ( $\bullet$ ), as determined by  $^1\text{H}$  NMR analyses, for **NOV-435** (100 mg) catalyzed polymerizations carried out (a) in the presence of 10 mg of Cloisite<sup>®</sup> 30B and (b) 100 mg of Cloisite<sup>®</sup> 30B.

First, it is worth pointing out that Cloisite<sup>®</sup> 30B organoclay bears some hydroxyl groups brought by the ammonium salts used as organo-modifier (two -OH groups on each ammonium). This organoclay, being more hydrophobic, has less bound water compared to unmodified montmorillonite and sepiolite, thus the possible amount of water brought by the clay in the medium should be very low. It is thus expected that the main variations are resulting from the different content in -OH groups, at the clay surface.

Interestingly, here again in both cases the polymerization kinetics is not affected by the clay addition, the conversion reaching values higher than 90% within 2 hours, attesting for the lack of negative impact from this nanoclay on the lipase polymerization activity. However, at high monomer conversion, increasing polymerization times result in transesterification reactions reducing the average PCL chain length.

As expected, when a low amount of organoclay is added, the lower content of water molecules present at the surface of montmorillonite platelets results in PCL molecular weights higher than those obtained in presence of sepiolite and MMT- $\text{Na}^+$ , at the same content (Figure 4.7a). Interestingly, the PCL chains length obtained in presence of 10 mg of Cloisite<sup>®</sup> 30B and in absence of clay are very similar (ca. 8000 g/mol). Such similar values observed when adding 10 mg of Cloisite<sup>®</sup> 30B compared

to the "no clay" case can be explained by the small amount of clay and thus a very limited number of -OH groups which participate to the polymerization as co-initiator.

Figure 4.7b clearly highlights the impact of the organoclay content, and thus the amount of -OH groups involved in the polymerization, on the PCL average molecular weight. Logically, when increasing the content in organoclay the number of -OH groups acting as co-initiators is much more higher resulting in a marked decrease in the PCL average molecular weight. Indeed, an increase in the organomodified montmorillonite content from 10 to 100 mg in the reaction medium results in a two fold decrease in the polymer chain length. This clearly attests for the effective participation of the clay -OH groups on the PCL chains grafting and growth from the clay platelets.

#### 4.2.4 Scale-up of PCL synthesis in presence of clays

To follow the effect of scale-up in reaction conditions, some experiments were carried out in the presence of sepiolite and Cloisite<sup>®</sup> 30B, by increasing five times the amount of solvent, catalyst and clay content. As it can be seen from Figure 4.8, augmenting reaction volumes and amount of sepiolite did not involve any drastic effect on the reaction kinetics and the molecular weight of PCL chains. While for the case of modified montmorillonite, an important increase in molar masses of PCL was observed (Figure 4.9b).

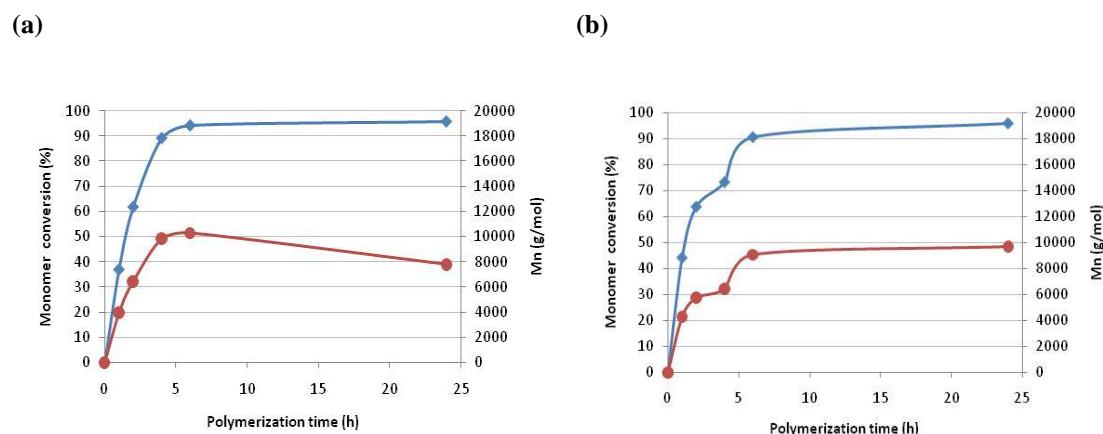


**Figure 4.8 :** Time-evolution curves of  $\epsilon$ -CL conversion (◆) and molecular weight ( $M_n$ ) of obtained PCL (●), as determined by  $^1\text{H}$  NMR analyses. Reaction mixture constituents as (a) 2 ml toluene; 1 ml  $\epsilon$ -CL; 20 mg NOV-435; 10 mg sepiolite and (b) 10 ml toluene; 5 ml  $\epsilon$ -CL; 100 mg NOV-435; 50 mg sepiolite.

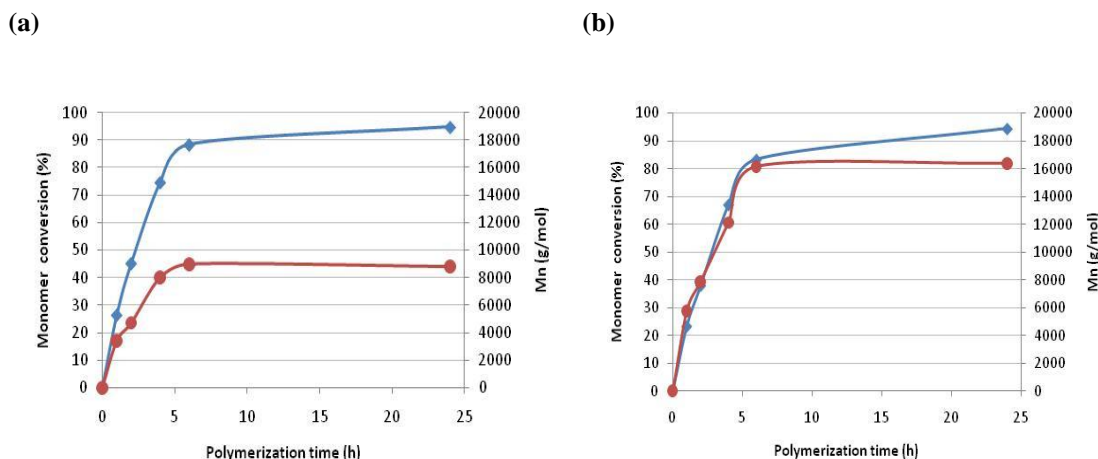


**Figure 4.9 :** Time-evolution curves of  $\epsilon$ -CL conversion (♦) and molecular weight ( $M_n$ ) of obtained PCL (●), as determined by  $^1\text{H}$  NMR analyses. Reaction mixture constituents as (a) 2 ml toluene; 1 ml  $\epsilon$ -CL; 20 mg NOV-435; 10 mg Cloisite® 30B and (b) 10 ml toluene; 5 ml  $\epsilon$ -CL; 100 mg NOV-435; 50 mg Cloisite® 30B.

### 4.3 Lipase (CALB) Immobilization on Clays

After determining the influence of clay addition in the reaction medium, such nanoclays were used for lipase immobilization and the resulting derivatives were further tested for  $\epsilon$ -CL polymerization. In a first batch of immobilization tests, the commercially available natural sepiolite (SEP) and Cloisite® 30B (commercial organo-modified montmorillonite) have been used as supports and compared.

For both clays, various loadings in lipase were tested (respectively 7.5; 13.5 and 27 mg of proteins per gram of clay). In the sample coding, the number 1, 2 or 3 stands for the corresponding amounts of enzyme loading and the last letter (a, b...) denotes the derivatives resulting from different batch of immobilization. The results reported on Table 4.1 present the percentage of immobilized enzyme and the determined hydrolytic activity of the different systems.

The results evidenced that too high enzyme loadings result in a lower immobilization efficiency, both for sepiolite and montmorillonite clays. This allowed to determine the optimized lipase content to use for immobilization as 7.5 mg of proteins per gram of clay derivative. Indeed, it is well known that increasing the amount of enzyme loading can lead to higher amount of immobilized enzyme but the formation of a thicker layer of adsorbed lipases usually results in a loss of specific activity due to

the first enzymes being “buried” and no longer accessible to the substrate (Mei et al., 2003b).

**Table 4.1** : Immobilization loading of lipase on different supports.

Derivative	mg added protein/ g derivative (clay added)	mg fixed protein/ g derivative (clay added)	Immobilization (%)	Specific activity (U/mg)
<b>SEPL1a</b>	7.5	6.7	90	<b>13</b>
<b>SEPL2a</b>	13.5	10.2	75	<b>19</b>
<b>SEPL3a</b>	27.0	17.8	66	<b>23</b>
<b>MMTMODL1a</b>	7.5	7.2	96	<b>101</b>
<b>MMTMODL2a</b>	13.5	13.2	97	<b>95</b>
<b>MMTMODL3a</b>	27.0	19.4	72	<b>80</b>

\* **SEPL**: CALB immobilized on natural sepiolite;

**MMTMODL**: CALB immobilized on Cloisite® 30B as support.

#### 4.3.1 Influence of the type of clay support: MMT, MMTMOD, SEP or SEPMOD

Higher immobilization efficiency and specific activity values shown by MMTMODL derivatives when compared to SEPL derivatives could be explained by the presence of organo-modifiers at the surface providing a better conformational positioning and accessibility of the active center of the enzyme. To demonstrate if this difference comes from the natural structure of these two clays or from the effect of organo-modification, a new set of immobilization was performed where natural montmorillonite and organo-modified sepiolite were also tested as supports (Table 4.2).

The results of this immobilization study highlighted the great impact of clay surface organo-modification on the lipase immobilization efficiency and more importantly on the hydrolytic activity. This is particularly marked for sepiolite-based systems which show great enhancement in hydrolytic activity when using their organo-modified forms for lipase immobilization. It can be assumed that enzyme molecules preferentially interact with surfactant molecules in the case of modified sepiolite support compared with the case of natural sepiolite.



**Table 4.2 :** Immobilization loading of lipase on different clay supports.

Derivative	Loading (mg added protein/ g clay)	Immobilization (%)	Specific Activity (U/mg)	GA treatment →	Specific Activity (U/mg)
<b>SEPL1b</b>	7.5	<b>88</b>	<b>37</b>		<b>13</b>
<b>SEPL2b</b>	13.5	<b>74</b>	<b>45</b>		<b>14</b>
<b>SEPL3b</b>	27.0	<b>56</b>	<b>35</b>		<b>16</b>
<b>SEPMODL1b</b>	7.5	<b>96</b>	<b>210</b>		<b>241</b>
<b>SEPMODL2b</b>	13.5	<b>98</b>	<b>199</b>		<b>222</b>
<b>SEPMODL3b</b>	27.0	<b>96</b>	<b>132</b>		<b>200</b>
<b>MMTL1b</b>	7.5	<b>99</b>	<b>117</b>		<b>132</b>
<b>MMTL2b</b>	13.5	<b>90</b>	<b>93</b>		<b>99</b>
<b>MMTL3b</b>	27.0	<b>73</b>	<b>91</b>		<b>80</b>
<b>MMTMODL1b</b>	7.5	<b>95</b>	<b>165</b>		<b>283</b>
<b>MMTMODL2b</b>	13.5	<b>97</b>	<b>145</b>		<b>246</b>
<b>MMTMODL3b</b>	27.0	<b>67</b>	<b>145</b>		<b>217</b>
<b>Free CALB</b>			<b>117</b>		<b>257</b>

\***SEPL**: CALB immobilized on natural sepiolite; **SEPMODL**: CALB immobilized on modified sepiolite; **MMTL**: CALB immobilized on natural montmorillonite; **MMTMODL**: CALB immobilized on Cloisite® 30B as support.

Moreover, the performances of the montmorillonite-based systems are generally greater than for the sepiolite-based counterparts. Such differences in lipase immobilization and hydrolytic activities could be due to the differences in the electrostatic interactions between the enzyme, the various clay surfaces and the organomodifier functional groups. It can be suggested that specific surfaces may direct enzyme molecules towards a particular orientation so that the active site of the enzyme becomes more accessible for the substrate and finally enhancing its activity.

The loss of activity of CALB after its immobilization on natural sepiolite can be explained by different reasons as: the possible reaction of amino acids which are essential for bonding or catalysis with the surface of natural clay mineral, steric hindrance of the approach of the substrate, disruption of the three dimensional structure of the enzyme protein and diffusional limitations for solute transport near particles.

Due to immobilization mechanism, the active center of the lipase is in close contact with the surface of the clay support and this creates a hydrophobic environment around the active center. Therefore, some differences derived from the nature of the support as its hydrophobicity or internal morphology, can change the adsorption



strength of the lipase on the support and also the structure of the active center surroundings and subsequently the final catalytic features of the lipase (Fernandez-Lorente et al., 2008).

Fernandez-Lafuente et al. (1998), have suggested that the adsorption of lipases to a hydrophobic support may be induced by some factors more complex than just the hydrophobicity of the support. But after all, they have concluded that the amount of lipases adsorbed is higher for more hydrophobic support. This can explain the higher activity of MMTL derivatives over SEPL derivatives, since CALB is expected to show higher enzymatic activity when adsorbed on more hydrophobic support as montmorillonite compared to sepiolite which is more hydrophilic. Another possible explanation regarding the lower activity of the sepiolite-based systems is the difference in terms of available surface area and location of the immobilized enzyme.

The derivatives (CALB immobilized on clays) were characterized by XRD analysis to possibly determine the location of the adsorbed enzyme. Modified and natural clays were also compared to determine the effect of organo-modification and lipase immobilization on the clay structure (Figure 4.10).

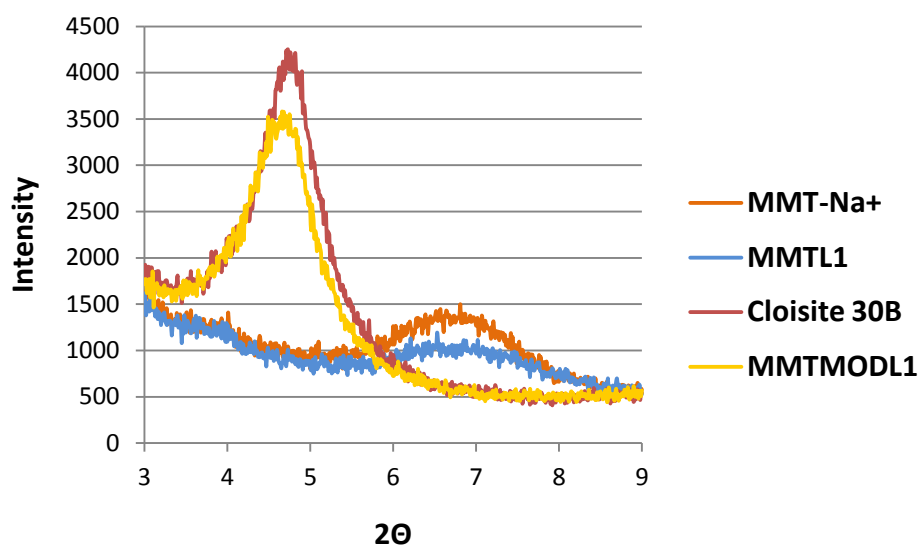


**Figure 4.10 :** XRD patterns of natural montmorillonite (MMT-Na<sup>+</sup>); modified montmorillonite (Cloisite<sup>®</sup> 30B); natural montmorillonite onto which CALB is immobilized (MMTL1); modified montmorillonite onto which CALB is immobilized (MMTMODL1).

As expected, the characteristic reflection peak (001) of natural montmorillonite is shifted to lower angles due to the expansion of the interlayer space by the

intercalation of alkylammonium molecules as organomodifier. After the organomodification, the basal spacing of natural montmorillonite which is 1.38 nm ( $2\theta = 6.8^\circ$ ), is expanded to 1.88 nm ( $2\theta = 4.8^\circ$ ).

Besides, the adsorption of the enzyme onto both natural and modified montmorillonite seems to be limited to the external surface of the clays since only a slight decrease in peak intensities of MMT- $\text{Na}^+$  and Cloisite<sup>®</sup> 30B is observed and no peak shift is detected (Figure 4.10). Taking into consideration the specific dimensions of CALB (3 x 4 x 5 nm), the enzyme cannot be intercalated between clay nanosheets. A possible probability can be the intercalation of some amino acid residues while the polypeptide backbone remains outside of the interlayer gallery.

For the case of sepiolite, both enzyme immobilization and surfactant adsorption appear to occur on the external surfaces or edges of the clay since any shift on reflection angles is observed (Figure 4.11). The basal spacing of natural sepiolite (1.21 nm;  $2\theta = 7.3^\circ$ ) remained unchanged confirming the already known fact that the alkylammonium salt cations used for the modification of natural sepiolite could not penetrate inside the micropores of sepiolite and occupied just the external surface (Chivrac et al., 2010).

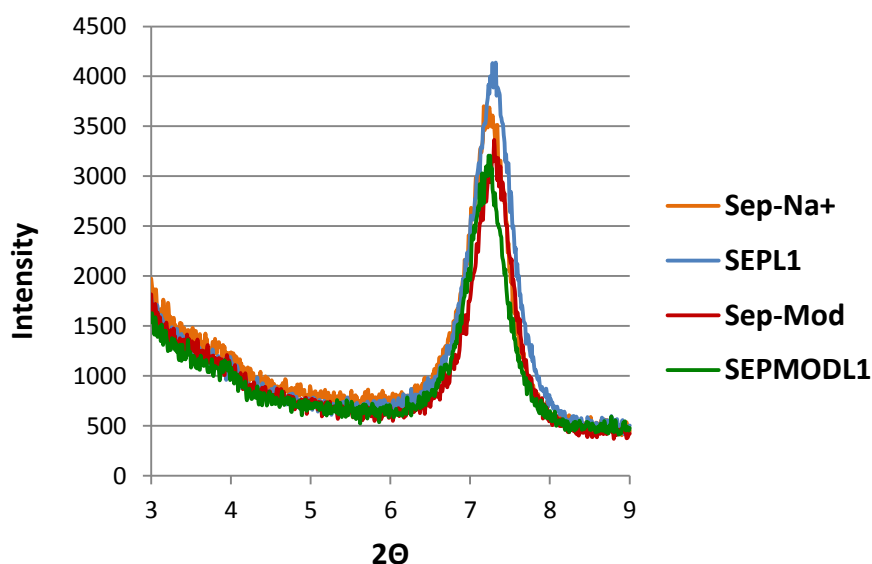


**Figure 4.11 :** XRD patterns of natural sepiolite ( $\text{Sep-Na}^+$ ); modified sepiolite ( $\text{Sep-Mod}$ ); natural sepiolite onto which CALB is immobilized ( $\text{SEPL1}$ ); modified sepiolite onto which CALB is immobilized ( $\text{SEPMODL1}$ ).

Here again, due to the CALB dimensions, the sepiolite internal channel is not available to the lipase so all immobilization occurs at the external surface of the sepiolite needles.

Nevertheless, to explain the differences in hydrolytic activity, one can suppose that due to clay swelling in solution the interlayer space of montmorillonite becomes partially accessible to the substrate and/or enzyme, resulting in a larger surface area available for the reaction components. On the other hand, the more aggregated structure of the non-modified sepiolite, resulting in low surface area, could explain the lower efficiency of the corresponding catalytic systems.

Besides, the non-modified clays both show a global negative charge on their surface which may be not fully appropriate for lipase immobilization and further catalytic activity. Indeed, the immobilization procedure being performed in a pH 7.0 buffer solution, which is above the lipase isoelectric point (pI 6.0), one may assume that the enzyme globally bears a slightly negative charge and thus may show limited interactions (or even some repulsion) with the clay surface. On the other hand, organo-modified supports could present an apparent positive charge on their surface, brought by the ammonium salts, which could interact favorably with the globally negatively charged enzyme at pH 7.0, thus promoting the immobilization.

Furthermore, it can also be supposed that the adsorption mechanism for silicates is promoted by cationic interactions between silanol groups and positive charges (protonated lysine) of the enzymes. However, such protonated form of the enzyme for a more efficient lipase immobilization would require the use of acidic condition during immobilization procedure which may alter the clay structure integrity.

Nevertheless, the lower activity observed with the non-modified sepiolite cannot be attributed to an issue of immobilized enzyme amounts since the content in immobilized enzyme can reach values as high as 90% which are very similar to the values obtained with montmorillonite.

Thus, even if the precise explanation is not fully known yet, it is quite obvious that the clay surface organo-modification dramatically improves the efficiency of the immobilized lipase catalysts. In addition, catalytic systems based on montmorillonite seem to give higher performances compared to the sepiolite ones.

### 4.3.2 Influence of lyophilization and glutaraldehyde treatment

Glutaraldehyde (GA) which is known for its protein cross-linking ability was used in the next step to increase the stability and specific activity of resulting derivatives. GA is a linear 5-carbon dialdehyde, in liquid form that is soluble in all proportions in water, alcohol and in organic solvents. It is widely used for enzyme immobilization, however its structure in aqueous solutions and cross-linking mechanism remain as a debate subject (Migneault et al., 2004). The cross-linking of proteins to a solid support or between protein molecules (support-free) usually implies  $\epsilon$ -amino groups of lysine residues. These lysine residues, in most cases are not involved in the catalytic site of the enzyme and this allows moderate cross-linking to preserve the conformation of the protein and its catalytic activity (Avrameas, 1969).

The precise chemical nature of the reaction of GA with proteins is not clearly understood. Several mechanisms are proposed for protein crosslinking reaction. It is suggested that there is no single mechanism which can define the reaction of GA with proteins since GA is present in different forms depending on the pH of the solution even for specific and controlled reaction conditions. There may be a simultaneous series of reactions which can proceed one after the other. On the Figure 4.12, the reaction of GA with enzymes in acidic or neutral conditions proposed by Walt and Agayn (1994) is shown.

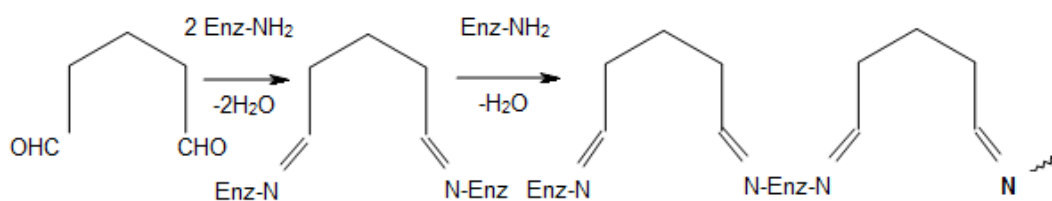


**Figure 4.12 :** Reaction of glutaraldehyde with proteins under acidic or neutral conditions (Walt and Agayn, 1994).

For more details on glutaraldehyde possible structures and the enzyme cross-linking proposed mechanisms readers can refer to a review article by Migneault et al. (2004).

Generally two protocols are used for immobilization of proteins with GA. In the first one, the supports are previously activated with GA. In the second one, previously adsorbed proteins on supports with primary amino groups are treated with GA (Lopez-Gallego et al., 2005). It has been suggested that both protocols follow the same mechanism where there is first a rapid adsorption of the protein by ionic

exchange followed by the covalent reaction. Fernandez-Lafuente et al. (1995) highlighted that in the first strategy where immobilization is carried out on previously activated supports, the chemical modification of the enzyme is limited to only the groups of protein which are involved in the immobilization whereas in the second strategy involving the modification of previously immobilized enzyme by GA, all protein surface can be modified.

Under mild conditions, when the enzyme is firstly adsorbed onto the support, all primary amino groups of the enzyme and support may be activated with one molecule of glutaraldehyde. It has been suggested that in this form, GA bound to the  $\epsilon$ -amino groups of lysine residues of the enzyme could covalently react with another GA molecule bound to the activated support and create a multipoint covalent enzyme-support attachment (Lopez-Gallego et al., 2005).

The derivatives (CALB adsorbed onto clay supports) were incubated with 0.5% glutaraldehyde solution in 25 mM sodium phosphate buffer at pH 7.0 and 25 °C for 1 h under mild stirring. By this treatment, a full modification of primary amino groups of the enzyme and the support was expected. Samples were centrifuged at 6000 rpm for 20 min at 4 °C. Resulting pellets containing derivatives were washed with 25 mM sodium phosphate buffer (pH 7.0) to remove the excess of GA and then centrifuged with three repeats. Final derivatives were incubated for an additional 24 h at 25 °C to achieve a more intense cross-linking between the enzyme and the support. To verify if the *p*NPB substrate is degraded by the presence of GA, blank tests, for which only the substrate solution was incubated with 0.5% GA solution, were performed and no degradation due to the action of GA was detected.

As it can be seen from the results (Table 4.2), after GA treatment an enhancement in hydrolytic activities was observed for derivatives with organo-modified supports. This effect was mostly marked for modified-montmorillonite based derivatives. On the contrary, for natural sepiolite derivatives, a decrease in specific activities was observed whereas the catalytic activities for natural montmorillonite derivatives remained almost unchanged.

We can assume that GA molecules have a positive interaction with organo-modifier groups and the surface of modified-montmorillonite clay to render the enzyme active center more accessible to substrate. This positive effect of the glutaraldehyde

treatment on the systems based on organo-modified clays is confirmed with the catalyst system based on surface modified sepiolite which also shows a slight increase in hydrolytic activity after crosslinking by GA. However, due to surface properties of non-modified sepiolite, GA treatment led to the formation of a structure not promoting the catalytic activity of the lipase and even induced a negative effect on the hydrolytic activity of the derivative.

In order to explain the activity increase for free CALB after GA treatment, it can be hypothesized that a large complex composed of dissolved enzyme molecules linked to each other has formed. As a result, an over-concentrated microenvironment in the substrate solution (*p*NPB) could have been created around this complex, providing a better diffusion of substrate molecules and thus an increased probability for the enzyme to meet a substrate molecule.

Since the main variations in catalyst activities could be assigned to differences in clay structure and surface properties, morphological studies of the various systems have been carried out by scanning electron microscopy (SEM).

SEM photographs of the different clays and derivatives recorded at two distinct magnification are shown below on Figures 4.13 to 4.22.

As far as non-modified sepiolite is concerned, one can clearly see the large aggregates formed by the needle-shape nanoclay (Figure 4.13).

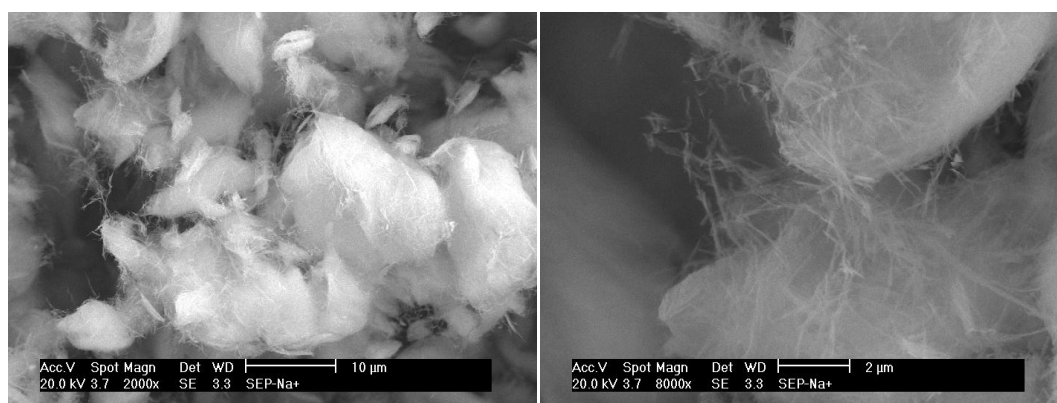


**Figure 4.13 :** SEM pictures of natural sepiolite (SEP) at 2000x magnification (left) and 8000x magnification (right).

Enzyme immobilization on this non-modified sepiolite retains the highly aggregated morphology but the individual needles that can be observed at higher magnification seem to be embedded in the immobilized enzyme at the clay surface (Figure 4.14).

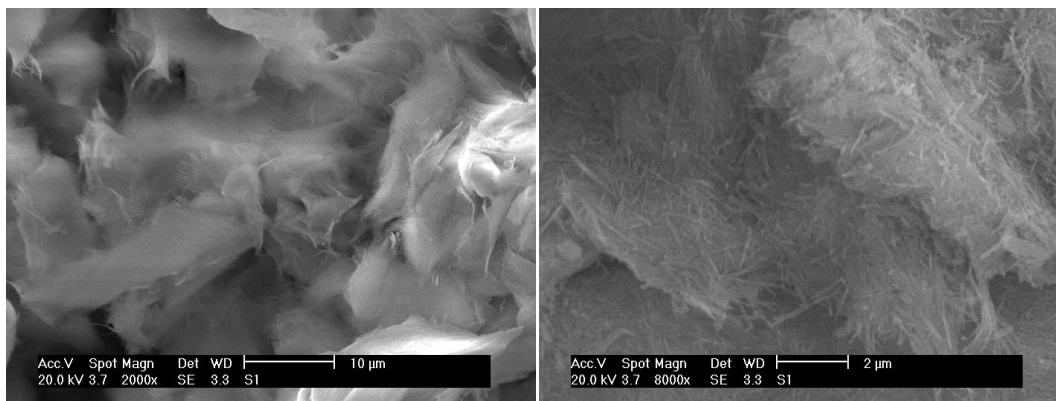


**Figure 4.14 :** SEM pictures of natural sepiolite after the immobilization of CALB (SEPL) at 2000x magnification (left) and 8000x magnification (right).

After sepiolite organo-modification, SEM analysis seems to show that clay aggregates remain but they are not so large. This trend is confirmed at higher magnification, where much more individually separated needles can be observed for the modified clay, due to the surface modification (Figure 4.15).

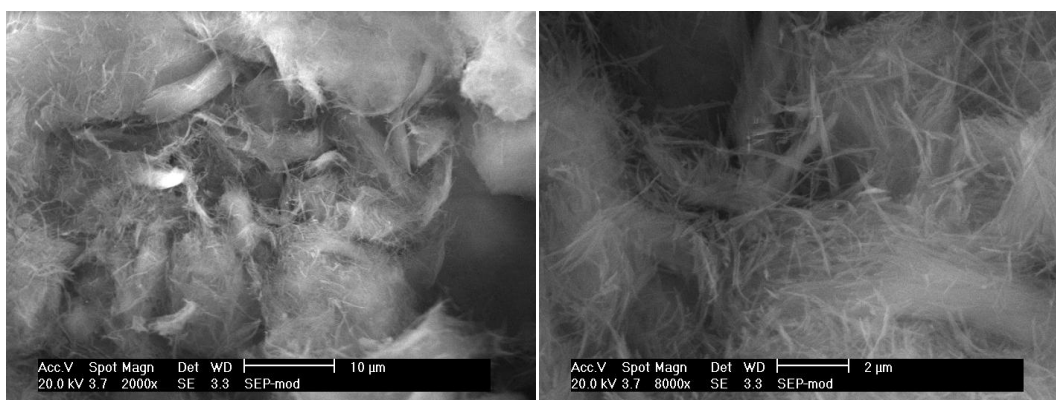


**Figure 4.15 :** SEM pictures of modified sepiolite (SEPMOD) at 2000x magnification (left) and 8000x magnification (right).

Here again (Figure 4.16), the SEM picture of the organo-modified sepiolite with immobilized lipase seems to show that the individual needles are embedded in the immobilized enzyme at the clay surface.

Since the sepiolite needle-like particles are covalently attached to each other, it is very difficult to separate individually all the particles.

Also, due to the non-swelling character of the sepiolite clay, organo-modification and enzyme adsorption are assumed to occur just at the clay surface.

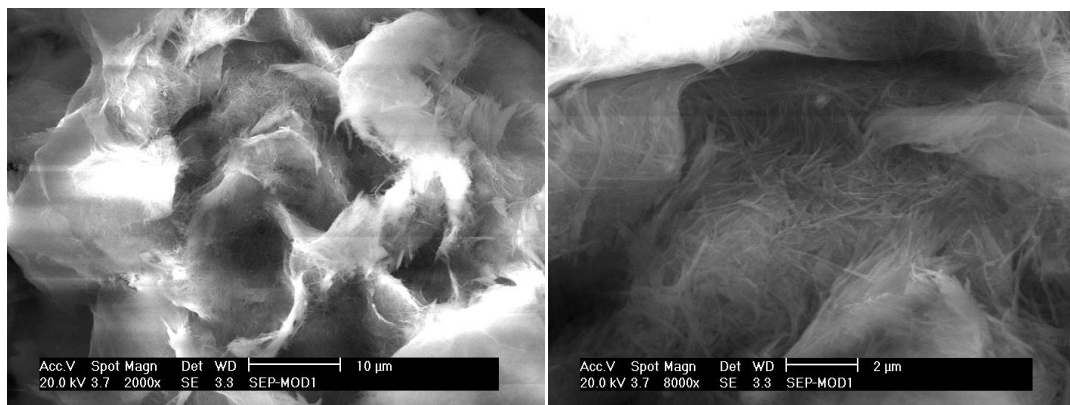


**Figure 4.16 :** SEM pictures of modified sepiolite after immobilization of CALB (SEPMODL) at 2000x magnification (left) and 8000x magnification (right).

Regarding the cross-linking reaction by GA treatment, the SEM observations do not show significant differences compared to the previous systems. Individual clay needles are still embedded in crosslinked enzyme and large clay aggregated are still present (Figure 4.17).

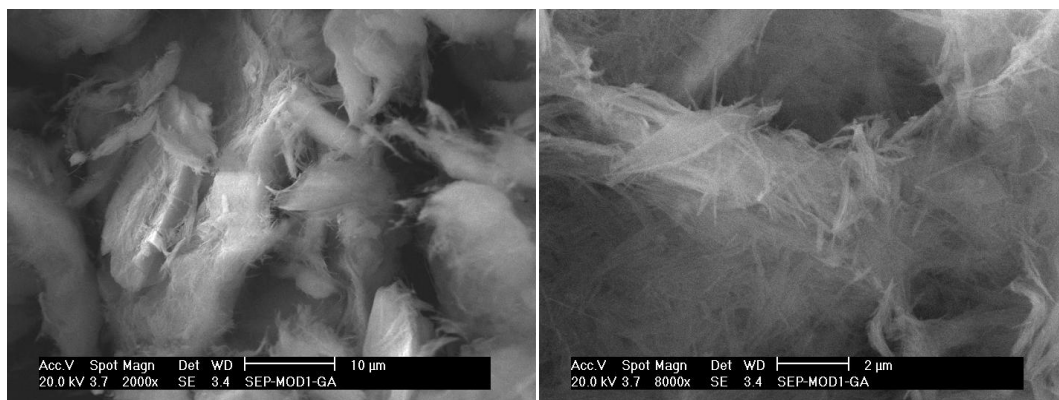


**Figure 4.17 :** SEM pictures of modified sepiolite after immobilization of CALB and treated with GA (SEPMODL G) at 2000x magnification (left) and 8000x magnification (right).

The morphologies observed for montmorillonite and its derivatives are totally different than for the sepiolite.

As far as non-modified montmorillonite is concerned, large aggregates of clay platelets stacks are observed (Figure 4.18). These clay platelets seem to be more visible for the natural montmorillonite after immobilization of CALB on its surface.

The clay aggregates also seem to present a smoother surface after lipase immobilization (Figure 4.19).



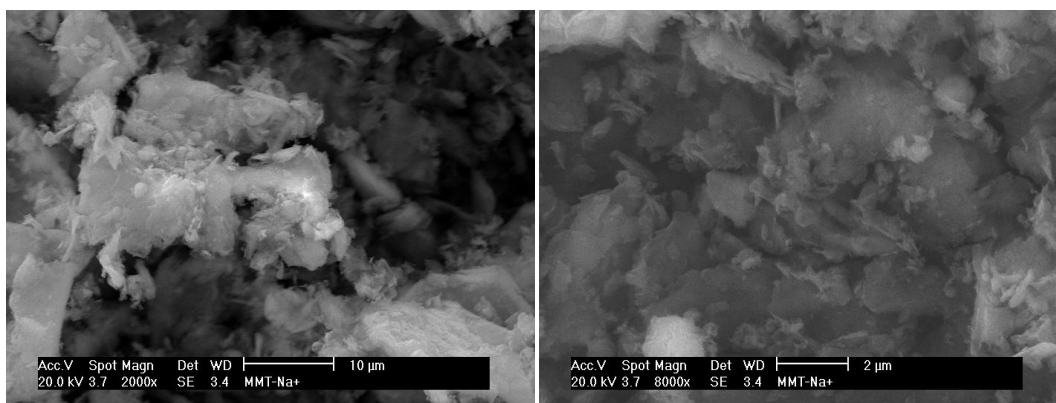


**Figure 4.18 :** SEM pictures of natural montmorillonite (MMT) at 2000x magnification (left) and 8000x magnification (right).

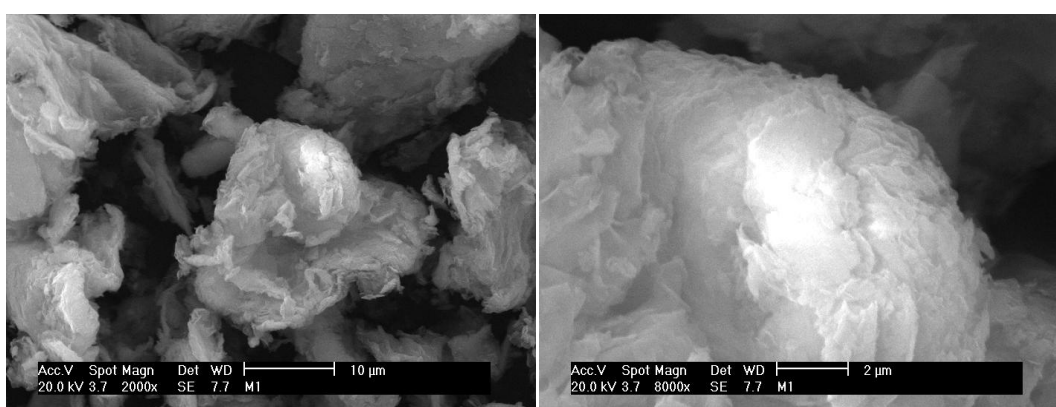


**Figure 4.19 :** SEM pictures of natural montmorillonite after immobilization of CALB (MMTL) at 2000x magnification (left) and 8000x magnification (right).

The morphologies observed for the organo-modified montmorillonite first highlight the benefits of surface organo-modification since the clay aggregates are smaller (Figure 4.20).

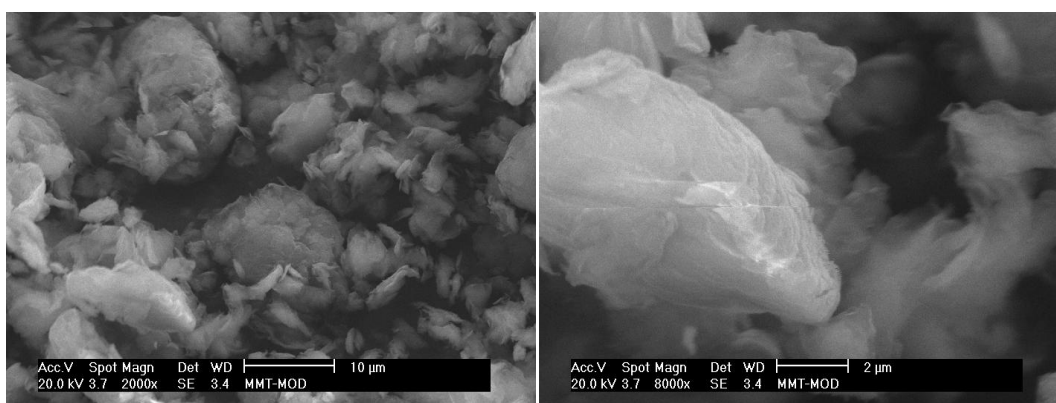


**Figure 4.20 :** SEM pictures of modified montmorillonite (MMTMOD) at 2000x magnification (left) and 8000x magnification (right).

Here again, the clay platelets can be detected in these aggregates and lipase immobilization on the external surface seems to result in a smoother surface for the clay stacks (Figure 4.21).

After GA treatment for enzyme cross-linking, no significant differences can be observed from SEM analyses except at higher magnification where smoother surface is visible with the clay platelets that appear to be fully embedded in the cross-linked enzyme (Figure 4.22).

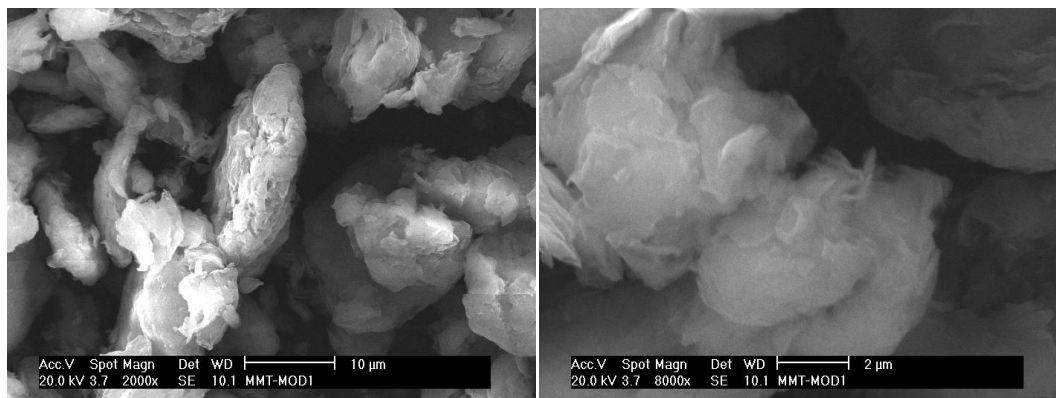


**Figure 4.21 :** SEM pictures of modified montmorillonite after immobilization of CALB (MMTMODL) at 2000x magnification (left) and 8000x magnification (right).

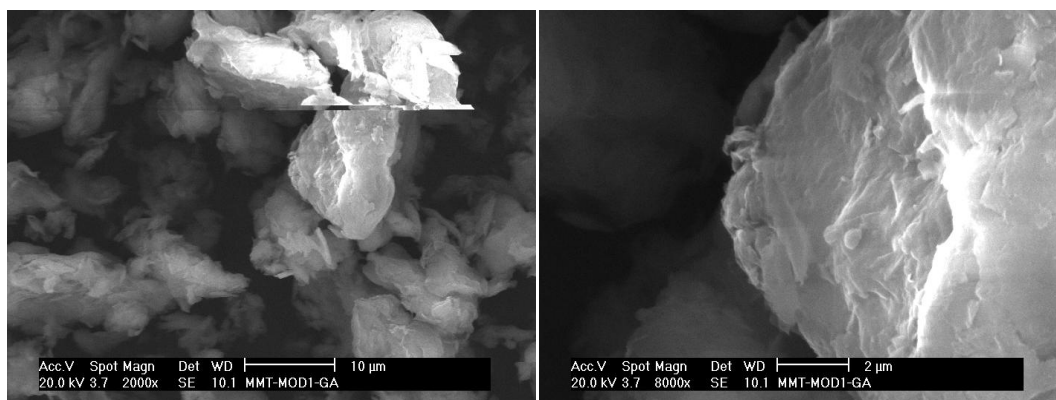


**Figure 4.22 :** SEM pictures of modified montmorillonite after immobilization of CALB and treated with GA (MMTMODL G) at 2000x magnification (left) and 8000x magnification (right).

Thus, all these SEM observations seem to confirm the expected location of immobilized lipase at the surface of the clay aggregates together with the benefits of clay organo-modification which seems to induce smaller aggregates and thus higher surface area for enzyme immobilization.

A major issue with enzymatic catalysis is the stability of the lipase over time. Thus, samples treated with GA were kept at 4 °C for two months to follow the effect of GA on stabilities of these derivatives (see Table 4.3). At the end of two weeks of incubation, for modified-clay derivatives an increase in enzymatic activities were detected. This may be due to some new favorable arrangement and interaction between GA, enzyme and support, providing a better positioning and availability for the lipase catalytic active site. After two months, for all derivatives, approximately 50% of activity loss were recorded.

**Table 4.3 :** Stability test on glutaraldehyde treated derivatives.

<b>Derivative</b>	<b>A (U/mg)</b>
<b>SEPL1b G</b>	<b>13</b>
<b>SEPL1b G (2 months)</b>	<b>6</b>
<b>SEPMODL1b G</b>	<b>241</b>
<b>SEPMODL1b G (1 week)</b>	<b>273</b>
<b>SEPMODL1b G (2 weeks)</b>	<b>276</b>
<b>SEPMODL1b G (2 months)</b>	<b>149</b>
<b>MMTL1b G</b>	<b>132</b>
<b>MMTL1b G (2 months)</b>	<b>70</b>
<b>MMTMODL1b G</b>	<b>283</b>
<b>MMTMODL1b G (1 week)</b>	<b>293</b>
<b>MMTMODL1b G (2 weeks)</b>	<b>341</b>
<b>MMTMODL1b G (2 months)</b>	<b>183</b>
<b>CALB dialyzed G</b>	<b>257</b>
<b>CALB dialyzed G (2 months)</b>	<b>157</b>

\* **G:** treated with glutaraldehyde

These preliminary studies highlighted that derivatives prepared with 7.5 mg of protein loading per gram of clay show highest immobilization efficiency and specific hydrolytic activity. Besides, protein cross-linking by glutaraldehyde treatment allows to enhance the lipase hydrolytic activity for the derivatives based on organo-modified clays. Thus, MMTMODL1 G and SEPMODL1 G derivatives showing higher activity values were chosen as the best candidates in terms of clay type and protein loading amount and were further analyzed for their ROP catalytic capacities. For that, same immobilization procedure with same conditions (7.5 mg of protein loading/ g of clay) was repeated but with higher amount of material (lipase + clay) to get adequate quantities of derivatives to be used as catalysts in polymerization reactions (Table 4.4).

Similar increase tendencies in activities were detected after GA treatment especially for modified-montmorillonite based system. It is important to point out that some variations in terms of specific activities can be observed from one batch of immobilization to another for the same type of support. Beside the typical variations in immobilization procedure, these differences can also be due to dilutions performed for the lipase activity assay and slight differences in ambient temperature during the assay readings. Thus, all lipase hydrolytic activity assays are performed in triplicate and the measured differences are acceptable with condition that the specific activities in different immobilization series for the same type of support are in the same range.

Since these derivatives are to be used as catalysts in polymerization reactions in organic media, a lyophilization step was performed to eliminate the water from the systems, prior to their usage, to provide a long term stability. In this step a drastic loss of activity occurred due to dehydration process causing substantial structural modifications in enzymes (Table 4.4). During the lyophilization freezing step, the exposure of proteins to ice-water interface might have led to their denaturation (Bedu-Addo, 2004).

**Table 4.4 :** Immobilization of lipase on modified clay supports.

Derivative	Loading (mg added protein/ g clay)	Immobilization (%)	Specific Activity (U/mg)
<b>MMTMODL1c</b>	7.5	<b>98</b>	<b>174</b>
<b>MMTMODL1c G</b>			<b>318</b>
<b>MMTMODL1c G LYOPH</b>			<b>177</b>
<b>SEPMODL1c</b>	7.5	<b>97</b>	<b>223</b>
<b>SEPMODL1c G</b>			<b>245</b>
<b>SEPMODL1c G LYOPH</b>			<b>82</b>

\* **G:** treated with glutaraldehyde; **LYOPH:** lyophilized

#### 4.4 Synthesis of PCL Catalyzed by CALB Immobilized on Clays

To study the efficiency of the derivatives for esterification reactions, model polymerization reactions were performed by these lyophilized immobilized enzymes. According to the previously reported results, we know that the amount of nanoclay as well as the quantity of lipase can affect the polymerization reaction, thus both parameters must be investigated.

In order to compare MMT and SEP based catalysts, the presence of same quantity of clay in the reaction medium was chosen as a first reference condition. For this, 300 mg of MMTMODL1c G LYOPH and SEPMODL1c G LYOPH were put as catalyst into the reaction medium. For MMTMODL1c G LYOPH, the amount of immobilized lipase after lyophilization was calculated as 9.19 mg of protein per gram of clay. Therefore, in 300 mg of clay derivative, there will be 2.757 mg of enzyme fixed and this quantity of enzyme has a total unit of activity calculated as  $177 \text{ U/mg} \times 2.757 \text{ mg enzyme} = 488 \text{ U}$ . For all reactions, the total enzyme activity units were calculated this way. This resulted, for these derivatives, in different amounts of total units of activity available for the two reactions; 488 and 215 U, respectively. The catalytic performances of these systems for  $\epsilon$ -CL ROP are presented below (Figures 4.23 a-b).

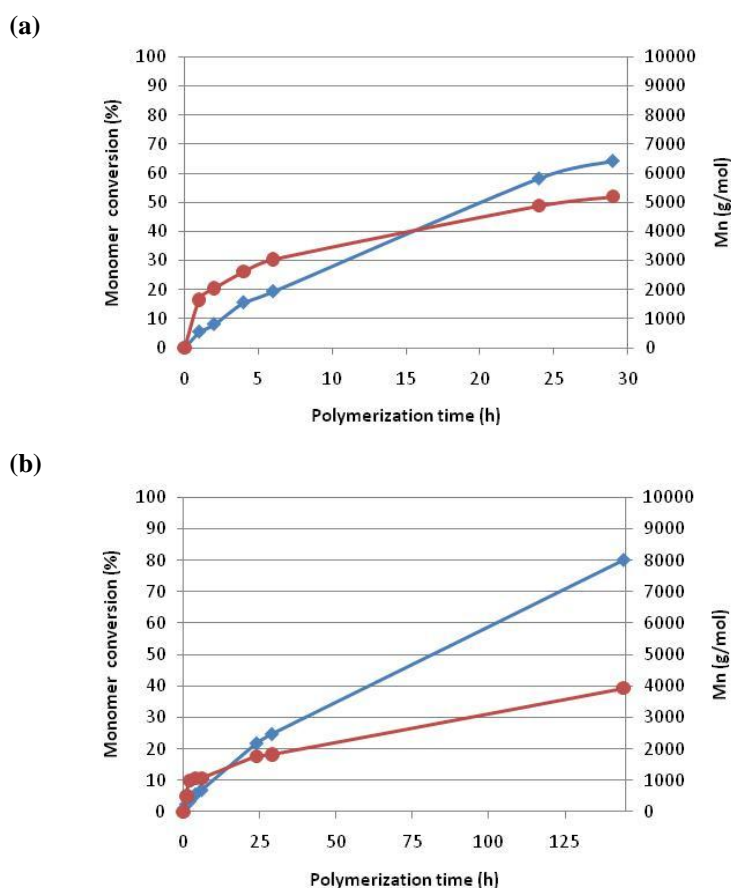


**Figure 4.23 :** Time-evolution curves of  $\epsilon$ -CL conversion ( $\blacklozenge$ ) and molecular weight ( $M_n$ ) of obtained PCL ( $\bullet$ ), as determined by  $^1\text{H}$  NMR analyses for polymerizations (10 ml toluene; 3 ml  $\epsilon$ -CL) catalyzed by (a) 300 mg of MMTMODL1c G LYOPH (488 U) and (b) 300 mg of SEPMODL1c G LYOPH (215 U).

For SEPMODL1c G LYOPH, six days are needed to reach a monomer conversion of 80% and PCL average molecular weight remains quite low (4000 g/mol) (Figure 4.23b). But interestingly, this system still shows some activity towards  $\epsilon$ -CL polymerization in these reaction conditions, which was not observed with the natural sepiolite derivative (data not shown here).

Regarding the reaction kinetics for MMTMODL1c G LYOPH, one can clearly see that the polymerization proceeds faster (ca. 60% monomer conversion after 24 hours) with slightly longer PCL chain (5000 g/mol), compared to the catalytic system based on organo-modified sepiolite (Figure 4.23a).

However, it is also interesting to compare this system with the commercial immobilized lipase NOV-435 for  $\epsilon$ -CL polymerizations with and without the presence of organo-modified montmorillonite in the reaction media. For this, the reactions were carried out in the same conditions with 10 ml of toluene and 3 ml of monomer at 70 °C, using similar clay quantity (i.e. 300 mg) (Figures 4.24 a-b).

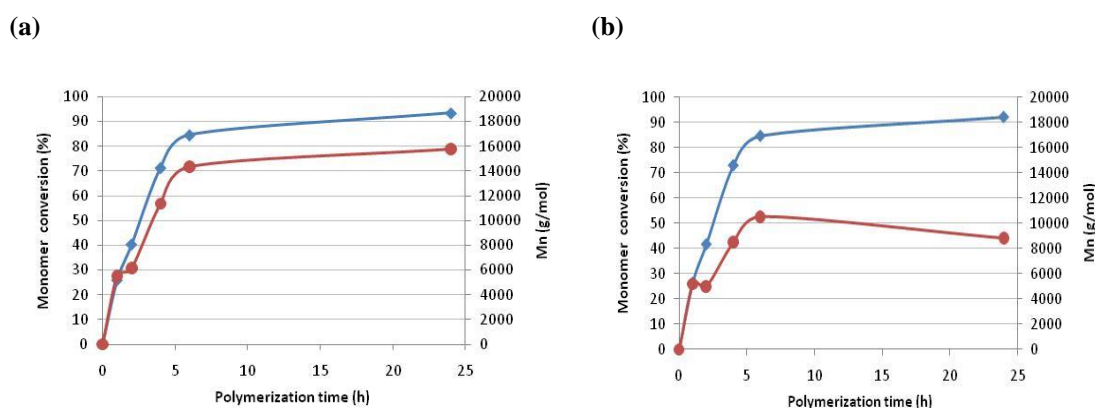


**Figure 4.24 :** Time-evolution curves of  $\epsilon$ -CL conversion ( $\blacklozenge$ ) and molecular weight ( $M_n$ ) of obtained PCL ( $\bullet$ ), as determined by  $^1\text{H}$  NMR analyses for polymerizations (10 ml toluene; 3 ml  $\epsilon$ -CL) catalyzed by (a) 50 mg NOV-435, (b) 50 mg NOV-435 in presence of 300 mg Cloisite® 30B.

As it has already been observed in previous kinetic studies, a drastic decrease in molecular weights of PCL chains is observed with NOV-435, by the addition of organomodified montmorillonite into the reaction medium (Figure 4.24b).

When comparing NOV-435 to the MMTMODL1c G LYOPH, this latter catalytic system shows lower polymerization rate and products of lower molecular weights (i.e 5000 g/mol) are formed. Indeed, the MMTMODL1 catalytic system allows to reach 60% monomer conversion after 24 hours (Figure 4.23a) whereas the NOV-435

system leads to 85% monomer conversion within 6 hours of polymerization time (Figure 4.24b). Moreover, the PCL average molecular weights are slightly higher when the polymerization is catalyzed by NOV-435 in presence of the Cloisite<sup>®</sup> 30B montmorillonite (ca. 8000 g/mol).

However, the commercial catalyst NOV-435 is supposed to contain 10 wt% of protein, thus introducing 50 mg of this catalyst corresponds to the addition of 5 mg protein. As far as MMTMODL1c G LYOPH is concerned, by the addition of 300 mg of clay derivative, there will be 2.757 mg of enzyme introduced in the reaction medium as already presented. So, even if the specific hydrolytic activity of the NOV-435 catalyst cannot be determined, the amount of enzyme involved in the reaction is much more lower for the clay-immobilized lipase system and thus one can expect such lower catalytic activity towards the  $\epsilon$ -CL polymerization.

A new series of immobilization was carried out with the same four types of support, with a loading of 7.5 mg protein per gram of clay, with the purpose to analyze the potential effects of GA on the lipase hydrolytic activity after lyophilization and on the polymerization reaction performances (Table 4.5).

**Table 4.5 :** Immobilization of lipase on different clay supports to test the effect of GA.

Derivative	Loading (mg added protein/g clay)	Immobilization (%)	Specific Activity prior lyophilization (U/mg)	Specific Activity after lyophilization (U/mg)
SEPL1d	7.5	86	39	2.3
SEPL1d G			16	2.0
SEPMODL1d	7.5	98	210	60
SEPMODL1d G			287	117
MMTL1d	7.5	100	178	35
MMTL1d G			210	31
MMTMODL1d	7.5	98	300	130
MMTMODL1d G			382	162

\* G: treated with glutaraldehyde

At the end of the conventional immobilization method used so far, the derivatives in form of a paste were separated into two equal parts. One part was directly lyophilized (e.g., SEPL1) while the other part was treated with GA and then lyophilized (SEPL1G). When looking at the results, no significant protective effect of GA



treatment on enzymes during lyophilization process can be seen (Table 4.5). Derivatives, GA treated or not, lost an important part of their hydrolytic activities after lyophilization. To make a comparison between GA treated and non-treated derivatives in terms of their transesterificative activities, catalysts SEPMODL1/ G and MMTMODL1/ G, having highest specific activities were tested for  $\epsilon$ -CL polymerization (Figures 4.25 and 4.26).

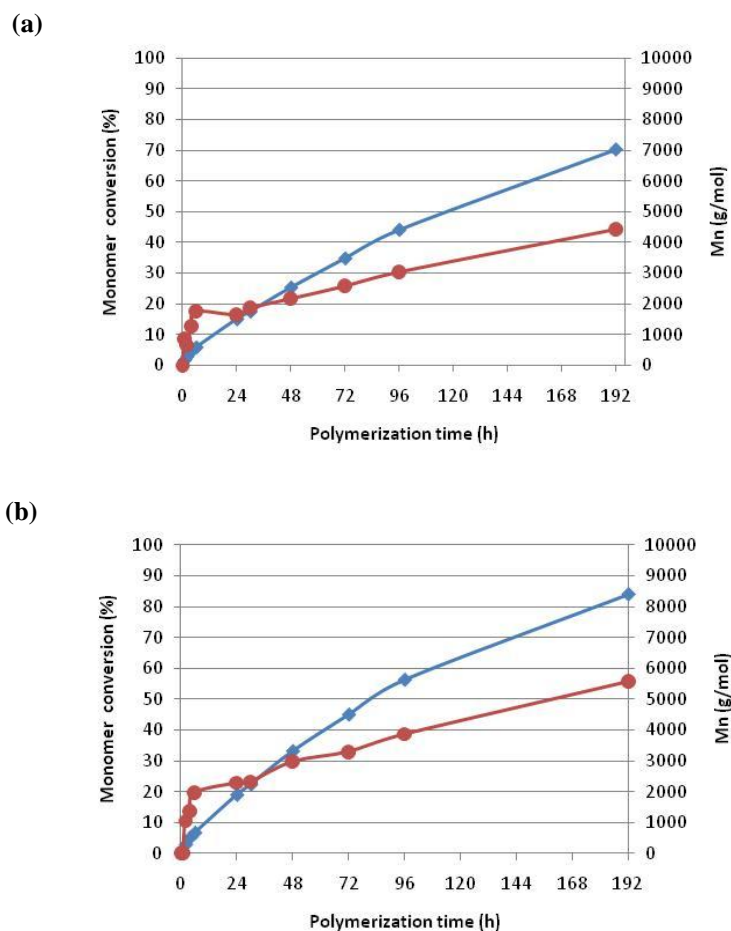


**Figure 4.25 :** Time-evolution curves of  $\epsilon$ -CL conversion ( $\blacklozenge$ ) and molecular weight ( $M_n$ ) of obtained PCL ( $\bullet$ ), as determined by  $^1\text{H}$  NMR analyses, for polymerizations (10 ml toluene; 3 ml  $\epsilon$ -CL) catalyzed by (a) 300 mg of **SEPMODL1d** (120 U) and (b) 300 mg of **SEPMODL1d G** (304 U).

Regarding the SEPMODL1d derivatives, even if the amount of total unit activity present for the GA treated system (304 U) is almost three times the one of the non treated (120 U), polymerization rates and molar masses of the PCLs are almost similar for the two cases. Interestingly sepiolite based systems showed a low activity resulting in a very slow reaction with monomer conversion reaching 80%, only after 8 days. For both systems, the PCL average chain length first increases rapidly and



then the increase in molecular weight proceeds more slowly at higher monomer conversion. This is more likely due to a competition between the insertion of new monomer units and transesterification reactions.

It was concluded that the influence of GA treatment was limited for modified sepiolite type derivatives. Moreover, the huge differences in the measured hydrolytic activity of derivatives do not lead to significant differences in their catalytic ROP behavior. It can be hypothesized that there may be a fixed amount of enzyme interacting with the monomer or more likely that the derivatives may present a totally different catalytic behavior than their hydrolytic activity when catalyzing transesterification systems in organic media.

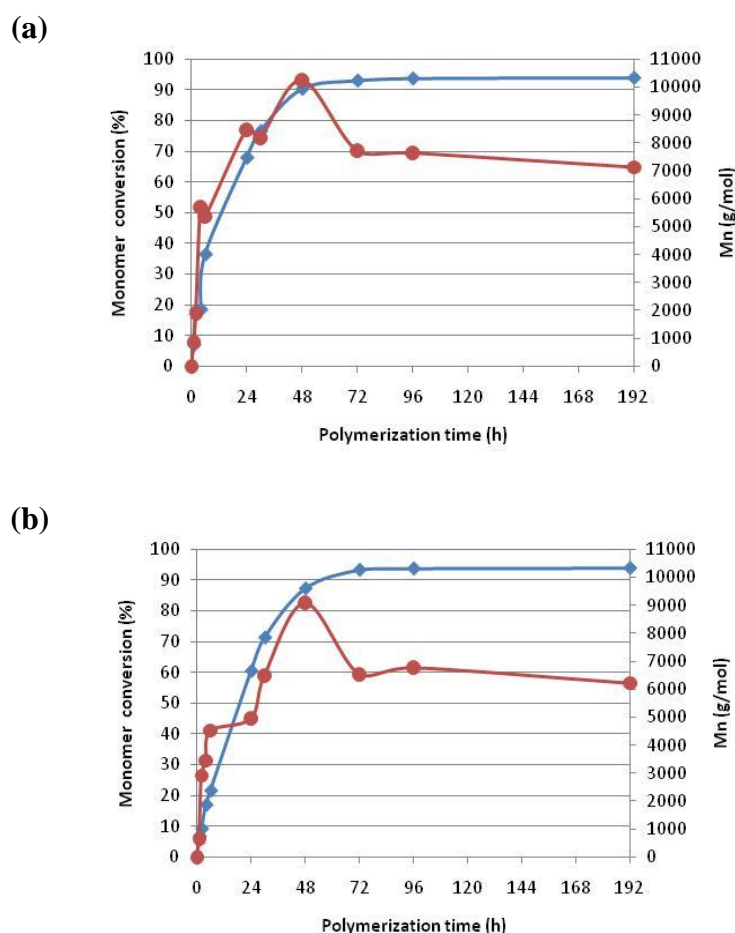


**Figure 4.26 :** Time-evolution curves of  $\epsilon$ -CL conversion ( $\blacklozenge$ ) and molecular weight ( $M_n$ ) of obtained PCL ( $\bullet$ ), as determined by  $^1\text{H}$  NMR analyses, for polymerizations (10 ml toluene; 3 ml  $\epsilon$ -CL) catalyzed by (a) 300 mg of MMTMODL1d (317 U) and (b) 300 mg of MMTMODL1d G (393 U).

The reactions catalyzed with MMTMODL1d derivatives proceeded faster (90% of monomer conversion in 48 h) and higher  $M_n$  values of PCL chains (i.e 10000 g/mol)

were obtained compared to those catalyzed by SEPMODL1d derivatives (Figure 4.26). For both cases (MMTMODL1d treated and non-treated with GA), a decrease in  $M_n$  values was detected after 48 hours due to transesterification reactions. Here again, no significant difference between the two reactions was detected, so it can be assumed that there is a very limited influence of cross-linking by GA treatment onto the enzyme performance. In addition, despite the initial difference between the catalysts in terms of hydrolytic activity, no significant variations can be observed on their polymerization behavior.

This point is confirmed by the fact that even if SEPMODL1d G (304 U) and MMTMODL1d G (393 U) showed similar hydrolytic activities for *p*NPB substrate in aqueous solution, their catalytic behavior was totally different for  $\epsilon$ -CL polymerizations in toluene. This fact is important to understand the different affinities of the derivatives and lipase for different substrates in different catalysis media. This also confirms that no direct correlation can be made between the hydrolytic activities and efficiencies of the corresponding lipases towards  $\epsilon$ -CL polymerization, which also explain why all catalytic systems had to be tested for the ROP reaction.

Therefore, despite the slower kinetics and slightly lower molecular weight obtained, the original MMTMODL1 system shows significant ROP activity which clearly highlights the great potential of our catalytic system.

As already discussed, Cloisite<sup>®</sup> 30B organoclay has proven to be the most appropriate clay-based support for lipase immobilization. Interestingly, as previously mentioned, this organo-clay displays at the clay surface some hydroxyl groups (from the ammonium organomodifier) which can participate in the polymerization reaction as co-initiator, promoting the ring-opening of the lactone and thus the PCL chain grafting and growth from the clay surface.

Thus, in a next step, we aimed at taking profit of these clay hydroxyl groups participating in the polymerization reaction, leading to PCL chain grafting and growth from the clay surface, to elaborate the so-called PCL/clay organic/inorganic nanohybrids and further characterize the properties of these materials.

## 4.5 Elaboration and Characterization of PCL/Clay Nanohybrids

### 4.5.1 Nanohybrids synthesized by NOV-435

Aiming at elaborating and characterizing such organic/inorganic nanohybrids, also called “nano-biocomposites” (Avérous and Pollet, 2012a; Bordes et al., 2009), the scale-up of the most efficient reactions was performed to obtain larger quantities of the final products but also to reach longer chains grafted onto the clays that could result in better dispersed nanohybrid structures.

As a first approach, the NOV-435 immobilized form of the lipase, showing the highest catalytic activity, has been first studied for the  $\epsilon$ -CL polymerization carried out in the presence of different nanoclays to elaborate these organic/inorganic nanohybrids (Figure 4.27).

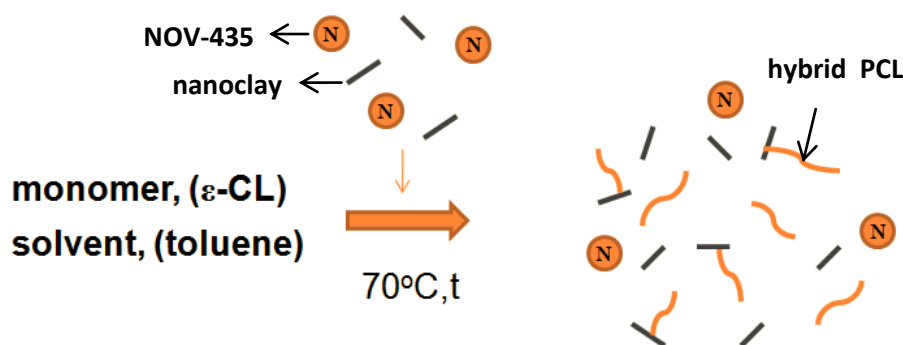


**Figure 4.27 :** Schematic representation of polymerization reactions catalyzed by NOV-435 in the presence of nanoclays.

First, a reference reaction without the addition of clay was performed (NOV0). For other reactions, Cloisite<sup>®</sup> 30B (commercially organomodified montmorillonite), natural form of montmorillonite and sepiolite were used as nanoclays added into the medium (NOV1 to NOV5).

At the end of the reactions, NOV-435 beads were separated and the resulting mixtures were directly precipitated in cold methanol to obtain PCL/nanoclay hybrids, except for NOV1 where clay-rich and PCL-rich fractions were separated by successive chloroform washing/ centrifugation steps.

Reaction conditions are listed below on Table 4.6.

**Table 4.6 :** Larger scale  $\epsilon$ -CL polymerization experiments catalyzed by NOV-435 in presence of different types of clay.

Name	Reaction conditions	Nanoclay added
NOV0	50 ml toluene + 10 ml $\epsilon$ -CL + 50 mg NOV-435	none
NOV1	50 ml toluene + 10 ml $\epsilon$ -CL + 50 mg NOV-435	300 mg Cloisite <sup>®</sup> 30B
NOV2	50 ml toluene + 10 ml $\epsilon$ -CL + 50 mg NOV-435	300 mg Cloisite <sup>®</sup> 30B
NOV3	10 ml toluene + 3 ml $\epsilon$ -CL + 50 mg NOV-435	300 mg Cloisite <sup>®</sup> 30B
NOV4	50 ml toluene + 10 ml $\epsilon$ -CL + 50 mg NOV-435	300 mg Sepiolite-Na <sup>+</sup>
NOV5	50 ml toluene + 10 ml $\epsilon$ -CL + 50 mg NOV-435	300 mg MMT-Na <sup>+</sup>

The nanohybrids obtained at the end of each reaction and the fractions recovered after the separation procedure, were characterized by TGA. The measured inorganic clay content present within the nanohybrid as well as the types of nanoclays are given in Table 4.7, for each product.

DSC analysis was conducted to determine the thermal properties of resulting polymer and organic/inorganic PCL/clay nanohybrids. The obtained results are also reported on Table 4.7.

**Table 4.7 :** Molecular weights and thermal properties of PCL and PCL/clay nanohybrids synthesized by NOV-435 and clay percentages present in the hybrid structures determined by SEC, DSC and TGA analyses.

PCL	M <sub>n</sub> * (g/mol)	T <sub>g</sub> (°C)	T <sub>m</sub> (°C)	$\Delta H_f$ (J/g)	$\chi$ (%)	T <sub>c</sub> (°C)	$\Delta H_c$ (J/g)
<b>NOV0 PCL</b> (no clay)	18000	-61	58	57.8	42	32	62.9
<b>NOV1 PCL</b> (Cloisite <sup>®</sup> 30B; 0.4%)	13000	-	57	67.2	49	37	65.4
<b>NOV2 PCL</b> (Cloisite <sup>®</sup> 30B; 3%)	12000	-	58	69.6	51	37	67.0
<b>NOV3 PCL</b> (Cloisite <sup>®</sup> 30B; 7%)	11000	-	57	67.5	49	36	65.5
<b>NOV4 PCL</b> (Sep-Na <sup>+</sup> ; 3.5%)	14000	-	58	77.4	57	38	74.0
<b>NOV5 PCL</b> (MMT-Na <sup>+</sup> ; 3%)	15000	-60	58	60.1	44	38	62.0

\*determined by <sup>1</sup>H NMR of the final product recovered after precipitation

Since the glass transition phenomenon is related to the amorphous region within the material, it is not surprising that  $T_g$  values were more easily detected on samples having lower crystallinity rates. It can be seen that  $T_g$  values of only two samples could be estimated. Concerning crystallinity percentages, the PCL sample (NOV4 PCL) having 3.5 wt% of natural sepiolite shows a higher crystallinity compared to two other samples (NOV2 and NOV5) containing approximately the same amount but different types of clay. This may be due to the needle-like structure of sepiolite clay which could favorize the PCL crystallization of these hybrid materials.

Regarding crystallization, neat PCL product (NOV0 PCL) displays lower crystallization temperature upon cooling compared to the nanohybrid products. This is an expected behavior since the presence of clay nanoparticles is known to serve as nucleation points for crystal growth (Chivrac et al., 2007). Besides, no significant differences are observed on thermal properties of PCL/Cloisite<sup>®</sup> 30B nanohybrids (NOV1-2-3 PCLs) containing different amounts of organoclays. It can be stated that the content in Cloisite<sup>®</sup> 30B is not a factor affecting the final thermal properties of nanohybrid.

In the case of PCL/MMT- $\text{Na}^+$  (NOV5 PCL), the final product displays characteristic temperatures,  $T_g$  and  $T_m$  values, very similar to pure PCL, except its  $T_c$  value (38 °C) which is higher than the  $T_c$  of neat PCL (32 °C) due to the presence of montmorillonite clays which can promote the crystallization nucleation step.

The resulting PCL/clay nanohybrids were also characterized by X-ray diffraction (XRD). XRD measurements provide a powerful tool to evaluate the changes in the organization of clay platelets and the quality of clay dispersion allowing to determine the different types of nanocomposite structures formed. Small angle X-ray scattering (SAXS) is a conventional method to characterize the interlayer distance between clay particles in layered silicate-based nanocomposites (Bordes et al., 2009). As the intercalation of polymer chains proceeds, the clay interlayer space increases, resulting in a shift of the characteristic reflection peak to lower angles. If the complete exfoliation takes place, this peak is no longer observed in the X-ray diffraction pattern at low angle range. In Figure 4.28, it can be seen that the well ordered structure of layered mineral (Cloisite<sup>®</sup> 30B) is no longer observed in the nanohybrids (NOV2 and NOV3) due to the intercalation of PCL chains between clay platelets.

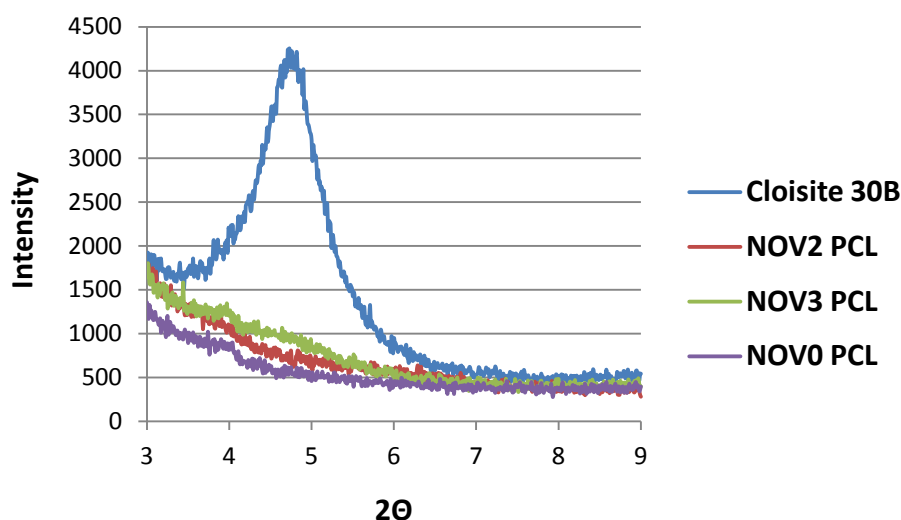


**Figure 4.28 :** XRD patterns of neat PCL(NOV0 PCL), Cloisite<sup>®</sup> 30B and PCL/Cloisite<sup>®</sup> 30B nanohybrids (NOV2-3 PCLs).

The needle-like sepiolite displays a diffraction peak at low angle which corresponds to the internal channel of the clay (Chivrac et al., 2010). Since the layers are joined together by covalent bondings, the clay structure is not modified during polymerization. The layers cannot be delaminated and the polymer chains do not penetrate the channel. Thus, the NOV4 PCL nanohybrid shows a diffraction peak at the same position as the neat sepiolite clay. The lower intensity of the peak is simply due to the dilution effect since sepiolite is present in small percentage within the polymer (Figure 4.29).

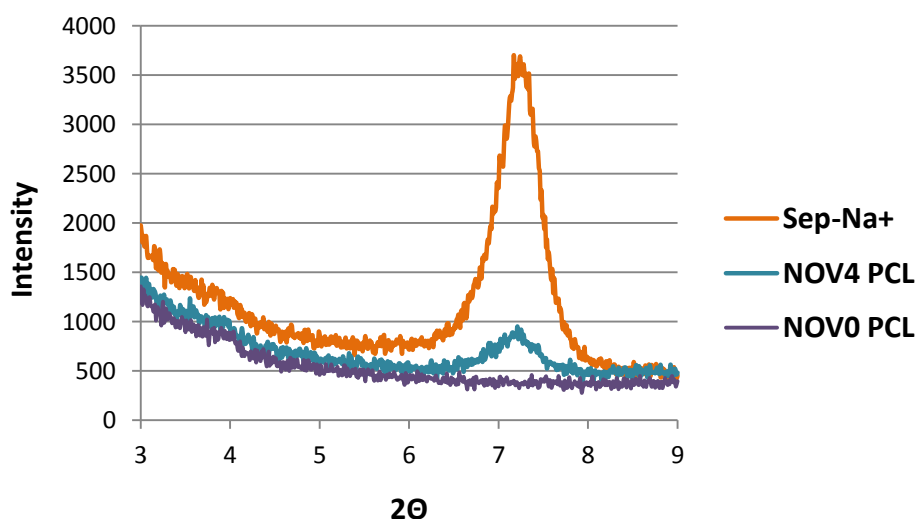


**Figure 4.29 :** XRD patterns of neat PCL (NOV0 PCL), natural sepiolite (Sep-Na<sup>+</sup>) and PCL/sepiolite nanohybrid (NOV4 PCL).

In the case of non-modified montmorillonite (MMT- $\text{Na}^+$ ), the resulting NOV5 PCL nanohybrid seems to present significant intercalation of PCL chains between the clay platelets since the characteristic peak of the clay is no longer observed (Figure 4.30).

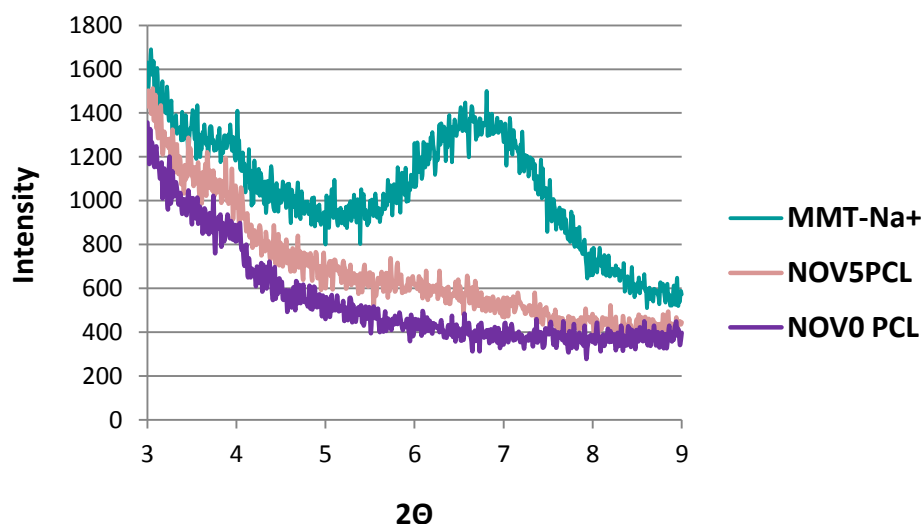


**Figure 4.30 :** XRD patterns of neat PCL (NOV0 PCL), non-modified montmorillonite (MMT- $\text{Na}^+$ ) and PCL/MMT- $\text{Na}^+$  nanohybrid (NOV5 PCL).

PCL/clay nanohybrids based on the different types of clay, but containing approximately the same clay content, were characterized by Scanning Electron Microscopy (SEM) and their visual appearance has been compared (Figure 4.31).

In the case of nanohybrids based on organo-modified montmorillonite (Cloisite<sup>®</sup> 30B), the edges of clay platelets, possibly coated with polymer chains, can be identified at the surface of the final product NOV2 PCL (Figure 4.31a).

While in the presence of non-modified montmorillonite in NOV5 PCL, polymer surface seems slightly rougher but the clay platelets can not be clearly detected (Figure 4.31b).

The presence of sepiolite gives a totally different surface aspect to the nanohybrid product with the needle-like particles that can be seen in a large number on the whole surface of the material (Figure 4.31c).

Nevertheless, SEM observations only give information about the material surface aspect and do not allow to analyze the nanohybrid structure at nanoscale. Thus, the NOV2 PCL, for which the clay platelets were clearly visualized by SEM, was also

analyzed with transmission electron microscopy (TEM) for the better understanding and monitoring of its structure.

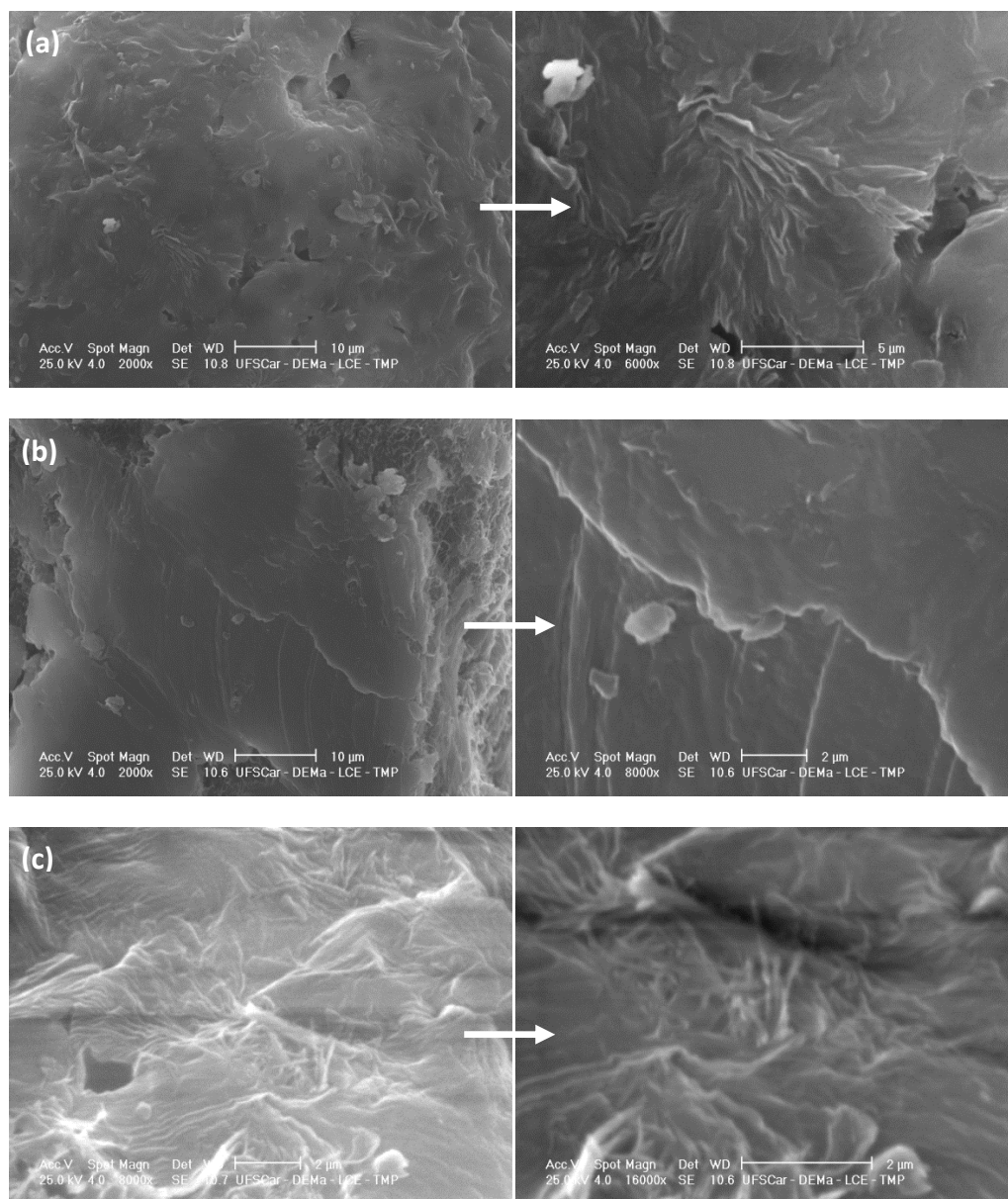


**Figure 4.31 :** SEM pictures of PCL/clay nanohybrids (a) NOV2 PCL (3% Cloisite<sup>®</sup> 30B); (b) NOV5 PCL (3% MMT-Na<sup>+</sup>); (c) NOV4 PCL (3.5% SEP-Na<sup>+</sup>) with their zoomed view on the right hand side.

On these TEM pictures, no big agglomerates of clay are detected but, on the contrary, well separated clay sheets are visible (dark parts on the microphotographs) as a result of the significant intercalation of PCL chains between the organo-modified MMT platelets. Even if a few clay stacks are observed, one can say that the OMMT clay is well dispersed within the material (Figure 4.32a).



The dimensions of the dark entities observed on TEM images match with the average size of montmorillonite sheets and it can also be observed that clay platelets tend to bend (Figures 4.32b-c).

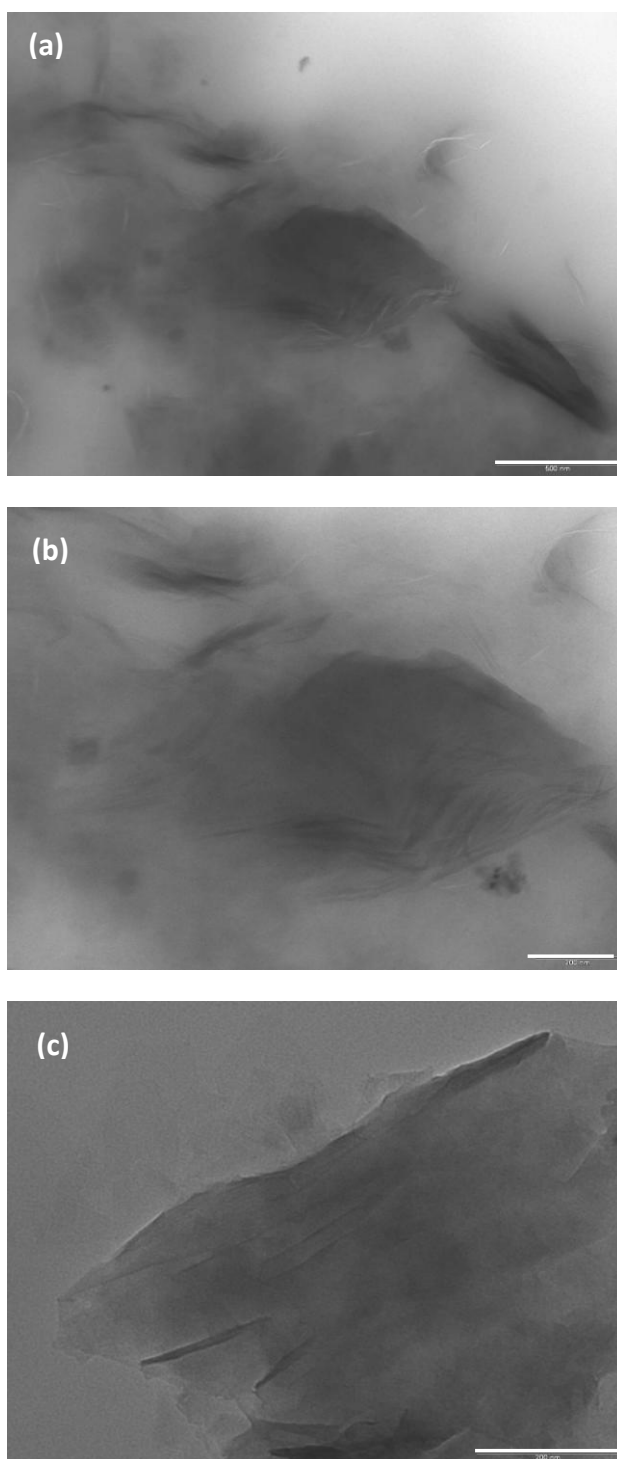


**Figure 4.32 :** TEM pictures of PCL/clay nanohybrids (a) (scale is 500 nm), (b) and (c) (scale is 200 nm).

#### 4.5.2 Nanohybrids synthesized by CALB immobilized on Cloisite<sup>®</sup> 30B

The second approach to elaborate these organic/inorganic nanohybrids by the "grafting from" strategy was to use the catalytic systems based on CALB immobilized on nanoclays. It is expected that, with the lipase being in close vicinity of the clay hydroxyl groups, the anchoring and growth of polyester chains directly from these hydroxyl groups could be favored, leading to higher PCL chain grafting at the clay surface (Figure 4.33).

This original route was compared to the more direct one which was performed by conducting the "grafting from" polymerization using the NOV-435 catalyst in presence of corresponding clays in the reaction medium, as previously described.

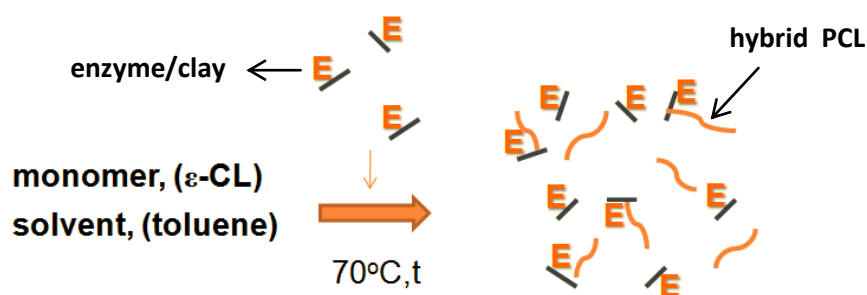


**Figure 4.33 :** Schematic representation of polymerization reactions catalyzed by CALB immobilized on nanoclays.

Recently, Sun et al. (2010) have emphasized on the lack of systematic approach in the current literature, for the immobilization of CALB by adsorption in organic medium. Xin et al. (1999), have suggested that since lipases are insoluble in the solvent, they can be only present within the thin aqueous film layer surrounding the support which is formed by a little amount of solution and in this manner higher immobilization efficiencies can be reached by adsorption in organic media. It has been concluded that highest activity recoveries for CALB can be obtained from immobilizations conducted in more hydrophobic solvents (Sun et al, 2010).

Thus, based on this concept, two different media and two different drying procedures were employed in order to test their respective effects on the resulting immobilized enzyme activity. CALB immobilization onto Cloisite<sup>®</sup> 30B was performed both in phosphate buffer as the aqueous medium and in toluene as the organic medium with a loading ratio of 7.5 mg protein per g of clay. For each case, the resulting paste

composed of enzyme adsorbed onto clay was separated into two equal parts and dried by two different techniques, namely lyophilization and vacuum drying at 30 °C.

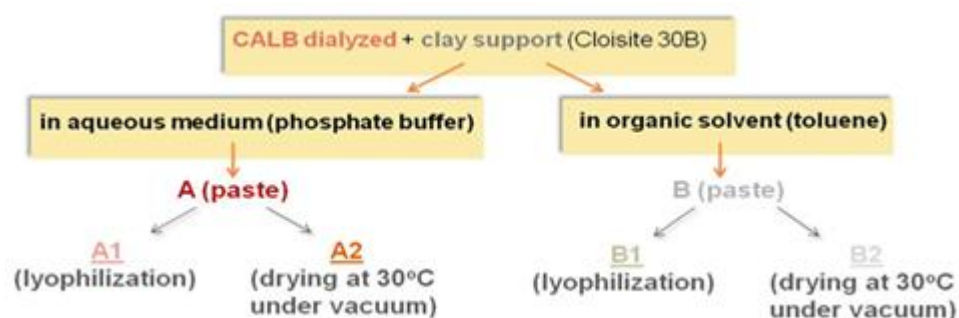


**Figure 4.34 :** Procedures for immobilization in aqueous and organic media with two different drying techniques.

Hydrolytic activities of free, dialyzed, lyophilized CALB and lipase derivatives (CALB immobilized onto Cloisite<sup>®</sup> 30B) were determined and are reported in Table 4.8.

**Table 4.8 :** Effect of immobilization media and drying techniques on final specific activity of the lipase derivatives (CALB immobilized onto Cloisite<sup>®</sup> 30B).

Enzyme	A (U/mg)
<b>CALB</b>	<b>170</b>
<b>CALB dialyzed</b>	<b>159</b>
<b>A (paste)</b>	<b>138</b>
<b>A1 lyoph</b>	<b>126</b>
<b>A2 dried (30°C)</b>	<b>173</b>
<b>B1 dried (30°C)</b>	<b>167</b>
<b>B2 dried (30°C)</b>	<b>179</b>
<b>CALB LYOPH</b>	<b>127</b>

No important difference in final hydrolytic activities of the enzyme was observed between the systems neither for the usage of two different media nor for the distinct drying procedures. It is worth noting that B1, which must have normally been lyophilized, was dried under vacuum due to technical limitations for the evaporation of the organic solvent in lyophilizator.

Interestingly, no significant activity loss was observed after the lyophilization process and immobilization procedure performed in aqueous medium gave good

results thus, these two process parameters were further retained for the lipase/clay derivatives preparation.

Nevertheless, all these new catalyst systems (lipase/clay derivatives) were used for the ROP of  $\epsilon$ -CL in typical conditions. 10 ml of toluene, 3 g of  $\epsilon$ -CL and 300 mg derivative (CALB/clay) as catalyst were used for the polymerization reactions (Table 4.9). At the end of reaction (48 h), an aliquot was withdrawn from the medium and analyzed by  $^1\text{H}$  NMR to determine the monomer conversion. Then, the whole mixture was directly precipitated in methanol to recover the resulting organic/inorganic nanohybrid. Then the precipitated product was filtrated, washed and dried. The final product recovered as a powder was then characterized.

**Table 4.9 :**  $\epsilon$ -CL conversion percentages and molar masses of PCLs observed in polymerizations catalyzed by A1 and B2 catalysts.

Catalyst	t (h)	Monomer conversion (%)	$M_n$ (g/mol)*
<b>A1</b>	48	95	8000
<b>A2</b>	48	90	3500
<b>B2</b>	48	86	3000

\*determined by  $^1\text{H}$  NMR on the final powder product

Even if the difference in terms of hydrolytic activity was not very important between A1 and B2 catalysts, their performances for PCL chain synthesis were very different from each other. They almost reached similar monomer conversion percentages but B2 catalyst (for which the CALB immobilization was performed in organic medium) tend to produce much smaller PCL chains. It can be concluded that CALB immobilized onto Cloisite<sup>®</sup> 30B in toluene medium leads to an active catalyst system but showing lower performances compared to the immobilized lipase obtained in aqueous solution.

To explain such a behavior it is suggested that, when lipase is immobilized in the organic media, it has a very limited amount of water, as a thin film surrounding the enzyme, available for its catalytic activity. When it was assayed for the hydrolysis of *p*NPB in buffer solution, it could find water molecules necessary for its configuration change so that its active site was more accessible to the substrate. By this way it could reach similar hydrolytic activities with A derivatives (lipase immobilization performed in water). On the other hand, during the catalyzed polymerization carried

out in toluene, due to the scarce of water molecules, some motion restrictions might occur, due to the low hydration of the enzyme, causing a limited availability of its active site.

Besides, it is expected that derivatives which are lyophilized would present lower water content than the derivatives recovered by a simple vacuum drying at 30 °C which could contain more water due to the difficulty to remove all water molecules from the clay structure. As a consequence, these water molecules may be involved as co-initiators for the polymerization, thus explaining the obtained PCL chains displaying lower molecular weights (A2 PCL) (see Table 4.9).

It is then interesting to compare the performances of the clay-immobilized lipase derivatives to the NOV-435 commercial catalytic system. First, it is worth pointing out that for reactions performed in similar conditions, the effective amount of enzyme varies. Indeed, 300 mg of A or B derivatives contained approximately 2.5 mg of CALB protein, while when using 50 mg NOV-435 as catalyst for the synthesis of NOV3 PCL, the enzyme amount was 5 mg. It can be seen that, in our system, the lower amount of CALB compared to NOV-435 was able to synthesize PCL chains with a molar mass of 8000 g/mol, whereas NOV-435 containing an enzyme amount twice of it, produced a PCL with a  $M_n$  value of 11000 g/mol.

PCLs synthesized by A1, A2 and B2 derivatives were characterized by TGA analysis (Figure 4.35). Their degradation behavior is very similar pursuing a four step process. As far as the thermogravimetric analyses are concerned, one can see that the recorded weight loss evolutions are very similar for the three nanohybrid materials. Thus, it can be concluded that the slight differences in terms of PCL molecular weights and clay contents do not influence the PCL main degradation temperature. The three samples show identical degradation behavior with two main degradation steps and very close main degradation temperatures (around 267 and 366 °C). This first two-steps weight loss corresponds to PCL chains degradation while the weight loss recorded at 466 and 569 °C are more likely due to some degradation of the clay. This degradation behavior is quite different from the results reported in the literature for PCL/montmorillonite nano-biocomposites usually showing a single degradation step at higher temperatures (above 400 °C) (Lepoittevin et al., 2003). This difference is most likely due to the lower PCL molecular weights obtained in the present study, as it has already been reported (Persenaire et al., 2001).

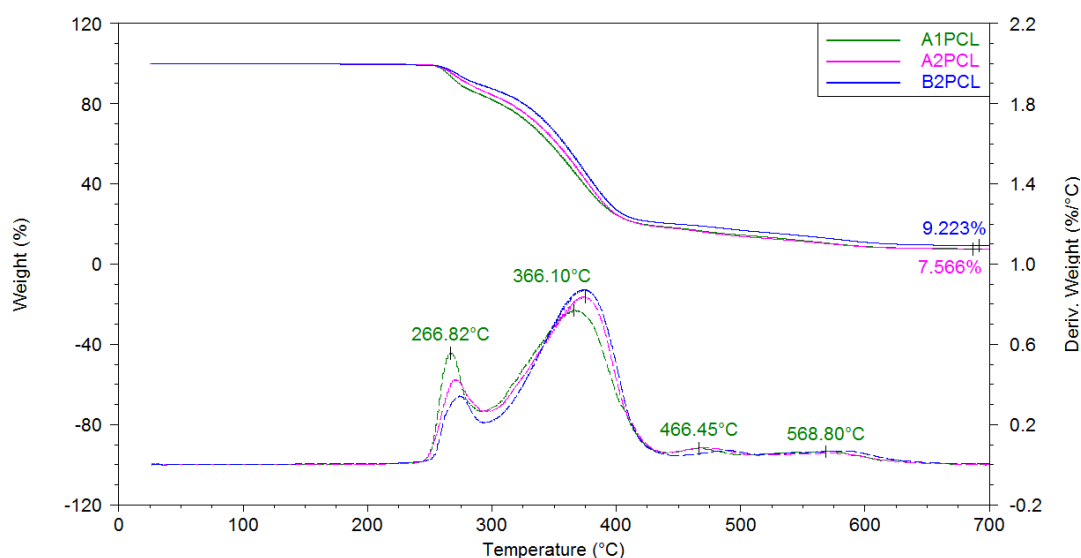


**Figure 4.35 :** TGA curves (weight loss and its temperature derivative) of the PCL/clay nanohybrids obtained from the polymerization catalyzed by A1, A2 and B2 derivatives.

However, these TGA results allowed to determine the inorganic clay content in the nanohybrid material as the unburnt residue left at 700 °C. These values are reported in Table 4.10.

From these results, one can see that the PCL/clay nanohybrid obtained from the B2 derivative shows a higher final clay content due to the slightly lower monomer conversion (and thus lower content in organic material in the final product).

**Table 4.10 :** Thermal properties of resulting PCL/Cloisite<sup>®</sup> 30B nanohybrids synthesized by CALB immobilized onto Cloisite<sup>®</sup> 30B and clay percentages present in the nanohybrids as determined by DSC and TGA.

PCL	T <sub>g</sub> (°C)	T <sub>m</sub> (°C)	ΔH <sub>fusion</sub> (J/g)	χ (crystallinity %)	T <sub>c</sub> (°C)	ΔH <sub>c</sub> (J/g)
<b>A1 PCL</b> (Cloisite <sup>®</sup> 30B; 7.6%)	-60	58	67	48	35	66
<b>A2 PCL</b> (Cloisite <sup>®</sup> 30B; 7.5%)	-60	57	76	55	35	71
<b>B2 PCL</b> (Cloisite <sup>®</sup> 30B; 9%)	-57	57	66	48	37	63

As far as the DSC results are concerned, one can see that the different PCL/clay nanohybrids obtained with our clay-immobilized lipase derivatives show very similar

thermal properties. No clear trend can be observed between the nanohybrids; all three samples display equivalent melting and crystallization temperatures and similar crystallinity contents, regardless of the catalyst system used and final clay content.

Additionally, the thermal degradation behavior of the nanohybrid product obtained from our A1 catalyst (CALB immobilized on Cloisite<sup>®</sup> 30B) was compared to the NOV3 PCL synthesized in the same conditions by the catalysis of NOV-435 in presence of the organo-clay (Figure 4.36).

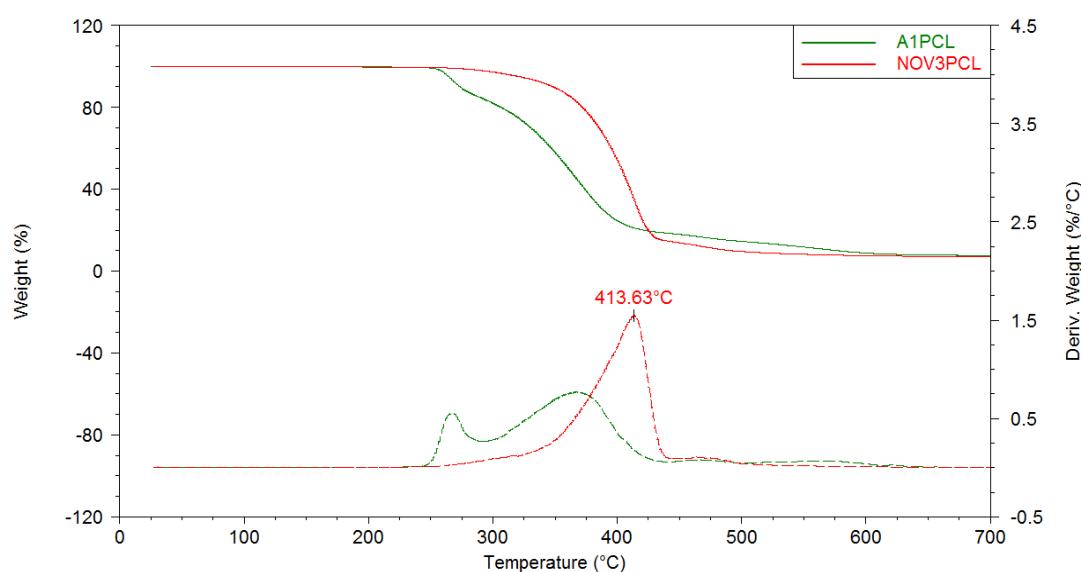


**Figure 4.36 :** TGA spectrum of A1 PCL synthesized by CALB immobilized onto Cloisite<sup>®</sup> 30B, and NOV3 PCL synthesized by NOV-435 in the presence of Cloisite<sup>®</sup> 30B.

From these TGA curves, it can be observed that A1 PCL starts to degrade at lower temperature compared to NOV3 PCL which may be due to its lower molecular weight. The derivative weight loss curve of NOV3 PCL shows a peak at 413 °C which represents the main degradation of PCL whereas A1 shows a multiple step degradation process with maximum degradation rates at respectively 267 and 366 °C.

Such a marked two-steps degradation could be due to sample heterogeneity in terms of PCL average molecular weights combined to the grafted or non-grafted nature of these chains. However, one cannot exclude that the first degradation step of A1 in the range of 225-290 °C may be related with the decomposition of surfactant molecules of the organoclay and degradation of loose enzymes (protein molecules attached onto previously adsorbed ones, rather than bind onto the support surface). The degradation step which follows between 290 and 450 °C corresponds to the main degradation of

PCL and can also be attributed to the pursuing decomposition of organoclay surfactant molecules and the degradation of anchored enzymes adsorbed at the surface of the support and thus more protected.

XRD analyses of the PCL/clay nanohybrids obtained by clay-immobilized CALB catalysts (A1, A2 and B2 derivatives) were performed and their nanostructure compared to NOV3 PCL synthesized in the same conditions but by the catalysis of commercial NOV-435 in presence of Cloisite<sup>®</sup> 30B (Figure 4.37).

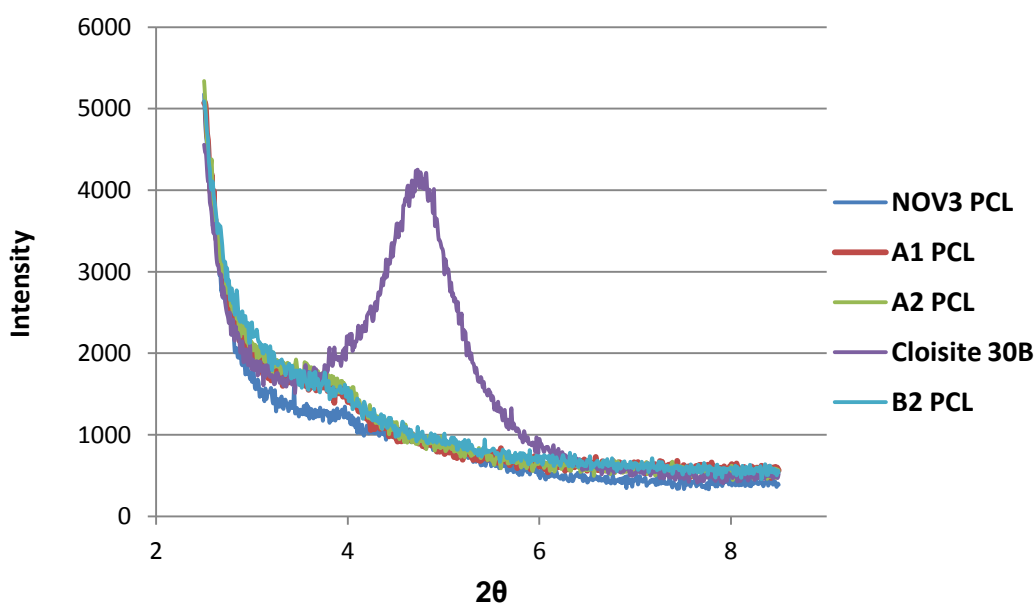


**Figure 4.37 :** XRD patterns of modified montmorillonite (Cloisite<sup>®</sup> 30B) and PCL/Cloisite<sup>®</sup> 30B nanohybrids (NOV3, A1, A2, B2 PCLs).

Analyzing the XRD patterns of these nanohybrids, it can be seen that the specific diffraction peak of Cloisite<sup>®</sup> 30B is shifted to lower angles and shows a very low intensity for all the PCL/clay nanohybrids. This clearly demonstrates the occurrence of a significant PCL chain intercalation with a possible partial exfoliation of clay sheets in the PCL matrix of these nanohybrids.

When the polymerization was catalyzed by the enzyme immobilized onto nanoclay, it can be assumed that the adsorbed lipase and clay hydroxyl groups close vicinity favored the grafting of polymer chains and thus enhanced the intercalation/exfoliation of clay nanoparticles.

Such grafting of polymer chains at the surface of clay nanoparticles is also well-known for allowing the elaboration of organic/inorganic nanohybrids displaying



finely dispersed and well distributed nanoparticles within the polymeric matrix. This has been confirmed by performing SEM analyses of the recovered PCL/Cloisite<sup>®</sup> 30B nanohybrids. From the SEM pictures of these nanohybrid materials synthesized by CALB immobilized onto Cloisite<sup>®</sup> 30B (A1 and B2 derivatives), the edges of the clay platelets can be identified at the surface of the material (Figure 4.38).

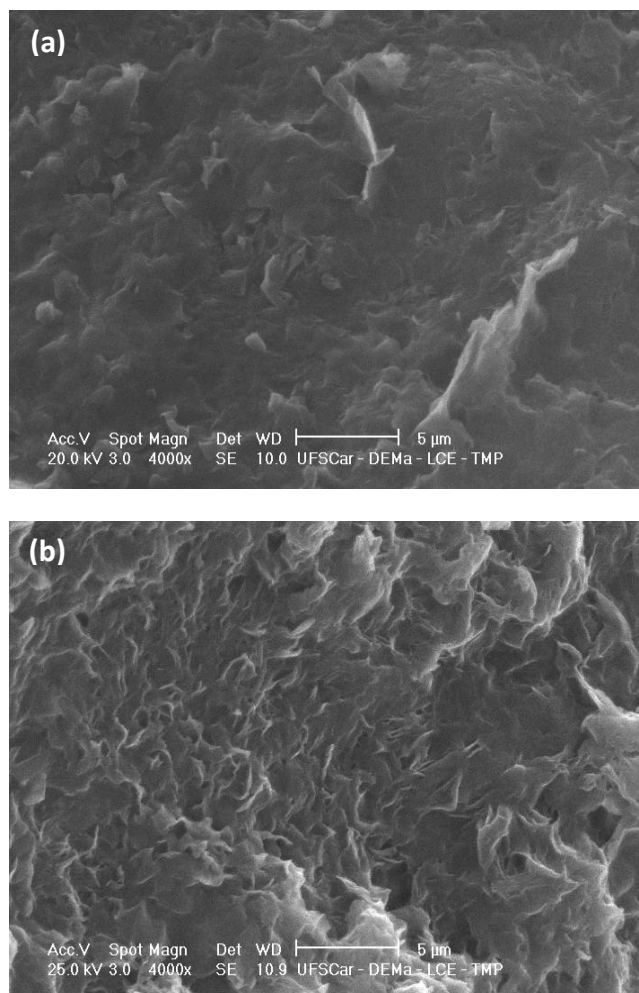


**Figure 4.38 :** SEM pictures of PCL/Cloisite<sup>®</sup> 30B nanohybrids synthesized by A1 and B2 catalysts (a) A1 PCL (7.6 wt% Cloisite<sup>®</sup> 30B); (b) B2 PCL (9.2 wt% Cloisite<sup>®</sup> 30B).

The surface of the B2 PCL nanohybrid clearly shows higher roughness and highly visible clay platelets. This difference in surface aspect between the two nanohybrids could be due to the lower clay content for A1 PCL (7.6 wt% Cloisite<sup>®</sup> 30B) combined to the higher average molecular weight of PCL chains that could result in a more pronounced coating of the clay platelets by the PCL matrix.

#### 4.6 Nanohybrid Characterization for Evidencing Polymer Grafting on Clay

As it has been shown and discussed before, the analysis of the polymerization kinetic trends and material characterization such as molecular weight evolution, brought several elements. They seem to indicate that the -OH groups available at the clay surface participate to the enzymatically catalyzed ROP reaction leading to the grafting of PCL chains at the surface of the organoclay. However, direct demonstration of such grafting is difficult to obtain and additional characterizations are necessary to bring supplementary evidences of the PCL chain grafting onto clay nanoparticles.

In order to evidence such polymer grafting at the clay surface, the final product mixture recovered was dissolved in chloroform and then separated into a clay-rich fraction and a PCL-rich fraction, by three successive chloroform washing/centrifugation steps. The solid clay-rich phase, collected as a pellet after each centrifugation was washed by chloroform and after three successive washing/centrifugation repeats, it was dried. Besides, the non-grafted PCL was recovered from the supernatant solution by precipitation in methanol and further dried to obtain the PCL-rich phase as a fine white powder (Figure 4.39). Both fractions were characterized by thermogravimetric analysis (TGA).

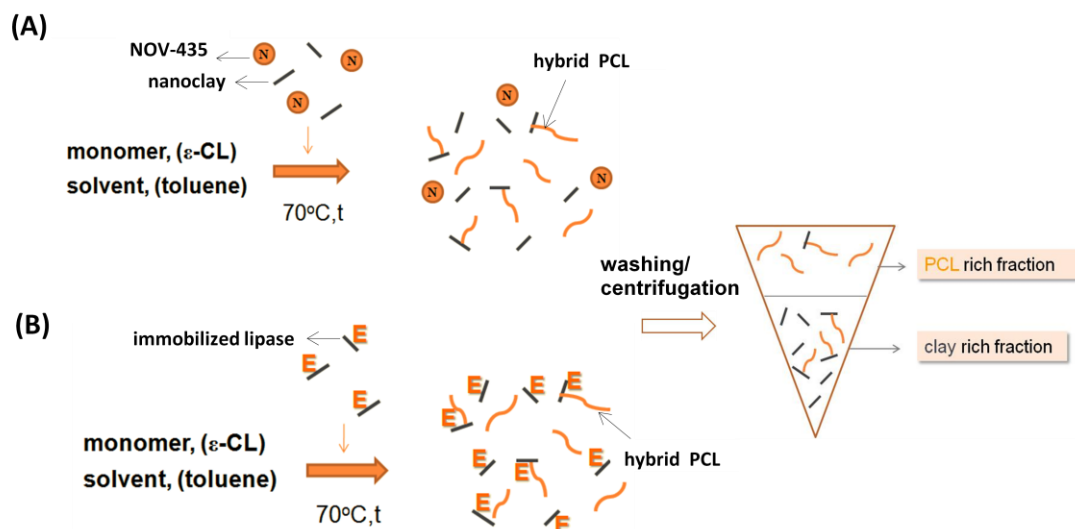


**Figure 4.39 :** Schematic representation of the separation procedure for different types of nanohybrids.

First, it has been verified that the fraction separation procedure was efficient by simply solution-blending PCL chains with clays in solution. After the centrifugation

separation procedure, both fractions were analyzed by TGA and the results (data not shown here) have confirmed that the PCL-rich fraction did not contain any residual clay and similarly that the clay-rich fraction was not displaying thermal degradation of organic materials.

In a first series of experiments, separation procedure was performed on the PCL/clay nanohybrids obtained from  $\epsilon$ -CL polymerization catalyzed by commercial NOV-435 catalyst carried out in presence of clays.

Figure 4.40 presents the weight loss curves of these PCL-rich and clay-rich phases, compared to the neat nanoclay, for the polymerization reaction carried out in the presence of 100 mg of unmodified sepiolite (SEP) clay with 2 ml of toluene; 1 ml of  $\epsilon$ -caprolactone and 100 mg of NOV-435.

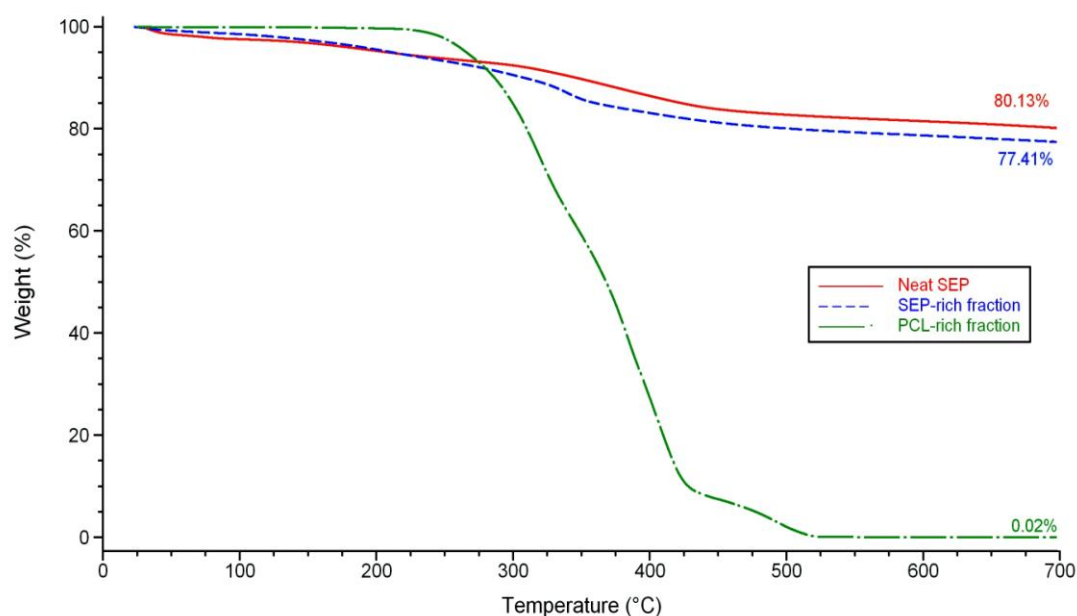


**Figure 4.40 :** Weight loss curves of neat SEP, SEP-rich fraction and PCL-rich fraction of PCL/clay nanohybrid obtained from NOV-435 catalyzed polymerization. TGA performed under air atmosphere.

As shown in this figure, neat sepiolite undergoes a multistep dehydration process when heated from 20 to 700 °C. The first step is due to the loss of hydration water (zeolitic water) which is physically bonded to sepiolite. This weight loss may strongly depend on the atmospheric relative humidity. In the second step sepiolite loses half of its coordinated water and then the remaining, more tightly bonded part, is lost in the third step occurring at higher temperatures. As it can also be seen, the

curve recorded for the SEP-rich fraction is very similar to the neat clay but only differs by a slightly higher weight loss occurring between 250 and 400 °C. This temperature range corresponds to the PCL main degradation step. The content in unburnt residues (at 700 °C) for these two samples allows to show that the SEP-rich fraction may contain approximately 2.7 wt% of grafted PCL chains. The non-modified sepiolite clay having hydroxyl groups at the clay platelets surface (more precisely on the edges) such polymer grafting could be expected.

The extracted PCL-rich fraction shows a multistep degradation process, with the main weight loss (more than 90%) occurring between 200 and 450 °C (Figure 4.40). A very low content (ca. 0.02 %) of unburnt inorganic residues in this PCL-rich fraction also indicates that some clay nano-platelets are present in the polymeric phase due to the grafting of the PCL at their surface allowing some of these clay nano-platelets to be extracted in the PCL-rich fraction during the separation procedure.

The same characterization was performed on another nanohybrid (Figure 4.41) for which the synthesis was carried out with larger volumes of solvent and monomer (respectively 10 ml of toluene and 5 ml of  $\epsilon$ -CL) but same amount of enzyme (100 mg NOV-435) and in the presence of only 50 mg of sepiolite.

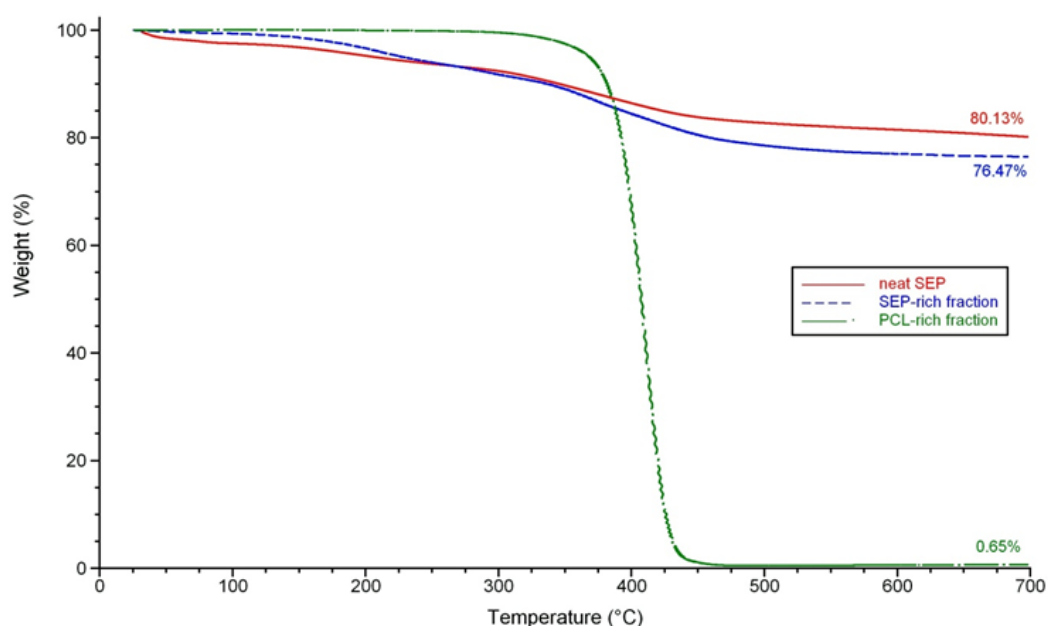


**Figure 4.41 :** Weight loss curves of neat SEP, SEP-rich fraction and PCL-rich fraction of PCL/clay nanohybrid obtained from NOV-435 catalyzed polymerization. TGA performed under air atmosphere.

As shown by the TGA, the result was similar to the previous one, reaching a percentage of ca. 3.7 wt% of grafted PCL chains in the clay-rich fraction (see Figure 4.41).

A second type of polymerization reaction was carried out in the presence of 300 mg of Cloisite<sup>®</sup> 30B organo-modified montmorillonite (MMTMOD) clay with 10 ml of toluene; 3 ml of  $\epsilon$ -caprolactone and 50 mg of NOV-435. Figure 4.42 presents the weight loss curves of the PCL-rich and clay-rich phases obtained from this reaction, compared to the neat MMTMOD nanoclay.

After the separation procedure, the PCL-rich phase recovered from the polymerization carried out with organo-modified montmorillonite displays a degradation behavior similar to the one of the PCL-rich fraction recovered from the reaction performed with sepiolite. The only difference is that the PCL main degradation occurs at slightly higher temperature likely because of the higher chain molecular weights obtained when the polymerization is performed in presence of the organo-modified montmorillonite compared to the hydrophilic non-modified sepiolite.

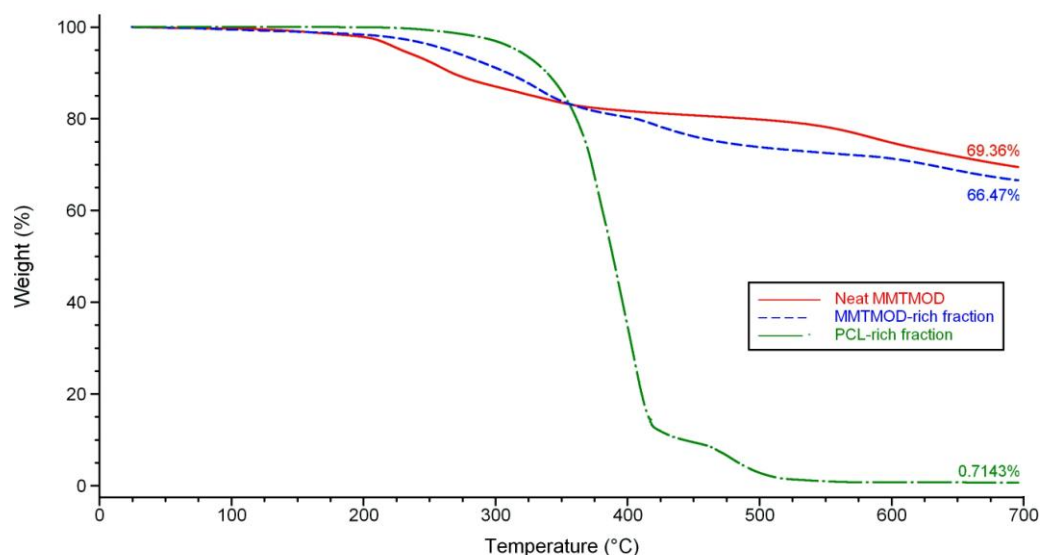


**Figure 4.42 :** Weight loss curves of neat MMTMOD, MMTMOD-rich fraction and PCL-rich fraction of PCL/clay nanohybrid obtained from NOV-435 catalyzed polymerization. TGA performed under air atmosphere.

According to the measured weight loss, it can be estimated that the MMTMOD-rich fraction contains approximately 2.9 wt% of grafted PCL chains.

The effective PCL chain grafting at the clay surface is further confirmed by the TGA results of the PCL-rich fraction which shows unburnt residues (ca 0.7 wt% at 700 °C) arising for the inorganic clay fraction dragged to the supernatant solution by its grafted polymer chains.

As previously described for sepiolite-based systems, the same characterization was performed on another nanohybrid for which the synthesis was carried out with larger volumes of solvent and monomer but same amounts of MMTMOD and enzyme. The TGA result was similar to the previous one, reaching a percentage of ca. 3 wt% grafted PCL chains in the clay-rich fraction (not shown here).

It is worth pointing out that similar polymerization and characterization were performed using organo-modified sepiolite which should have a different content and availability of surface hydroxyl groups but the TGA analyses (not presented here) demonstrated that the amount of grafted PCL chains on the clay-rich fraction was similar (between 1 and 3 wt%) and still very limited.

Similarly, no significant PCL-grafting on the clay was evidenced when the polymerization was carried out with the non-modified montmorillonite (not shown here). This result is not surprising since MMT- $\text{Na}^+$  does not have hydroxyl groups and thus polymer grafting is unlikely to occur.

These results clearly evidenced the PCL chain grafting from the clay surface due to the well-known participation of the hydroxyl groups as co-initiators to the polymerization. However, such PCL chain grafting at the clay surface remains limited when polymerization reactions are performed with the NOV-435 catalytic system. One may suppose that this heterogeneous catalyst formed of CALB immobilized on porous acrylic resin may favor the formation of free PCL chains rather than grafted ones as a result of the hydroxyl groups at clay surface being difficult to reach for the immobilized enzyme and thus unlikely to participate in a large extent to the polymerization reaction.

It has been shown before that the catalytic systems based on CALB immobilized onto nanoclays display interesting catalytic performances and could lead to significant PCL chain grafting at the surface of organoclays. Indeed, it is expected that the close proximity between the clay surface hydroxyl groups and the immobilized CALB enzyme significantly favors the probability for these -OH groups

to be involved in the catalyzed ROP reaction leading to higher PCL grafting at the surface of the organoclay. Thus, similar separation/extraction procedure was performed on these nanohybrids followed by thermogravimetric analyses aiming at evidencing the effective polymer grafting onto the clay nanoparticles.

As previously described, the SEPL derivatives showed low activity for the  $\epsilon$ -CL polymerization. Nevertheless, attempts were made to characterize the recovered PCL/sepiolite nanohybrids after separation/extraction procedure. A polymerization reaction was performed by the catalysis of 250 mg of SEPL3 (derivative constituted of ~5 mg of protein fixed (CALB) onto 250 mg of sepiolite) with 1 ml of  $\epsilon$ -CL in 2 ml of toluene. By analyzing the TGA results, it can be clearly seen that there was no significant grafting on sepiolite since the SEP-rich fraction shows exactly the same weight loss as the neat clay (Figure 4.43).

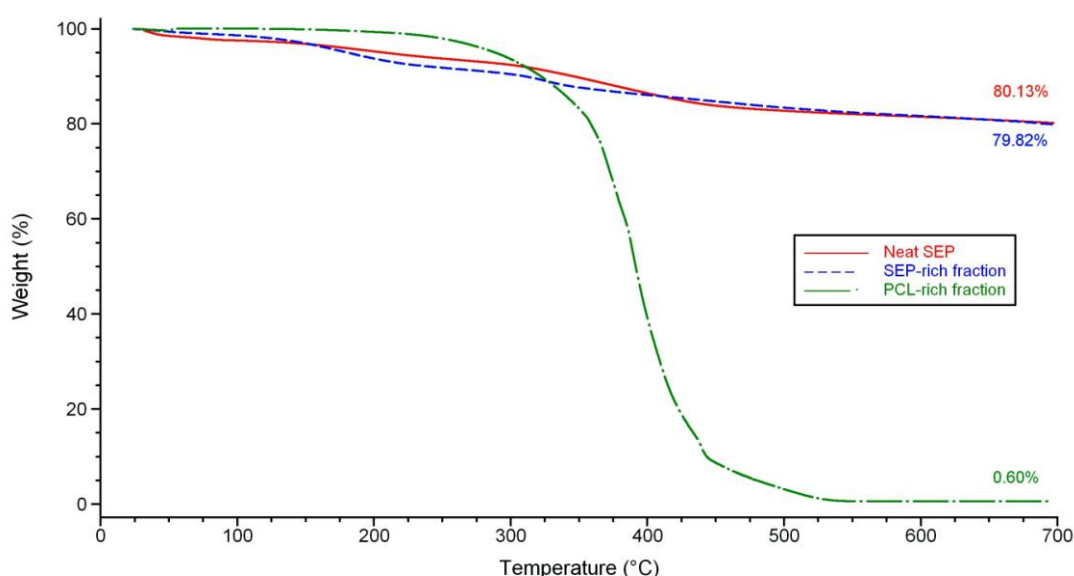


**Figure 4.43:** Weight loss curves of neat SEP, SEP-rich fraction and PCL-rich fraction of PCL/clay nanohybrid obtained from the polymerization catalyzed by CALB immobilized on sepiolite (SEPL3). TGA performed under air atmosphere.

This absence of grafting for non-modified sepiolite is due to a very low polymerization rate and a likely limited availability of the clay surface hydroxyl groups. Similar results were obtained for non-modified montmorillonite (not shown here). Thus efforts have been concentrated on the characterization of nanohybrids obtained from catalytic systems based on organo-modified clays.

As previously described, different catalytic systems have been prepared by performing the lipase immobilization with a loading of 7.5 mg protein per g of clay (as the system showing the best activity) followed or not by glutaraldehyde treatment. It was thus interesting to investigate the performance of these systems (CALB immobilized onto clays) towards PCL chain grafting on clay surface and analyzing the possible impact of glutaraldehyde treatment.

As far as organo-modified sepiolite (SEPMOD) is concerned, polymerization reactions were performed by the catalysis of 300 mg of SEPMODL1 (derivative constituted of ~2 mg of protein fixed onto 300 mg of modified sepiolite) and SEPMODL1 G (derivative constituted of ~2.6 mg of protein fixed onto 300 mg of modified sepiolite) with 3 ml of  $\epsilon$ -CL in 10 ml of toluene.

The TGA results evidenced the occurrence of polymer grafting with the sepiolite rich fractions containing approximately 1.3 and 2.3 wt% of PCL chains grafted at the clay surface for respectively SEPMODL1 and SEPMODL1 G catalyzed reactions (Figures 4.44 and 4.45).

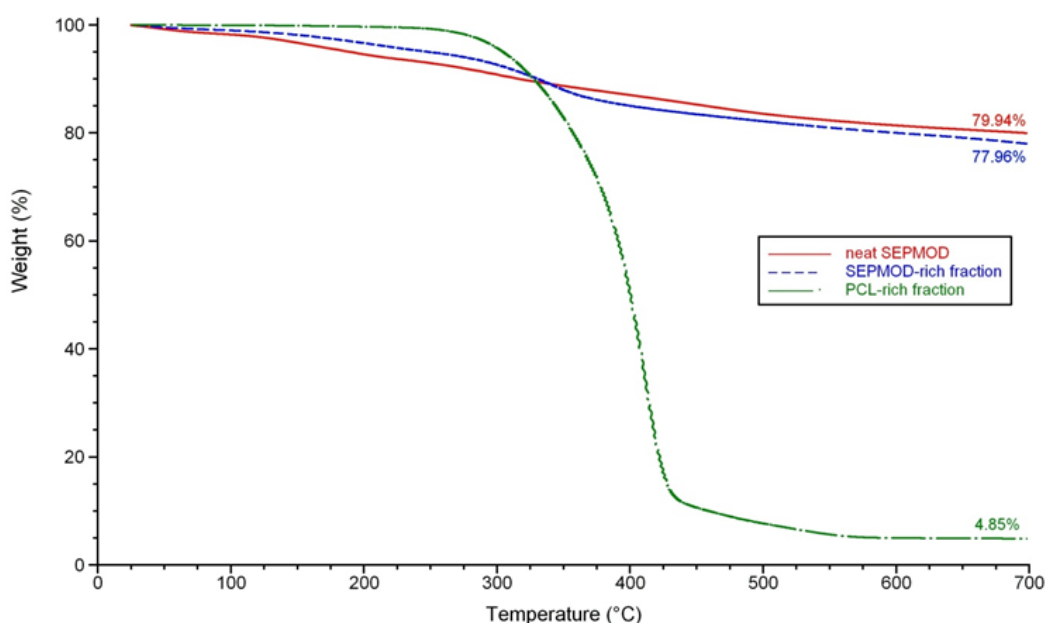


**Figure 4.44 :** Weight loss curves of neat modified SEP (SEPMOD), SEPMOD-rich fraction and PCL-rich fraction of PCL/clay nanohybrid obtained from the polymerization catalyzed by CALB immobilized on modified sepiolite (SEPMODL1). TGA performed under air atmosphere.



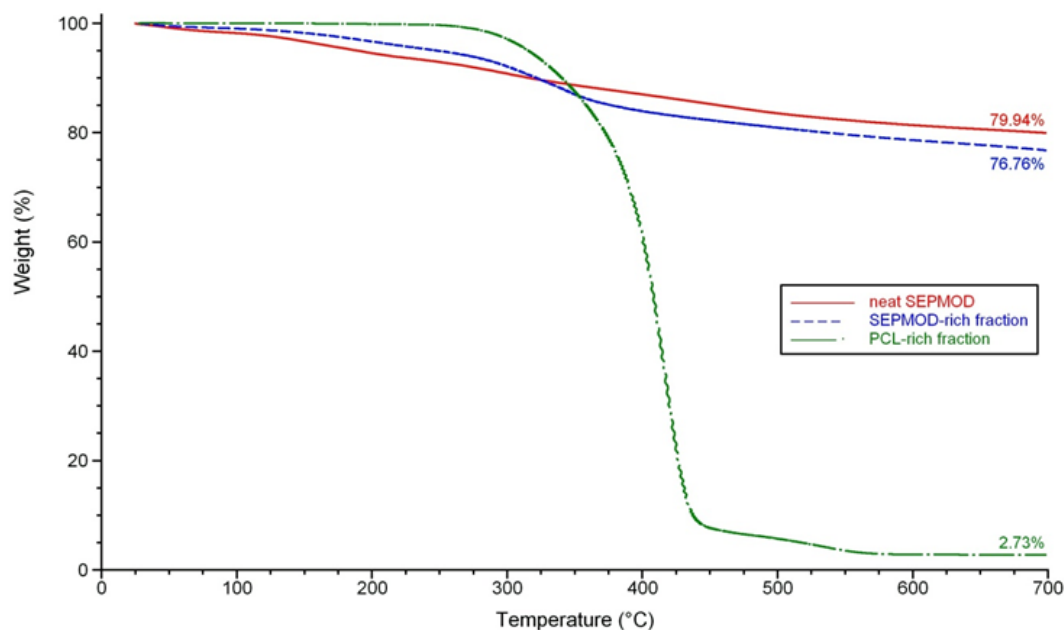


**Figure 4.45 :** Weight loss curves of neat modified SEP (SEPMOD), SEPMOD-rich fraction and PCL-rich fraction of PCL/clay nanohybrid obtained from the polymerization catalyzed by CALB immobilized on modified sepiolite (SEPMODL1G). TGA performed under air atmosphere.

In both cases, the PCL-rich fraction displays a significant content in unburnt residues attributed to the inorganic clay present in the polymeric fraction. Regarding the glutaraldehyde treatment, no significant difference is observed between the two systems, showing that such procedure during the lipase immobilization does not impact on the PCL chain grafting on the clay surface. This behavior is also in agreement with the absence of significant influence of the glutaraldehyde treatment on the catalytic activity for polymerization, as previously described.

Finally, it can be concluded that -OH groups present on the surface of modified sepiolite induced the grafting and growth of some polyester chains from the clay surface, a case which could not be observed with non-modified sepiolite. Among the repeated reactions performed with CALB immobilized on SEPMOD, using the same polymerization conditions, the best results obtained in terms of PCL grafting showed a SEP-rich fraction containing approximately up to 5 wt% of grafted PCL chains.

As far as organo-modified montmorillonite (MMTMOD) is concerned, the TGA results evidenced the occurrence of a more important polymer grafting on the clay.

Polymerization reactions were performed by the catalysis of 300 mg of MMTMODL1 and MMTMODL1 G (derivatives constituted of ~2.44 mg of protein

fixed onto 300 mg of Cloisite<sup>®</sup> 30B) with 3 ml of  $\epsilon$ -CL in 10 ml of toluene. The weight loss curves of the clay-rich fractions for MMTMODL1 and MMTMODL1 G catalyzed reactions evidenced grafting of PCL chains onto the clay with respectively 13.0 and 13.6 wt% of grafted PCL chains in the inorganic clay fraction (Figures 4.46 and 4.47).

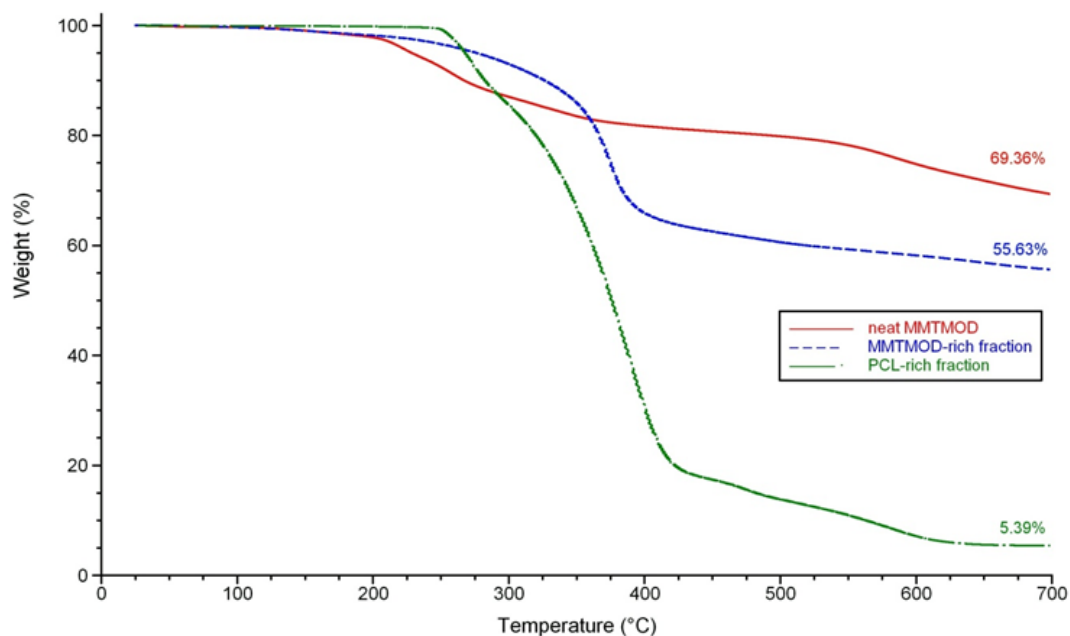


**Figure 4.46 :** Weight loss curves of neat modified MMT (MMTMOD), MMTMOD-rich fraction and PCL-rich fraction of PCL/clay nanohybrid obtained from the polymerization catalyzed by CALB immobilized on modified montmorillonite (MMTMODL1). TGA performed under air atmosphere.

Our catalytic systems based on MMTMOD can also be compared to the commercial immobilized lipase NOV-435 catalyst for  $\epsilon$ -CL polymerization carried out in the same reactions conditions with 10 ml of toluene and 3 ml of monomer at 70 °C, using similar catalytic conditions in terms of protein content (ca. 5 mg) and clay quantity (ca. 300 mg). TGA analysis realized on the products of these reactions demonstrated that lipase immobilized on MMTMOD provided a higher grafting efficiency (ca. 13 wt% of PCL chains grafted on the inorganic clay fraction) while with NOV-435 only ~ 3 wt% of grafting could be attained (Figures 4.46 and 4.47).

Such important PCL chain grafting at the surface of the organo-modified montmorillonite was expected, based on the polymerization kinetics trends and material characterization.

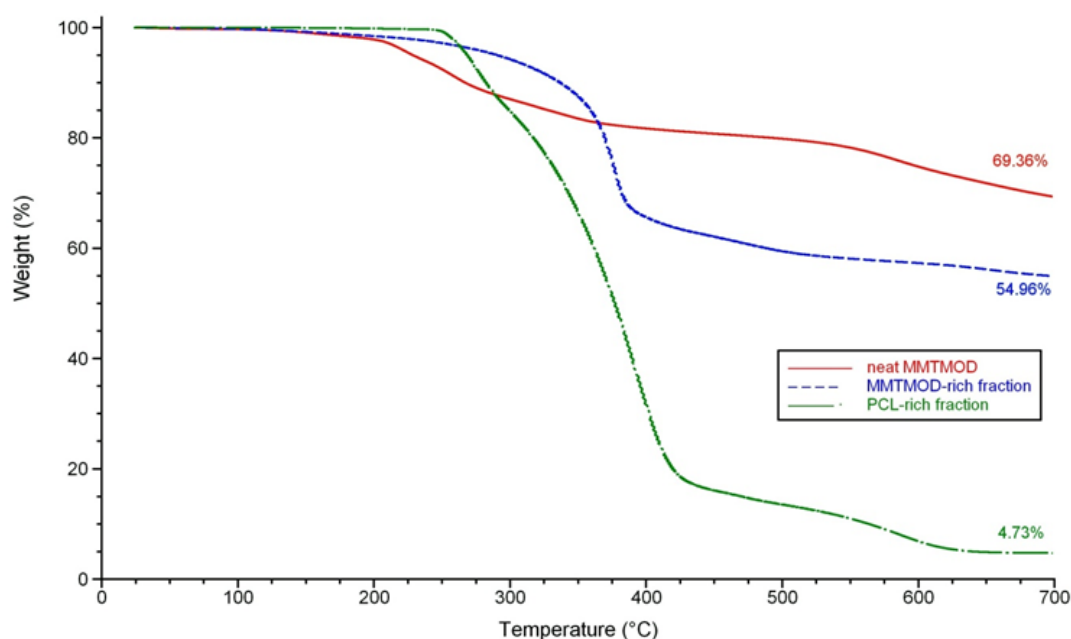


**Figure 4.47 :** Weight loss curves of neat modified MMT (MMTMOD), MMTMOD-rich fraction and PCL-rich fraction of PCL/clay nanohybrid obtained from the polymerization catalyzed by CALB immobilized on modified montmorillonite (MMTMODL1G). TGA performed under air atmosphere.

As already mentioned, it is suggested that the close proximity between the clay surface hydroxyl groups and the immobilized CALB enzyme significantly favors the probability for these -OH groups to be involved in the catalyzed ROP reaction leading to higher PCL grafting at the surface of the organoclay.

As shown and discussed before, the TGA analyses of the different fractions obtained from the separation procedure conducted on the PCL/clay nanohybrids seem to demonstrate the effective polymer grafting at the clay surface. Nonetheless, it is important to perform alternative characterizations on the recovered products with the aim to gather additional indirect proofs of this effective grafting.

Then, the thermogravimetric analyses on the separated polymer-rich and clay-rich fractions of the nanohybrids were completed by Energy Dispersive X-Ray Fluorescence spectroscopy (EDX) analyses performed on the fractionated samples. The material after being excited by bombarding of high-energy X-rays or gamma rays, emits secondary (or fluorescent) X-rays specific to its composition. By this way, elemental analysis of the polymer/clay PCL/MMTMOD nanohybrid has been assessed.

The determined compositions were compared to the analyses performed on the neat PCL and native organo-modified montmorillonite (see Table 4.11).

**Table 4.11** : Percentages and ratios of analytes present in neat PCL, Cloisite<sup>®</sup> 30B (MMTMOD), clay-rich and PCL rich fractions of PCL/MMTMOD nanohybrid determined by EDX.

<b>Analyte</b>	<b>MMTMOD</b>	<b>PCL</b>	<b>clay rich fraction</b>	<b>PCL rich fraction</b>
C	0	0	0	0
N	0	0	0	0
O	42.3	89.4	78.0	84.8
Na	0.1	4.5	0.9	0.4
Mg	1.1	0.2	0.1	0.1
Al	16.3	0.5	4.2	4.1
Si	33.2	0.1	15.7	8.4
Cl	1.1	5.3	0.2	1.3
Fe	5.9	0.1	1.0	0.9
Si/Al	2.0	0.2	3.8	2.0
O/Si	1.3	1314.7	5.0	10.1
Si/Fe	5.6	0.9	15.2	10.0
O/Fe	7.1	1131.6	75.9	100.3

As it can be seen from EDX analysis, components which are specific to the modified montmorillonite and which compose most of its structure are, except from oxygen, Al and Si. Interestingly, the Cloisite<sup>®</sup> 30B montmorillonite also contains some Fe. PCL is mostly composed of O since C is a too light element to be detected on such an equipment.

The ratios O/Si and O/Fe which are very high for the pure PCL, are dramatically decreased in the case of purified polymeric fraction due to the presence of clay nanoparticles in the PCL-rich fraction. This is more likely due to the PCL chains grafted at the clay surface leading some clay platelets to be dragged down in the PCL-rich supernatant during the centrifugation/washing separation procedure.

Besides, these ratios which are naturally low for neat Cloisite<sup>®</sup> 30B significantly increase for the clay rich fraction by the grafting of polymer chains on the clay surface.

One can also note that these variations in the O/Si and O/Fe ratios are not consistent. This can be explained by the fact that the Si content of a sample can be erroneous due to possible contamination by silicon-based grease, glassware residues... leading to overestimate the Si content of the product. Thus, it is believed that the O/Fe ratio is the more accurate one to determine the sample composition variations.

These analyses, even if they are less sensitive than TGA measurements, give additional indirect proof of the effective grafting of the PCL chains at the surface of the organoclay, at least for the nanohybrids obtained from polymerization catalyzed by NOV-435 and carried out in presence of Cloisite<sup>®</sup> 30B. Unfortunately, it was not possible to analyze nanohybrids obtained with the MMTMODL catalysts (CALB immobilized on organoclay).

Nevertheless, such grafting of polymer chains at the surface of clay nanoparticles is also well-known for allowing the obtaining of nanohybrids displaying finely dispersed and well distributed nanoparticles within the polymeric matrix. This could be confirmed by performing SEM analyses of the recovered PCL/clay nanohybrids (MMTMODL G PCL) obtained from the enzymatic polymerization catalyzed by CALB immobilized on Cloisite<sup>®</sup> 30B (MMTMODL G catalyst) (Figure 4.49). This corresponds to the sample for which the TGA analyses evidenced the presence of ca. 13 wt% of grafted PCL chains present in the clay-rich fraction extracted from the nanohybrid.

For the sake of comparison, the SEM pictures of the surface of the corresponding MMTMODL G catalyst (CALB immobilized on organo-modified montmorillonite and treated with GA) are also shown in Figure 4.48.

From these microphotographs, one can clearly see different surface morphologies between the nanohybrid clay-rich fraction and the starting catalyst. On the extracted clay-rich fraction pictures (Figure 4.49), one can easily detect the montmorillonite clay platelets with the edges of these clay platelets appearing as white lines. The very fine dispersion and distribution of the clay in the PCL matrix are clearly evidenced and one can also observe that the clay platelets are randomly oriented. This attests for

the advantageous effect of PCL grafting at the clay surface for the good and efficient delamination of the clay particle stacks.

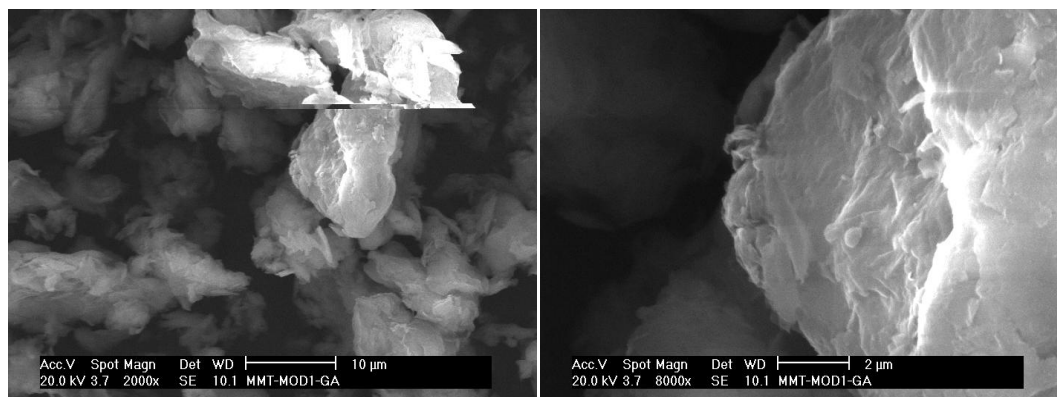


**Figure 4.48 :** SEM pictures of organo-modified montmorillonite after immobilization of CALB and treated with GA (MMT-MODL G) at 2000x magnification (left) and 8000x magnification (right).

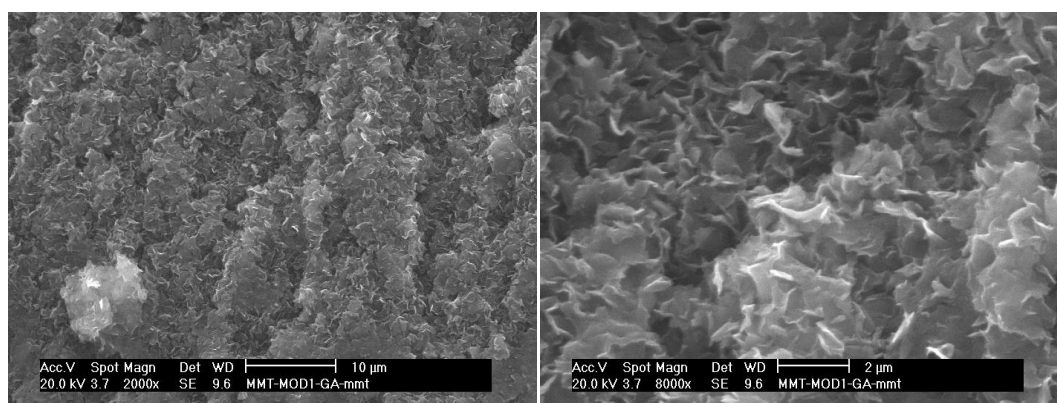


**Figure 4.49 :** SEM pictures of the clay-rich fraction of PCL/montmorillonite nanohybrid obtained from the polymerization catalyzed by MMT-MODL G and showing the PCL chains grafting on clay surface at 2000x magnification (left) and 8000x magnification (right).

From these microphotographs, one can clearly see different surface morphologies between the nanohybrid clay-rich fraction and the starting catalyst. On the extracted clay-rich fraction pictures (Figure 4.49), one can easily detect the montmorillonite clay platelets with the edges of these clay platelets appearing as white lines. The very fine dispersion and distribution of the clay in the PCL matrix are clearly evidenced and one can also observe that the clay platelets are randomly oriented. This attests for the advantageous effect of PCL grafting at the clay surface for the good and efficient delamination of the clay particle stacks.

It was then interesting to compare these observations with the SEM pictures obtained from the sepiolite-based systems for which only a very limited PCL chain grafting is observed. Figure 4.50 presents the SEM images of organo-modified sepiolite with immobilized lipase (the SEPMODL G catalyst) and Figure 4.51 presents the clay-rich fraction extracted from the final nanohybrid product.

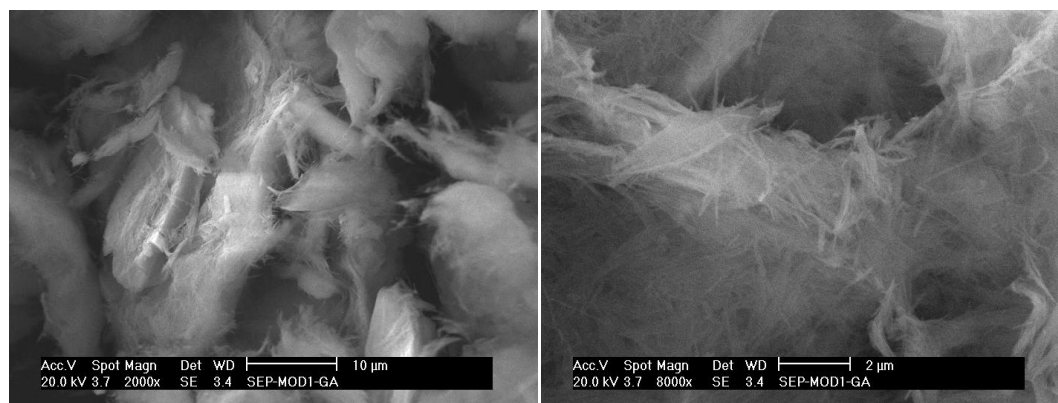


**Figure 4.50 :** SEM pictures of modified sepiolite after immobilization of CALB and treated with GA (SEPMODL G) at 2000x magnification (left) and 8000x magnification (right).

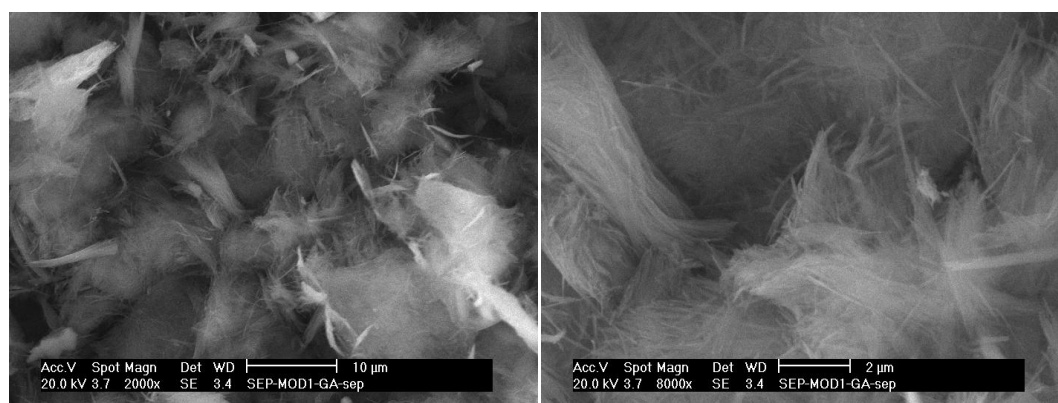


**Figure 4.51 :** SEM pictures of the clay-rich fraction of PCL/sepiolite nanohybrid obtained from the polymerization catalyzed by SEPMODL G PCL at 2000x magnification (left) and 8000x magnification (right).

Since the content of PCL chains grafted to sepiolite on the clay-rich fraction is only of 2.3 wt%, no polymeric matrix could be visually detected. After the polymerization, the recovered clay-rich fraction shows surface morphology identical to the original SEPMODL G catalyst with the characteristic sepiolite fibrous or needle-like structure largely observed (Figure 4.51).

#### 4.7 Test of Different Lipases for the ROP of $\epsilon$ -CL

The next step consisted in the polymerization of  $\epsilon$ -CL by different types of lipases derived from various species. A lipase kit containing several commercial lipases isolated from *Aspergillus*, *Candida rugosa*, *Mucor miehei*, *Pseudomonas cepacia*, *Pseudomonas fluorescens*, *Rhizopus arrhizus*, *Rhizopus niveus* species and from hog (porcine) pancreas was used to test the activity of these enzymes towards *p*NPB in aqueous media and also  $\epsilon$ -CL in organic media. Table 4.12 presents the calculated hydrolytic specific activities of these lipases for *p*NPB and also their specific activity values, provided by the producer, towards fatty acids.

**Table 4.12 :** Specific activities of lipases depending on different types of substrate.

Lipase from	Specific activity based on <i>p</i> NPB as substrate A (U/mg)	Specific activity determined by the producer on other substrates A (U/mg)	
<i>Rhizopus arrhizus</i>	69	10	(butyric acid)
<i>Rhizopus niveus</i>	2	1.5	(fatty acid)
porcine pancreas	4	15-35	(fatty acid)
<i>Pseudomonas cepacia</i>	29	50	(oleic acid)
<i>Aspergillus species</i>	2	0.5	(acetic acid)
<i>Candida antarctica</i>	57	1.5	(oleic acid)
<i>Candida rugosa</i>	170	2	(oleic acid)
<i>Mucor mihei</i>	22	1	(oleic acid)
<i>Pseudomonas fluorescens</i>	96	40	(oleic acid)

As seen from Table 4.12, lipases showed different specific hydrolytic activities depending on the type of the substrate. A correlation in terms of performance could not been established between them since they behaved with a different mechanism for each substrate.

These free lipases were then tested for their esterification activity in polymerization reactions where 1 ml of  $\epsilon$ -CL was aimed to be polymerized by 50 mg of lipase in



2 ml of toluene at temperatures of 40 and 70 °C. Monomer conversion percentages and molar masses of PCL chains were determined by NMR (Tables 4.13 and 4.14).

**Table 4.13 :** The use of different lipases for polymerization of  $\epsilon$ -CL; specific activities on *p*NPB substrate, monomer conversion and reaction time at different temperatures.

Lipase from	Monomer conversion (%) (40 °C)		Monomer conversion (%) (70 °C)		A (U/mg)
<i>Rhizopus arrhizus</i>	-		2.4	(7 days)	69
<i>Rhizopus niveus</i>	-		-		2
porcine pancreas	5	(6 days)	22	(6 days)	4
<i>Pseudomonas cepacia</i>	3.5	(6 days)	7	(6 days)	29
<i>Aspergillus species</i>	-	(7 days)	2	(7 days)	2
<i>Candida antarctica</i>	54	(3 days)	95	(1 day)	57
<i>Candida rugosa</i>	-		-		170
<i>Mucor mihei</i>	-	(7 days)	-	(7 days)	22
<i>Pseudomonas fluores.</i>	Not tested		26	(12 days)	96

First, one can notice that, except for CALB, the monomer conversion percentages at 70 °C were very low for all types of free lipases. Only porcine pancreatic lipase showed a slightly better activity compared to others, polymerizing 22% of the  $\epsilon$ -CL monomer after six days and producing a PCL of 1000 g/mol (Table 4.14). Since these catalytic systems are based on free lipases, and because the reaction had to be carried out for very long times, one can raise the issue of possible deactivation of the free enzymes at 70 °C. Thus, a lower temperature (40 °C) was used to prevent the possible thermal deactivation of the lipases, but almost no polymerization was observed except again for CALB. From these results, it can be concluded that this temperature was too low to ring open these  $\epsilon$ -CL monomer (Table 4.13).

As it can be noticed from the Table 4.13, *Candida rugosa*, *Pseudomonas fluorescens* and *Rhizopus arrhizus* lipases which had shown the best activities towards *p*NPB in aqueous media, were not able to polymerize efficiently  $\epsilon$ -CL. This showed again that

lipases can exhibit very dissimilar catalytic behavior according to the substrate in variant media.

**Table 4.14 :** Molecular weights ( $M_n$ ) of PCLs synthesized at 70°C by different lipases for different reaction times.  $M_n$  values determined by  $^1\text{H}$  NMR.

Lipase from	Monomer conversion (%) (70 °C)	Polymerization time	$M_n$ (g/mol)
<i>Rhizopus arrhizus</i>	2.4	(7 days)	200
<i>Rhizopus niveus</i>	-	-	-
porcine pancreas	22	(6 days)	1000
<i>Pseudomonas cepacia</i>	7	(6 days)	900
<i>Aspergillus species</i>	2	(7 days)	580
<i>Candida antarctica</i>	95	(1 day)	4000
<i>Candida rugosa</i>	-	-	-
<i>Mucor mihei</i>	-	-	-
<i>Pseudomonas fluores.</i>	26	(12 days)	900

Nevertheless, such low activity towards  $\epsilon$ -CL polymerization for these alternative commercial lipases was not totally surprising and unexpected. Since it has been clearly demonstrated that immobilized forms of lipases can be much more efficient than their free counterparts, it was of prime interest to test immobilized forms of some of these lipases for the synthesis of PCL. Among these lipases, the porcine pancreas lipase showing the best performance after CALB was thus immobilized onto Cloisite<sup>®</sup> 30B montmorillonite clay.

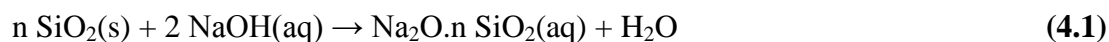
This new derivative when used as a catalyst for the polymerization showed a very poor activity; it converted just the 8% of the monomer in 5 days and produced PCL chains having very low molecular weights (ca. 500 g/mol). This polymerization rate was lower than for the free porcine pancreas lipase and attests for an obvious loss of activity resulting from the immobilization procedure.

After all, CALB remained as the best performant lipase among the commercial lipases tested for our system. Nevertheless, this preliminary study could pave the way for future works on screening alternative lipases and testing their immobilization on inexpensive and appropriate solid supports to develop new efficient catalysts for polyester synthesis by ring opening polymerization.

#### **4.8 Synthesis of PCL Catalyzed by Lipase Immobilized on Alternative Inorganic Supports**

In order to test another inorganic compound (rich in silica) as lipase support, silicates derived from rice hull ash were used for lipase immobilization. The aim is to promote the use of (and give added value to) rice hull, as a cheap and largely available material, for lipase immobilization in the perspective to elaborate PCL/silicate nanohybrids.

Rice hull ash (RHA) has a high silica content over 60 % SiO<sub>2</sub> (w/w) and is used in the production of several silicon compounds. Kamath and Proctor (1998) have extracted the silica in RHA with NaOH to obtain a sodium silicate solution as an alternative process to the conventional high temperature metallurgical process. The extraction process can be presented as in the following reaction (4.1).



Pure silica xerogels, synthetic magnesium silicates with high surface area of over 650 m<sup>2</sup>/g, calcium, barium, zinc and aluminum silicates with also high surface areas were produced through further studies from sodium silicate solutions extracted by utilizing the Kamath and Proctor's method. Various micro structural forms of silicas such as, individual particles (fume silicas), precipitated silicas and silicate networks, and random closed packed structures of silica gels are well known and used in industrial applications.

Nano-structured silicates with an open framework structure have been formed from sodium silicate solution by Johnston et al. (2008) with a large surface area of about 350–600 m<sup>2</sup>/g depending upon the synthesis method. The same novel structured silicates were recently produced from rice hull ash, provided by an industrial rice company in Thrace region (Turkey), in the laboratories of ITU Chemical Engineering Department, by the group of Prof. Taşpınar.

In the study of Johnston et al. (2008), diethylene glycol was also used as a spacer compound to obtain a framework structure for the nano-sized calcium silicate which was produced from the reaction of  $\text{Na}_2\text{SiO}_3$  (from rice hull ash) and  $\text{CaCl}_2$ . Ca silicate was obtained as a precipitate (ppt.) according to the possible reaction between  $\text{Na}_2\text{SiO}_3$  and  $\text{CaCl}_2$  as follows (4.2). Other types of silicates were prepared according to the same method by using different anion-chloride solutions depending on the type of silicate desired.



Mg, Ca, Ca+Mg, Zn, Ba silicates synthesized by this way, were used as lipase supports in our study. CALB was physically immobilized on these samples and derived silica type catalysts were used for the polymerization of  $\epsilon$ -CL according to the typical reaction conditions (Sections 4.3-4.4).

CALB enzyme was immobilized by the same physical adsorption procedure onto different types of silicate samples. Table 4.15 shows the immobilization percentages and specific hydrolytic activities of these derivatives. In terms of protein adsorption on silicate surface, except Zn silicate, other types of silicates provided rather good immobilization efficiencies.

Nonetheless, resulting enzymatic activities were lower than the specific activity of free CALB. This highlighted that the interaction between the silicate surface and the CALB molecule caused some limitations for the conformation of the enzyme so that the access to its active site remained restricted for the *p*NPB substrate.

**Table 4.15 :** Immobilization of CALB onto various silicates.

<b>CALB/silicate derivative</b>	<b>Loading (mg added protein/ g silicate)</b>	<b>Immobilization (%)</b>	<b>Specific Activity (U/mg)</b>	<b>Specific Activity (U/mg) after lyoph.</b>
CALB/Mg silicate	7.5	62	46	3
CALB/Ca silicate	7.5	76	41	15
CALB/Ca+Mg silicate	7.5	78	49	11
CALB/Zn silicate	7.5	11	n.d.*	n.d.*
CALB/Ba silicate	7.5	69	36	9
Free CALB	-	-	116	-

\*n.d.: not detected

These new silica type derivatives were then tested as catalysts for the polymerization of  $\epsilon$ -CL. 1 ml of  $\epsilon$ -CL was polymerized in 2 ml of toluene at 70 °C. The amount of catalyst (CALB/silicate) was different for each reaction (see Table 4.16). Indeed, the specific activities of these catalysts being low, it has been decided to use the maximum available amount of the derivatives which was dependent of the limited quantity of silicates provided by another research group. Since immobilization percentages were different for each type of silicate, adsorbed amount of protein was consequently different and this resulted in different values of total units of activity available for each polymerization reaction.

Monomer conversion percentages and molar masses of products after 5 days of reaction are presented on Table 4.16.

**Table 4.16 :** Use of silica type derivatives as catalyst for  $\epsilon$ -CL polymerization reactions.

<b>CALB/silicate derivative</b>	<b>Quantity used of each derivative (mg)</b>	<b>Total units of activity present (U)*</b>	<b>Monomer conversion (%)</b>	<b>M<sub>n</sub> of PCL (g/mol)</b>
CALB/Mg silicate	200	3.3	20	1000
CALB/Ca silicate	100	9.0	38	1700
CALB/Ca+Mg silicate	145	10.0	80	2800
CALB/Zn silicate	170	-	7	800
CALB/Ba silicate	50	2.5	20	2000

\* Total units of activity calculated basing on hydrolytic activities in aqueous media.

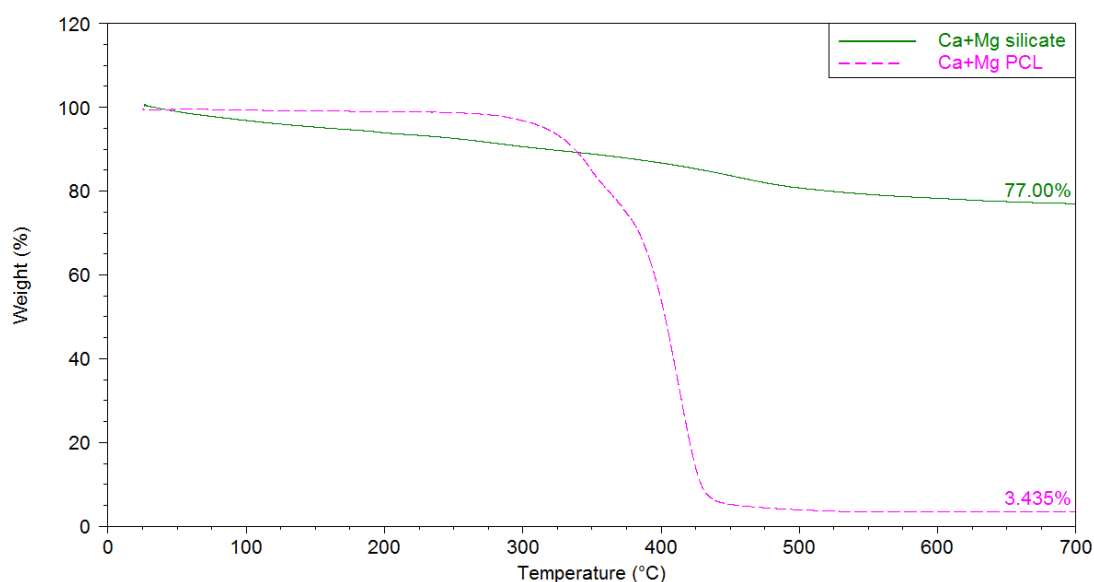
As previously mentioned, activities of CALB/silicate derivatives measured for *p*NPB in aqueous media were totally different than those observed for  $\epsilon$ -CL substrate in organic media. CALB/Ba silicate despite having the lowest total units of hydrolytic activity (2.5 U) for the reaction, was capable of synthesizing a PCL with a M<sub>n</sub> of 2000 g/mol. CALB/Ca+Mg silicate derivative has a similar hydrolytic activity as CALB/Ca silicate catalyst but allowed to reach a higher monomer conversion percentage (80% compared to 38% for CALB/Ca).

The obtained PCL showing the highest molecular weight, which was synthesized by the catalysis of CALB immobilized on Ca+Mg silicate, was analyzed by DSC (Table 4.17). The T<sub>m</sub> and T<sub>c</sub> values were determined as 55 and 34 °C, respectively, and the product showed 60% of crystallinity.

**Table 4.17 :** Characteristics of PCLs synthesized by silica type derivatives.

PCL	T <sub>m</sub> (°C)	ΔH <sub>fusion</sub> (J/g)	χ (crystallinity %)	T <sub>c</sub> (°C)	ΔH <sub>c</sub> (J/g)
Ca+Mg silicate PCL (3.4 wt% of silicate)	55	83.9	60	34	84.4
Zn silicate PCL (1.6 wt% of silicate)	47	86.0	62	27	83.6
Ba silicate PCL (4.3 wt% of silicate)	52	71.0	51	33	71.9

The silica content within the Ca+Mg silicate/PCL hybrid material was estimated to be 3.4 wt% by the TGA analysis (Figure 4.52).

**Figure 4.52 :** Weight loss curves of neat Ca+Mg silicate and PCL produced by the catalysis of CALB/Ca+Mg silicate.

About 4.3 and 1.6 wt% of silica contents were determined for the PCL hybrid materials with Ba silicate and Zn silicate, respectively. TGA analyses showed that Ca+Mg silicate/PCL nanohybrid started to degrade at 230 °C whereas the Ba silicate/PCL started its degradation at 225 °C and the Zn silicate/PCL nanohybrid at 250 °C (data not shown).

The morphological appearance of Ca+Mg silicate/PCL was analyzed by SEM and compared to the structure of the native Ca+Mg silicate observed by TEM which is presented on Figure 4.53.

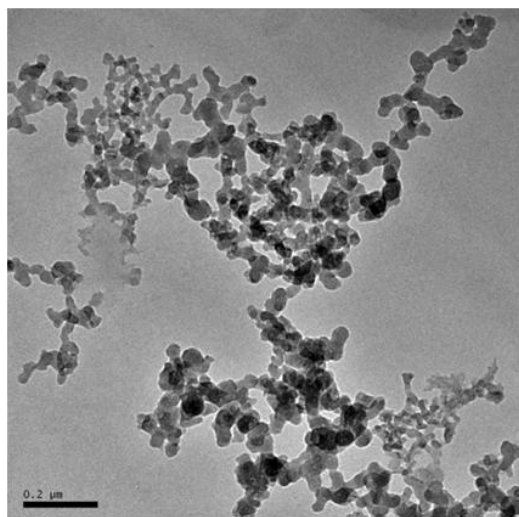


**Figure 4.53 :** TEM micrograph of calcium-magnesium silicate from rice hull ash (scale is 200 nm).

TEM analysis of this silicate shows calcium-magnesium oxide nano-sized particles structured in a highly porous framework.

As far as the SEM analyses of Ca+Mg silicate/PCL are concerned, it can be clearly seen that the structure of the silicate/PCL nanohybrid presents a totally different morphology compared to clay/PCL nanohybrids (Figure 4.54).

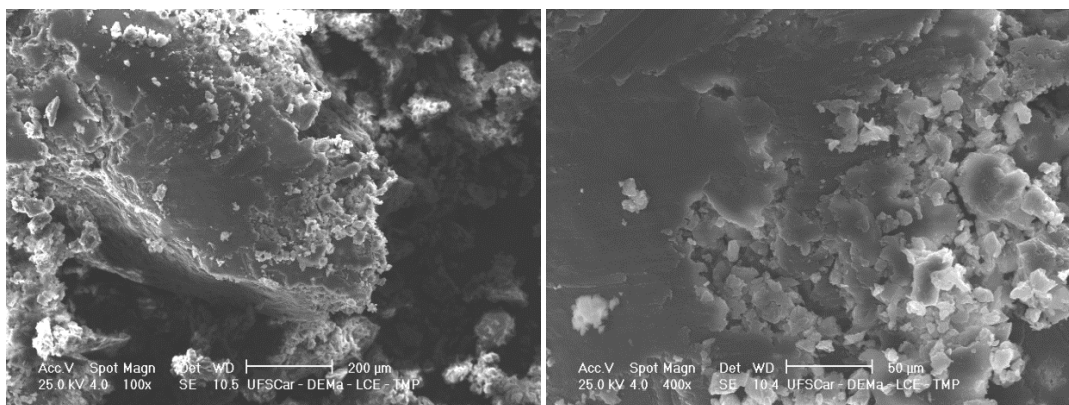


**Figure 4.54 :** SEM pictures of PCL synthesized by CALB immobilized on Ca+Mg silicate at 100x magnification (left) and 400x magnification (right).

Even if the silicate nanoparticles can not be distinguished precisely, the general view of the silicate/PCL product and its surface roughness display some characteristic visual features of this silicate.

## 4.9 Synthesis of PLA by Enzymatic Catalytic Systems

Having completed this detailed study about the ring opening polymerization of  $\epsilon$ -CL by lipase catalysis and the characterization of resulting PCLs, it was of great interest to extend this study to the synthesis of polylactic acid (PLA) especially because of the several contradictory works reported so far in the literature about the ROP of the lactide isomers. For this, NOV-435, free CALB and CALB immobilized onto montmorillonite clay were tested as catalysts for the ROP of D-, L- and D/L-lactides with the aim to obtain PLA.

### 4.9.1 Synthesis of PLA by NOV-435 and free CALB

As a preliminary study, we focused on different factors affecting the monomer conversion rate and molecular weight of polymers (PLAs) in the ROP of lactides. Various ratios of lactide/solvent and lactide/ catalyst were assayed. Additionally, temperatures between 60-110 °C were tested for lactide polymerization in solvent by the catalysis of NOV-435. The performances of free and immobilized CALB were compared. Reaction conditions optimized for ROP of  $\epsilon$ -CL have also been tested.

Similarly to the  $\epsilon$ -CL polymerization, lactide enzymatic polymerization were followed by  $^1\text{H}$  NMR. A typical  $^1\text{H}$  NMR spectrum of PLA with the peak assignments is presented in Figure 4.55.

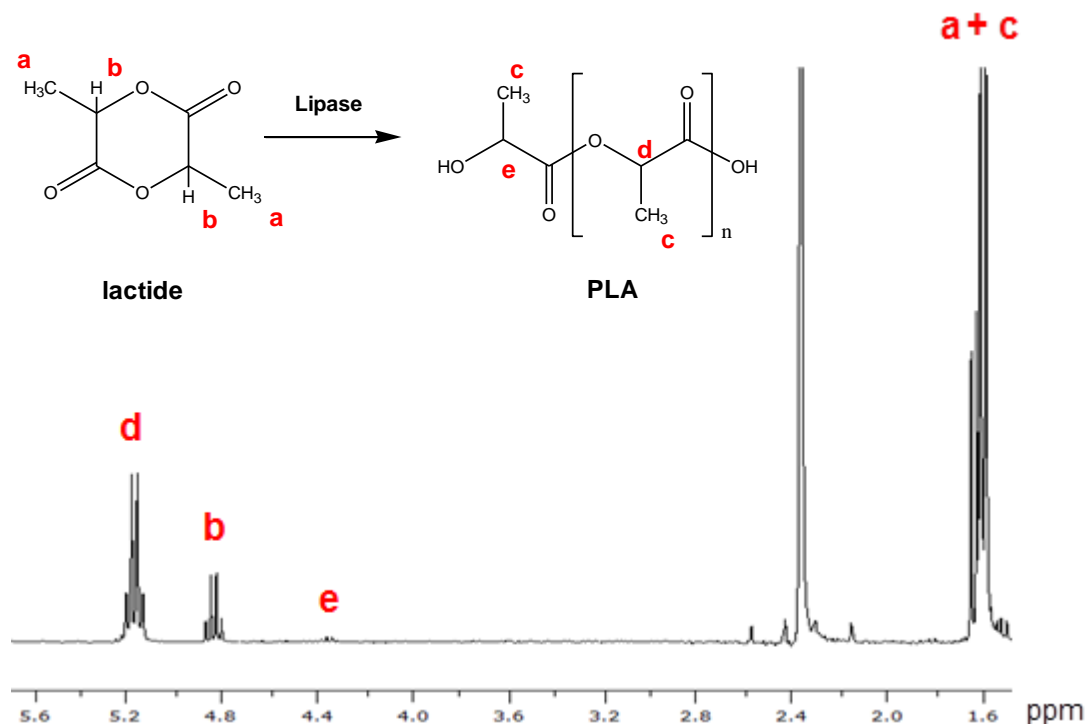
Monomer signals can be observed at 1.68 ppm for ( $\text{CH}_3$ ) and 4.85 ppm for ( $\text{CH}$ ) groups whereas the signals related to the polymer are seen at 1.6 ppm ( $\text{CH}_3$ ); 4.3 ppm ( $\text{CHOH}$ ) and 5.1 ppm ( $\text{CH}$ ).

Figure 4.56 represents a zoomed view on the 4 to 6 ppm range which allows the determination of the monomer conversion and estimation of the degree of polymerization versus time. The consumption of the monomer (D-lactide) and the formation of the polymer (PDLA) can be clearly observed from the  $^1\text{H}$  NMR spectrum.

Monomer conversion was determined by the comparison of integrated peak areas of the methylene groups next to the carbonyl group in the lactide monomer (4.85 ppm) and the polymer (5.1 ppm). In addition, the degree of polymerization was estimated



from the ratio of integral of the signal at 5.1 ppm assigned for CH groups of PLA main chain to the integral of the signal at 4.3 ppm assigned for the chain-end.



**Figure 4.55 :** Typical  $^1\text{H}$  NMR spectrum of PLA synthesized by lipase catalyzed ROP of at  $70^\circ\text{C}$ . The proton assignments and corresponding peaks are shown in the spectrum.

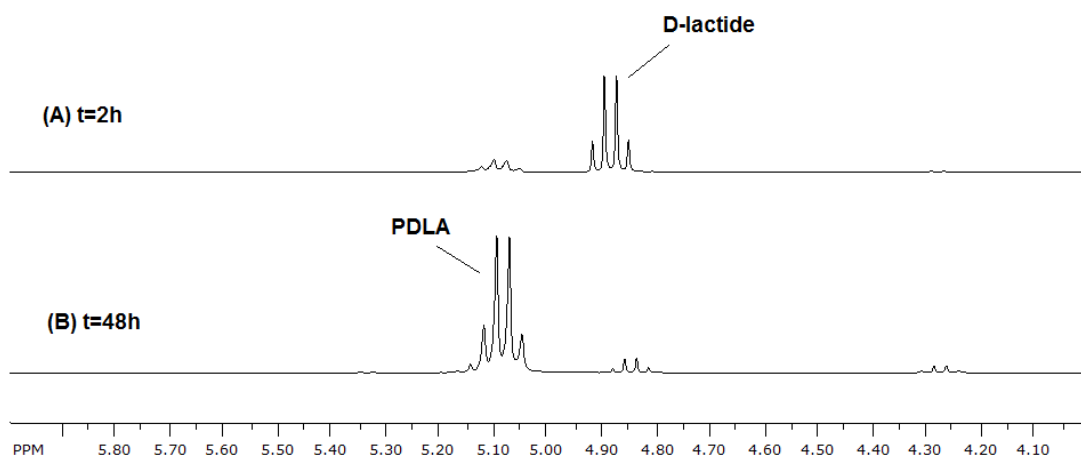


**Figure 4.56 :** Zoomed view of  $^1\text{H}$  NMR spectra of samples withdrawn from the reaction mixture of D-lactide polymerization by NOV-435 showing the methylene signals of monomer, polymer and chain end recorded after (A)  $t=2\text{ h}$  and (B)  $t=48\text{ h}$  of reaction.

These NMR analyses of aliquots from the reaction mixture allowed the monitoring of PLA polymerization kinetics.

According to the preliminary study results, the best reaction conditions within the studied parameter range for lactide polymerization by NOV-435 were estimated as; 70 °C,  $m_{\text{lactide}}/m_{\text{solvent}}=1/3$ ,  $m_{\text{NOV435}}/m_{\text{lactide}}=1.5/10$ . Thus, D-, L- and D/L-lactide polymerizations were performed by the catalysis of 150 mg NOV-435 for 1g of lactide monomer in 3 ml of toluene. Lactide conversion percentages and molecular weights of PLAs determined from  $^1\text{H}$  NMR analysis are reported in Table 4.18.

**Table 4.18 :** Lactide polymerization reactions carried out with 1 g of lactide, 3 ml of toluene and 150 mg of NOV-435 catalyst.

Isomer type	t (hours)	Monomer conversion (%)	$M_n$ (g/mol)*
D-lactide	48	99	2600
L-lactide	48	6	200
D/L-lactide	48	7	230

\*Molecular weight ( $M_n$ ) determined by  $^1\text{H}$  NMR.

As far as NOV-435 is concerned, it can be observed that this catalyst is more active for the ROP of D-lactide compared to the other lactide isomers. This data is in accordance with a recent work presented by Hans et al. (2009) indicating the polymerizability of D-lactide. Interestingly, the monomer conversion percentage is much more higher in our case (99% after 48 h compared to 33% after 3 days in their case) and molar mass of the final product (PDLA) is quite similar (2600 compared to 3300 g/mol).

Besides, even if they are very low, some monomer conversions are observed for L- and D/L- lactides when using NOV-435 catalyst. Thus, this fact seems to be in contradiction with the results and remarks reported by Hans et al. (2009) stating the impossibility for the L-lactide isomer to be polymerized by such lipase catalyst.

However, one can admit that the monomer conversion is very low in these cases with NOV-435 and that the obtained small oligomers are only based on one or two opened lactide monomers. This would support the conclusions made by Hans et al. (2009) stating that once the first L-lactide monomer unit is opened the resulting S-configuration of the secondary alcohol cannot undergo further monomer addition.

Thus, this still possibly allows the opening of one lactide monomer which could correspond to the observed  $M_n$  values around 200 g/mol.

One can also easily notice that the NOV-435 catalyzed ROP of D-lactide proceeds much more slower than for the  $\epsilon$ -CL polymerization (see Section 4.1) but this is globally in perfect agreement with all studies reported so far on lactide enzymatic polymerization (Lasalle and Ferreira, 2008; Hans et al., 2009).

Similarly to NOV-435, a preliminary work was also conducted on lactide polymerization catalyzed by free CALB. In this case, the most appropriate reaction conditions were estimated to be 70 °C,  $m_{\text{lactide}}/m_{\text{solvent}}=1/2$ ,  $m_{\text{CALB}}/m_{\text{lactide}}=1/20$ . According to these informations, D-, L- and D/L- lactide were polymerized using the free CALB in toluene at 70 °C. Polymerizations were carried out in the presence of 2 ml of toluene; 1 g of lactide monomer and 50 mg CALB as the catalyst. The monomer conversion percentages and molecular weights of resulting PLAs were determined by  $^1\text{H}$  NMR analysis and reported below (Table 4.19).

**Table 4.19 :** Lactide polymerization reactions carried out with 1 g of lactide, 2 ml of toluene and 50 mg of free CALB catalyst.

Isomer type	t (hours)	Monomer conversion (%)	$M_n$ (g/mol)*
D-lactide	48	70	1000
L-lactide	48	84	500
D/L-lactide	48	60	350

\*Molecular weight ( $M_n$ ) determined by  $^1\text{H}$  NMR.

As it can be seen from the above results, a similar trend is observed for the free form of the lipase, since CALB is more effective towards D-lactide monomer compared to the other stereoisomers. However, the molecular weight of the final PDLA is lower compared to the polyester obtained with NOV-435 and the final product is rather an oligomer. In addition, the D-lactide conversion is only of 70% when free CALB is used as catalytic system which, in turn, could explain the lower average molecular weight obtained for the PDLA in this case.

Besides, in the reactions catalyzed by NOV-435, the introduced amount of lipase B enzyme is about 15 mg (10 wt% of NOV-435) whereas in the free lipase catalyzed reaction 50 mg of CALB is used. This could also explain the lower molecular weight of final product obtained with the free lipase since one can assume that a higher amount of enzyme could induce a higher number of propagating chains and thus

lower  $M_n$  values for the PDLA. This also shows that the immobilized form of CALB can be preferably chosen for the D-lactide polymerization.

Interestingly, much higher monomer conversions are observed for L-lactide and D/L-lactide (84 and 60% respectively) when free form of CALB is used compared to the NOV-435 catalyst. As a consequence, the average molecular weights obtained for the resulting PLLA and PDLLA are slightly higher than in the case of NOV-435 catalysis even if the final products are still considered as oligomers.

However, molar mass of the final PLLA (500 g/mol) remains low when compared with the results of the study of Yoshizawa et al. (2008), where for a reaction conducted in toluene at 90 °C for 24 hours with 1 g of L-lactide and 100 mg CALB, they obtained 55% of monomer conversion and a PLLA with a  $M_n$  of 6400 g/mol. Obviously these values are extremely low when compared to the ones reported in the same study (Yoshizawa et al. 2008) when performing the polymerization at 120 or 130 °C either in bulk or in ionic liquid solvent. They obtained PLLA  $M_n$  values as high as 40000 to 55000 g/mol. But, in these cases, thermal initiation of lactide ROP cannot be excluded.

Nonetheless, it is worth pointing out that these results concerning the ability of CALB enzyme to polymerize L-lactide, are in agreement on this specific point with the results reported by Yoshizawa et al. (2008), but are in contradiction with the hypothesis formulated by Hans et al. (2009) discussed before. Thus, from these results, we could complete the statements proposed by Hans et al. (2009) and conclude that the impossibility for the L-lactide to be enzymatically ring-opened via CALB catalysis, due to the resulting S-configured secondary alcohol formed, seems to be observed only experimentally for the immobilized form of CALB. And that, even if the reason is still unknown, the lipase free form seems to be able to accommodate such S-configured intermediate during the polymerization and thus could ring-open the L-lactide stereoisomer.

#### **4.9.2 PLA synthesis catalyzed by lipase (CALB) immobilized on montmorillonite**

After having tested the free form and commercially immobilized form of CALB for ROP of lactides, CALB immobilized by physical adsorption on natural and organomodified montmorillonite was assayed as new catalyst for D-lactide

polymerization. For this, 200 mg of derivative (CALB on clay) were used for the catalysis of 1g D-lactide in 3 ml of toluene. The enzyme content of the derivative was approximately 7.5 mg. The monomer conversion percentages and molecular weights of resulting PDLAs were determined by  $^1\text{H}$  NMR analysis and reported below (Table 4.20).

**Table 4.20 :** Lactide polymerization reactions carried out with 1g of D- lactide in 3 ml of toluene and 200 mg of CALB/clay derivatives as catalysts.

Catalyst	t (hours)	Monomer conversion (%)	$M_n$ (g/mol)*
CALB on Cloisite <sup>®</sup> 30B	96	67	516
CALB on MMT- $\text{Na}^+$	96	71	521

\*Molecular weight ( $M_n$ ) determined by  $^1\text{H}$  NMR.

Monomer conversion values reached after 48 hours by using the free CALB as catalyst (i.e. 70%, see Table 4.19) seem to be only reached after 4 days when D-lactide polymerization is catalyzed by CALB immobilized on clays. This lower polymerization rate may be due to the much lower amount of enzyme involved in the reaction (ca. 7.5 mg of enzyme for these derivatives compared to 50 mg of enzyme for the free CALB).

This could also be due to the presence of clay in the reaction media acting as co-initiator for the polymerization, as previously described for  $\epsilon$ -CL polymerization. This effect of the clay participation to the reaction could also explain the lower average molecular weight for the obtained PDLA when using lipase/clay derivatives.

#### 4.9.3 PLA synthesis catalyzed by an alternative lipase: Amano lipase PS

Matsumura and his coworkers (1997) have reported the better functioning of Amano lipase PS enzyme for ROP of lactides, more particularly when conducted in bulk, in terms of monomer conversion and product molar masses. They reported almost complete monomer conversion within 7 days of reaction at 100 °C and  $M_w$  values as high as 70000 g/mol for the final product (PDLLA) by the catalysis of 3 wt% of lipase PS based on the monomer amount. On the other hand, molecular weights of the final products at slightly lower temperature (80 °C) when using the same amount of enzyme remained in a lower range (13000-27000 g/mol).

Later on, Matsumura and his group (1998) have just tested this lipase PS for the ROP of D/L-lactide in toluene at 80 °C using 50 mg of lipase (5 wt% based on the monomer) for 1 g of monomer. At the end of 7 days, they have obtained a monomer conversion of 34% and a  $M_w$  equal to 1700 g/mol. This result was quite different and much less promising than the ones observed in the reactions performed in bulk.

However, such good results observed for lactide polymerization catalyzed by lipase PS were further confirmed by the work of Malberg et al. (2010) who obtained, in bulk at 125 °C, high monomer conversion of L-lactide and average molecular weight values, confirming thus the great potential of this enzyme for lactide polymerization.

To investigate the behavior of this lipase PS enzyme in toluene, ROP of  $\epsilon$ -CL and of D- and L-lactides were performed in our typical conditions (temperature and enzyme amount) and also in the conditions proposed by Matsumura et al. (1998). Performing the polymerizations in toluene allowed to overcome both the high viscosity of the reaction mixture and the low solubility of lactide isomers at temperatures of 80 and 100 °C. Amano lipase used in our reactions was purchased from Sigma-Aldrich. It is isolated from *Burkholderia cepacia*. The corresponding results are reported in Table 4. 21.

**Table 4.21 :** Reaction conditions for ROP of  $\epsilon$ -CL and D-, L-lactides catalyzed by Amano lipase PS.

Monomer (1g)	T (°C)	Enzyme quantity (mg)	Toluene amount (ml)	Time (days)	Monomer conversion (%)	$M_n$ of the product (g/mol)*
$\epsilon$ -CL	70	100	2	7	34	1200
D-lactide	80	100	3	7	11	500
	100	30	3	5	6	250
L-lactide	100	30	3	7	16	520

\*Molecular weight ( $M_n$ ) determined by  $^1\text{H}$  NMR.

The reactions proceeded very slowly and poor monomer conversions and low molar masses for the products were obtained. When comparing these values to the results reported by Matsumura for D/L lactide polymerization in toluene (Matsumura et al., 1998) one can consider that the difference is not so important. The low values obtained for the lactide polymerization catalyzed by lipase PS in solvent medium could be explained by the deactivation of the enzyme. Indeed, according to the

product information data provided by the manufacturer (Amano), the enzyme loses 70% of its initial activity after 60 minutes at 65 °C at pH 7.0 and its optimum activity ranges between 55 and 70 °C. Thus one may consider that the combined effect of long reaction times and elevated temperatures may lead to significant lipase loss of activity. Nevertheless, it is still quite surprising to see in the work of Matsumura et al. (1997) such high values of molar masses for PDLLA (i.e. 126000 g/mol) and monomer conversion rates (100%) at 130 °C at the end of 7 days.

Unfortunately all these results did not allow us to fully clarify the contradictory trends and advanced statements reported so far in the literature on the lactide polymerization. Clearly, when polymerization is carried out at elevated temperatures there is the issue of enzyme deactivation and possible thermally-induced lactide polymerization. As far as average molecular weights are concerned, one has also to mention that most of the published studies that report high molecular weights for final PLA product present results (mainly from SEC analyses) obtained on "purified" PLA. Such purification procedure by PLA solubilization and precipitation in ethanol is also known to possibly lead to product fractionation. The PLA oligomers and shorter chains could be solubilized while only a very small amount of the largest chain precipitate and are further the only ones to be analyzed. This could be supported by the very low yield often reported in such studies, even in case of complete lactide conversion. On the contrary, our studies present results obtained by  $^1\text{H}$  NMR analyses performed directly on aliquot samples from the raw reaction mixture. This could explain part of the discrepancies observed between our studies and previously published data on similar results.

#### **4.10 Copolymerizations of $\epsilon$ -CL and Lactide Isomers Catalyzed by NOV-435**

PCL and PLA are well-known biodegradable polymers (Bordes et al., 2009). On one hand, PLA has good biocompatibility and high stiffness, but its brittleness is one of its major disadvantage. On the other hand, PCL is highly flexible and shows a good biodegradability, nevertheless its mechanical strength is relatively low and its melting point at 60 °C causes limitations for many applications (Wang et al., 1998).

Blending both polyesters is regarded as an attractive route for the improvement of the properties. However, the direct blend suffers from limited miscibility and weak adhesion between phases. Resulting materials often show poor mechanical

properties. In this case, copolymerization can be considered as an alternative to avoid the poor miscibility issues. For this reason, the elaboration of PCL/PLA copolymers was targeted with the aim to obtain compatibilized systems with improved properties. It is also an excellent opportunity to test the reactivity of the lipase-based catalyst towards copolymerization of  $\epsilon$ -CL and lactide isomers.

It is already known that immobilized form of CALB is highly active for the ROP of lactones of all ring size while it has been suggested that it is reversibly inhibited by the L and D/L-lactides.

As a first strategy, to analyze the system, equal amounts of  $\epsilon$ -CL and D-lactide (1 g of each) were put in the same reaction tube in the presence of toluene (2 ml) as solvent. The reaction was catalyzed by 100 mg of NOV-435 and carried out at 70 °C for 48 h. Conversion percentages for both monomers were followed during the polymerization by NMR analysis.

On Figure 4.57, a typical  $^1\text{H}$  NMR spectrum of a poly( $\epsilon$ -CL-co-lactide) can be seen with the peaks attributed to their related protons groups.

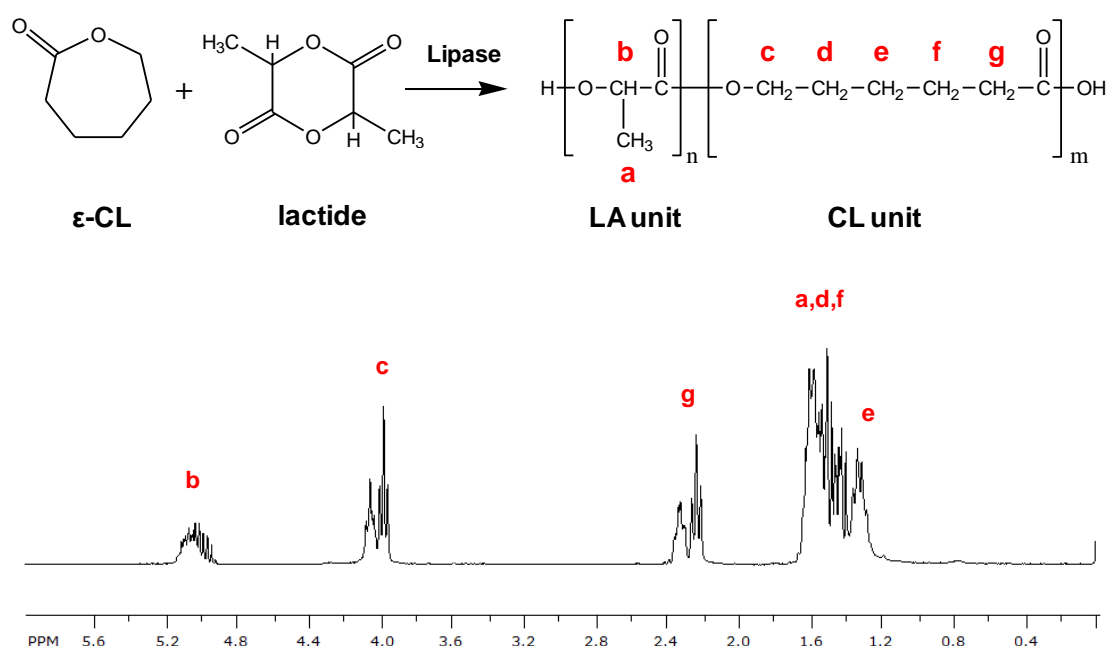


**Figure 4.57 :**  $^1\text{H}$  NMR spectrum of poly( $\epsilon$ -CL-co-D-lactide) copolymer synthesized by NOV-435, with proton assignments and corresponding peaks.

In Figure 4.58, a zoomed view of  $^1\text{H}$  NMR spectra representing the reaction mixture compositions along the copolymerization reaction at  $t=2$  and 48 h can be seen. The consumption of the D-lactide and  $\epsilon$ -CL monomers and the formation of respectively



LA (4.95-5.15 ppm) and CL (3.95-4.10 ppm) units can be clearly observed from the appearing peaks at 48h. Monomer conversion percentages were determined for each monomer by taking the ratios of integrated peak areas of the methylene groups next to the carbonyl group of the monomers and resulting polymers.

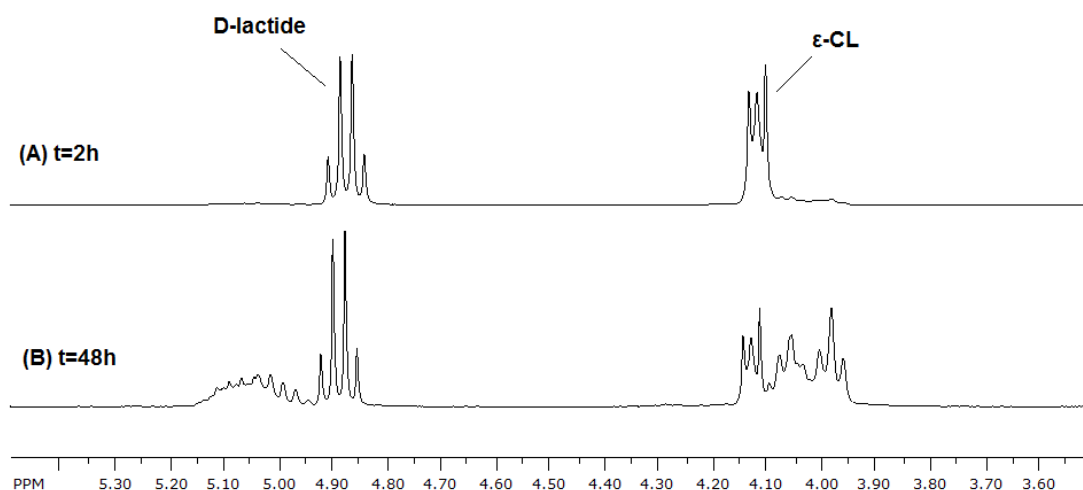


**Figure 4.58 :** Zoomed view of  $^1\text{H}$  NMR spectra of samples withdrawn from the reaction mixture (A) at  $t=2$  h and (B) at  $t=48$  h.

As it can be seen from the Table 4.22, the polymerization of  $\epsilon$ -CL which is normally promoted by CALB was initially slowed by the presence of D-lactide. In contrast to this, a significant consumption for D-lactide was observed. Final product had an  $M_n$  value of 2700 g/mol, determined by SEC with PS standard equivalent.

Thus, by this “one pot” strategy, limited monomer conversions were obtained with a final product still remaining as an oligomer as attested by the NMR and SEC results.

**Table 4.22 :** Monomer conversion evolution for the copolymerization of 1 ml of  $\epsilon$ -CL and 1 g of D-lactide in 2 ml of toluene catalyzed by 100 mg NOV-435.

<b>t (hours)</b>	<b><math>\epsilon</math>-CL conversion (%)</b>	<b>D-lactide conversion (%)</b>
2	15	8
20	52	30
48	74	52

In a second strategy (Figure 4.59), PCL was firstly synthesized from  $\epsilon$ -CL (1 g) keeping the same conditions of reactions (2 ml of toluene, 100 mg NOV-435 at 70 °C). After 2 hours,  $\epsilon$ -CL conversion reached 95% and PCL chains having a  $M_n$  value of 12000 g/mol (SEC; PS standard) were obtained. After the synthesis of PCL chains, D-lactide was introduced into the reaction tube by the addition of an extra

3 ml of toluene to prevent a too high increase of viscosity in reaction medium. The mixture was left to react at 70 °C for 48 h.

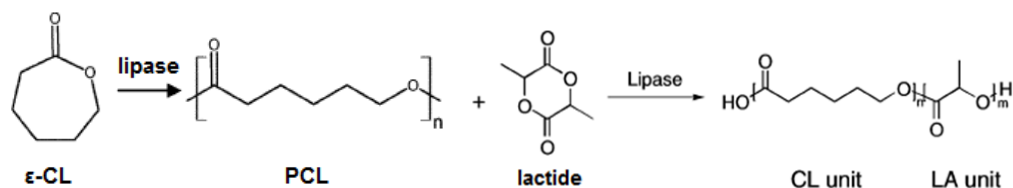


**Figure 4.59 :** Representation of a two steps copolymerization where PCL is firstly synthesized from  $\epsilon$ -CL by lipase catalysis followed by subsequent addition and polymerization of the lactide monomer.

D-lactide consumption was followed during the whole reaction time (Table 4.23). At the end of 2 days the D-lactide monomer was almost totally consumed (97% conversion) as it can be also seen from  $^1\text{H}$  NMR spectrum (Figure 4.60).

**Table 4.23 :** Time evolution of D-lactide monomer conversion after its subsequent addition in copolymerization medium composed of ~ 1 g PCL, 5 ml of toluene and 100 mg NOV-435 catalyst.

t (hours)	D-lactide conversion (%)
2	17
20	71
48	97

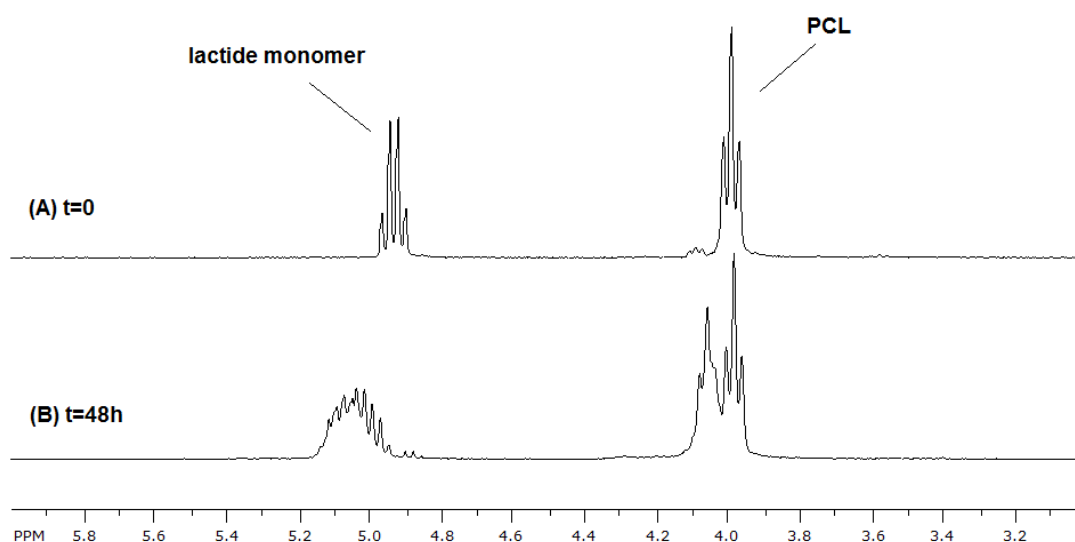


**Figure 4.60 :** Zoomed view of  $^1\text{H}$  NMR spectra of samples (A) at  $t=0$ , where D lactide monomer is added to the reaction mixture containing the preformed PCL chain, (B) at  $t=48$  h, final purified copolymer.

When looking at the specific peak of the monomer at  $t=0$  (4.9 ppm), it can be seen that after 48 hours, the lactide is almost totally consumed. But the sharp  $-CH$  peak of PDLA which is normally present as a quadruplet at 5.1 ppm is not observed. Instead, a broad peak (4.9-5.2 ppm) is obtained, representing the formation of some short sequences of LA units which might be incorporated within the PCL chains. The typical peak of the  $-CH_2O$  protons (at 4.0 ppm) of PCL chains is also altered, thus confirming the insertion of short sequences of LA units within the main chain of PCL, causing some differences on its original NMR signal.

Copolymer formation can be visualized from  $^{13}C$  NMR spectra, specifically from the expanded carbonyl carbon ( $C=O$ ) region between  $\delta=169$ -174 ppm. The peak at 173.5 ppm represents the carbonyl signal of the PCL homopolymer (Figure 4.61A). After 2 hours of polymerization, lactide monomer has not been consumed yet as attested by the presence of the typical carbonyl signal for the monomer at  $\delta=167$  ppm (Figure 4.61A). At the end of copolymerization, after 2 days, a total disappearance of the lactide monomer signal is observed but the typical peak ( $\delta=169.7$  ppm) for a PLA homopolymer chain or large sequence of LA units cannot be visualized. Instead, there are various small peaks having different intensities corresponding to intermediate carbonyl signals (Figure 4.61B). These peaks clearly demonstrate that short sequences of lactide units are inserted within the PCL chain due to transesterification reactions and confirm the formation of a random copolymer since two single peaks corresponding to each homopolymer are not present, which is normally the case for PCL/PLA block copolymers.

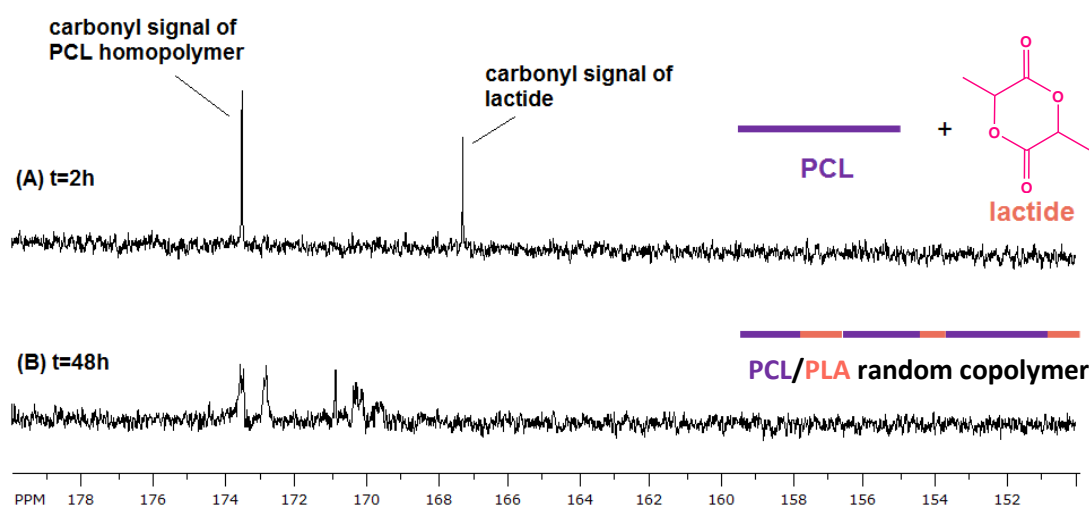


**Figure 4.61 :** Carbonyl signals in  $^{13}C$  NMR spectra of copolymerization products of PCL+ D-lactide system; (A) at  $t=2$  h and (B) at  $t=48$  h.

The final derived copolymer synthesized at the end of this polymerization had a molecular weight of 7500 g/mol (SEC; PS standard). This result attests for a decrease in the polymer average molecular weight (which was initially 12000 g/mol for PCL) during lactide polymerization, confirming the occurrence of transesterification reactions and thus the random copolymer structure.

The same strategy i.e., synthesizing first the PCL and introducing secondly the lactide monomer, was also assayed with L- and D/L- lactides but very poor monomer conversions were observed for these stereoisomers. The resulting products were mainly composed of PCL homopolymer (Table 4.24).

Table 4.24 presents the various reactions carried out for the synthesis of PCL/PLA copolymers and the characteristics of the resulting products.

**Table 4.24 :** Results of  $\epsilon$ -CL/PCL- lactide copolymerizations catalyzed by NOV-435.

Copolymerization reaction	% Lactide conv. (48h)	Product		PDI	T <sub>g</sub> (°C)	T <sub>m</sub> (°C)	$\Delta H_{fus}$ (J/g)	T <sub>c</sub> (°C)	$\Delta H_c$ (J/g)
		M <sub>n</sub> (g/mol)	(SEC)						
$\epsilon$ -CL+D-lactide	52	2700	2.9	-28	-	-	-	-	-
PCL+D-lactide	97	7500	2.6	-23	-	-	-	-	-
PCL+L-lactide	4	7300	2.9	-	53	75	31	77	77
PCL+D/L-lactide	3	10800	2.5	-	55	67	35	75	75
PCL + Cloisite® 30B + D-lactide (CLDMMT)	93	-	-	-29	54	0.56	-	-	-
CLDMMT after clay removal	-	6600	2.4	-30/ -55	55	9	-	-	-

As already mentioned, when both monomers ( $\epsilon$ -CL + D-lactide) were copolymerized at the same time, good D-lactide conversion but low molecular weight of the product were observed. Besides, when PCL block was firstly synthesized and D-lactide monomer was subsequently added, higher conversion rates and molecular weight for final product were obtained.

It was observed that copolymerization proceeded better with D-lactide (97% conversion) than L- or D/L-lactide (3-4% conversion). This is in perfect accordance with the results obtained for the lactide homopolymerization reactions for which only the D-lactide monomer could be polymerized by NOV-435 catalyst.

As far as D-lactide is concerned, the resulting P(CL-co-LA) copolymers did not show any melting or crystallization temperature revealing their amorphous morphology. Here again, the amorphous character is a direct consequence of the formation of a random copolymer due to the transesterificative effect of the lipase. A single clear, well defined  $T_g$  value (-29 to -23 °C) positioning between the  $T_g$  values of PCL (-60 °C) and PLA (60 °C) homopolymers was determined for these D-lactide containing copolymers, confirming the random structure of the copolyesters.

By using the Fox equation (4.3), it is usually possible to determine the expected glass transition temperature in statistical copolymers with a very good accuracy (Hiemenz and Lodge, 2007).

$$\frac{1}{T_g} = \frac{w_1}{T_{g1}} + \frac{w_2}{T_{g2}} \quad (4.3)$$

Where  $w_1$  and  $w_2$  are weight fractions of components 1 and 2, respectively.

Interestingly, when the Fox equation was used to estimate the copolymer composition from its  $T_g$  value, the calculated weight fraction of LA units is lower than the content expected from the monomer conversions. For instance, according to the Fox equation, the  $T_g$  value of -28 °C should correspond to a copolymer with ca. 36 wt% of LA while the monomer conversions measured for this experiment would lead to a copolyester having 41 wt% in LA units. This seems to indicate that some of the converted lactide monomers are not inserted into the copolyester chains and rather remain as short homopolymers (oligomers).

Considering the polymers synthesized in the presence of L- and D/L-lactide, their  $T_m$  and  $T_c$  values were very similar to those of pure PCL ( $T_m$ :58 °C and  $T_c$ :32 °C), proving that their final structure is mostly, if not totally, composed of PCL homopolymer (Table 4.24). However, in all cases a decrease in the average molecular weight was observed after the second step of copolymerization highlighting the occurrence of transesterification reactions.

To finalize the experimental studies on such copolyesters, one experiment was carried out in presence of Cloisite<sup>®</sup> 30B. The results obtained from this reaction are also reported on Table 4.24. The addition of Cloisite<sup>®</sup> 30B at the same time with D-lactide monomer did not have a negative impact on reaction kinetics since the lactide conversion is similar to the reaction performed without clay. In addition, the DSC results clearly confirmed that in this case an amorphous random copolymer structure is again obtained. Unfortunately, the possible presence of organoclay residues (ammonium organomodifiers and/or inorganic moieties) in the final product did not allow us to perform SEC analyses on this sample. However, an estimation can be made regarding the final copolymer average molecular weight by analyzing the product after clay removal.

For this, and also to verify if the final copolymer is grafted onto the organoclay, clay rich and polymer rich fractions were separated by centrifugation and several washing steps made on the clay rich fraction to eliminate unbound polymer chains.

The SEC analysis performed on the recovered purified polymer-rich fraction shows a chromatogram displaying a large molecular weight distribution with the main peak having an average molecular weight of 6600 g/mol. This result is consistent with the value obtained for the same copolymerization conducted without clay (7500 g/mol). The slightly lower  $M_n$  value can be explained by the effect of clay, as previously observed and discussed for  $\epsilon$ -CL homopolymerization. However, the separation procedure may result in polymer chains separation according to their length and composition (as it will be demonstrated below) and thus the analyzed sample fraction may not be fully representative of the whole product.

It is most likely that, at the end of the polymerization reaction, the product recovered from the reaction mixture is composed of long and short, grafted and free chains and of copolymers with different composition percentages. Thus, it is quite difficult to make a precise interpretation on the TGA and DSC spectra. TGA analysis was performed on the final clay/copolymer hybrid product (CLDMMT) and on its clay and polymer rich fractions (Figure 4.62).

From the TGA results, one can see that the amount of unburnt residue at 700 °C for CLDMMT (the copolymer/clay nanohybrid recovered directly by precipitation at the

end of the reaction) and for its purified polymer rich fraction (after separation by centrifugation) are quite similar (~12 wt%).

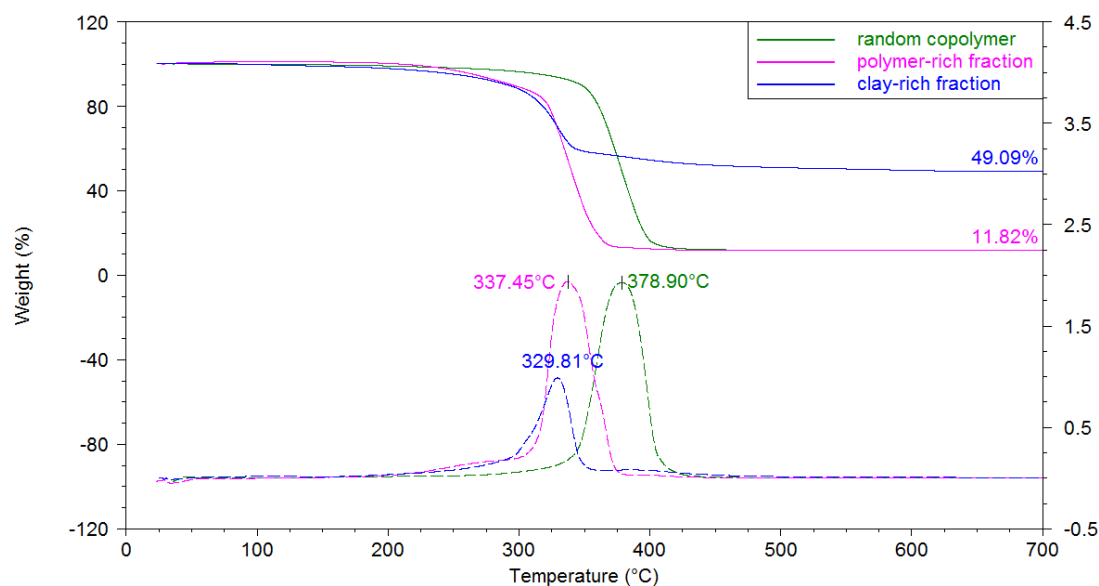


**Figure 4.62 :** TGA spectrum of hybrid random copolymer (CLDMMT), its polymer rich and clay rich fractions.

Even if it cannot be deduced that the whole clay within the material is grafted with polymer chains, the presence of clay on the polymer-rich fraction separated by centrifugation clearly shows that some part of copolyester chains extracted in the supernatant are grafted to inorganic clay platelets.

Moreover, the clay-rich fraction shows a 49 wt% of residue (Figure 4.62), meaning that the weight loss due to organic compounds degradation is of 51 wt%. By subtracting from this value the clay organo-modifier weight content (approximately 30 wt%), it can be deduced that there is the presence of about 20 wt% of polymer within the clay-rich fraction. All these TGA results seem to confirm a significant grafting of P(CL-co-LA) random copolyester chains at the surface of the Cloisite<sup>®</sup> 30B clay platelets and thus the successful preparation of clay/copolyester nanohybrid materials.

Regarding the DSC analysis, it can be hypothesized that the recovered purified polymer-rich fraction is a mixture of both PCL homopolymer chains and P(CL-co-LA) copolymer chains since it shows two  $T_g$  values (Figure 4.63). The first value recorded at -55 °C is attributed to pure PCL homopolymer while the  $T_g$  at -30 °C is assigned to the copolymer.

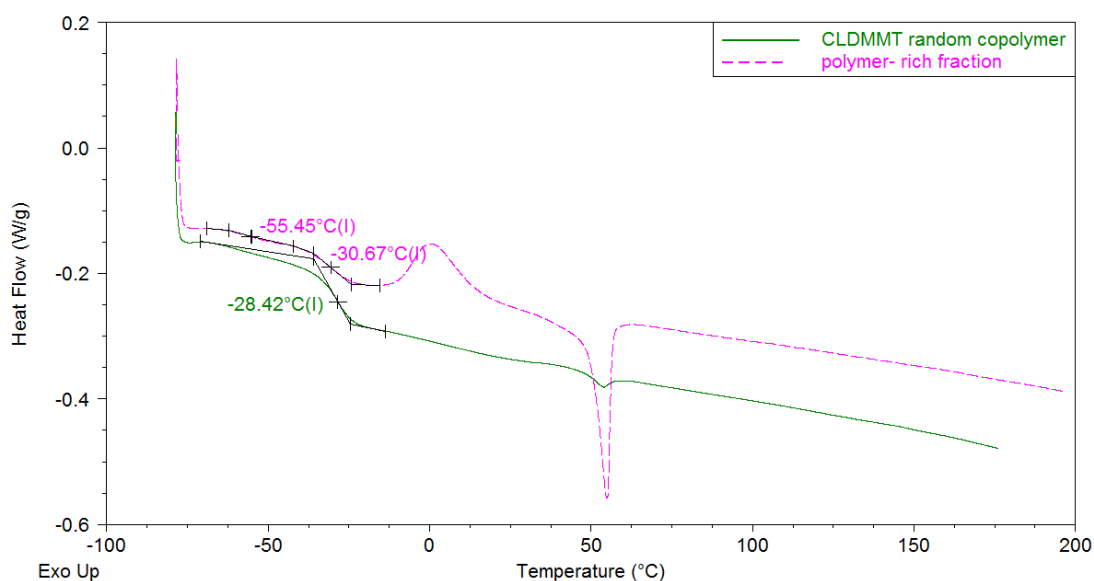


**Figure 4.63 :** DSC thermograms of CLDMMT hybrid random copolymer and its purified polymer-rich fraction.

From these DSC analyses it can be concluded that PCL homopolymer chains which are not clearly detectable in the whole precipitated material (CLDMMT) can be found out in the purified polymer-rich product, attesting for the formation of homopolymer chains and thus the heterogeneity of the final product.

In addition, one can clearly see that the DSC analysis of polymer-rich fraction obtained after centrifugation separation shows an exothermic crystallization peak (around 0 °C) followed by a melting endotherm (around 52 °C). This result evidences the presence of PCL crystalline domains on the analyzed sample. On the contrary, the copolyester/clay nanohybrid sample recovered after the reaction does not show such marked PCL melting endotherm and crystallization. It is more likely that in this case, the centrifugation separation procedure induces a polymer chain separation according to their length and composition.

It is assumed that long free chains as well as the long clay-grafted PCL or copolymer chains remain on the supernatant while short grafted chains are precipitated with the clay during the centrifugation separation process. Indeed, the long (co)polymer chains grafted on clay are also more likely to be extracted on the supernatant together with the long free chains. Besides, due to heterogeneity in the copolyester composition and because of the lipase transesterification activity, it is assumed that the longest macromolecules are mostly PCL homopolymer chains while copolymers with higher and significant amount of LA units result in shorter chains. Thus, these



short grafted chains are not able to crystallize either because they are oligomers and/or because of the amorphous character of the P(CL-co-LA) copolymer. In contrast, the extracted polymer-rich fraction enriched in the longer free or grafted chains, which are mostly PCL homopolymer chains, shows partial crystallization with a higher  $\Delta H_f$  value (9 J/g) compared to the value obtained for the clay/copolymer nanohybrid CDLMMT (0.56 J/g).

Moreover, one cannot exclude the additional influence of the presence of nanoclay in higher amounts on the clay/copolymer nanohybrid compared to the polymer-rich fraction resulting in the clay platelets hindering the polymer crystallization.

## 5. CONCLUSIONS AND PERSPECTIVES

This multidisciplinary study combining biotechnology, with the use of enzymatic catalysis, and polymer science, with the elaboration of organic/inorganic nano-biocomposites, had the aim to develop original catalysts based on lipase immobilized onto clays which would be efficient for the synthesis of biopolyester/clay nanohybrids.

Contrary to the conventional chemical synthesis of polymers and the common approaches used for the preparation of nano-biocomposites, this study focused on using and analyzing in details original enzymatic catalyst systems for their elaboration.

The use of lipase/clay derivatives to catalyze the polymerization of  $\epsilon$ -CL and lactide isomers and to elaborate the corresponding biopolyester/clay nanohybrid materials has not been investigated and reported so far in the literature.

In this work, the use of clays as lipase supports and also as nanofillers within organic/inorganic nanohybrids appeared as a judicious choice due to their intrinsic properties (high specific surface area, high aspect ratio, natural origin, etc.) and their large availabilities.

This work was structured into three main distinct and complementary parts:

- (i) immobilization of CALB onto nanoclays and obtention of CALB/clay derivatives,
- (ii) the use of commercial free and immobilized lipases and the CALB/clay derivatives as catalysts in the ring-opening polymerization reactions for the synthesis of PCL and PLA and the test of their catalytic performances,
- (iii) subsequent elaboration of polyester/clay nanohybrids by polyester chain grafting onto clay surface by enzymatic catalysis and their characterization.

In the first part of the study, where  $\epsilon$ -CL polymerization kinetics were analyzed, it has been confirmed that the NOV-435 immobilized system is much more efficient than the non-immobilized counterpart when considering the catalytic activity with

the effective amount of enzyme. This fact confirmed the benefits of CALB immobilization and reported results on the high activity of NOV-435.

Moreover, determination of the polymerization rate for the reactions performed in the presence of clays showed that the addition of clay in the medium does not have a negative impact on the kinetic of lipase-catalyzed polymerization of  $\epsilon$ -CL. Nevertheless, the addition of clay, results in a decrease in the PCL average molecular weights. Analyses evidenced a clear dependence between the decrease in PCL chain lengths and the increasing amount of hydroxyl groups available at the clay surface. The hydrophobic organo-modified montmorillonite, bearing less hydroxyl groups, leads to PCL chains with highest molecular weights. These results demonstrated that the hydroxyl groups at the clay surface are effectively involved in the polymerization reaction, leading to the grafting and growth of PCL chains from the clay surface.

After determining the influence of clay addition in the reaction medium, such nanoclays were used for lipase immobilization and the resulting derivatives were further tested for  $\epsilon$ -CL polymerization. The main results from this part of the study concern the successful elaboration of clay-immobilized lipase catalysts efficient for the  $\epsilon$ -CL polymerization. Our results highlighted important differences in catalytic performance between montmorillonite and sepiolite-based systems as well as the influence of clay-organomodification. Indeed, it has been demonstrated that lipases immobilized on montmorillonite show better performances compared to the sepiolite-based ones. In addition, the clay surface organo-modification performed using quaternary ammonium salts has shown to greatly enhance the lipase immobilization procedure and thus the catalytic activity of the corresponding systems. It has been suggested that such differences in the catalytic behavior of the systems could be explained by differences of electrostatic interactions between the enzyme and the clay surface.

Therefore, despite the slower kinetics and slightly lower molecular weight obtained, our original MMTMODL catalytic systems (CALB immobilized on organomodified montmorillonite) showed significant ROP activity towards  $\epsilon$ -CL which clearly highlighted its great potential. These performant catalytic systems provided a monomer conversion of 90% in 48 hours and PCL chains with  $M_n=10000$  g/mol.

In a next step, taking advantage of the specific behavior of the clay hydroxyl groups participating in the polymerization reaction and leading to PCL chain grafting and growth from the clay surface, the successful elaboration of PCL/clay organic/inorganic nanohybrids was achieved using the most efficient catalytic systems.

The properties of these PCL/clay nanohybrid materials were further characterized. The selective extraction procedures carried out on the reaction mixture and the performed thermogravimetric analyses evidenced the effective grafting of PCL chains from the clay surface. They also showed that the longer and higher amount of grafted chains are obtained with the organo-modified montmorillonite clay. SEM analyses further demonstrated the positive effect of such PCL chain grafting at the clay surface to obtain finely dispersed clay nanoparticles in the polymer matrix.

The study extended to the synthesis of polylactic acid (PLA) did not allow us to clarify the contradictory trends reported so far in the literature about the polymerizability of D- and L-lactide isomers. Nevertheless, one can note that we have successfully polymerized L-lactide. By the catalysis of NOV-435, only a very low monomer conversion (6%) and small PLLA oligomers with  $M_n=200$  g/mol could be obtained in 48 hours. However, monomer conversion reached 84% by the catalysis of free CALB but still oligomers were formed ( $M_n=500$  g/mol), indicating the opening of only one or two lactide monomers.

In the case of P(CL-co-LA) copolymer synthesis by NOV-435, it was observed that copolymerization proceeded better with D-lactide (97% conversion) than L- or D/L-lactide (3-4% conversion). The performed analyses revealed the random structure of the copolymers synthesized with D-lactide whereas the final products were mostly composed of PCL homopolymer with L- or D/L-lactide.

After all, the rapid screening of various commercial lipases tested for ROP of  $\epsilon$ -CL showed that CALB remained as the most performant lipase. This preliminary study could pave the way for future works on screening alternative lipases from different microorganisms or other sources and testing their immobilization on inexpensive and appropriate solid supports to develop new efficient catalysts for polyester synthesis by ring opening polymerization. The future perspectives to this work should be a part of the next projects to be developed in the BioTeam group.

Additional characterization, such as mechanical properties determination could be accomplished on the PCL/clay nano-biocomposites, after upscaling the process to produce larger quantities. Besides, different reaction conditions such as scanning a broader temperature range or testing different reaction media like ionic liquids, would worth to be tested aiming at improving the polymerization kinetics and molecular weights of final products.

At a longer term, it would be interesting to study the properties and behavior of these biopolyesters/clays nano-biocomposites for biomedical purposes since these advanced organic/inorganic hybrids obtained by enzymatic catalysis would preferably stand on such high value added applications rather than a use for large-scale and inexpensive materials as packaging.

The interest of using clays within inorganic/organic nano-biocomposites and their positive contribution to the material were supported by several studies conducted on biomedical applications. It has been demonstrated that the presence of clay platelets influence the biodegradation rate and mechanical stability of the material (Zhuang et al., 2007).

Among possible applications, encapsulation of active components for drug delivery system, or scaffolds for bone and cartilage reconstruction can be envisaged. For instance, in polymer/clay nanocomposites, the montmorillonite interlayer gallery or the sepiolite internal channels can be used to adsorb specific drugs to stimulate e.g., the cells growth (Ruiz-Hitzky et al., 2010). In the literature, it has been demonstrated that biodegradable and biocompatible polyesters used as scaffolds for tissue engineering provide good porosity, appropriate pore size for specific cells, permeability for nutrient diffusion and surface characteristics for cell adhesion and growth (Agarwal and Ray, 2001). As an example, it could be interesting to elaborate scaffolds from PLA or PCL organic/inorganic nanohybrids by electrospinning which is a technique developed in the laboratory.

PCL and PLA are FDA-approved polyesters for the contact with living tissues in biomedical applications. Nanohybrids based on PCL/PLA with hydroxyapatite are already widely investigated as scaffolds for bone regeneration (Steinbuechel, 2003). Therefore, it would be interesting to replace hydroxyapatite within the structure of

these nano-biocomposites by the largely available and inexpensive nanoclays (sepiolite and montmorillonite) for such applications.

Then, some in vitro tests demonstrating the growth and adhesion of the cells and the lack of toxicity of these materials on living organism, would have to be performed. In addition, it has also been shown that the surface properties of biodegradable polymer scaffolds (hydrophilicity, surface charge density, micromorphology, etc.) have an important influence on cell adsorption, spreading and biological functions. In this context, PLA suffers from its hydrophilic nature limiting the penetration of cells into the pores of the polymeric matrix.

At this point, the interest for the synthesis of PCL/PLA copolyesters would emerge to tune the properties of the biodegradable polymers and their correspondings nano-biocomposites for such biomedical applications. Interestingly, PLA and copolymers obtained from D-lactide and  $\epsilon$ -CL have been used as drug delivery carriers (Soppimath et al., 2001). Improvements in terms of active agent effect, prolonged biological activity and controlled drug release rate have been observed.



## REFERENCES

- Agarwal, C. M. and Ray, R. B.** (2001). Biodegradable polymeric scaffolds for musculoskeletal tissue engineering. *J. Biomed. Mater. Res.*, **55**, 141-150.
- Albertsson, A.C and Varma, I.K.** (2003). Recent developments in ring opening polymerization of lactones for biomedical applications. *Biomacromolecules*, **4**, 1466-1486.
- Albertsson, A.C. and Srivastava, R.K.** (2008). Recent developments in enzyme-catalyzed ring- opening polymerization. *Adv. Drug. Deliv. Rev.*, **60**, 1077-1093.
- Alexandre, M. and Dubois, P.** (2000). Polymer layered silicate nanocomposites: preparation, properties and uses of a new class of materials. *Mater. Sci. Eng. R:Rep.*, **28**, 1-63.
- Avérous, L.** (2008). PLA: synthesis, properties, applications. (Chapter 21) in *Monomers, polymers and composites from renewable resources* (eds. Belgacem, M.N. and Gandini, A.), Elsevier Ltd., Amsterdam, Netherlands.
- Avérous, L. and Pollet, E.** (2011). Biorenewable nanocomposites. *MRS Bull.*, **36**, 703-710.
- Avérous, L. and Pollet, E.** (2012a). Biodegradable polymers. (Chapter 2) in *Environmental silicate nano-biocomposites* (eds. Avérous, L. and Pollet, E.), Springer-Verlag, London.
- Avérous, L. and Pollet, E.** (2012b). Green nano-biocomposites. (Chapter 1) in *Environmental silicate nano-biocomposites* (eds. Avérous, L. and Pollet, E.), Springer-Verlag, London.
- Avérous, L., Moro, L., Dole, P. and Fringant, C.** (2000). Properties of thermoplastic blends: starch–polycaprolactone. *Polymer*, **41**, 4157-4167.
- Avrameas, S.** (1969). Coupling of enzymes to proteins with glutaraldehyde. Use of the conjugates for the detection of antigens and antibodies. *Immunochemistry*, **6**, 43-52.
- Basko, M. and Kubisa, P.** (2006). Cationic copolymerization of  $\epsilon$ -caprolactone and L,L-lactide by an activated monomer mechanism. *J. Polym. Sci. A Polym. Chem.*, **44**, 7071-7081.
- Bastioli, C.** (1998). Biodegradable materials-present situation and future perspectives. *Macromol. Symp.*, **135**, 193-204.



- Bastioli, C., Cerutti, A., Guanella, I., Romano, G.C. and Tosin, M.** (1995). Physical state and biodegradation behavior of starch–polycaprolactone systems. *J. Environ. Polym. Degrad.*, **3**, 81-95.
- Becker, J.M. and Dove A.P.** (2011). Poly(lactide)s as robust renewable materials. (Chapter 9) in *Green polymerization methods* (eds. Mathers, R.T. and Meier, M.A.R.), Wiley-VCH, Weinheim, Germany.
- Bedu-Addo, F.K.** (2004). Understanding lyophilization formulation development. *Pharmaceutical Technology*, Lyophilization, 10-18.
- Benali, S. and Dubois, P.** (2012). PCL/Clay nano-biocomposites. (Chapter 5) in *Environmental silicate nano-biocomposites* (eds. Avérous, L. and Pollet, E.), Springer-Verlag, London.
- Bergaya, F., Jaber, M. and Lambert, J.F.** (2011). Organophilic clay minerals. (Chapter 2) in *Rubberclay nanocomposites*. Science, technology and application (edt. Galimberti, M.), Wiley, Chichester.
- Bergaya, F., Jaber, M. and Lambert, J.F.** (2012). Clays and clay minerals as layered nanofillers for (bio)polymers. (Chapter 3) in *Environmental silicate nano-biocomposites* (eds. Averous, L. and Pollet, E.), Springer-Verlag London.
- Blanco, R.M., Terreros, P., Perez, M.F., Otero, C. and Gonzalez, G.** (2004). Functionalization of mesoporous silica for lipase immobilization characterization of the support and the catalysts. *J. Mol. Catal. B: Enzym.*, **30**, 83-93.
- Bokobza, L. and Chauvin, J.** (2005). Reinforcement of natural rubber: use of in situ generated silicas and nanofibres of sepiolite. *Polymer*, **46**, 4144-4151.
- Bordes, P., Pollet, E. and Avérous, L.** (2009). Nano-biocomposites: Biodegradable polyester/nanoclay systems. *Prog. Polym. Sci.*, **34**, 125-155.
- Bradford, M.M.** (1976). A rapid and sensitive method for the quantitation of microgram quantities of protein utilizing the principle of protein dye binding. *Anal. Biochem.*, **72**, 248-254.
- Brady, L., Brzozowski, A. M., Derewenda, Z. S., Dodson, E., Dodson, G., Tolley, S., Turkenburg, J. P. et al.** (1990). A serine protease triad forms the catalytic center of a triacylglycerol lipase. *Nature*, **343**, 767-770.
- Brigatti, F., Galan, E., Theng, B.K.G.** (2006). Structures and mineralogy of clay minerals. *Handbook of clay science* (eds. Bergaya, F., Theng, B.K.G., Lagaly, G.), Elsevier, Amsterdam, 19-86.
- Brigida, A., Pinheiro, A., Ferreira, A. and Gonçalves, L.** (2008). Immobilization of *Candida antarctica* Lipase B by adsorption to green coconut fiber. *Appl. Biochem. Biotechnol.*, **146**, 173-187.
- Brzozowski, A., Derewenda, U., Derewenda, Z.S., Dodson, G.G., Lawson, D.M., Turkenburg, J.P., Bjorkling, F. et al.** (1991). A model for interfacial activation in lipases from the structure of a fungal lipase-inhibitor complex. *Nature*, **351**, 491-494.

- Carrasco, M.S., Rad, J.C. and Gonzalez-Carcedo, S.** (1995). Immobilization of alkaline phosphatase by sorption on Na-sepiolite. *Bioresource Technol.*, **51**, 175-181.
- Ceccorulli, G., Scandola, M., Kumar, A., Kalra, B. and Gross, R.A.** (2005). CocrySTALLIZATION of random copolymers of  $\omega$ -pentadecalactone and  $\epsilon$ -caprolactone synthesized by lipase catalysis. *Biomacromolecules*, **6**, 902-907.
- Chang, J.H., An, Y.U., Cho, D. and Giannelis, E.P.** (2003). Poly(lactic acid) nanocomposites: comparison of their properties with montmorillonite and synthetic mica (II). *Polymer*, **44**, 3715-3720.
- Chen, B., Hu, J., Miller, E.M., Xie, W., Cai, M. and Gross, R.A.** (2008). *Candida antarctica* Lipase B chemically immobilized on epoxy-activated micro and nanobeads: catalysts for polyester synthesis. *Biomacromolecules*, **2**, 463-471.
- Chen, G. and Yoon, J.S.** (2005). Nanocomposites of poly[(butylene succinate)- co-(butylene adipate)] (PBSA) and twice-functionalized organoclay. *Polym. Int.*, **54**, 939-945.
- Chivrac, F., Pollet, E. and Av  rous, L.** (2007). Nonisothermal crystallization behavior of poly(butylene adipate-co-terephthalate)/clay nanobiocomposites. *J. Polym. Sci. Polym. Phys.*, **45**, 1503-1510.
- Chivrac, F., Pollet, E. and Av  rous, L.** (2009). Progress in nano-biocomposites based on polysaccharides and nanoclays. *Mat. Sci. Eng. R.*, **67**, 1-17.
- Chivrac, F., Pollet, E., Schmutz, M. and Av  rous, L.** (2010). Starch nanobiocomposites based on needle-like sepiolite clays. *Carbohydr. Polym.*, **80**, 145-153.
- Chow, T.S.** (1978). Effect of particle shape at finite concentration on the elastic moduli of filled polymers. *J. Polym. Sci., Part B: Polym. Phys.*, **16**, 959-965.
- Connor, E.F., Nyce, G.W., Myers, M., Mock, A. and Hedrick, J.L.** (2002). First example of N-heterocyclic carbenes as catalysts for living polymerization: organocatalytic ring-opening polymerization of cyclic esters. *J. Am. Chem. Soc.*, **124**, 914-915.
- Coulembier, O., Dove, A.R., Pratt, R.C., Sentman, A.C., Culkin, D.A., Mespouille, L., Dubois, P., Waymouth, R.M. and Hedrick, J.L.** (2005). Latent, thermally activated organic catalysts for the on-demand living polymerization of lactide. *Angew. Chem. Int. Ed.*, **44**, 4964-4968.
- Cruz, J.C., Pfromm, P.H., Rezac, M.E.** (2009). Immobilization of *Candida antarctica* Lipase B on fumed silica, *Process Biochem.*, **44**, 62-69.
- Csihony, S., Culkin, D.A., Sentman, A.C., Dove, A.P., Waymouth, R.M. and Hedrick, J.L.** (2005). Single-component catalyst/initiators for the organocatalytic ring-opening polymerization of lactide. *J. Am. Chem. Soc.*, **127**, 9079-9084.
- De Paiva, L.B., Morales, A.R. and Valenzuela Diaz, F.R.** (2008). Organoclays: properties, preparation and applications. *Appl. Clay Sci.*, **42**, 8-24.

- Degee, O., Dubois, P., Jacobsen, S., Fritz, S.G. and Jerome, R.** (1999). Beneficial effect of triphenylphosphine on the bulk polymerization of L,L-lactide promoted by 2-ethylhexanoic acid tin (II) salt. *J. Polym. Sci. A Polym. Chem*, **37**, 2413-2420.
- Degli Innocenti, F.** (2005). Biodegradation behaviour of polymers in the soil. (Chapter 3) in *Handbook of biodegradable polymers* (edt. Bastioli, C.), Rapra Technology Ltd., UK.
- Degn, P. and Zimmermann, W.** (2001). Optimization of carbohydrate fatty acid ester synthesis in organic media by a lipase from *Candida antarctica*. *Biotechnol. Bioeng.*, **74**, 483-491.
- Deng, F. and Gross, R.A.** (1999). Ring-opening bulk polymerization of  $\epsilon$ -caprolactone and trimethylene carbonate catalyzed by lipase Novozym 435. *Int. J. Biol. Macromol.*, **25**, 153-159.
- Di, Y., Iannace, S., Di Maio, E. and Nicolais, L.** (2003). Nanocomposites by melt intercalation based on polycaprolactone and organoclay. *J. Polym. Sci. B Polym Phys.*, **41**, 670-678.
- Dove, A.P.** (2009). Metal-free catalysis in ring-opening polymerization (Chapter 14) in *Handbook of ring-opening polymerization* (edts. Dubois, P., Coulembier, O. and Raquez, J.M.), Wiley-VCH Verlag GmbH&Co., Weinheim, Germany.
- Dove, A.P., Pratt, R.C., Lohmeijer, B.G.G., Waymouth, R.M. and Hedrick, J. L.** (2005). Thiourea-based bifunctional organocatalysis:  $\square$  supramolecular recognition for living polymerization. *J. Am. Chem. Soc.*, **127**, 13798-13799.
- Dove, A.P., Pratt, R.C. , Lohmeijer, B.G.G. , Li, H., Hagberg, E.C., Waymouth, R.M. and Hedrick, J.L.** (2006). N-heterocyclic carbenes as organocatalysts. In *N- Heterocyclic carbenes in synthesis* (edt. Nolan, S.P.), Wiley-VCH Verlag GmbH, Weinheim, p. 275.
- Dubois, P., Jacobs, C., Jérôme, R. and Teyssié, P.** (1991). Macromolecular engineering of polylactones and polylactides. 4. Mechanism and kinetics of lactide homopolymerization by aluminum isopropoxide. *Macromolecules*, **24**, 2266-2270.
- Duda, A.** (1996). Polymerization of  $\epsilon$ -caprolactone initiated by aluminum isopropoxide carried out in the presence of alcohols and diols. Kinetics and mechanism. *Macromolecules*, **29**, 1399-1406.
- Duda, A. and Penczek, S.** (1994). Determination of the absolute propagation rate constants in polymerization with reversible aggregation of active centers. *Macromolecules*, **27**, 4867-4870.
- Duquesne, E., Moins, S., Alexandre, M., Dubois, P.** (2007). How can nanohybrids enhance polyester/sepiolite nanocomposite properties? *Macromol. Chem. Phys.*, **208**, 2542-2550.
- Ema, Y., Ikeya, M., Okamoto, M.** (2006). Foam processing and cellular structure of polylactide-based nanocomposites. *Polymer*, **47**, 5350-5359.

- Endo, T.** (2009). General mechanisms in ring-opening polymerization. (Chapter 2) in *Handbook of ring-opening polymerization* (eds. Dubois, P., Coulembier, O. and Raquez, J.M.), Wiley-VCH Verlag GmbH&Co., Weinheim, Germany.
- Feng, H. and Dong, C.M.** (2006). Preparation and characterization of chitosan-graft-poly ( $\epsilon$ -caprolactone) with an organic catalyst. *J. Polym. Sci. A Polym. Chem.*, **44**, 5353-5361.
- Fernandez-Lafuente, R., Armisen, P., Sabuquillo, P., Fernandez-Lorente, G. and Guisan, J.M.** (1998). Immobilization of lipases by selective adsorption on hydrophobic supports. *Chem. Phys. Lipids*, **93**, 185-197.
- Fernandez-Lorente, G., Cabrera, Z., Godoy, C., Fernandez-Lafuente, R., Palomo, J.M. and Guisan, J.M.** (2008). Interfacially activated lipases against hydrophobic supports: Effect of the support nature on the biocatalytic properties. *Process Biochem.*, **43**, 1061-1067.
- Fuentes, I.E., Viseras, C.A., Ubiali, D., Terreni, M. and Alcantara, A.R.** (2001). Different phyllosilicates as supports for lipase immobilisation. *J. Mol. Catal. B: Enzym.*, **11**, 657-663.
- Gazeau-Bureau, S., Delcroix, D., Martin-Vaca, B., Bourissou, D., Navarro, C. and Magnet, S.** (2008). Organo-catalyzed ROP of  $\epsilon$ -caprolactone: methanesulfonic acid competes with trifluoromethanesulfonic acid. *Macromolecules*, **41**, 3782-3784.
- Ghiaci, M., Aghaei, H., Soleimani, S. and Sedaghat, M.E.** (2009a). Enzyme immobilization: Part 2. Immobilization of alkaline phosphatase on Na-bentonite and modified bentonite. *Appl. Clay Sci.*, **43**, 308-316.
- Ghiaci, M., Aghaei, H., Soleimani, S. and Sedaghat, M.E.** (2009b). Enzyme immobilization Part 1. Modified bentonite as a new and efficient support for immobilization of *Candida rugosa* lipase. *Appl. Clay Sci.*, **43**, 289-295.
- Gitlesen, T., Bauer, M. and Adlercreutz, P.A.** (1997). Adsorption of lipase on polypropylene powder. *Biochim. Biophys. Acta*, **1345**, 188-196.
- Gopinath, S. and Sugunan, S.** (2007). Enzymes immobilized on montmorillonite K 10: effect of adsorption and grafting on the surface properties and the enzyme activity. *Appl. Clay Sci.*, **35**, 67-75.
- Griebenow, K. and Klivanov, A.M.** (1996). On protein denaturation in aqueous-organic mixtures but not in pure organic solvents. *J. Am. Chem. Soc.*, **118**, 11695-11700.
- Gross, R.A. and Kalra, B.** (2002). Biodegradable polymers for the environment. *Science*, **297**, 803-807.
- Gross, R.A. Kalra B. and Kumar, A.** (2001). Polyester and polycarbonate synthesis by in vitro enzyme catalysis. *Appl. Microbiol. Biotechnol.*, **55**, 655-660.
- Hakkarainen, M. and Wistrand, A.F.** (2011). Developments in the polymerization of polylactide-based materials. (Chapter 2) in *Update on polylactide based materials*, Smithers Information Ltd.

- Hakkarainen, M., Karlsson, S. and Albertsson, A.C.** (2000). Influence of low molecular weight lactic acid derivatives on degradability of polylactide. *J. Appl. Polym. Sci.*, **76**, 228-239.
- Hans, M., Keul, H. and Moeller, M.** (2009). Ring-opening polymerization of D,D-lactide catalyzed by Novozyme 435. *Macromol. Biosci.*, **9**, 239-247.
- Henderson, L.A., Svirkin, Y.Y., Gross, R.A., Kaplan, D.L. and Swift, G.** (1996). Enzyme-catalyzed polymerizations of  $\epsilon$ -caprolactone: effects of initiator on product structure, propagation kinetics, and mechanism. *Macromolecules*, **29**, 7759-7766.
- Hiemenz, P. C. and Lodge, T. P.** (2007). *Polymer Chemistry*. CRC Press, Boca Raton, Florida, USA.
- Ho, K.L.G., Pometto, A.L., Gadea-Rivas, A., Briceno, J.A. and Rojas, A.** (1999). Degradation of polylactic acid (PLA) plastic in costa rican soil and iowa university compos rows. *J. Environ. Polym. Degr.*, **7**, 173-177.
- Honda, Y. and Osawa, Z.** (2002). Microbial denitrification of wastewater using biodegradable polycaprolactone. *Polym. Degrad. Stab.*, **76**, 321-327.
- Huang, S.J.** (2005). Poly(lactic acid) and copolyesters. (Chapter 9) in *Handbook of biodegradable polymers* (edt. Bastioli, C.), Rapra Technology Ltd., UK.
- Ikada, Y. and Tsuji, H.** (2000). Biodegradable polyesters for medical and ecological applications. *Macromol. Rapid Commun.*, **21**, 117-132.
- Jaeger, K.E., Dijkstra, B.W. and Reetz, M.T.** (1999). Bacterial biocatalysts: Molecular biology, three-dimensional structures, and biotechnological applications of lipases. *Annu. Rev. Microbiol.*, **53**, 315-351.
- Jimenez, G., Ogata, N., Kawai, H. and Ogihara, T.** (1997). Structure and thermal/mechanical properties of poly( $\epsilon$ -caprolactone)-clay blend. *J. Appl. Polym. Sci.*, **64**, 2211-2220.
- Johnston, J.H., McFarlane, A.J. and Borrmann, T.** (2008). Nano-structured silicate, functionalized forms thereof, preparation and uses. The Patent Description & Claims data from USPTO Patent Application 20080305027, Class: 4233309 (USPTO).
- Kamath, S.R. and Proctor, A.** (1998). Silica gel from rice hull ash: Preparation and characterization. *Cereal Chem.*, **75**, 484-487.
- Kamber, N.E., Jeong, W., Waymouth, R.M., Pratt, R.C., Lohmeijer, G.G. and Hedrick, J.L.** (2007). Organocatalytic ring-opening polymerization. *Chem. Rev.*, **107**, 5813-5840.
- Kennedy, J.F., White, C.A. and Melo, E.H.M.** (1988). *Chimica Oggi*, **5**, 21-29.
- Kiersnowski, A. and Piglowski, J.** (2004). Polymer-layered silicate nanocomposites based on poly( $\epsilon$ -caprolactone). *Eur. Polym. J.*, **40**, 1199-1207.
- Kiersnowski, A., Dabrowski, P., Budde, H., Kressler, J. and Piglowski, J.** (2004). Synthesis and structure of poly( $\epsilon$ -caprolactone)/synthetic montmorillonite nano-intercalates. *Eur. Polym. J.*, **40**, 2591-2598.

- Kikuchi, H., Uyama, H. and Kobayashi, S.** (2000). Lipase-catalyzed enantioselective copolymerization of substituted lactones to optically active polyesters. *Macromolecules*, **33**, 8971-8975.
- Klibanov, A.M.** (1997). Why are enzymes less active in organic solvents than in water? *Trends Biotechnol.*, **15**, 97-101.
- Knani, D., Gutman, A.L. and Kohn, D.H.** (1993). Enzymic polyesterification in organic media. Enzyme-catalyzed synthesis of linear polyesters. I. Condensation polymerization of linear hydroxyester. II. Ring-opening polymerization of  $\epsilon$ -caprolactone. *J. Polym. Sci. A Polym. Chem.*, **31**, 1221-1232.
- Kobayashi, S.** (2006). Enzymatic ring-opening polymerization of lactones by lipase catalyst: Mechanistic aspects. *Macromol. Symp.*, **240**, 178-185.
- Kobayashi, S., Takeya, K., Suda, S. and Uyama, H.** (1998a). Lipase-catalyzed ring-opening polymerization of medium-size lactones to polyesters, *Macromol. Chem. Phys.*, **199**, 1729-1736.
- Kobayashi, S., Uyama, H. and Namekawa, S.** (1998b). In vitro biosynthesis of polyesters with isolated enzymes in aqueous systems and organic solvents. *Polym. Degrad. Stab.*, **59**, 195-201.
- Koenig, M.F. and Huang, S.J.** (1994). Evaluation of crosslinked poly(caprolactone) as a biodegradable, hydrophobic coating. *Polym. Degrad. Stab.*, **45**, 139-144.
- Kowalski, A., Duda, A. and Penczek, S.** (1998). Kinetics and mechanism of cyclic esters polymerization initiated with tin(II) octoate: 1. Polymerization of  $\epsilon$ -caprolactone. *Macromol. Rapid Commun.*, **19**, 567-572.
- Kowalski, A., Duda, A. and Penczek, S.** (2000a). Kinetics and mechanism of cyclic esters polymerization initiated with tin(II) octoate. 3. Polymerization of L,L-dilactide. *Macromolecules*, **33**, 7359-7370.
- Kowalski, A., Libiszowski, J., Duda, A. and Penczek, S.** (2000b). Polymerization of L,L-dilactide initiated by tin(II) butoxide. *Macromolecules*, **33**, 1964-1971.
- Kricheldorf, H. R. and Eggerstedt, S.** (1998). Living macrocyclic polymerization of  $\epsilon$ -caprolactone with 2,2-dibutyl-2-stanna-1,3-dioxepane as initiator. *Macromol. Chem. Phys.*, **199**, 283-290.
- Kricheldorf, H. R., Kreiser-Saunders, I. and Stricker, A.** (2000). Sn(Oct)<sub>2</sub>-initiated polymerizations of lactide: a mechanistic study. *Macromolecules*, **33**, 702-709.
- Krikorian, V. and Pochan, D.J.** (2003). Poly(L-lactic acid)/layered silicate nanocomposite: fabrication, characterization and properties. *Chem. Mater.*, **15**, 4317-4324.
- Kubies, D., Pantoustier, N., Dubois, P., Rulmont, A. and Jerome, R.** (2002). Controlled ring-opening polymerization of  $\epsilon$ -caprolactone in the presence of layered silicates and formation of nanocomposites. *Macromolecules*, **35**, 3318-3320.

- Kumar, A. and Gross, R.A.** (2000a). *Candida antartica* lipase B catalyzed polycaprolactone synthesis: Effects of organic media and temperature. *Biomacromolecules*, **1**, 133-138.
- Kumar, A. and Gross, R.A.** (2000b). *Candida antarctica* lipase B-catalyzed transesterification: New synthetic routes to copolyesters. *J. Am. Chem. Soc.*, **122**, 11767-11770.
- Kumar, A., Kalra, B., Dekhterman, A. and Gross, R.A.** (2000c). Efficient ring-opening polymerization and copolymerization of  $\epsilon$ -caprolactone and  $\omega$ -pentadecalactone catalyzed by *Candida antartica* lipase B. *Macromolecules*, **33**, 6303-6309.
- Kwak, S.Y. and Oh, K.S.** (2003). Effect of thermal history on structural changes in melt-intercalated poly( $\epsilon$ -caprolactone)/organoclay nanocomposites investigated by dynamic viscoelastic relaxation measurements. *Macromol. Mater. Eng.*, **288**, 503-508.
- Labet, M. and Thielemans, W.** (2009). Synthesis of polycaprolactone: a review. *Chem. Soc. Rev.*, **38**, 3484-3504.
- Lafuente, F.R., Armisen, P., Sabuquillo, P., Fernandez-Lorente, G. and Guisan, J.M.** (1998). Immobilization of lipases by selective adsorption on hydrophobic supports. *Chem. Phys. Lipids*, **93**, 185-197.
- Lagaly, G., Ogawa, M. and Dekany, I.** (2006). Clay mineral organic interaction. *Handbook of clay science*. (eds. Bergaya, F., Theng, B.K.G., Lagaly, G.), Elsevier, Amsterdam, **1218**, 309-377.
- Lassalle, V.L. and Ferreira, M.L.** (2008). Lipase-catalyzed synthesis of polylactic acid: an overview of the experimental aspects. *J. Chem. Technol. Biotechnol.*, **83**, 1493-1502.
- Lecomte, P. and Jérôme, C.** (2012). Recent developments in ROP of lactones. *Adv. Polym. Sci.*, **245**, 173-218.
- Lee, Y.H., Lee, J.H., An, I.G., Kim, C., Lee, D.S., Lee, K., et al.** (2005). Electrospun dual-porosity structure and biodegradation morphology of montmorillonite reinforced PLLA nanocomposite scaffolds. *Biomaterials*, **26**, 3165-3172.
- Lee, Y.S., Hong, J.H., Jeon, N.Y., Won, K. and Kim, B.T.** (2004). Highly enantioselective acylation of rac-alkyl lactates using *Candida antarctica* lipase B. *Org. Process Res. Dev.*, **8**, 948-951.
- Lepoittevin, B., Devalckenaere, M., Pantoustier, N., Alexandre, M., Kubies, D., Calberg, C. et al.** (2002a). Poly( $\epsilon$ -caprolactone)/clay nanocomposites prepared by melt intercalation: mechanical, thermal and rheological properties. *Polymer*, **43**, 4017-4023.
- Lepoittevin, B., Pantoustier, N., Alexandre, M., Calberg, C., Jerome, R. and Dubois, P.** (2002b). Layered silicate/polyester nanohybrids by controlled ring opening polymerization. *Macromol. Symp.*, **183**, 95-102.
- Lepoittevin, B., Pantoustier, N., Alexandre, M., Calberg, C., Jerome, R. and Dubois, P.** (2002c). Polyester layered silicate nanohybrids by controlled grafting polymerization. *J. Mater. Chem.*, **12**, 3528-3532.

- Lepoittevin, B., Pantoustier, N., Devalckenaere, M., Alexandre, M., Calberg, C., Jerome, R., et al.** (2003). Polymer/layered silicate nanocomposites by combined intercalative polymerization and melt intercalation: a masterbatch process. *Polymer*, **44**, 2033-2040.
- Loeker, F.C., Duxbury, C.J., Kumar, R., Gao, W., Gross, R.A. and Howdle, S.M.** (2004). Enzyme-catalyzed ring-opening polymerization of  $\epsilon$ -caprolactone in supercritical carbon dioxide. *Macromolecules*, **37**, 2450-2453.
- Lohmeijer, B.G.G., Pratt, R.C., Leibfarth, F., Logan, J.W., Long, D.A., Dove, A.P., Nederberg, F., Choi, J., Wade, C., Waymouth, R.M. and Hedrick, J.L.** (2006). Guanidine and amidine organocatalysts for ring-opening polymerization of cyclic esters. *Macromolecules*, **39**, 8574-8583.
- Lopez-Gallego, F., Betancor, L., Mateo, C., Hidalgo, A., Alonso-Morales, N., Dellamora-Ortiz, G., Guisan, J.M. and Fernandez-Lafuente, R.** (2005). Enzyme stabilization by glutaraldehyde crosslinking of adsorbed proteins on aminated supports. *J. Biotechnol.*, **119**, 70-75.
- Löfgren, A., Albertsson, A.C., Dubois, A.C., Jérôme, R. and Teyssié, P.** (1994). Synthesis and characterization of biodegradable homopolymers and block copolymers based on 1,5-dioxepan-2-one. *Macromolecules*, **27**, 5556-5562.
- Löfgren, A., Albertsson, A.C., Dubois, P., Jérôme, R.** (1995). Recent advances in ring-opening polymerization of lactones and related compounds. *J. Macromol. Sci. C Polym. Rev.*, **35**, 379-418.
- MacDonald, R.T., Pulapura, S., Svirkin, Y., Gross, R.A., Kaplan, D.A., Akkara, J., Swift, G. and Wolk, S.** (1995). Enzyme-catalyzed  $\epsilon$ -caprolactone ring-opening polymerization. *Macromolecules*, **28**, 73-78.
- Malachová, K., Praus, P., Pavlíčková, Z. and Turicová, M.** (2009). Activity of antibacterial compounds immobilised on montmorillonite. *Appl. Clay Sci.*, **43**, 364-368.
- Malberg, S., Wistrand, A.F. and Albertsson, A.C.** (2010). The environmental influence in enzymatic polymerization of aliphatic polyesters in bulk and aqueous mini emulsion. *Polymer*, **51**, 5318-5322.
- Marcilla, R., De Geus, M., Mecerreyes, D., Duxbury, C.J., Koning, C.E. and Heise, A.** (2006). Enzymatic polyester synthesis in ionic liquids. *Eur. Polym. J.*, **42**, 1215-1221.
- Martin, E., Dubois, P., Jerome, R.** (2003a). Polymerization of  $\epsilon$ -caprolactone initiated by Y alkoxide grafted onto porous silica. *Macromolecules*, **36**, 7094-7099.
- Martin, E., Dubois, P. and Jerome, R.** (2003b). Preparation of supported yttrium alkoxides as catalysts for the polymerization of lactones and oxirane. *J. Polym. Sci. A Polym. Chem.*, **41**, 569-578.



- Martino, V.P., Ruseckaite, R.A., Jiménez, A. and Avérous, L.** (2010). Correlation between composition, structure and properties of poly(lactic acid) - polyadipate based nano-biocomposites. *Macromol. Mater. Eng.*, **295**, 551-558.
- Martino, V.P., Jiménez, A., Ruseckaite, R.A. and Avérous, L.** (2011). Structure and properties of clay nano-biocomposites based on poly(lactic acid) plasticized with polyadipates. *Polym. Advan. Technol.*, **22**, 2206-2213.
- Mateo, C., Palomo, J.M., Fernandez-Lorente, G., Guisan, J.M. and Fernandez-Lafuente, R.** (2007). Improvement of enzyme activity, stability and selectivity via immobilization techniques. *Enzyme Microb. Technol.*, **40**, 1451-1463.
- Matsumura, S.** (2006). Enzymatic synthesis of polyesters via ring-opening polymerization. *Adv. Polym. Sci.*, **194**, 95-132.
- Matsumura, S., Mabuchi, K. and Toshima, K.** (1997). Lipase-catalyzed ring-opening polymerization of lactide. *Macromol. Rapid Commun.*, **18**, 477-482.
- Matsumura, S., Mabuchi, K. and Toshima, K.** (1998). Novel ring-opening polymerization of lactide by lipase. *Macromol. Symp.*, **130**, 285-304.
- Mei, Y., Kumar, A. and Gross, R.A.** (2002). Probing water-temperature relationships for lipase-catalyzed lactone ring-opening polymerizations. *Macromolecules*, **35**, 5444-5448.
- Mei, Y., Kumar, A., and Gross, R.A.** (2003a). Kinetics and mechanism of *Candida antarctica* lipase B catalyzed solution polymerization of  $\epsilon$ -caprolactone. *Macromolecules*, **36**, 5530-5536.
- Mei, Y., Miller, L., Gao, W. and Gross, R.A.** (2003b). Imaging the distribution and secondary structure of immobilized enzymes using infrared microspectroscopy. *Biomacromolecules*, **4**, 70-74.
- Messersmith, P.B. and Giannelis, E.P.** (1993). Polymer-layered silicate nanocomposites: in situ intercalative polymerization of  $\epsilon$ -caprolactone in layered silicates. *Chem. Mater.*, **5**, 1064-1066.
- Messersmith, P.B. and Giannelis, E.P.** (1995). Synthesis and barrier properties of polycaprolactone-layered silicate nanocomposites. *J. Polym. Sci. Polym. Chem.*, **33**, 1047-1057.
- Migneault, I., Dartiguenave, C., Bertrand, M.J. and Waldron, K.C.** (2004). Glutaraldehyde: behavior in aqueous solution, reaction with proteins, and application to enzyme crosslinking. *BioTechniques*, **37**, 790-802.
- Miola-Delaite, C., Hamaide, T. and Spitz, R.** (1999). Anionic coordinated polymerization of  $\epsilon$ -caprolactone with aluminium, zirconium and some rare earths alkoxides as initiators in the presence of alcohols. *Macromol. Chem. Phys.*, **200**, 1771-1778.
- Miola-Delaite, C., Colomb, E., Pollet, E. and Hamaide, T.** (2000). Anionic ring opening polymerization of oxygenated heterocycles with supported zirconium and rare earths alkoxides as initiators in protic conditions. Towards a catalytic heterogeneous process. *Macromol. Symp.*, **153**, 275-286.

- Mochizuki, M., Hirano, M., Kanmuri, Y., Kudo, K. and Tokiwa, Y.** (1995). Hydrolysis of polycaprolactone fibers by lipase: Effects of draw ratio on enzymatic degradation. *J. Appl. Polym. Sci.*, **55**, 289-296.
- Myers, M., Connor, E.F., Glauser, T., Mock, A., Nyce, G. and Hedrick, J.L.** (2002). Phosphines: nucleophilic organic catalysts for the controlled ring-opening polymerization of lactides. *J. Polym. Sci. A Polym. Chem.*, **40**, 844-851.
- Namekawa, S., Suda, S., Uyama, H. and Kobayashi, S.** (1999). Lipase-catalyzed ring-opening polymerization of lactones to polyesters and its mechanistic aspects. *Int. J. o Biol. Macromol.*, **25**, 145-151.
- Namekawa, S., Uyama, H. and Kobayashi, S.** (2001). Lipase-catalyzed ring-opening polymerization of lactones in the presence of aliphatic polyesters to ester copolymers. *Macromol. Chem. Phys.*, **202**, 801-806 .
- Nederberg, F., Connor, E.F., Moller, M., Glauser, T. and Hedrick, J.L.** (2001). New paradigms for organic catalysts: the first organocatalytic living polymerization. *Angew. Chem. Int. Ed.*, **40**, 2712-2715.
- Nikolic, M. A. L., Dean, K. and Halley P. J.** (2012). Biodegradation and applications of nanobiocomposites. (Chapter 16) in *Environmental silicate nano-biocomposites* (etds. Avérous, L. and Pollet, E.), Springer-Verlag, London.
- Nomura, N., Akita, A., Ishii, R. and Mizuno, M.** (2010). Random copolymerization of  $\epsilon$ -caprolactone with lactide using a homosalen-Al complex. *J. Am. Chem. Soc.*, **132**, 1750-1751.
- Nyce, G.W., Glauser, T., Connor, E.F., Mock, A., Waymouth, R.M. and Hedrick, J.L.** (2003). In situ generation of carbenes: a general and versatile platform for organocatalytic living polymerization. *J. Am. Chem. Soc.*, **125**, 3046-3056.
- Ogata, N., Jimenez, G., Kawai, H., Ogihara, T.** (1997). Structure and thermal/mechanical properties of poly(L-lactide)-clay blend. *J. Polym. Sci. Polym. Phys.*, **35**, 389-396.
- Okamoto, M.** (2012). Polylactide/clay nano-biocomposites. (Chapter 4) in *Environmental silicate nano-biocomposites* (edts. Avérous, L. and Pollet, E.), Springer-Verlag, London.
- Oshimura, M., Tang, T. and Takasu, A.** (2011). Ring-opening polymerization of  $\epsilon$ -caprolactone using perfluoroalkanesulfonates and perfluoroalkanesulfonimides as organic catalysts. *J. Polym. Sci. A Polym. Chem.*, **49**, 1210–1218.
- Pantoustier, N., Alexandre, M., Degée, P., Calberg, C., Jerome, R., Henrist, C., et al.** (2001). Poly( $\epsilon$ -caprolactone) layered silicate nanocomposites: effect of clay surface modifiers on the melt intercalation process. *e-Polymers*, no. 009.

- Pantoustier, N., Lepoittevin, B., Alexandre, M., Kubies, D., Calberg, C., Jerome, R. et al.** (2002). Biodegradable polyester layered silicate nanocomposites based on poly( $\epsilon$ -caprolactone). *Polym. Eng. Sci.*, **42**, 1928-1937.
- Pantoustier, N., Alexandre, M., Degée, P., Kubies, D., Jerome, R., Henrist, C., et al.** (2003). Intercalative polymerization of cyclic esters in layered silicates: thermal vs catalytic activation. *Compos. Interfaces*, **10**, 423-433.
- Parzuchowski, P. G., Grabowska, M., Tryznowski, M. and Rokicki, G.** (2006). Synthesis of glycerol based hyperbranched polyesters with primary hydroxyl groups. *Macromolecules*, **39**, 7181-7186.
- Paul, M.A., Alexandre, M., Degée, P., Calberg, C., Jerome, R. and Dubois, P.** (2003a). Exfoliated polylactide/clay nanocomposites by in-situ coordination-insertion polymerization. *Macromol. Rapid Commun.*, **24**, 561-566.
- Paul, M.A., Alexandre, M., Degée, P., Henrist, C., Rulmont, A. and Dubois, P.** (2003b). New nanocomposite materials based on plasticized poly(L-lactide) and organo modified montmorillonites: thermal and morphological study. *Polymer*, **44**, 443-450.
- Paul, M.A., Delcourt, C., Alexandre, M., Degée, P., Monteverde, F., Rulmont, A. et al.** (2005). Plasticized polylactide/organo-clay nanocomposites by in situ intercalative polymerization. *Macromol. Chem. Phys.*, **206**, 484-498.
- Peeters, J.W., Van Leeuwen, O., Palmans, A.R.A., Meijer, E.W.** (2005). Lipase catalyzed ring-opening polymerizations of 4-substituted  $\epsilon$ -caprolactones: mechanistic considerations. *Macromolecules*, **38**, 5587-5592.
- Penczek, S.** (2000). Cationic ring-opening polymerization (CROP) major mechanistic phenomena. *J. Polym. Sci. A Polym. Chem.*, **38**, 1919-1933.
- Persenaire, O., Alexandre, M., Degée, P. and Dubois, P.** (2001). Mechanisms and kinetics of thermal degradation of poly( $\epsilon$ -caprolactone). *Biomacromolecules*, **2**, 288-294.
- Pluta, M., Paul, M.A., Alexandre, M. and Dubois, P.** (2006). Plasticized polylactide/ clay nanocomposites. I. The role of filler content and its surface organo-modification on the physico-chemical properties. *J. Polym. Sci. Polym. Phys.*, **44**, 299-311.
- Poojari, Y., Palsule, A.S., Cai, M., Clarson S.J. and Gross, R.A.** (2008). Synthesis of organosiloxane copolymers using enzymatic polyesterification. *Europ. Polym. J.*, **44**, 4139-45.
- Potts, J.E., Clendinning, R.A., Ackart, W.B. and Niegish, W.D.** (1973). Biodegradability of synthetic polymers. *Polym. Sci. Technol.*, **3**, 61.

- Pratt, R.C., Lohmeijer, B.G.G., Long, D.A., Lundberg, P.N.P., Dove, A.P., Li, H., Wade, C.G., Waymouth, R.M. and Hedrick, J.L.** (2006). Exploration, optimization, and application of supramolecular thiourea-amine catalysts for the synthesis of lactide (co)polymers. *Macromolecules*, **39**, 7863-7871.
- Pucciariello, R., Villani, V., Belviso, S., Gorrasi, G., Tortora, M. and Vittoria, V.** (2004). Phase behavior of modified montmorillonite-poly( $\epsilon$ -caprolactone) nanocomposites. *J. Polym. Sci. Polym. Phys.*, **42**, 1321-1332.
- Puskas, J.E., Chiang, C.K. and Sen, M.Y.** (2011). Green cationic polymerizations and polymer functionalization for biotechnology. (Chapter 14) in *Green polymerization methods* (eds. Mathers, R.T. and Meier, M.A.R.), Wiley-VCH, Weinheim, Germany.
- Qian, Z.** (2007). Engineering *Candida antarctica* lipase B by circular permutation and incremental truncation. PhD Thesis, Emory University.
- Reeve, S.M.S., McCarthy, P., Downey, M.J. and Gross, R.A.** (1994). Polylactide stereochemistry: effect on enzymic degradability. *Macromolecules*, **27**, 825-831.
- Ruiz-Hitzky, E., Aranda, P., Dardera, M. and Rytwobc, G.** (2010). Hybrid materials based on clays for environmental and biomedical applications. *J. Mater. Chem.*, **20**, 9306-9321.
- Rutkowska, M., Jastrzebska, M. and Janik, H.** (1989). Biodegradation of polycaprolactone in sea water. *React. Funct. Polym.*, **38**, 27-30.
- Sarda, L. and Desnuelle, R.** (1958). Action de la lipase pancreatique sur les esters en emulsion. *Biochim. Biophys. Acta*, **30**, 513 -521.
- Sawada, H.** (1994). Field testing of biodegradable plastics. *Biodegradable Plastics and Polymers* (eds. Doi, Y. and Fukuda, K.) Elsevier Science, Amsterdam, The Netherlands, p.298.
- Schmid, R. and Verger, R.** (1998). Lipases: Interfacial enzymes with attractive applications. *Angew. Chem. Int. Ed.*, **37**, 1608-1633.
- Schmidt, D., Shah, D. and Giannelis, E.P.** (2002). New advances in polymer/layered silicate nanocomposites. *Curr. Opin. Solid St. M.*, **6**, 205-212.
- Schwach, G., Coudane, Engel, R. and Vert, M.** (1996). Zn lactate as initiator of D-L-lactide ring opening polymerization and comparison with Sn octoate. *Polym. Bull.*, **37**, 771-776.
- Sedaghat, M.E., Ghiaci, M., Aghaei, H. and Soleimanian-Zad, S.** (2009). Enzyme immobilization. Part 4. Immobilization of alkaline phosphatase on Na-sepiolite and modified sepiolite. *Appl. Clay Sci.*, **46**, 131-135.
- Sharma, R., Chisti, Y. and Banerjee, U. C.** (2001). Production, purification, characterization, and applications of lipases. *Biotechnol. Adv.*, **19**, 627-662.

- Shen, Z.Q., Shen, Y.Q., Sun, J. Q., Zhang, F. Y. and Zhang, Y. F.** (1995). Ring opening polymerization of epsilon-caprolactone by rare earth alkoxide- CCl<sub>4</sub> systems. *Polym. J.*, **27**, 59-64.
- Shibasiki, Y., Sanada, H., Yokoi, M., Sanda, F. and Endo, T.** (2000). Activated monomer cationic polymerization of lactones and the application to well-defined block copolymer synthesis with seven-membered cyclic carbonate. *Macromolecules*, **33**, 4316-4320.
- Shibata, M., Someya, Y., Orihara, M. and Miyoshi, M.** (2006). Thermal and mechanical properties of plasticized poly(L-lactide) nanocomposites with organo-modified montmorillonites. *J. Appl. Polym. Sci.*, **99**, 2594-2602.
- Shibata, M., Teramoto, N., Someya, Y. and Tsukao, R.** (2007). Nanocomposites based on poly(ε-caprolactone) and the montmorillonite treated with dibutylamine-terminated-ε-caprolactone oligomer. *J. Appl. Polym. Sci.*, **104**, 3112-3119.
- Sinha Ray, S. and Okamoto, M.** (2003a). Biodegradable polylactide and its nanocomposites: opening a new dimension for plastics and composites. *Macromol. Rapid Commun.*, **24**, 815-840.
- Sinha Ray, S. and Okamoto, M.** (2003b). Polymer/layered silicate nanocomposites: a review from preparation to processing. *Prog. Polym. Sci.*, **28**, 1539-1641.
- Sinha Ray, S. and Bousmina, M.** (2005). Biodegradable polymers and their layered silicate nanocomposites: In greening the 21<sup>st</sup> century materials world. *Prog. Mater. Sci.*, **50**, 962-1079.
- Sinha Ray, S., Maiti, P., Okamoto, M., Yamada, K. and Ueda, K.** (2002a). New polylactide/layered silicate nanocomposites. 1. Preparation, characterization and properties. *Macromolecules*, **35**, 3104-3110.
- Sinha Ray, S., Yamada, K., Ogami, A., Okamoto, M. and Ueda, K.** (2002b). New polylactide/layered silicate nanocomposite: nanoscale control over multiple properties. *Macromol. Rapid Commun.*, **23**, 943-947.
- Sinha Ray, S., Yamada, K., Okamoto, M. and Ueda, K.** (2002c). Polylactide-layered silicate nanocomposite: a novel biodegradable material. *Nano Lett.*, **2**, 1093-1096.
- Sinha Ray, S., Yamada, K., Okamoto, M., Fujimoto, Y., Ogami, A. and Ueda, K.** (2003a). New polylactide/layered silicate nanocomposites. 5. Designing of materials with desired properties. *Polymer*, **44**, 6633-6646.
- Sinha Ray, S., Yamada, K., Okamoto, M., Ogami, A. and Ueda, K.** (2003b). New polylactide/layered silicate nanocomposites. 3. High-performance biodegradable materials. *Chem Mater.*, **15**, 1456-1465.
- Sinha Ray, S., Yamada, K., Okamoto, M., Ogami, A. and Ueda, K.** (2003c). New polylactide/ layered silicate nanocomposites. 4. Structure, properties and biodegradability. *Compos. Interfaces*, **10**, 435-450.

- Sinha Ray, S., Yamada, K., Okamoto, M. and Ueda, K.** (2003d). Biodegradable polylactide/ montmorillonite nanocomposites. *J. Nanosci. Nanotechnol.*, **3**, 503-510.
- Sinha Ray, S., Yamada, K., Okamoto, M. and Ueda, K.** (2003e). New polylactide layered silicate nanocomposites. 2. Concurrent improvements of material properties, biodegradability and melt rheology. *Polymer*, **44**, 857-866.
- Soppimath, K. S., Aminabhavi, T. M., Kulkarni, A. R. and Rudzinski, W. E.** (2001). Biodegradable polymeric nanoparticles as drug delivery devices. *J. Controlled Release*, **70**, 1-20.
- Södergard, A. and Inkinen, S.** (2011). Production, chemistry and properties of polylactides. (Chapter 3) in *Biopolymers-New materials for sustainable films and coatings* (edt. Plackett, D.), John Wiley and Sons Ltd., United Kingdom.
- Srivastava, R.K. and Albertsson A.C.** (2005). High-molecular-weight poly(1,5-dioxepan-2-one) via enzyme-catalyzed ring-opening polymerization. *J. Polym. Sci. A Polym. Chem.*, **43**, 4206-4216.
- Steinbuchel, A.** (2003). Biopolymers, general aspects and special applications. Weinheim, Germany: Wiley-VCH.
- Stevens, W., Dijkstra, P. J., Feijen, J.** (1997). New initiators for the ring opening polymerization of cyclic esters. *Trends Polym. Sci.*, **5**, 300-305.
- Stridsberg, K. M., Ryner, M. and Albertsson, A.C.** (2001). Controlled ring-opening polymerization: polymers with designed macromolecular architecture. *Adv. Polym. Sci.*, **157**, 41-65.
- Sun, J., Jiang, Y., Zhou, L. and Gao, J.** (2010). Immobilization of *Candida antarctica* lipase B by adsorption in organic medium. *New Biotechnology*, **27**, 53-58.
- Takamoto, T., Uyama, H. and Kobayashi, S.** (2001). Lipase-catalyzed synthesis of aliphatic polyesters in supercritical carbon dioxide. *e-Polymers*, **4**, 1-6.
- Tartaglione, G., Tabuani, D. and Camino, G.** (2008). Thermal and morphological characterization of organically modified sepiolite. *Microporous Mesoporous Mater.*, **107**, 161-168.
- Thostenson, E., Li, C. and Chou, T.** (2005). Review: nanocomposites in context. *J. Compos. Sci. Technol.*, **65**, 491-516.
- Thurecht, K.J., Heise, A., De Geus, M., Villarroya, S., Zhou, J., Wyatt, M.F. and Howdle, S.M.** (2006). Kinetics of enzymatic ring-opening polymerization of  $\epsilon$ -caprolactone in supercritical carbon dioxide. *Macromolecules*, **39**, 7967-7972.
- Tokiwa, Y. and Suzuki, T.** (1977). Hydrolysis of polyesters by lipases. *Nature*, **270**, 76-78.
- Trodler, P. and Pleiss J.** (2008). Modeling structure and flexibility of *Candida antarctica* lipase B in organic solvents. *BMC Structural Biology*, **8**, 9-19.

- Tsuji, H. and Suzuyoshi, K.** (2002). Environmental degradation of biodegradable polyesters. 2. Poly( $\epsilon$ -caprolactone), poly[(R)-3-hydroxybutyrate], and poly(L-lactide) films in natural dynamic seawater. *Polym. Degrad. Stab.*, **75**, 347-355.
- Turner, N.A., Duchateau, D.B. and Vulfson, E.N.** (1995). Effect on hydration on thermostability of serine esterases. *Biotech. Lett.*, **17**, 371-376.
- Turner, N.A. and Vulfson, E.N.** (2000). At what temperature can enzymes maintain their catalytic activity? *Enzyme Microb. Technol.*, **27**, 108-113.
- Tzialla, A.A., Kalogeris, E., Enotiadis, A., Taha, A.A., Gournis, D. and Stamatis, H.** (2009). Effective immobilization of *Candida antarctica* lipase B in organic-modified clays: Application for the epoxidation of terpenes. *Mater. Sci. Eng. B*, **165**, 173-177.
- Tzialla, A.A., Pavlidis, I.V., Felicissimo, M.P., Rudolf, P., Gournis, D. and Stamatis, H.** (2010). Lipase immobilization on smectite nanoclays: Characterization and application to the epoxidation of  $\alpha$ -pinene. *Bioresour. Technol.*, **101**, 1587-1594.
- Uppenberg, J., Hansen, M.T., Patkar, S. and Jones, T.A.** (1994). The sequence, crystal-structure determination and refinement of 2 crystal forms of lipase-B from *Candida antarctica*. *Structure*, **2**, 293-308.
- Uppenberg, J., Oehrner, N., Norin, M., Hult, K., Kleywegt, G.J., Patkar, S., Waagen, V., Anthonsen, T., Jones, T.A.** (1995). Crystallographic and molecular-modeling studies of lipase B from *Candida antarctica* reveal a stereospecificity pocket for secondary alcohols. *Biochemistry*, **34**, 16838-16851.
- Uyama, H. and Kobayashi, S.** (1993). Enzymic ring-opening polymerization of lactones catalyzed by lipase. *Chem. Lett.*, 1149-1150.
- Uyama, H., Takeya, K. and Kobayashi, S.** (1995). Enzymatic ring-opening polymerization of lactones to polyesters by lipase catalyst: unusually high reactivity of macrolides. *Bull. Chem. Soc. Jpn.*, **68**, 56-61.
- Uyama, H., Suda, S., Kikuchi, H. and Kobayashi, S.** (1997). Extremely efficient catalysis of immobilized lipase in ring-opening polymerization of lactones. *Chem. Lett.*, 1109-1110.
- Varma, I.K., Albertsson, A.C., Rajkhowa, R. and Srivastava, R.K.** (2005). Enzyme catalyzed synthesis of polyesters. *Prog. Polym. Sci.*, **30**, 949-981.
- Vert, M.** (2000). Lactide polymerization faced with therapeutic application requirements. *Macromol. Symp.*, **153**, 333-342.
- Viville, P., Lazzaroni, R., Pollet, E., Alexandre, M., Dubois, P., Borgia, G., et al.** (2003). Surface characterization of poly( $\epsilon$ -caprolactone)-based nanocomposites. *Langmuir*, **19**, 9425-9433.
- Viville, P., Lazzaroni, R., Pollet, E., Alexandre, M. and Dubois, P.** (2004). Controlled polymer grafting on single clay nanoplatelets. *J. Am. Chem. Soc.*, **126**, 9007-9012.

- Wahlberg, J., Persson, P.V., Olsson, T., Hedenström, E. and Iversen, T.** (2003). Structural characterization of a lipase-catalyzed copolymerization of  $\epsilon$ -caprolactone and D,L-lactide. *Biomacromolecules*, **4**, 1068-1071.
- Walt, D.R. and Agayn, V.** (1994). The chemistry of enzyme and protein immobilization with glutaraldehyde. *Trends Anal. Chem.*, **13**, 425-430.
- Wang, L. and Sheng, J.** (2005). Preparation and properties of polypropylene/org-attapulgit nanocomposites. *Polymer*, **46**, 6243-49.
- Wang, L., Ma, W., Gross, R.A. and McCarthy, S.P.** (1998). Reactive compatibilization of biodegradable blends of poly(lactic acid) and poly( $\epsilon$ -caprolactone). *Polym. Degrad. Stab.*, **59**, 161-168.
- Winkler, F. K., D'Arcy, A. and Hunziker, W.** (1990). Structure of human pancreatic lipase. *Nature*, **343**, 771-774.
- Xiao, Y., Coulembier, O., Koning, C.E., Heise, A. and Dubois, P.** (2009). Cumulated advantages of enzymatic and carbene chemistry for the non-organometallic synthesis of (co)polyesters. *Chem. Commun.*, **18**, 2472-2474.
- Xin, J.Y., Li, S., Xu, Y., Wang, L.S. and Yu, C.** (1999). Study on the immobilization and stability of lipase in organic media. *J. Mol. Catal.*, **13**, 103-108.
- Yoshizawa, M., Saito, C., Takeoka, Y. and Rikukawa, M.** (2008). Lipase-catalyzed polymerization of L-lactide in ionic liquids. *Polym. Adv. Technol.*, **19**, 1396-1400.
- Zaks, A. and Klibanov, A.M.** (1988). Enzymatic catalysis in nonaqueous solvents. *J. Biol. Chem.*, **263**, 3194-3201.
- Zhang, L., Nederberg, F., Pratt, R.C., Waymouth, R.M., Hedrick, J.L. and Wade, C.G.** (2007). Phosphazene bases: a new category of organocatalysts for the living ring-opening polymerization of cyclic esters. *Macromolecules*, **40**, 4154-4158.
- Zhou, J.X., Wang, W.X., Thurect, K.J., Villarroya, S. and Howdle, S.M.** (2006). Simultaneous dynamic kinetic resolution in combination with enzymatic ring-opening polymerization. *Macromolecules*, **39**, 7302-7305.
- Zhuang, H., Zheng, J. P., Gao, H. and Yao, K. D.** (2007). In vitro biodegradation and biocompatibility of gelatin/montmorillonite-chitosan intercalated nanocomposite. *J. Mater. Sci. Mater. Med.*, **18**, 951-957.
- Zinck, P.** (2011). Synthetic strategies for biomedical polyesters specialties (Chapter 21) in *Biomedical engineering, trends in materials science* (edt. Laskovski, N.A.), InTech.
- Url-1** < [http://www.bpf.co.uk/Topics/Standards\\_for\\_compostability.aspx](http://www.bpf.co.uk/Topics/Standards_for_compostability.aspx)>, date retrieved 25.05.2012.
- Url-2** < <http://www.okcompost.be/data/pdf-document/Doc-09e-a-Requirements-of-norm-EN-13432.pdf>>, date retrieved 25.05.2012.
- Url-3** <<http://en.european-bioplastics.org>>, date retrieved 29.06.2012.





## CURRICULUM VITAE

**Name Surname:** Mediha Hale ÖZTÜRK DÜŞKÜNKORUR

**Place and Date of Birth:** İstanbul – 10/04/1980

**Address:** 12 rue de la Grange, 67000, Strasbourg

**E-Mail:** medihaleozturk@gmail.com

**B.Sc.:** Chemical Engineering- Istanbul Technical University,  
Bachelor's degree in Business Administration - Anadolu University

**M.Sc.:** Molecular Biology, Genetics and Biotechnology-  
Istanbul Technical University

### Professional Experience :

2005- 2009

Istanbul Technical University - Chemical Engineering Department - Research Assistant

2002- 2004

Istanbul Technical University- Department of Molecular Biology-Genetics and  
Biotechnology - Lab. Assistant

### PUBLICATIONS/PRESENTATIONS ON THE THESIS

- **H. Öztürk**, E. Pollet, A. Hebraud, L. Averous. Lipase catalyzed synthesis of biopolyester and related clay-based nanohybrids, *Biodegradable Polymers and Sustainable Polymers (BIOPOL-2009)*, A. Jiménez, G.E. Zaikov (Eds); ISBN 979-1-61209-520-2; Pages 117-136.
- **Hale Öztürk Düşkünkörur**, Eric Pollet, Philippe Debeire, Vincent Phalip, Yüksel Güvenilir, Luc Avérous, "Lipase Catalyzed Synthesis of Biopolyester and Related Clay-Based Nanohybrids", submitted to *Biomacromolecules*.
- **Hale Öztürk Düşkünkörur**, Eric Pollet, Philippe Debeire, Vincent Phalip, Luc Avérous, Yüksel Güvenilir. Synthesis of biopolyester/clay nanohybrids by lipase catalysis. *3rd International Conference on Biodegradable and Biobased Polymers - BIOPOL 2011*, August 29-31, 2011 Strasbourg, France.



# BIOPOLYESTER SYNTHESIS BY ENZYMATIC CATALYSIS AND DEVELOPMENT OF NANOHYBRID SYSTEMS

## Résumé

L'objectif de ce travail est de développer des catalyseurs originaux et performants à base de lipases immobilisées sur argiles pour la synthèse de biopolyesters et d'obtenir des nanohybrides organique/inorganique par greffage de chaînes polyesters sur les nanoparticules d'argiles. Deux argiles (sépiolite et montmorillonite) ont été utilisées pour l'immobilisation de *Candida antarctica* lipase B (CALB) et les catalyseurs obtenus ont été testés en polymérisation de l' $\epsilon$ -caprolactone et des isomères de lactide. Les cinétiques de polymérisation et la caractérisation des polyesters ont montré que les lipases immobilisées sur montmorillonite sont plus performantes que celles immobilisées sur sépiolite. L'organo-modification de ces argiles améliore l'activité catalytique des systèmes obtenus. L'utilisation de CALB immobilisée sur montmorillonite a permis l'élaboration de nanohybrides organique/inorganique via le greffage et la croissance des chaînes polyesters à partir de la surface de l'argile. Finalement, des copolyesters statistiques PCL/PLA ont été obtenus avec succès par polymérisation enzymatique du D-lactide avec l' $\epsilon$ -caprolactone.

**Mots-clés :** Lipase, polymérisation, immobilisation, argile, polyester/argile nano-biocomposites (ou nanohybrides)

## Résumé en anglais

This thesis aims at presenting the use and development of original catalytic systems based on lipases immobilized on clays which are efficient for the synthesis of biopolyesters and allowing the preparation of organic/inorganic nanohybrids based on clay nanoparticles (sepiolite and montmorillonite) grafted with such polyesters. These nanoclays were used as lipase supports and the clay-immobilized forms of *Candida antarctica* lipase B (CALB) were tested for  $\epsilon$ -caprolactone and lactide isomers polymerization. Polymerization kinetics and characterization of resulting materials have shown that lipases immobilized on montmorillonite show better performances compared to the ones immobilized on sepiolite. Clay surface organo-modification has proved to greatly enhance the catalytic activity of the corresponding systems. CALB immobilized on montmorillonite allowed the elaboration of organic/inorganic nanohybrids as evidenced by the effective grafting of polyester chains from the clay surface. Finally, random PCL/PLA copolyesters were successfully obtained by lipase-catalyzed copolymerization of D-lactide with  $\epsilon$ -caprolactone.

**Keywords :** Lipase, polymerization, immobilization, clay, polyester/clay nano-biocomposites (or nanohybrids)